



University
of Glasgow

Stirrat, Alison (2002) *Effect of endogenous mediators in secondary pulmonary hypertension: an in vitro study of pulmonary resistance arteries.*

PhD thesis

<http://theses.gla.ac.uk/4361/>

Copyright and moral rights for this thesis are retained by the author

A copy can be downloaded for personal non-commercial research or study, without prior permission or charge

This thesis cannot be reproduced or quoted extensively from without first obtaining permission in writing from the Author

The content must not be changed in any way or sold commercially in any format or medium without the formal permission of the Author

When referring to this work, full bibliographic details including the author, title, awarding institution and date of the thesis must be given

**Effect of endogenous mediators in
Secondary pulmonary hypertension:
an *in vitro* study of pulmonary resistance arteries**

Alison Stirrat

A thesis submitted for the degree of Doctor of Philosophy (June 2002)

from

**The Division of Neuroscience and Biomedical Systems, Faculty of
Medicine, University of Glasgow, Glasgow, G12 8QQ.**

Declaration

I hereby declare that this thesis has been composed by myself and has not been submitted in any previous applications for a degree. The work presented in this thesis, except where specifically acknowledged, has been carried out by myself and all sources of information have been specifically acknowledged by means of reference to the work of the authors.

Clison Sturral 8.10.02

Acknowledgements

First and foremost, I would like to thank Professor Mandy MacLean for all the help and support she has given me throughout the tenure of my study.

I would also like to express my gratitude to Dr. Ian Morecroft for all his help and patience in teaching me myography. Thank you for your support and friendship.

I would like to thank Mr. John Lu and Mr Michael Flynn for their human LVD *in vivo* study results.

I would like to thank my parents, Ian and Isabel, for their continued love and encouragement throughout my studies. I have finally made it, just like you told me I would, and I think that you deserve some of the credit. To Lorna, thank you for being my friend as well as my sister. I hope you know how much I appreciate everything you, my family, have done for me. I love you all.

And last, but by no means least, to my darling Frank. I may have just written a thesis, and should know the entire contents of my thesaurus (which is still smoking), but I have been unable to find the words to articulate my feelings of love and gratitude to you. Suffice to say that I love you and couldn't have done this without you. Thank you.

Contents

Declaration
Acknowledgements
List of contents
List of figures
List of abbreviations
Summary

<u>Chapter 1: Introduction</u>	Page No.
1.1. The need for research	2
1.2. History of blood vessels	2
1.3. Classification of arteries	5
1.4. Vascular smooth muscle cell phenotypes	8
1.5. Diversity in the pulmonary and systemic circulations	10
1.6. The normal pulmonary circulation	12
1.7. Regulation of pulmonary vascular tone	14
1.8. Pulmonary hypertension	16
1.9. Hypoxic pulmonary vasoconstriction	19
1.10. The identity of the O₂ sensor	27
1.11. The indirect theory of HPV	29
1.12. Genetic basis for primary PHT	30
1.13. Investigations undertaken in this thesis	33
<u>Chapter 2: Materials and methods</u>	
2.1. Background of myography	36
2.2. Myography application	36
2.3. Myography equipment	37
2.4. Dissection of resistance arteries	
2.4.1. Rat pulmonary resistance arteries	39
2.4.2. Human pulmonary resistance arteries	41
2.4.3. Human abdominal systemic resistance arteries	42
2.5. Mounting procedure	43
2.6. Calibration of a myograph	47
2.7. Setting of transmural pressure	49
2.8. Small animal hypobaric hypoxic chamber design	52
2.9. Maintenance of animals	54
2.10 Validation of hypobaric hypoxic rat model	55
2.11. Data analysis	58
2.12. Statistical analysis	61
2.13. Drugs and solutions	61

Chapter 3: The mediators involved in the ACh-induced Vasodilator response: the effect of chronic hypoxia

3.1.1 Vasodilator response to ACh in control and chronic hypoxic rats	64
3.1.2. Endogenous vasodilator mediators of pulmonary arteries	65
3.2. Methods	70
3.3. Results:	73
3.3.1. Presence of pulmonary hypertension	73
3.3.2. Differences between the ACh-induced vasodilatation in control and chronic hypoxic rats	74
3.3.3. Control Wistar rat PRAs	77
3.3.4. Hypoxic Wistar rat PRAs	83
3.4. Discussion:	89
3.4.1. Chronic hypoxic rat model of PHT	89
3.4.2. ACh-induced vasodilatation in control and chronic hypoxic rats	89
3.4.3. Mediators of ACh-induced vasodilatation in control rat PRAs	90
3.4.4. Mediators of ACh-induced vasodilatation in chronic hypoxic rat PRAs	94
3.4.5. Interaction of the mediators involved in the ACh-induced vasodilatation	99
3.5 Conclusion	101

Chapter 4: Effect of human urotensin-II on human small muscular arteries of the pulmonary and systemic circulations

4.1.1. History of urotensin-II	103
4.1.2. U-II synthesis	103
4.1.3. U-II isoforms	105
4.1.4. U-II action	107
4.2. Methods	111
4.3. Results:	114
4.3.1. Human PRAs	114
4.3.2. Human abdominal SRAs	124
4.3.3. U-II isoforms in normotensive rat PRAs	127
4.4. Discussion	128
4.4.1. Vasodilator effect of U-II in human PRAs and SRAs	128

4.4.2. Mediators involved in the hU-II-induced vasodilatation in human PRAs	129
4.4.3. Possible pathophysiological role of hU-II	131
4.5. Conclusion	132

Chapter 5: The effect of mixed ET_A/ET_B antagonists in the treatment of human PHT secondary to left ventricular dysfunction

5.1.1. Endothelin structure	134
5.1.2. Endothelin biosynthesis and expression	134
5.1.3. Endothelin receptors	136
5.1.4. Endothelin action	138
5.1.5. Role of endothelin in chronic heart failure	140
5.1.6. Role of endothelin in pulmonary hypertension	141
5.1.7. Endothelin receptor second messenger systems	142
5.1.8. Another endothelin receptor subtype	144
5.1.9. Characterisation of endothelin receptors	147
5.1.10. Chronic heart failure and secondary PHT	149
5.1.11. ET antagonists in heart failure	151
5.1.12. Novel mixed ET _A /ET _B antagonists	154
5.2. Methods:	156
5.2.1. <i>In vivo</i> study	156
5.2.2. <i>In vitro</i> study	157
5.3. Results:	159
5.3.1. <i>In vivo</i> study	159
5.3.2. <i>In vitro</i> study	
5.3.2.1. Comparison of ET-1 response between groups	161
5.3.2.2. The effect of mixed ET _A /ET _B antagonists in the control group	165
5.3.2.3. The effect of mixed ET _A /ET _B antagonists in the good group	168
5.3.2.4. The effect of mixed ET _A /ET _B antagonists in the moderate group	171
5.3.2.5. The effect of mixed ET _A /ET _B antagonists in the poor group	174
5.4. Discussion:	177
5.4.1. <i>In vivo</i> study	177
5.4.2. <i>In vitro</i> study	
5.4.2.1. Comparison of ET-1 response between different patient groups	178
5.4.2.2. Effect of the mixed ET _A /ET _B antagonists	179
5.5. Conclusion	182

Chapter 6: The effect of mixed ET_A/ET_B antagonists in the treatment of hypoxia-induced PHT using the chronic hypoxic rat model

6.1.1. Introduction	184
6.1.2. ET-1 in PHT	184
6.1.3. Effect of chronic hypoxia on ET-1 response	184
6.1.4. ET receptors in control and chronic hypoxic rat PRAs	185
6.1.5. Novel mixed ET _A /ET _B antagonists	185
6.2. Methods	187
6.3. Results	189
6.3.1. Development of PHT	189
6.3.2. Control rat PRAs in the presence of the mixed ET _A /ET _B antagonists	190
6.3.3. Chronic hypoxic rat PRAs in the presence of the mixed ET _A /ET _B antagonist, SB 247083	193
6.3.4. Chronic hypoxic rat PRAs in the presence of the mixed ET _A /ET _B antagonist, SB 234551	197
6.3.5. Chronic hypoxic rat PRAs in the presence of the mixed ET _A /ET _B antagonist, SB 217242	201
6.3.6. Comparison of control and chronic hypoxic rat PRAs	205
6.4. Discussion:	207
6.4.1. Comparison of control and chronic hypoxic rat PRAs	207
6.4.2. Control normotensive rat PRAs	208
6.4.3. Chronically hypoxic rat PRAs	209
6.5. Conclusion	212

Chapter 7: General Discussion

7.1. Role of ET-1 in PHT	214
7.2. The mediators of ACh-induced vasodilatation: effect of chronic hypoxia	216
7.3. The vasodilator role of hU-II in the pulmonary circulation	218
7.4. Regulation of pulmonary vascular tone	220
7.5. Conclusion	222

Chapter 8: References 223

List of figures

Chapter 1:

- Figure 1.1** Diagram of the structure of a classic elastic artery
Figure 1.2 Muscularisation of the precapillary arterioles in rat lung in the presence of PHT
Figure 1.3 Diagrammatic representation of the pulmonary vascular tree

Chapter 2:

- Figure 2.1** Schematic diagram of 500A model of Mulvaney / Halpern wire myograph
Figure 2.2 Diagram of the left lobe of the rat lung
Figure 2.3 Diagram of the mounting procedure for pulmonary and systemic resistance arteries
Figure 2.4 Diagrammatic representation of hypobaric chamber
Figure 2.5 Diagram of the heart

Chapter 3:

- Figure 3.1** Vasodilator response to ACh in control and chronic hypoxic Wistar rat PRAs (graph)
Figure 3.2 Vasodilator response to ACh in the control Wistar rat PRAs in the presence and absence of various vasodilator inhibitors (graph)
Figure 3.3 Vasodilator response to ACh in the hypoxic Wistar rat PRAs in the presence and absence of various vasodilator inhibitors (graph)

Chapter 4:

- Figure 4.1** Amino acid sequences for (a) goby; (b) human; (c) porcine U-II. The predicted sequence for (d) mouse U-II
Figure 4.2 Vasodilator response to hU-II in the control human small PRAs in the presence and absence of various vasodilator inhibitors (graph)
Figure 4.3 Vasodilator response to hU-II and porcine U-II in the control human small PRAs (graph)
Figure 4.4 Vasodilator response to hU-II in the control human small PRAs in the presence and absence of 1 μ M indomethacin (graph)
Figure 4.5 Vasodilator response to hu-II in the control human small PRAs in the presence and absence of 0.1 μ M apamin and charybdotoxin (graph)
Figure 4.6 Vasodilator response to hu-II and porcine U-II on human abdominal adipose tissue small SRAs (graph)

Chapter 5:

- Figure 5.1** Amino acid heterogeneity of the endothelin isoforms, in their 21 amino acid sequence, from various species
- Figure 5.2** The vasoconstrictor response to ET-1 in the human small PRAs of the various LVF groups (graph)
- Figure 5.3** The vasoconstrictor response to ET-1 in the human small PRAs in the presence and absence of 1 μ M of a mixed ET_A/ET_B antagonist in the control group (graph)
- Figure 5.4** The vasoconstrictor response to ET-1 in the human small PRAs in the presence and absence of 1 μ M of a mixed ET_A/ET_B antagonist in the good LVF group (graph)
- Figure 5.5** The vasoconstrictor response to ET-1 in the human small PRAs in the presence and absence of 1 μ M of a mixed ET_A/ET_B antagonist in the moderate LVF group (graph)
- Figure 5.6** The vasoconstrictor response to ET-1 in the human small PRAs in the presence and absence of 1 μ M of a mixed ET_A/ET_B antagonist in the poor LVF group (graph)

Chapter 6:

- Figure 6.1** Contractile response to ET-1 in the presence and absence of 1 μ M of the mixed ET_A/ET_B antagonists in normotensive Wistar rat PRAs (graph)
- Figure 6.2** Contractile response to ET-1 in the presence and absence of 1, 0.3, and 0.1 μ M of the mixed ET_A/ET_B antagonists, SB 247083, in chronic hypoxic Wistar rat PRAs (graph)
- Figure 6.3** Contractile response to ET-1 in the presence and absence of 1, 0.3, and 0.1 μ M of the mixed ET_A/ET_B antagonists, SB 234551, in chronic hypoxic Wistar rat PRAs (graph)
- Figure 6.4** Contractile response to ET-1 in the presence and absence of 1, 0.3, and 0.1 μ M of the mixed ET_A/ET_B antagonists, SB 217242, in chronic hypoxic Wistar rat PRAs (graph)

List of publications

MacLean, M.R., Alexander, D., Stirrat, A., Gallagher, M., Douglas, S.A., Ohlstein, E.H., Morecroft, I. & Pollard, K. (2000) Contractile responses to human urotensin-II in rat and human pulmonary arteries: effect of endothelial factors and chronic hypoxia in the rat. *Br. J. Pharmacol.*, **130**, 201-204.

Stirrat, A., Gallagher, M., Douglas, S.A., Ohlstein, E.H., Berry, C., Richardson, M. & MacLean, M.R. (2001) Potent vasodilator responses to human urotensin-II in human pulmonary and abdominal resistance arteries. *Am. J. Physiol.*, **280**, H925-H928.

List of abbreviations

Acetylcholine (ACh)

Adenosine triphosphate (ATP)

Adenylate cyclase (AC)

ATP-activated potassium channels (K_{ATP})

4-aminopyridine (4-AP)

Calcium (Ca^{2+})

Calcium activated potassium channels (K_{Ca})

Cardiac index (CI)

Cardiac output (CO)

Charybdotoxin (ChTX)

Chronic heart failure (CHF)

Chronic hypoxia (CH)

Classic elastic artery (CE)

Cumulative concentration response curve (CCRC)

Cyclic adenosine 3'5' monophosphate (cAMP)

Cyclic guanosine 3'5' monophosphate (cGMP)

Cyclo-oxygenase (COX)

Diacyl glycerol (DAG)

Endothelium-derived contracting factor (EDCF)

Endothelium-derived hyperpolarizing factor (EDHF)

Endothelial nitric oxide synthase (eNOS)

Endothelin-1 (ET-1)

Endothelin converting enzyme (ECE)

Food and Drug Administration (FDA)

Guanosine triphosphate (GTP)

Guanylate cyclase (GC)

Human urotensin-II (hU-II)

Hydrogen peroxide (H₂O₂)

5-Hydroxytryptamine (5-HT)

5-Hydroxytryptamine transporter (5-HTT)

Hypoxic pulmonary vasoconstriction (HPV)

Inositol triphosphate (IP₃)

Intracellular calcium concentration ($\{Ca^{2+}\}_i$)

Left ventricular dysfunction (LVD)

Left ventricular end diastolic pressure (LVEDP)

Left ventricular function (LVF)

Mean pulmonary arterial pressure (MPAP)

Mitochondrial electron transport chain (mitochondrial ETC)

Myosin light chain kinase (MLCK)

Nitric oxide (NO)

Nitric oxide synthase (NOS)

Non-muscular artery (NM)

Ordinary muscular artery (OM)

Partially muscular artery (PM)

Phosphatidylinositol diphosphate (PIP₂)

Phosphodiesterase (PDE)

Phospholipase C (PLC)

Potassium (K⁺)

Potassium current (I_k)

Prostacyclin (PGI₂)

Prostaglandin E₂ (PGE₂)

Protein kinase A (PKA)

Protein kinase G (PKG)

Pulmonary artery smooth muscle cell (PASMC)

Pulmonary hypertension (PHT)

Pulmonary resistance arteries (PRAs)

Pulmonary vascular resistance (PVR)

Reactive oxygen species (ROS)

Renin-angiotensin-aldosterone system (RAAS)

Right ventricular/ left ventricular + septum ratio (R.V./L.V. + S)

Sarafotoxin (STX_{s6c})

Sarcoplasmic reticulum (SR)

Cu, Zn Superoxide dismutase (SOD)

Systemic resistance arteries (SRAs)

Systemic vascular resistance (SVR)

Tetraethylammonium (TEA)

Total peripheral resistance (TPR)

Transforming growth factor-β (TGF-β)

Transitional elastic artery (TE)

Urotensin-II (U-II)

Voltage-dependent calcium channels (VDCC)

Voltage-gated potassium channels (K_v)

Vascular smooth muscle cell (VSMC)

World health organisation (WHO)

Summary

Pulmonary hypertension (PHT) is a chronic and progressive condition, which can result in right ventricular failure, and, eventually death. There are two main categories of PHT: primary and secondary PHT. Primary PHT is idiopathic in origin, however, recent studies have suggested a genetic basis for the condition. Secondary PHT occurs as a result of pre-existing lung or heart disease, such as chronic obstructive pulmonary disease or chronic heart failure due to left ventricular dysfunction. PHT, regardless of aetiology, is resistant to commonly used antihypertensive therapies which successfully manage systemic hypertension. This lack of therapeutic effect of existing treatments results from the differences between the pulmonary and systemic circulations. These variations account for the differences in mean arterial pressures, total peripheral resistances, and responses to hypoxia observed in the pulmonary and systemic resistances. Investigation into the unique properties of pulmonary arteries could provide the focus for novel antihypertensive treatments which would be therapeutically beneficial in the pulmonary circulation without causing hypotension of the systemic circulation. As the pulmonary resistance arteries (PRAs) are the primary site of increased peripheral resistance through vascular remodelling, these are the vessels studied throughout this thesis using the small vessel technique of wire myography. Therefore, this thesis investigates the response to, the receptors mediating, and signalling pathways involved in the effect of various endogenous vasoactive substances found in the pulmonary circulation in the PRAs of various species using an *in vitro* pharmacological approach, and also investigated whether these parameters change in the presence of secondary PHT of different aetiologies.

The vasodilator response to acetylcholine (ACh) was investigated in the hypobaric chronic hypoxic rat model of secondary PHT. The maximum vasodilator response to ACh was significantly increased in the PRAs of chronic hypoxic rats when compared to normoxic control rats. The presence of hypoxia-induced PHT influenced the mediator profile responsible for the ACh-induced vasodilatation. In control rat PRAs, the ACh-induced vasodilator response appears to be mediated by endothelium-derived hyperpolarising factor (EDHF) via small and large Ca^{2+} -activated K^+ channels (SK_{Ca} and BK_{Ca} , respectively). In chronic hypoxic rat PRAs, the ACh-induced vasodilatation was mediated by nitric oxide (NO), prostacyclin (PGI_2), and EDHF. However, the involvement of EDHF in the ACh-induced vasodilator response requires confirmation through the use of electrophysiology.

The novel vasoconstrictor peptide human urotensin-II (hU-II) was shown to only elicit vasoconstriction in 30% of human PRAs in the presence of the NO synthase (NOS) inhibitor, L-NAME. However, hU-II was revealed as a vasodilator of human pulmonary and systemic resistance arteries (SRAs) which was equipotent with another potent endogenous vasodilator peptide, adrenomedullin. The hU-II-induced vasodilatation was shown to be mediated by PGI_2 and EDHF via BK_{Ca} and SK_{Ca} channels. Again, the involvement of EDHF in the hU-II-induced vasodilator response awaits confirmation through electrophysiological studies.

The *in vivo* and *in vitro* response to endothelin-1 (ET-1) was investigated in the PRAs of patients with different severities of left ventricular dysfunction (LVD), using PRAs from patients undergoing lung resection for bronchial carcinoma as controls. The LVD patients groups were classified according to their ejection fraction, as assessed

by echocardiographic assessment. The patients were divided into the following groups: an ejection fraction (EF) of >40% = good LVD; an EF of 30-40% = moderate LVD; and an EF of <30% = poor LVD. The *in vivo* experiments (which were not conducted by myself) showed a significant increase in the baseline measurement of pulmonary vascular resistance (PVR) between the good and poor groups, demonstrating the development of PHT as a consequence of severe LVD. The *in vitro* experiments revealed no significant increase in the potency of, or maximum contractile response to, ET-1 as the severity of LVD progressed. Three novel mixed ET_A/ET_B antagonists significantly decreased the potency of, and attenuated the maximum contractile response to, ET-1 in all patient groups. Therefore, the mixed ET_A/ET_B antagonists could prove to be therapeutically beneficial in the treatment of PHT secondary to chronic heart failure.

The response to ET-1 was investigated in the presence and absence of three novel mixed ET_A/ET_B antagonists in the hypobaric chronic hypoxic rat model. The maximum contractile response to, and potency of, ET-1 was significantly increased in the PRAs from the chronic hypoxic rat when compared to control rat PRAs.

The three mixed ET_A/ET_B antagonists significantly decreased the potency of ET-1 in the chronic hypoxic rat PRAs, but had no effect on control rat PRAs. Therefore, the mixed ET_A/ET_B antagonists could be an effective treatment for hypoxia-induced PHT.

These studies show that PHT of different aetiologies results in an increase in pulmonary vascular tone due, in part, to an imbalance of endogenous vasoconstrictor (ET-1) and vasodilator (hU-II and ACh) action. Therefore, readdressing this balance may result in the development of new treatments for PHT of different aetiologies.

Chapter 1

Introduction

1.1. The need for research:

Pulmonary hypertension is a chronic condition, existing most commonly as a secondary condition resulting from pre-existing lung and heart disease, but can also exist as a primary disease. Pulmonary hypertension (PHT) is a condition for which there is no effective cure as yet. Existing treatments are of little therapeutic value as they fail to exploit the differences between the pulmonary and systemic circulations. These variations result in treatment for PHT being of limited clinical use in the pulmonary circulation and the creation of side effects in the systemic circulation.

1.2. Histology of blood vessels:

Arteries are the blood vessels that carry oxygenated blood to peripheral tissues from the heart via the systemic circulation. However, the arteries of the pulmonary circulation differ from the systemic arteries as they deliver deoxygenated blood from the heart to the lungs where gaseous exchange occurs to re-oxygenate the blood. Despite this major difference in the oxygen content of the blood carried by systemic and pulmonary arteries, their general structural composition is similar, although the pulmonary arteries are structurally and functionally adapted to their specific role (Tortora, 1992; Ross & Rommel, 1989).

Arterial walls are comprised of three distinct layers of tissues, the composition and relative thickness of these layers determine the class of artery being studied. The three distinct layers of an arterial wall are the *tunica intima*; the *tunica media*; and the *tunica adventitia*. Arteries are generally classed as large elastic arteries; medium muscular arteries; or small non-muscular arteries and arterioles. This classification is

rather general and, as will be demonstrated later, does not suffice when classifying pulmonary arteries.

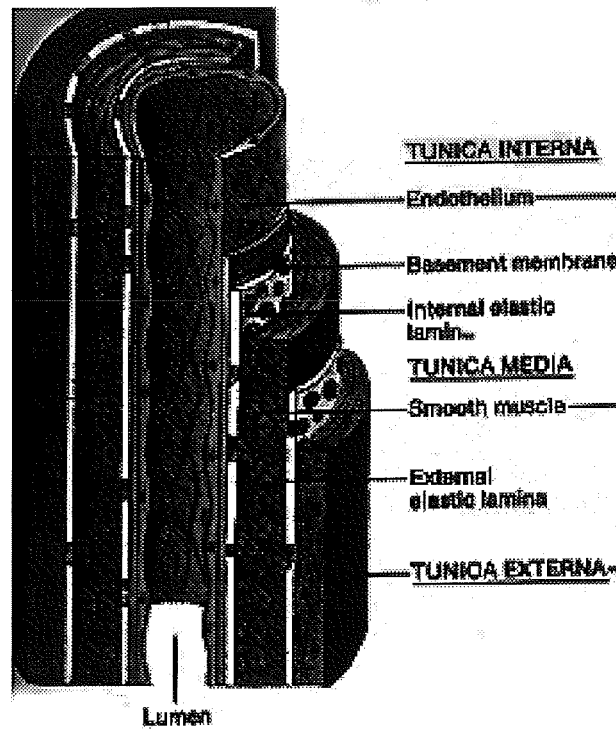


Figure 1.1: Diagram of the structure of a classic elastic artery. Illustration adapted from the Principles of human anatomy, sixth edition, Tortora G. J., Harper Collins, 1992.

The *tunica intima* is the innermost layer of the arterial wall with its surface forming the wall of the arterial lumen. This coat is further subdivided into three layers: the endothelium; the basement membrane; and the internal elastic lamina. The endothelium is the innermost layer of the *tunica intima* and is comprised of simple squamous epithelium joined by the *zona occludens* (tight junctions) and gap junctions. The endothelial cell is the site of receptor for many vasoactive substances such as

nitric oxide and endothelin. The tight junctions between the endothelial cells act as a barrier to substances in the blood which must diffuse through the endothelial cell or be moved via active transport by the pinocytotic vesicles within the cell in order to affect surrounding extravascular tissues. The middle layer of the *tunica intima* is the basal lamina consists of a thin layer of connective tissue which helps the endothelium perform its barrier function to substances in the blood. The outer layer of the *tunica intima* is the internal lamina which is comprised of elastic fibres (Tortora, 1992; Ross & Rommel, 1989).

The *tunica media* is the middle layer of the arterial wall. This layer is comprised of vascular smooth muscle cells and connective tissue cells in the form of collagenous and elastic fibres. The relative amounts of these two tissue types within the *tunica media* depends on the class of the artery that is being studied. The vascular smooth muscle cells in this layer are arranged in a spiral orientation, often with each muscle layer being separated by an elastic lamina. The smooth muscle cells are joined by gap junctions and the elastic laminae have fenestrations along their length. Both of these features contribute to the transport of substances by diffusion through the arterial wall. Sometimes, there is an external elastic lamina separating the *tunica media* from the *tunica adventitia* (Tortora, 1992; Ross & Rommel, 1989).

The *tunica adventitia* is the outermost layer of the arterial wall. This layer is comprised of connective tissue, especially collagenous and elastic fibres. The relative amounts of collagenous and elastic fibres is again dependent on the class of artery, but the *tunica adventitia* is usually principally comprised of collagenous fibres; fibroblasts; and macrophages. The *tunica adventitia* is itself supplied by small blood

vessels called the *vasa vasorum*, whereas the *tunica adventitia* is also the site of the arterial nerve innervation called the *nervi vascularis* (Tortora, 1992; and Ross & Rommel, 1989).

1.3. Classification of arteries:

The general composition of an artery has been discussed above. However, such a general look at the arterial wall structure is too simplistic as different sizes of arteries at different locations within the pulmonary arterial tree have subtle variations. The studies described in this thesis are conducted in rat and human vessels so all further discussion of arterial histology will be with regards to these pulmonary arteries. It is currently thought that there are six structurally distinct subtypes of pulmonary artery within two main categories, and that these structural differences form the basis of the varied response to numerous stimuli and their effect on pulmonary pressure (Brenner, 1935; and Sasaki *et al.*, 1995).

The first main category is the elastic artery, of which there are two subtypes. Both of these subtypes have a great mass of extracellular matrix consisting of collagenous and elastic fibres, interspersed with vascular smooth muscle cells and numerous elastic laminae in their *tunica media*'s. The phenotype of the vascular smooth muscle cells in this type of artery have copious amounts of cytoplasmic organelles and sparse actin filaments which would result in a weak smooth muscle cell contraction. The *tunica adventitia* of both subtypes of elastic artery is densely packed with collagenous and elastic fibres and was more substantial in width than the *tunica media* (Brenner, 1935; and Sasaki *et al.*, 1995).

The first of the elastic artery subtypes is known as the *classic elastic artery (CE)*. The concentric interleaved elastic laminae of the *tunica media* are very prominent and the vascular smooth muscle cell layers that they separate are arranged away from the circumferential axis, each layer with a slightly different orientation from the next layer. The internal and external laminae are also very pronounced in these arteries. The pulmonary arteries with CE morphology are the main pulmonary arteries; the left and right pulmonary artery branches; and the main interlobar arteries (Sasaki *et al.*, 1995).

The second of the elastic artery subtypes shares much of its morphology with the CE segments and is known as the *transitional elastic artery (TE)*. The TE segment differs from the CE segment in two ways. While the TE artery has many prominent elastic laminae in its *tunica media*, they are not interleaved and the vascular smooth muscle cell layers are orientated around the circumferential axis. The pulmonary arteries with TE morphology are the proximal half of the branches that come off of the interlobar artery (Sasaki *et al.*, 1995).

The second main category is the muscular artery, of which there are four subtypes. All of these subtypes have vascular smooth muscle cells which are densely packed with actin filament bundles to allow a strong contraction compared to the elastic arteries, and the smooth muscle cells are orientated around the circumferential axis (Brenner, 1935; and Sasaki *et al.*, 1995).

The first of the muscular artery subtypes is known as the *thick muscular artery (TM)*. The vascular smooth muscle cells of the TM segment often contain glycogen

aggregates to provide extra energy for contraction if needed. The *tunica media* of the TM segment is very thick as it is comprised of up to ten layers of densely packed vascular smooth muscle cells which are very sparsely interspersed by extracellular matrix. The *tunica adventitia* is not very substantial. The pulmonary arteries with TM morphology are the distal half of the branches of the interlobar artery in the rat and human lung biopsies. These are the type of vessels used in the rat and human studies in this thesis (100 - 250 μ M i.d.) (Sasaki *et al.*, 1995).

The second of the muscular artery subtypes is known as the *ordinary muscular artery* (OM). The *tunica media* of the OM segment is comprised of one or two layers of vascular smooth muscle cells with very little extracellular matrix interspersing the cells. The pulmonary arteries with OM morphology are very small arteries that branch off from the branches of the interlobar artery (Sasaki *et al.*, 1995).

The third of the muscular artery subtypes is known as the *partially muscular artery* (PM). The *tunica media* of the PM segment consists of one discontinuous layer of vascular smooth muscle cells. Where the *tunica media* of the PM segment has no smooth muscle cells, the internal and external laminae fuse and appear as one single elastic lamina. As the circumference of the PM artery decreases, the amount of vascular smooth muscle cell coverage decreases resulting in larger patches of non-muscular *tunica media*. The *tunica adventitia* of the PM segment is very thin. The pulmonary arteries with PM morphology are arterioles (Sasaki *et al.*, 1995).

The fourth and final muscular artery subtype is known as the *non-muscular artery* (NM). The *tunica media* of the NM segment does not contain any vascular smooth

muscle cells at all, the *tunica media* is comprised of immature smooth muscle cells (pericytes) instead. The *tunica adventitia* of the NM segment is so thin as to be virtually non-existent. The pulmonary arteries with NM morphology are the alveolar capillaries (Sasaki *et al.*, 1995).

The internal elastic lamina disappears gradually as we travel down the pulmonary arterial tree. The external elastic lamina also disappears gradually as you move down the tree, but there is a large attenuation in the extent of the external lamina between the TE and the TM segments and is virtually non-existent by the PM segment (Brenner, 1935; and Sasaki *et al.*, 1995).

1.4. Vascular smooth muscle cell phenotypes:

Studies have revealed four phenotypically distinct cell subpopulations simultaneously exist in the medial smooth muscle cell (SMC) layer of arteries from both the pulmonary and systemic circulations *in vivo* and *in vitro* (Frid *et al.*, 1994; Frid *et al.*, 1997). These cell subpopulations were isolated and characterised according to their expression of smooth muscle (SM) and cytoskeletal proteins, cell morphology, immunobiochemical characteristics, and responses to various growth-promoting stimuli and hypoxia (Frid *et al.*, 1994; Frid *et al.*, 1997). The four cell subpopulations can be separated into two broad categories: two smooth muscle cell subpopulations and two nonmuscle-like cell populations. These phenotypically distinct cell subpopulations are from specific layers of the *tunica media*: L1-cells were isolated from the subendothelial layer of the media, L2-SMCs were isolated from the middle layer, while L3-“S” SMCs and L3-“R” cells were isolated from the outer layer of the media. The two SMC subpopulations (L2 and L3-“S” cells) were characterised by

their expression of the SMC contractile proteins α -SM-actin and SM-myosin, slow growth in 10% serum and no growth in 10% plasma, no proliferation in response to hypoxia, and do not secrete mitogenic factors. The L3-“S” SMCs also expressed the cytoskeletal contractile protein, metavinculin. The two nonmuscle-like subpopulations (L1 and L3-“R” cells) were characterised by their lack of expression of SMC contractile proteins, exhibit fast growth in 10% serum and growth in 10% plasma, exhibit growth in response to hypoxia, and secrete mitogenic factors (Frid *et al.*, 1994; Frid *et al.*, 1997). However, despite the morphological and phenotypic differences between these four cell subpopulations, they all expressed the SMC contractile protein α -SM-actin during their development, revealing them as being SMCs. The cells then differentiate into the four distinct phenotypes, which suggests that these cells have distinct cell lineages (Frid *et al.*, 1994; Frid *et al.*, 1997). These findings suggest that these four cell subpopulations contribute in their own ways to vascular wall homeostasis in normal physiological and pathophysiological conditions.

It is unclear whether all of the cell subpopulations are equally involved in the pathobiology of human vascular diseases such as arteriosclerosis and hypertension, or if only specific subpopulations are involved in these pathophysiological processes. It has been postulated that the subpopulations of nonmuscle-like cells which exhibit increased proliferation in response to pathological stimuli, such as hypoxia and mitogenic factors may be involved in the intimal thickening which occurs during several vascular diseases (Frid *et al.*, 1997). It has been demonstrated that heparin inhibited the serum-stimulated growth of L1 cells. As a heparin-like substance has been shown to be released from endothelial and SMCs, the L1 cells are quiescent under normal physiological conditions. However, should vascular injury occur which

results in the decreased release of the heparin-like substance, the L1 cell subpopulation which exhibit increased proliferation in response to hypoxia and secretes mitogens, could be activated (Frid *et al.*, 1997). Therefore, the existence of four distinct cell subpopulations could allow the continuation of the normal contractile function of the media in response to pathophysiological stimuli while other subpopulations contribute to the pathophysiological process by undergoing increased proliferation (Frid *et al.*, 1997).

The distinct morphological diversity within the arteries of the pulmonary circulation probably account for the observed variations in the response to various physiological stimuli and in the potency and efficacy of numerous vasoactive substances. These observations substantiate the practice of viewing the pulmonary circulation as a series of unique arteries rather than as a whole uniform entity.

The rat vessels used in this study are rat and human pulmonary resistance arteries. These vessels have an internal diameter in the range of 100-250 μ m and have TM morphology.

1.5. Diversity in the pulmonary and systemic circulations:

The pulmonary circulatory system is a unique and integral part of the body. Its importance is born from the fact that without it, the cardiovascular system ceases to implement its functional role of oxygenated perfusion of blood to all body tissues resulting in brain-stem death from oxygen and glucose starvation (Goerke & Mines, 1988). The uniqueness of the pulmonary circulation system is due to the differences that exist between it and the systemic circulation both functionally and

pharmacologically. The pulmonary system is a low pressure system with a mean arterial pressure of 12-15mmHg while the systemic system has a mean arterial pressure of 95mmHg. Therefore, the pulmonary system is also a low resistance system compared to the systemic system. This functional difference is a result of the fact that pulmonary arteries have very little endogenous tone and are almost fully dilated in their resting state while the systemic arteries and arterioles are always slightly constricted and provide much of the total systemic resistance (Fishman, 1988; Goerke & Mines; 1988; MacLean, 1998). One of the most striking distinctions between the two circulatory systems is their response to hypoxia. The systemic arteries will dilate in low PO₂ causing a decrease in mean arterial pressure while the pulmonary arteries will constrict in response to low PO₂ resulting in an increase in mean arterial pressure and is known as hypoxia-induced pulmonary vasoconstriction (HPV) (Heath *et al.*, 1973; Fishman, 1976; Fishman, 1988; Dominiczak & Bohr, 1995; MacLean, 1998). HPV is a beneficial mechanism in healthy lungs that allows the alveoli that are being ventilated to selectively receive an increased blood supply in order to ensure maximisation of ventilation-perfusion matching in times of hypoxia. However, in lungs that already have compromised ventilation-perfusion matching due to pre-existing lung disease such as cystic fibrosis; lung cancer; or emphysema, the HPV mechanism only serves to exacerbate the existing PHT (MacLean *et al.*, 1993). Therefore, we can see that the pulmonary circulation merits separate consideration from the systemic circulation and by understanding the differences between the two systems, it may be possible to develop therapies which alleviate PHT without causing undesirable systemic hypotension.

1.6. The normal pulmonary circulation:

The normal healthy pulmonary circulation is very efficient at ventilation-perfusion matching. The normal circulation is mainly regulated by the concentration of oxygen O_2 and CO_2 found in the blood. Neurotransmitters and locally produced mediators also have an effect on the pulmonary circulation, but, the principal influences are the respiratory gases.

When a healthy adult is at rest, the oxygen requirement of the peripheral tissues (metabolic rate) is easily matched by cardiac output. During exercise, the metabolic requirement for O_2 increases causing a corresponding increase in cardiac output. The blood entering the tissue via the arteriole contains a much greater concentration of O_2 than the blood leaving the tissue via the venule, thus, increasing the arteriovenous O_2 difference. As the exercise increases the cardiac output, the volume of blood flowing through the lung also increases but rarely causes any increase in pulmonary pressure, even though the increase in blood volume occurs at the expense of gaseous exchange, as the pulmonary circulation recruits reserve vessels found near the apex of the lung and other vessels that are already open dilate slightly. However, a person with heart failure cannot match cardiac output to tissue O_2 requirement and finds that slight exertion such as walking upstairs can leave them fatigued (Fishman, 1988).

The pulmonary system is a low resistance system compared to the systemic system, resulting in a small driving pressure. This lack of resistance is due to the fact that the pulmonary arteries are almost maximally dilated in their natural resting state. The resistance that does exist in the system appears to originate in the small muscular pulmonary arteries, which have an internal diameter of approximately 100-10000 μm

and the arterioles with diameters of $<100\mu\text{m}$. These arteries appear to be the arteries that are the most capable of vasoconstriction, and, for that reason, are known as the small pulmonary resistance arteries (PRAs). The arteries used in this study are the small PRAs with an internal diameter in the range of approximately $100\text{-}250\mu\text{m}$ (Fishman, 1988).

As previously mentioned, the pulmonary circulation is a low pressure system. The mean arterial pressure in a healthy adult is $12\text{-}15\text{mmHg}$, about an eighth of the mean systemic arterial pressure. As the mean left atrial pressure is $5\text{-}10\text{mmHg}$, there is only a very small drop in pressure across the whole pulmonary circulation from pulmonary artery to the left atrium. The small pressure drop that exists in the system appears to occur in the pulmonary capillaries which surround the alveoli and are the site of gaseous exchange. In order to carry out *in vitro* isolated vessel experiments in near physiological conditions, it is essential to set the vessels up with a transmural pressure equivalent to that which they experience *in vivo*. The transmural pressure is calculated by measuring the difference between the luminal and pleural pressure (Fishman, 1988). In the small muscular PRAs of $100\text{-}250\mu\text{m}$ in diameter used in this study, the transmural pressure is 16mmHg (Herget *et al.*, 1978; MacLean & M^cCulloch, 1998).

The volume of blood in the healthy pulmonary circulation at any given time is about a tenth of the total circulating blood volume. Any increase in the pulmonary blood volume would occur at the expense of air volume. Therefore, patients with congestive heart failure would eventually also have a decreased vital lung capacity. Patients with systemic hypertension are also at risk of having a decreased vital

capacity as systemic vasoconstriction displaces blood back into the pulmonary circulation. The pulmonary blood volume appears to be evenly distributed throughout the pulmonary circulation (Fishman, 1988).

The pulmonary arteries are constricted in response to a decrease in inspired PO_2 . This condition is known as hypoxia-induced pulmonary vasoconstriction (HPV), and is an important mechanism in ventilation-perfusion matching. This HPV occurs mainly in the small muscular PRAs and arterioles. The mechanism by which a low PO_2 elicits pulmonary vasoconstriction has yet to be fully elucidated, but many believe there to be a pharmacological mediator released in response to hypoxia which acts as a potent vasoconstrictor (Fishman, 1988; and Barnes & Liu, 1995). The theories underlying the mechanism of HPV are discussed in more detail later.

When the PCO_2 concentration of pulmonary arterial blood increases (hypercapnia) to a point which lowers the pH of the blood to less than 7.2 (acidosis), the HPV mechanism is stimulated. Hypercapnia that does not cause acidosis can synergistically enhance hypoxia-induced pulmonary vasoconstriction (Fishman, 1988).

1.7. Regulation of pulmonary vascular tone:

Regulation of the pulmonary circulation is not only influenced by mechanical stimuli, it is also influenced by pharmacological mediators and neurotransmitters.

In normal healthy adults living at sea level, the small PRAs are almost fully dilated and have little endogenous tone. This lack of endogenous tone could be due, in part,

to a preferential release of vasodilator mediators such as PGI₂ and NO. In this state, any additional release of vasodilators would make little difference to the tone. In normal healthy people living at high altitude, the small PRAs have a greater degree of endogenous tone. This increase in tone could be due in part, to a preferential release of vasoconstrictor agents such as endothelin or catecholamines (Fishman, 1988).

Both the sympathetic and parasympathetic nervous systems influence the systemic circulation, but, only the sympathetic nervous system appears to influence the pulmonary circulation (Fishman, 1988; and Goerke & Mines, 1988). Sympathetic nerve innervation activates both α - and β -adrenoceptor activation, with α -adrenoceptor activation causing vasoconstriction and β -adrenoceptor activation causing vasodilatation. As the small PRAs are normally fully dilated, sympathetic innervation usually results in vasoconstriction (Fishman, 1988; and Barnes & Liu, 1995).

There are also many mediators which can elicit vasodilatation in the pulmonary circulation. The vasodilator effects of these mediators, when administered exogenously, are very slight in the normal dilated pulmonary arteries, but, in those with PHT due to altitude or disease, where there is a significant increased vascular tone, the effects of the vasodilators are increased. Isoprenaline causes a vasodilatation by activating β_2 -adrenoceptors in the pulmonary arteries. Vasopressin causes vasodilatation in pre-contracted vessels via V₁ receptors. ANP vasodilates the pulmonary arteries via the ANP_A and ANP_B receptors. When the tone of the arteries is high, adenosine and ATP cause vasodilatation via the A₂ and P_{2y} receptors respectively. Acetylcholine activates NO production, which stimulates cGMP

production resulting in vasodilatation. There are also a few vasodilator prostaglandins. PGI₂ and PGE₁ cause vasodilatation via the IP and EP₂ receptors respectively. Bradykinin generally elicit a vasodilatation in the pulmonary arteries mediated mainly by the stimulated release of PGI₂ and NO, and by direct action of B₁ and/or B₂ receptors (Su & Bevan, 1976; Fishman, 1988; Barnes & Liu, 1995; Rang *et al.*, 1995). Endothelin-1 can mediated a transient vasodilatation by stimulating the production and release of PGI₂ and NO via the ET_B receptor (Rubyani & Polokoff, 1994). Shear stress causes vasodilatation also by stimulating production and release of NO (Barnes & Liu, 1995).

As well as causing PHT by eliciting vasoconstriction, several endogenous mediators have a mitogenic effect causing proliferation of the pulmonary vascular smooth muscle cells e.g. angiotensin-II, 5-HT and ET-1 (Rubyani & Botelho, 1991; Rubyani & Polokoff, 1994; Barnes & Liu, 1995).

1.8. Pulmonary hypertension:

The mean pulmonary arterial pressure of a normal adult at sea level is 12mmHg-15mmHg (25/10mmHg). When the mean pulmonary arterial pressure increases from 15 to 25mmHg (35/15mmHg), the person at sea level is classed as having PHT. However, adults native to high altitude (above 7000-8000ft) have a mean pulmonary arterial pressure of 25mmHg as normal (Fishman, 1988).

There are five main diagnostic classes, and four functional classes, of pulmonary hypertension (PHT). The models of PHT used in this thesis are characterised as resulting from left-sided atrial or ventricular heart disease (class 2.1 in World Health

Organisation [WHO] classification) and chronic high-altitude exposure (class 3.5 in WHO classification) (WHO website, 2002). Primary PHT (class 1.1 in WHO classification) is a disease that is usually idiopathic in origin and occurs in isolation from other disease (Fauzi, 2000; WHO website, 2002). However, secondary PHT arises as a consequence of another, pre-existing disease such as cardiac disease (classes 2.1 and 2.2) or other chronic obstructive pulmonary disease (class 3.1) such as cystic fibrosis or emphysema (WHO website, 2002). Despite the differences in origin of the two classes of PHT, the sustained pulmonary arterial pressure experienced by sufferers is caused by an increase in endogenous tone and increase in the proliferation of, and changes in the phenotype of, vascular smooth muscle cells of the small PRAs. These changes result in pulmonary vascular remodelling causing narrowing of the lumen, leading to an increase in vascular resistance and pressure. Prolonged PHT will result in *cor pulmonale*, when the right atrium becomes hypertrophied and dilated. As PHT and *cor pulmonale* progress, the right atrium will eventually fail, as a consequence of the increase in pulmonary arterial pressure and increased after-load on the right atrium experienced in PHT (Heath *et al.*, 1973; Fishman, 1976; Herget, 1978; Fishman, 1988).

PHT is characterised by a thickening of the muscular *tunica media* of medium sized PRAs (300-1000µm i.d.) and a progressive muscularisation of the previously non-muscular small PRAs (<300µm i.d.) from lung apex to base.

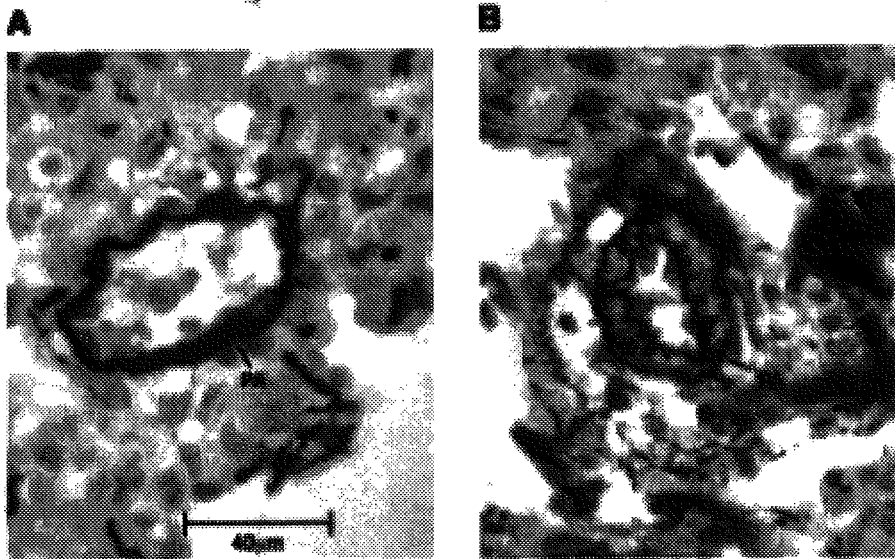


Figure 1.2: Muscularisation of the precapillary arterioles in rat lung in the presence of PHT. **A.** Normal rat lung with very little smooth muscle. **B.** Lungs of rat exposed to 2 weeks of hypobaric hypoxia resulting in the development of PHT. Illustration adapted from MacLean *et al.*, 2000.

As the phenotype of the vascular smooth muscle cell changes from immature pericyte to mature myocyte at a given site in the pulmonary vascular tree, the reactivity of the vessel to physical stimuli also alters due to the different K^+ channels, receptor populations, and contractile proteins in these cell phenotypes (MacLean, 1998). PRAs with a *tunica media* containing mature vascular smooth muscle cells, undergoes proliferation resulting in a thickening of the *media*. PRAs that previously had a *media* comprised of pericytes become muscularised. The stimulus for this vascular remodelling has yet to be elucidated. Hypoxia has been shown to elicit pulmonary vasoconstriction and vascular remodelling, yet the mechanism producing these effects has also eluded explanation so far. We do know that chronic hypoxia is associated with PHT. However, there are two theories on the mechanism underlying this

phenomenon: the **direct effect** theory and the **indirect effect** theory (Fishman, 1976; Fishman, 1988).

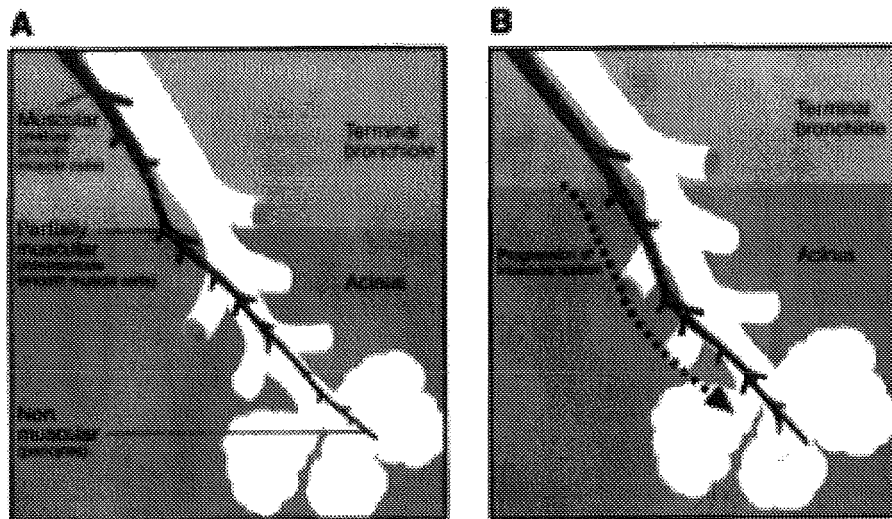


Figure 1.3: Diagrammatic representation of the pulmonary vascular tree. **A.** In the normal lung in which mature SMCs give way to immature SMCs as the vessel size decreases before petering out in the precapillary vessels. **B.** The pulmonary hypertensive lung exhibits progressive muscularisation into the normally non-muscular precapillary vessels as a result of hyperplasia and redistribution of SMC phenotypes. Illustration adapted from MacLean *et al.*, 2000.

1.9. Hypoxic pulmonary vasoconstriction:

The arteries of the pulmonary circulation have a unique response to low oxygen levels. The pulmonary artery smooth muscle myocytes contract in response to low oxygen tensions, while smooth muscle myocytes from a systemic artery relaxes in these conditions. Therefore, the pulmonary circulation undergoes vasoconstriction and the systemic circulation undergoes vasodilatation in low PO_2 conditions. This

vasoconstriction of the pulmonary circulation is known as ‘hypoxic pulmonary vasoconstriction (HPV)’ and is a very important physiological mechanism in this system (Sweeney & Yuan, 2000; Coppock *et al.*, 2001; Sylvester, 2001; Waypa *et al.*, 2001). The primary site of HPV is the small muscular pulmonary resistance arteries (PRAs) as the main and left and right branches of the pulmonary artery either do not respond or dilate slightly in response to low O₂ levels (Coppock *et al.*, 2001). The varied response to hypoxia between the pulmonary and systemic arteries and between the large conduit pulmonary arteries and the PRAs may be due to differences in the way myocytes from these loci sense O₂ or differential expression of O₂-sensitive ion channels. HPV has two phases, a transient contraction (phase 1) superimposed on a sustained contraction (phase 2) (Leach *et al.* 2001). It has been observed that glucose is necessary for the production of phase 2 of HPV as the inhibition of glycolysis inhibits the phase 2 component of HPV (Leach *et al.*, 2001). Further evidence to support this **direct effect** theory of HPV comes from the pulmonary vascular response to another physiological stimulus, hypercapnia. Acute hypercapnia can induce pulmonary vasoconstriction alone if the PCO₂ is sufficient to cause acidosis, or can synergistically augment vasoconstriction during hypoxia (Fishman, 1976; Fishman, 1988).

As the role of the lungs is to oxygenate the blood which then feeds the rest of the tissues, it is vital to maintain a good ventilation-perfusion matching ratio by diverting blood to areas of lung with good alveolar levels of O₂ where efficient gaseous exchange can occur (Sweeney & Yuan, 2000; Coppock *et al.*, 2001). The mechanism ensures blood reaches only well-ventilated alveoli is HPV. In healthy subjects, HPV

is beneficial in diverting blood away from any small areas of the lung where the alveoli are under-ventilated (Sweeney & Yuan, 2000; Coppock *et al.*, 2001). HPV can protect the physiological mechanism of ventilation-perfusion matching during cases of acute hypoxia, as seen in patients experiencing an asthma attack (Sweeney & Yuan, 2000; Coppock *et al.*, 2001). In the foetus, HPV is also the mechanism that allows blood to be diverted through the ductus arteriosus, bypassing the lungs as gaseous exchange is conducted through the placenta (Sweeney & Yuan, 2000). However, the nature of HPV becomes pathophysiological rather than protective in nature when there is sustained widespread hypoxia of the lungs, for example, in the presence of chronic obstructive pulmonary disease or in those living at high altitude (Sweeney & Yuan, 2000; Coppock *et al.*, 2001). In these cases, HPV only serves to make matters worse by causing a sustained vasoconstriction of the pulmonary circulation which leads to PHT and vascular remodelling. If these conditions are sustained for long enough, the PHT may progress, leading to right ventricular hypertrophy and a poor prognosis (Sweeney & Yuan, 2000; Coppock *et al.*, 2001). Therefore, understanding the mechanism of HPV could lead to new treatments for PHT.

Previous studies into the mechanism(s) underlying HPV have been conducted in the intact animal, isolated lungs, individual isolated vessels (endothelium-intact and –denuded), and pulmonary artery smooth muscle cells (PASMCs) and have shown contraction in all preparations in response to hypoxia. These results revealed that everything required for HPV is found intrinsically in the PASMC and that the endothelial layer of the pulmonary arteries are not required for the initiation of HPV (Sweeney & Yuan, 2000; Coppock *et al.*, 2001; Leach *et al.*, 2001; Sylvester, 2001;

Waypa *et al.*, 2001). However, the endothelium can modulate HPV by releasing either vasodilator endothelial factors (nitric oxide or prostacyclin) or vasoconstrictor factors (endothelin-1 or thromboxane A₂). It has been suggested that the release of endothelin-1 from the endothelium 'primes' the contractile machinery of the PASMC to HPV by increasing the Ca²⁺-sensitivity of the cell and by partially depolarising the membrane causing an increase in the intracellular Ca²⁺ concentration by allowing Ca²⁺ to enter the cell via voltage-gated Ca²⁺ channels (Sweeney & Yuan, 2000; Sylvester, 2001).

Many aspects of HPV are still under debate, such as the identity of the O₂ sensor and the pathways which mediate the vasoconstriction after low O₂ level has been sensed. However, it is now widely accepted that an increase in intracellular / cytosolic Ca²⁺ concentration ([Ca²⁺]_i) is the main mechanism underlying the contraction of the PRAs during HPV (Sweeney & Yuan, 2000; Coppock *et al.*, 2001; Leach *et al.*, 2001; Sylvester, 2001). The Ca²⁺ channel blocker, verapamil, inhibited HPV in isolated lung preparations and intact animals (Sweeney & Yuan, 2000). A current hypothesis is that hypoxia, sensed by an as yet unknown O₂ sensor, mediates the release of Ca²⁺ from the sarcoplasmic reticulum (SR) which causes an influx of Ca²⁺ into the cytosol from Ca²⁺ stores. This modulates the activity of the ion channels in the vascular smooth muscle cell (VSMCs) membrane leading to depolarisation of the membrane which causes the opening of voltage-gated Ca²⁺ channels (L-type channels). This further increases [Ca²⁺]_i leading to activation of the Ca²⁺-calmodulin complex which activates myosin light chain kinase causing contraction of the myocyte (Sweeney & Juan, 2000; Coppock *et al.*, 2001; Leach *et al.*, 2001; Sylvester, 2001; Waypa *et al.*,

2001). The increase in $[Ca^{2+}]_i$ may also be the trigger for the increased myocyte proliferation observed in chronic hypoxia (Sweeney & Yuan, 2000). In support of this theory, hypoxia has been shown to depolarise isolated arteries and PASMCs, the depolarisation of PASMCs by hypoxia was typically 15 – 20mV (Coppock *et al.*, 2001). The L-type channel blocker, verapamil, reduced the hypoxic response in isolated lung preparations (Sweeney & Yuan, 2000). These studies revealed that depolarisation of the PASMC membrane is a necessary requirement for HPV.

Some studies have proposed that the step between the release of Ca^{2+} from intracellular stores and the membrane depolarisation which allows the opening of L-type Ca^{2+} channels causing an increase in $[Ca^{2+}]_i$ is the inhibition of voltage-gated K^+ channels (Sweeney & Yuan, 2000; Coppock *et al.*, 2001; Sylvester *et al.*, 2001).

There are three different classes of K^+ channels present in VSMCs: ATP-activated K^+ channels (K_{ATP}), Ca^{2+} -activated K^+ channels (K_{Ca}), and voltage-gated K^+ channels (K_V). All three channel types are thought to be involved in the production of the K^+ current (I_K) which regulates the basal membrane potential and, therefore, regulates the basal tone of the pulmonary arteries (Evans *et al.*, 1996; Barman, 1998; Sweeney & Yuan, 2000; Coppock *et al.*, 2001). As the K_V channel blocker 4-aminopyridine (4-AP) caused a significant partial inhibition of the total I_K in the PASMC, the K_V channels are the main, but not the only, channels through which the I_K flows to regulate the low basal tone of pulmonary arteries (Sweeney & Yuan, 2000; Coppock *et al.*, 2001).

It has been shown that K_V channels are homo or heteromultimeric tetramers that are comprised of two different types of subunits, the membrane-spanning α -subunits

which form the pore of the channel and the outer β -subunits which regulate the activity of the channel (Sweeney & Yuan, 2000; Coppock *et al.*, 2001).

There are four subfamilies of genes which encode functional K_V channel α -subunits. These families are K_{V1} , K_{V2} , K_{V3} , and K_{V4} . There have been four subfamilies of electrically silent K_V channel α -subunits cloned. These families are K_{V5} , K_{V6} , K_{V8} , and K_{V9} . The electrically silent α -subunits must be co-expressed with a functional α -subunit in order to form a functional channel (Sweeney & Yuan, 2000; Coppock *et al.*, 2001). The electrically silent α -subunit modulates the properties of the K_V channels that they make up by determining the speed of activation and inactivation, voltage-dependence, and expression levels of the K_V channels (Sweeney & Yuan, 2000). The α -subunits $K_{V1.2}$, $K_{V1.5}$, $K_{V2.1}$, $K_{V3.1}$, $K_{V4.2}$, and $K_{V9.3}$ are proposed as the α -subunits which form O_2 -sensitive K^+ channels. A role for K_V channels in the O_2 sensing mechanism in O_2 -sensitive cells, such as neuroepithelial cells and cells of the aortic and carotid bodies (Sweeney & Yuan, 2000). However, these α -subunits are also expressed in VSMCs from systemic arteries yet systemic arteries dilate in response to hypoxia (Sweeney & Yuan, 2000; Coppock *et al.*, 2001). As there have been no qualitative differences in the α -subunits from these different circulations, the reason for the differential response to hypoxia in the pulmonary and systemic systems has yet to be elucidated.

There are three subfamilies of K_V channel β -subunits identified in mammalian VSMCs. These families are K_{V1} , K_{V2} , and K_{V3} . The β -subunits also modulate the properties of the K_V β -subunits they are coexpressed with by determining the

speed of activation and inactivation, and the protein kinase activation of the functional α -subunits (Sweeney *et al.*, 2000; Coppock *et al.*, 2001). A role for $K_V\beta$ -subunits in O_2 sensing has been proposed, especially for the $K_V\beta 1$ -subunit which binds specifically to $K_V 1$ α -subunits (Sweeney & Yuan, 2000; Coppock *et al.*, 2001). The β -subunits can also act as an open-channel blocker, thus, reducing the $I_{K(V)}$ (Sweeney & Yuan, 2000).

The homomeric K_V channels formed by $K_V 1.2$, $K_V 1.5$, $K_V 2.1$, and $K_V 3.1$ α -subunits, and the heteromultimeric K_V channels formed by $K_V 1.2/K_V 1.5$ and $K_V 2.1/K_V 9.3$ α -subunits have been proposed as the channels inhibited by hypoxia leading to membrane depolarisation (Sweeney & Yuan, 2000; Coppock *et al.*, 2001).

Therefore, it appears that acute hypoxia inhibits K_V channel function which causes membrane depolarisation which causes the opening of VDCCs and an increase in $[Ca^{2+}]_i$ resulting in HPV (Sweeney & Yuan, 2000; Coppock *et al.*, 2001; Leach *et al.*, 2001; Sylvester *et al.*, 2001; Waypa *et al.*, 2001). The mechanism by which hypoxia inhibits the K_V channels has not yet been elucidated but could involve altering the function of K_V channels by: increased superoxide production, inhibition of cytochrome P450, or inhibition of oxidative phosphorylation (Sweeney & Yuan, 2000). More than one of these mechanisms is probably involved in the inhibition of K_V channels in order to preserve the efficiency and sensitivity of HPV (Sweeney & Yuan, 2000).

A previous study investigating the effect of chronic hypoxia on K^+ current revealed that hypoxia altered the K^+ channels involved in regulating the pulmonary vascular

tone of intrapulmonary arteries. The K_V channel blocker, 4-AP, contracted the intrapulmonary arteries of chronic hypoxic rats but had little effect on these vessels from control rats. Therefore, the resting potential of VSMCs under normal conditions was regulated by a non-inactivating delayed rectifier K^+ current ($I_{K(N)}$), while the resting potential of chronically hypoxic VSMCs were regulated by a voltage-gated K^+ current ($I_{K(V)}$) (Osipenko *et al.*, 1998). In cases of chronic hypoxia, the $I_{K(V)}$ is decreased causing membrane depolarisation. Therefore, chronic hypoxia inhibits the function of K_V channels as did acute hypoxia, with probably the same mechanisms being involved in each case (Sweeney & Yuan, 2000; Coppock *et al.*, 2001). However, it has been observed that the HPV response was 'blunted' in chronically hypoxic rats, while the response to vasoconstrictor agonists, such as ET-1, was enhanced (Sweeney & Yuan, 2000; Sylvester, 2001). Therefore, this evidence suggests that chronic hypoxia affects the expression of K_V channels by up or down-regulating transcriptional factors (such as c-jun) which control the expression of functional K_V channels (Sweeney & Yuan, 2000; Coppock *et al.*, 2001). The down-regulation of the mRNA and protein expression of K_V -subunits causing a decrease in K_V channel expression may explain the increased basal tone observed in chronic hypoxic rat vessels (McCulloch & MacLean, 1998).

Although there are compelling arguments which point to the involvement of K_V channel inhibition as an effector mechanism of HPV, other studies have shown that 4-AP did not prevent HPV. However, it has been proposed that there is a 4-AP insensitive isoform of K_V channel which could be involved in regulating $I_{K(V)}$ in the PASMCs (Coppock *et al.*, 2001; Sylvester, 2001).

1.10. The identity of the O₂ sensor:

The mitochondria have recently been implicated as the O₂ sensor involved in HPV (Leach *et al.*, 2001; Sylvester, 2001; Waypa *et al.*, 2001). The role of mitochondria in O₂ sensing in the PSMCs had been previously discounted as the mitochondrial electron transport chain (ETC) inhibitor, cyanide, failed to inhibit HPV (Sylvester, 2001; Waypa *et al.*, 2001). However, newer studies have shown that inhibitors of the proximal region of the mitochondrial electron transport chain (ETC) (such as rotenone and myxothiazol) attenuated HPV in perfused lung preparations and PSMCs. These proximal inhibitors did not affect agonist-induced vasoconstriction in perfused lung preparations and PSMCs (Leach *et al.*, 2001; Waypa *et al.*, 2001). Both proximal and distal (cyanide and antimycin A) ETC inhibitors blocked oxidative phosphorylation. These results showed that mitochondrial electron transport was necessary for HPV, but mitochondrial ATP was not, and that the complex at which the ETC inhibitor acts is an important factor in whether HPV is abolished or not (Leach *et al.*, 2001; Sylvester *et al.*, 2001; Waypa *et al.*, 2001). Therefore, mitochondria could act as an O₂ sensor in PSMCs.

It has been postulated that the mitochondria generates reactive oxygen species (ROS) at complex III of the ETC, and that this production is increased in response to HPV (Leach *et al.*, 2001; Waypa *et al.*, 2001). The mechanism involved in the increase of ROS production has yet to be elucidated. Once the superoxide has been generated, it enters the cytosol through anion channels where it is dismutated to hydrogen peroxide (H₂O₂) by Cu, Zn superoxide dismutase (Cu, Zn SOD) (Sylvester, 2001; Waypa *et al.*, 2001). It is proposed that H₂O₂ acts as a second messenger that triggers other mechanisms involved in HPV. It was shown that HPV was inhibited by antioxidants

and antagonists of Cu, Zn SOD, revealing that conversion of superoxide to H₂O₂ is a necessary step in the mechanism of HPV (Sylvester, 2001; Waypa *et al.*, 2001). As a second messenger, H₂O₂ could reduce proteins of the K_V -subunits. This would inhibit the K_V channels causing membrane depolarisation and increased [Ca²⁺]_i resulting in contraction of the PSMCs. Therefore, only proximal mitochondrial ETC inhibitors which act at complex III and above inhibit the generation of ROS by fully oxidising the complex resulting in a lack of electrons and a decrease in superoxide generation and, subsequently, HPV (Leach *et al.*, 2001; Sylvester, 2001; Waypa *et al.*, 2001). The inhibition of the ETC by a distal inhibitor such as cyanide allows the complex to become fully reduced supplying a lot of electrons for the generation of superoxide and, thus, do not inhibit ROS generation or HPV (Waypa, *et al.*, 2001).

An increase in the generation of ROS in response to hypoxia is seen in endothelial cells, cardiac myocytes and macrophages as well as PSMCs. This suggests that there are differential responses to hypoxia in different cell types which is made possible by differentiation in the downstream signal transduction pathways, not by differences in O₂ sensing. This allows PSMCs to contract, systemic VSMCs to dilate, and cardiac myocytes to undergo ischaemic conditioning in response to hypoxia.

It had also been proposed that NADPH oxidase could act as an electron donor for the generation of superoxide and could also be involved in O₂ sensing in the PSMCs.

However, mice with the gp91^{phox} subunit of the NADPH oxidase complex knocked out were shown to exhibit vasoconstriction in response to hypoxia. Therefore,

NADPH oxidase is not involved in HPV (Coppock *et al.*, 2001; Leach *et al.*, 2001; Waypa *et al.*, 2001).

As these studies show, there is still no consensus on the mechanism underlying O₂ sensing and HPV. However, the elucidation of these mechanisms could one day herald a new therapeutic approach for the treatment of PHT.

1.11. The indirect effect theory of HPV:

Many people believe the **indirect effect** theory of HPV which states that the effect of hypoxia on pulmonary vasoconstriction is indirect, and elicited by the release of a chemical mediator or mediators from the lungs in response to hypoxia. As yet, no single mediator has appeared to be the effector of the vasoconstriction though many have been considered. The search has investigated the catecholamines (noradrenaline and adrenaline), histamine, angiotensin-II, prostaglandins (PGF_{2α} and PGE₂), leukotrienes (LTC₄), and 5-HT. None of these has satisfied all of the criteria for being the mediator of the response to hypoxia (Fishman, 1976; Fishman, 1988). All of these vasoactive substances could play a part in the increased tone of the small PRAs observed in PHT. However, the identification and isolation of a potent vasoconstrictor substance named endothelin (ET-1) in 1988 renewed the interest in the involvement of a chemical mediator in HPV (Yanagisawa *et al.*, 1988). Indeed, it has been demonstrated that there is an increase in the level of ET-1 in patients with PHT (Stewart *et al.*, 1991). It has also been shown that there is an increase in the response to ET-1 in the small PRAs of the chronic hypoxic rats (McCulloch *et al.*, 1998), and that this effect is concomitant with the alteration of the phenotype of

pulmonary vascular smooth muscle cells in these vessels (MacLean, 1998). The role of ET-1 will be discussed in more detail later (chapter 5).

1.12. Genetic basis for primary PHT:

Primary PHT is usually idiopathic in origin, but an increase in its incidence has been linked with the ingestion of a certain brand of appetite suppressant in 1965, aminorex (Fishman, 1988). A more recent increase in primary PHT cases in the 1990's was attributed to another appetite suppressant, Fenfluramine (see MacLean, 1999 for review). The mechanism by which aminorex caused primary PHT is unclear, but its ability to stimulate the release of endogenous catecholamine stores could account for the increase in tone observed in PHT vessels (Fishman, 1988). A novel feature of these lungs was their hyperreactivity to the administration of 5-HT, as pulmonary arteries exhibited an increase in 5-HT-induced maximum contractile response and mitogenesis (MacLean, 1999; Eddahibi *et al.*, 2001). As with idiopathic primary PHT, aminorex-induced PHT lungs showed plexiform lesions which appear as a dilated branch of muscular artery, as well as the characteristic progressive muscularization of PRAs. The plexiform lesion branches are not lined by vascular endothelium as normal arteries are, rather they are lined by fibrillary or myofibroblasts cells (Heath & Edwards, 1958; Heath *et al.*, 1987; Fishman, 1988). However, as not all of the people who ingested aminorex developed PHT, a genetic predisposition to the development of the disease has been suggested. Indeed, some patients in the early stages of aminorex-induced PHT found that their symptoms regressed without treatment (Fishman, 1988). There have been two main types of genetic differences found between patients with primary PHT and normal controls which suggest that there is a genetic predisposition for primary PHT. The first type of

variation involves the 5-HT transporter (5-HTT) which is expressed in various cell types including neurones, platelets, and both pulmonary arterial endothelial and smooth muscle cells (Eddahibi *et al.*, 2001). Polymorphism of the 5-HTT gene promoter has been found, resulting in the expression of either a long (L) or short (S) form of the gene promoter. The L-allelic form has been shown to promote an increased expression and activity of 5-HTT (Eddahibi *et al.*, 2001). This has important ramifications for the pulmonary vasculature as an increase in the expression of 5-HTT increases the internalisation of indoleamine which is necessary for the mitogenic and co-mitogenic actions of 5-HT. Therefore, the increase in expression of the 5-HTT resulted in an increase in pulmonary artery SMC growth. Indeed, hypoxia caused an increase in the expression of 5-HTT and mitogenic effect of 5-HT and an increase in 5-HTT expression was also observed in remodelled pulmonary arteries from animals with hypoxia-induced PHT (Eddahibi *et al.*, 2001). It was revealed that 65% of primary PHT patients had the L-allelic variant compared to only 27% of controls. Therefore, having the L-allelic variant of the 5-HTT gene promoter may confer an increased susceptibility for the development of primary PHT. There is also evidence of increased 5-HTT expression in the platelets of patients with chronic obstructive pulmonary disease. This suggests the involvement of a genetic predisposition in the form of polymorphism of the 5-HTT gene promoter in PHT of different aetiologies (Eddahibi *et al.*, 2001). The second genetic variation to be associated with primary PHT is a mutation of the bone morphogenetic protein type II receptor (BMPR-II) resulting from 10 different missense mutations causing deletions in the *BMPR2* gene sequence (Machado *et al.*, 2001). These mutations of the *BMPR2* gene alter highly conserved regions of the BMPR-II receptor resulting in structural alterations of the ligand-binding domain of the receptor and a loss of receptor function

(Machado *et al.*, 2001). The *BMPR-II* gene codes for the transforming growth factor- (TGF-) receptor. It is unclear how altering the TGF- pathway promotes primary PHT. However, as TGF- is involved in the response to injury of the pulmonary vasculature, the mutation of a gene encoding a receptor which mediates the effect of TGF- may result in a loss of this pathway allowing the survival of damaged cells which form plexiform lesions and hyperplasia of VSMCs. This study revealed that 72% of patients with familial primary PHT and 3 patients with sporadic primary PHT were identified as having a *BMPR2* mutation or show evidence of linkage to the *BMPR2* locus (Machado *et al.*, 2001). Therefore, mutation of the *BMPR2* gene may confer an increased susceptibility for the development of PHT.

It has been demonstrated that experimentally-induced PHT from chronic hypoxia can be reversed when the animals were subsequently returned to normoxic conditions for a number of weeks (Heath *et al.*, 1973; Herget *et al.*, 1978). When the mechanisms underlying pulmonary vascular remodelling are understood, steps to inhibit its progression can be undertaken. Secondary PHT can result from pre-existing pulmonary or cardiac disease. The pulmonary vascular vasoconstriction and vascular remodelling seen in primary PHT are also seen in secondary PHT but the vasoconstriction is enhanced by the hypoxia also caused by the pre-existing condition. This thesis describes a study involving patients with secondary PHT as a consequence of left ventricular dysfunction (LVD). LVD causes an increase in pulmonary venous pressure leading to an increase in capillary bed hydrostatic and filtration pressure which results in pulmonary oedema. Pulmonary oedema causes an increase in the respiration rate leading to high frequency, but shallow breathing. The increase in pulmonary arterial pressure is not proportional to the increase in left ventricular end-

diastolic pressure (LVEDP), suggesting that reflex mechanisms are involved in the pulmonary propagation of hypertension. The development of pulmonary oedema has three stages: congestion; interstitial oedema; and finally alveolar oedema. Alveolar oedema heralds a marked reduction in ventilation-perfusion matching and a decrease in pulmonary compliance. If pulmonary oedema persists, vascular resistance is increased, PHT is sustained and right atrium failure will also occur. As the compliance of the lungs is attenuated, breathing becomes more difficult and dyspnoea at rest becomes apparent. The pulmonary blood volume is redistributed away from the base of the lungs towards the apices. The pressure throughout the pulmonary circulatory system increases as a consequence of increased LVEDP, the result of LVD. However, the pressure increase was more marked in the pulmonary arteries than veins which implies that an increased pulmonary vasoconstriction of the arteries in response to hypoxia over and above that produced by the vascular remodelling that occurs in PHT (Fishman, 1988).

1.13. Investigations undertaken in this thesis:

The studies described in this thesis are conducted on both rat and human small muscular PRAs and human systemic resistance arteries (SRAs). Chapter 3 investigates the mediators involved in the ACh-induced vasodilatation of control and chronically hypoxic rat PRAs. This study investigates whether the presence of PHT has any effect on the mediator profile of the ACh-induced relaxation. Chapter 4 looks at the effect of human urotensin-II (hU-II) on human PRAs from patients undergoing bronchial carcinoma resection and on human SRAs from patients undergoing hernia repair. The mediators involved in the hU-II-induced vasodilatation of human PRAs is also investigated. Chapter 5 investigates the ET-1 response in the human PRAs from

patients undergoing bronchial carcinoma resection and patients with differing degrees of left ventricular dysfunction (LVD) to see whether the propagation of PHT secondary to LVD alters the ET-1 response. This study also looks at the effect that three novel mixed ET_A/ET_B antagonists, SB 247083, SB 234551, and SB 217242, have on the ET-1 response in these different patient groups. Chapter 6 looks at the effects of ET-1 on rat PRAs in the presence and absence of PHT induced by chronic hypoxia. The effect of the three novel mixed ET_A/ET_B antagonists is also investigated in the PRAs of control and chronic hypoxic rats.

Chapter 2

Materials and methods

2.1. Background of myography:

The most important vessels, with respect to hypertension, are the resistance arteries. The resistance arteries are the vessels responsible for the generation of 50-70% of the peripheral resistance in each organ, and therefore, the body as a whole (Mulvaney & Halpern, 1976; Mulvaney & Halpern, 1977; Bohlen, 1986; and Mulvaney & Aalkjaer, 1990). The classification of resistance vessels are the small muscular arteries with diameters of $<500\mu\text{m}$ and the arterioles with diameters of $<100\mu\text{m}$ in both the pulmonary and systemic circulations (Mulvaney & Halpern, 1976; Mulvaney & Halpern, 1977; Duling *et al.*, 1981; Mulvaney & Aalkjaer, 1990; and MacLean, 1998). This evidence suggests that the properties of resistance arteries should be studied in order to understand the mechanisms underlying hypertension. However, the very size of these vessels means that the traditional organ bath technique used in the study of isolated larger vessels cannot be employed here (Leach *et al.*, 1992). Therefore, there was a need to develop a technique that allowed the study of the small resistance vessels.

2.2. Myography application:

Mulvaney & Halpern (1977) developed a technique that allowed the study of the intrinsic mechanical and contractile properties of the microvasculature, vessels with diameters of $<300\mu\text{m}$. This technique was called wire myography. Mulvaney and Halpern were able to accurately determine the internal circumference of the resistance vessel being used. This information was used to calculate the transmural pressure which is required to hold the vessel at this internal circumference and wall tension whether the vessel is relaxed or contracted using an equation derived from the Laplace relationship (see page 50). The plotting of the wall tension against the

internal circumference of a vessel displays an exponential curve. The curve produced by the resting: internal circumference relationship can be used to determine the internal circumference of a vessel under a given transmural pressure in a relaxed state. The new technique of myography showed that the resting wall tension: internal circumference relationship of systemic resistance arteries of normotensive (WKY) and spontaneously hypertensive (SHR) rats were not significantly different. However, the wall tension: internal circumference relationship for vessels that are contracted by extracellular Ca^{2+} was significantly different in the WKY and SHR rat vessels with SHR rat resistance arteries having a greater wall tension for a given internal circumference than WKY rats. This technique showed the differences in the contractile properties of the systemic resistance arteries from SHR and WKY rats for the first time.

2.3. Myography equipment:

The myography apparatus consists of a stainless steel 5ml organ bath chamber containing two mounting jaws. One of the mounting jaws is fixed in place and is attached to an isometric force transducer while the other mounting jaw is attached to a sliding arm and micrometer which allows the distance between the jaws to be altered. The micrometer allows this distance to be calculated so that the internal diameter of the vessels can be measured. This measurement is then used to calculate the displacement of the jaws needed to set the vessels at a precise transmural pressure using the Laplace relationship. The myograph models used in these experiments were the 500A, 600M and the 610M. The myograph model 500A allows the insertion of two vessel preparations at a time. These myograph blocks were not moveable, so the vessels were inserted at the site with the aid of a microscope. The myograph models,

600 and 610M, has 4 individual myograph blocks which can be removed from the myograph interface to allow the vessels to be mounted in the chambers with the aid of a microscope. The microscope used was a Stemi 2000 (Zeiss) at a magnification of x2.5.

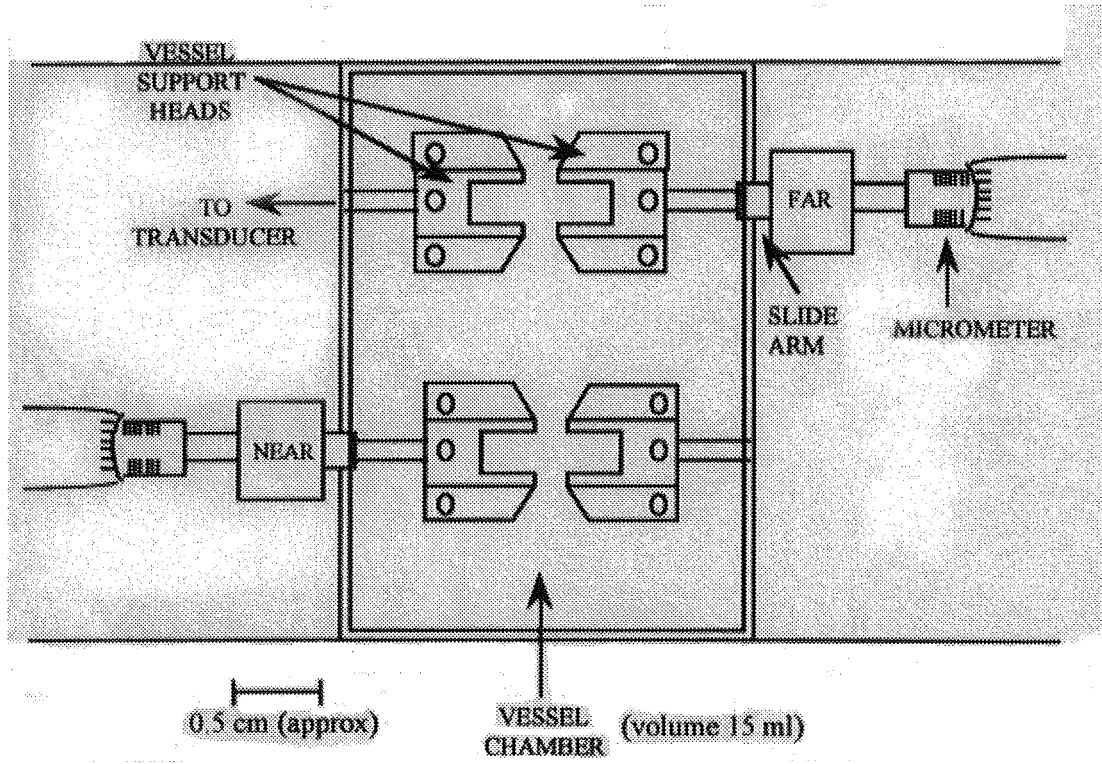


Figure 2.1: Schematic diagram (not to scale) of 500A model of Mulaney / Halpern wire myograph. All models allow *in vitro* measurement of isometric force changes. The vessels are mounted in the baths by the insertion of two wires (40 m i.d.) secured to the vessel support heads.

The tension, and therefore, the transmural pressure changes are recorded by a flatbed 4 channel L6514 Linseis chart recorder connected to myography models 500A, 600M and 610M. The pressure changes can be measured from the pen trace. Another of the 610M myograph interfaces is connected to a PC which records the pressure changes

using the Myodaq 2.01 programme and these are analysed using the same programme. The vessels are bathed in Krebs solution, the temperature of which is kept at $37^{\circ}\text{C} \pm 0.1$ by internal heating pads. A Douglas bag is filled with a mixture of 16% O_2 / 5% CO_2 /balance N_2 . The Douglas bag is connected to a vacuum pump which is then connected to the myograph interface where the aerator pipe is split up so that each of the aerators terminates in each individual chamber to bubble the Krebs solution.

2.4. Dissection of resistance arteries:

2.4.1. Rat pulmonary resistance arteries

The left lobe of the rat lung is cut from the left branch of the main pulmonary artery at the hilus. The lobe is placed on a dissecting dish with the costal surface lying down and the mediastinal surface exposed. The lobe is carefully pinned out and covered with ice cold Krebs solution. In this position, the interlobar vessels of the lung lie with the vein superior, and the artery inferior, to the bronchus. The point of a pair of spring scissors was inserted into the lumen of the bronchus and a cut extending to the apex of the lobe was made. This cut reveals the arteries which can be visualised beneath a layer of the bronchus wall. The bronchus wall is dissected from the top of the interlobar artery, taking care not to puncture the artery below. The bronchus wall still covers the branches of the interlobar artery and this is dissected away to allow the branches to be visualised more readily.

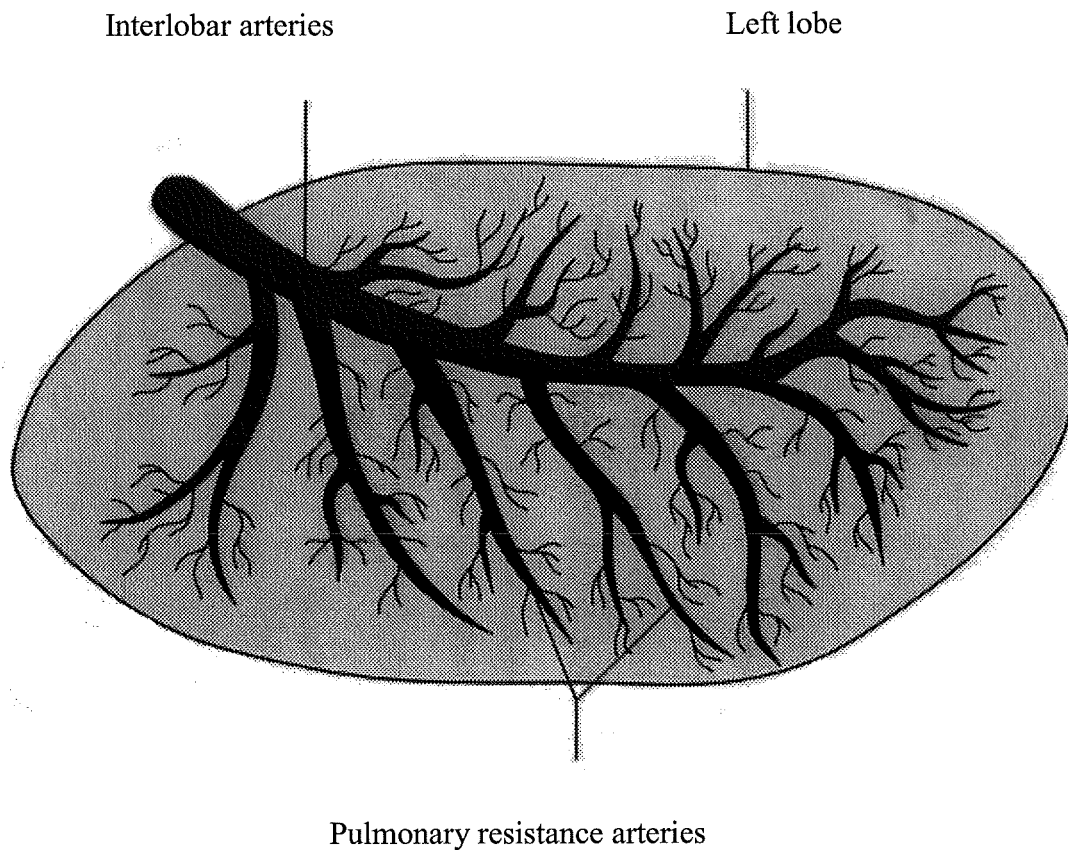


Figure 2.2: Diagram of the left lobe of the rat lung. The arteries used in the rat studies were the pulmonary resistance arteries.

After selecting a branch of the interlobar artery, the bronchus wall is dissected away and the surrounding parenchyma is carefully cut away so that the resistance artery can be cut from the interlobar artery and cleanly lifted free. The dissection preparation is washed with ice cold Krebs solution at regular intervals to prevent it from drying out caused by the microscope light. The dissected resistance artery is placed in another dissection dish full of Krebs solution so that any remaining parenchyma attached to the artery can be removed. The vessel is now ready for mounting or can be placed in

a glass vial of ice cold Krebs solution and kept in the fridge overnight for use the next day. All the vessels were either used on the day of sacrifice or the day after.

2.4.2. Human pulmonary resistance arteries

The biopsy tissue used in the human pulmonary artery experiments came from two sources. The control biopsies came from patients undergoing thoracotomies to remove cancerous lung tissue. These lung resections resulted in various sizes of lung being removed, however, the biopsy of macroscopically normal 'safety margin' tissue was usually in the region of 5x4x0.5cm. The chronic heart failure biopsies came from patients who were to undergo coronary artery bypass grafts and had consented to take part in a study which investigated whether the effect of various vasoactive substances was altered by the presence and degree of left ventricular dysfunction (LVD). This is discussed in more detail in chapter 5. Briefly, patients were assessed for degree of LVD using echocardiographic measurement of their ejection fraction. The patients were classified according to their ejection fractions. Patients with an ejection fraction of $\geq 40\%$ were classed as having good left ventricular function (good LVF), patients with an ejection fraction of 30-40% were classed as having moderate left ventricular function (moderate LVF), and patients with an ejection fraction of $< 30\%$ were classed as having poor left ventricular function (poor LVF). Before the bypass graft took place, *in vivo* experiments were conducted by infusing vasoactive substances into the forearm and recording the resulting changes in blood pressure (Singh *et al.*, 2002). Consent was also given to take a small (2x1.5x0.5cm) biopsy from the anterior costal surface of the superior lobe of the left lung to conduct *in vitro* wire myography experiments. However, the resistance arteries from the tissues of both sources were dissected in the same manner. The biopsy was placed on a dissecting dish and

covered in ice cold Krebs solution. The biopsy was carefully pinned out with any surface showing arteries uppermost. The resistance arteries are identified by their appearance and structure as they have thick walls with respect to their lumen and are often found to contain coagulated blood. The bronchi are identified by the fact that their walls are thinner than those of the arteries and are often found to contain mucous. The veins collapse and are generally not seen during dissection. When an artery is identified, the parenchyma is dissected from above the artery and it is followed until vessels in the correct size range were reached. The arteries branch frequently so that a biopsy of the aforementioned dimensions can yield a number of suitable vessels. Once a vessel of the correct size is found, parenchyma surrounding the artery is dissected away so that the resistance artery can be lifted out easily. The resistance artery is transplanted to another dish full of Krebs solution so that any remaining parenchyma attached to the artery can be removed. The vessel is now ready for mounting or can be placed in a glass vial of Krebs solution and kept in the fridge overnight.

2.4.3. Human abdominal systemic resistance arteries

The biopsies used in the human abdominal artery experiments came from patients undergoing a hernia repair operation. Consent was given to take an abdominal skin biopsy (4x0.5cm) with a section of subcutaneous fat (3x3x0.5cm) attached. The biopsy was pinned out carefully with any surface showing arteries uppermost. The resistance arteries in this biopsy can be found, the surrounding fat is dissected away and the resistance artery lifted clear. The resistance artery is placed in another dish full of Krebs solution so that any remaining fat attached to the artery can be removed.

The vessel is now ready for mounting or can be placed in a glass vial of Krebs solution and kept in the fridge overnight.

2.5. Mounting procedure:

Figure 2.3 shows the steps involved in mounting an artery on the Mulvaney / Halpern wire myograph. The resistance arteries are placed in a dissecting dish containing ice cold Krebs solution. The vessel is threaded with a 6cm length of tungsten wire with a diameter of 40 μ m under a Stemi 2000 (Zeiss) microscope on a magnification of x2.5. The proximal artery wall is held gently between the points of a pair of forceps in one hand. With the other hand, lift the mounting wire between the points of a pair of forceps. The tip of the mounting wire is gently placed into the proximal lumen of the resistance artery. This step can be hindered by the properties of the vessel as human resistance arteries generally have 'sticky ends' which can make the entry of the wire into the vessel difficult. Once the wire tip is in the artery lumen, the wire is gradually eased further into the lumen. The wire should remain in the centre of the lumen to prevent damaging the endothelial layer. Extra care should be taken if the artery is curled as the wire is more likely to scrape the wall during its advancement. Once the wire protrudes from the distal lumen of the artery, the wire is pushed further through the artery very slowly so that there is at least a 2cm length of wire on either side of the vessel. An individual myograph block is placed under the microscope with the micrometer on the right hand side and 5mls of Krebs solution was added to the organ chamber. **Step 1:** The wire skewering the vessel is then picked up by forceps and placed between the mounting jaws. The jaws are closed with the vessel situated in the 2cm gap between the prongs of the jaws. **Step 2:** The distal end of the wire is pulled across to the distal mounting screw on the left hand fixed jaw that is attached to the

transducer. The wire is wrapped around the mounting screw in a clock-wise direction before the screw is tightened. The proximal end of the wire is pulled across to the proximal mounting screw on the fixed transducer jaw. The wire is wound around the mounting screw in a clock-wise direction and the screw tightened. The first wire and, therefore, the artery are now secured to the mounting jaw of the fixed transducer arm.

Step 3: Any surplus wire around the screw is carefully removed to prevent pulling on the vessel during drug additions. The jaws are opened slightly to allow the insertion of the second 6cm long wire. **Step 4:** The wire is gently placed into the proximal lumen of the artery and is gradually advanced through the lumen until a length of approximately 2cm protrudes from the distal end of the lumen. When inserting the second wire, care must be taken to ensure that the wires run parallel and are not crossed before the ends are secured. **Step 5:** The distal end of the wire is pulled across to the distal mounting screw on the right hand moveable micrometer jaw. The wire is wrapped around the distal mounting screw in a clock-wise direction and the screw tightened. The proximal end of the wire is pulled across to the proximal mounting screw on the right hand jaw. The wire is wrapped around the mounting screw in a clock-wise direction and the screw tightened. **Step 6:** The jaws are moved apart so that a small but distinct gap between the two intraluminal wires can be seen. The myograph block is then plugged into the myo-interface. This procedure is repeated until all four chambers have been set up. The vessels are left to equilibrate for 45mins or until spontaneous tension generation has levelled off.

The vessel is then placed under a tension that is equal to the transmural pressure experienced by the vessels *in vivo*. As the pulmonary circulation is a low pressure system with respect to the systemic circulation, the transmural pressure of small

muscular pulmonary resistance arteries is 16mmHg (M^cCulloch & MacLean, 1996). The myography models 600M and one of the 610M and 500A are attached to a 4 channel flat bed L6514 Linseis pen recorder. The pens are manually placed at the top of the chart (left hand side) so that a full-scale deflection can be observed when the jaws are slowly closed together by turning the micrometer in a clock-wise direction. When the pen was deflected to the bottom of the chart (right hand side) the reading on the micrometer is written and denoted as 'X₀'. This is the point when the intraluminal wires are touching together. Further closure of the jaws may result in damage to the transducer and should be avoided. The jaws are then opened again by turning the micrometer in an anti-clock-wise direction. When the pen is back at the top of the chart, the intraluminal wires are the same distance apart as they were during the equilibration period. This full-scale deflection procedure was repeated for all four arteries. The pens were then manually moved to the bottom of the chart (right hand side) where they were spaced apart so that each individual trace can be distinguished easily seen. The transmural pressure was increased in the vessel by widening the gap between the jaws by turning the micrometer in an anti-clock-wise direction. The micrometer is turned until the pen has displaced by ten small boxes on the chart paper. Due to the calibration of the recorder, each small box represents 0.123mN so that the initial tension placed on the vessel is 1.23mN. The tension can slip off and have to be reapplied. When the trace has levelled off, the micrometer reading is recorded and denoted as 'X₁'. The difference in the micrometer readings (X₁-X₀) is then put into the equation to calculate the internal circumference of the artery. The internal circumference (IC) is used in the equation derived from the Laplace relationship to determine the exact number of small boxes of tension needed to create a transmural

pressure of $\sim 16\text{mmHg}$ with a final resting tension of between $0.54 - 0.95\text{mN}$ ($100 - 250 \text{ m i.d.}$) (see below).

When the trace has stabilised at a tension equal to 16mmHg , manually place the pens at a graduated baseline. The vessel is now ready to have its viability assessed. The physiological viability is demonstrated by a rapid vasoconstriction of the resistance artery in response to the addition of 2M KCl . Once the constriction has levelled off and the pressure change recorded, the chamber is flushed out and refilled with a 5ml of *Kreb's* solution. This washout procedure is repeated 4 times. When the trace has returned to its original baseline, the addition of 2M KCl is repeated and is washed out of the preparations after the vasoconstriction had stabilised. One of the myography models, 610M , is attached to a PC running the *Myodaq 2.01* programme. A file is opened up for each experiment in the *myodata* folder. The channels are zeroed and the jaws are closed by turning the micrometer in a clock-wise direction until the myograph display on the myo-interface reads $\sim 15\text{mN}$. This is the point where the two intraluminal wires are touching together. The reading on the micrometer is recorded as ' X_0 '. The jaws are moved apart by turning the micrometer in an anti-clock-wise direction until the myo-interface display reads 0mN again. Tension is placed on the vessel by increasing the gap between the jaws. The micrometer is moved in an anti-clock-wise direction until the display on the myo-interface and the force on the scale of the computer screen reads 1.23mN , which is equivalent to then small boxes on the *linseis* paper. Once the computer trace has levelled off, the second micrometer reading is taken as ' X_1 '. The internal circumference is calculated and used to work out the tension needed to place the artery under a transmural pressure of $\sim 16\text{mmHg}$. The equation calculates the number of displacement boxes needed and

multiply that by 0.123mN to determine the force in mN equal to 16mmHg. When the trace has stabilised at the desired tension the myograph channels are zeroed. The physiological viability is assessed with two additions of 2M KCl with a wash in between the additions and after.

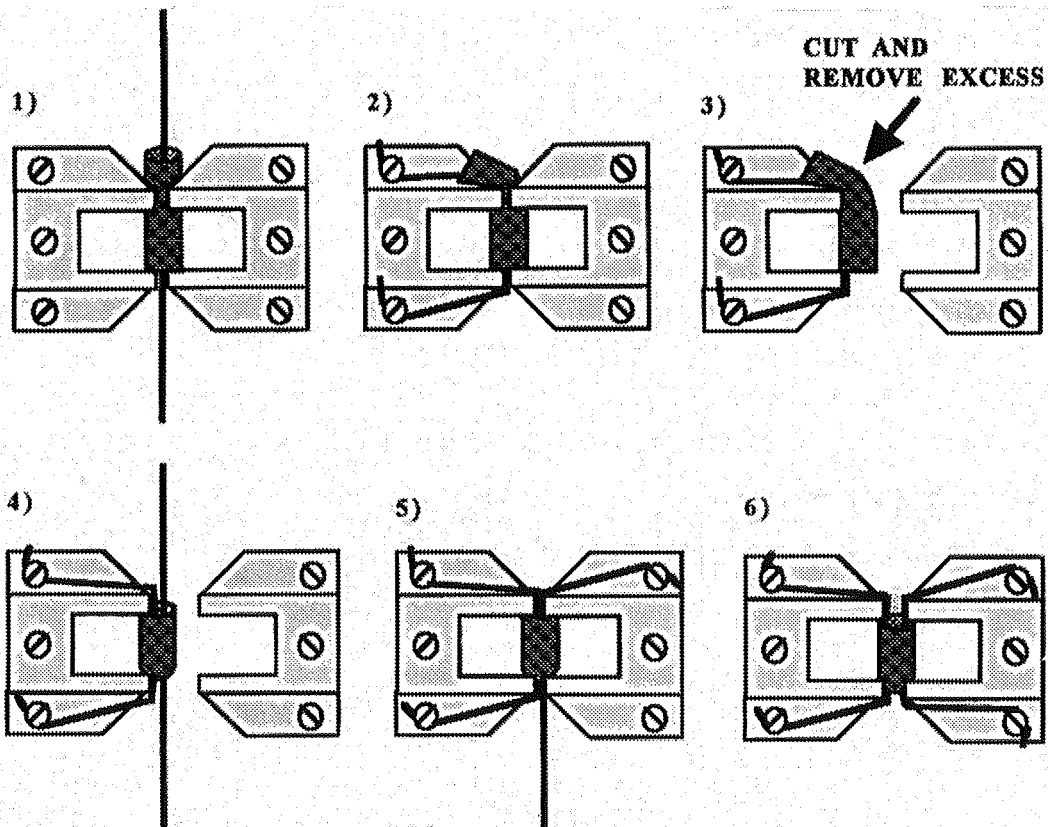


Figure 2.3: diagram of mounting procedure for pulmonary and systemic resistance arteries.

2.6. Calibration of a myograph:

The first step in calibrating a myograph is to attach a mounting wire to the support jaw attached to the transducer arm in each of the 4 chambers. The wire is secured with the mounting screws. The chamber is then filled with 5mls of Krebs solution and the chambers are left to settle to allow the Krebs solution to warm up to 37°C for 30mins. A pan-handle balance is placed over the chamber of the first myograph

block. The base of the balance is placed at right angles to the direction of movement of the jaws so that the transducer arm of the balance is inserted into the chamber between the mounting wire and the transducer jaw it is attached to. The transducer arm should be free-swinging so that it is touching neither wire nor jaw. The balance is left in this position for 30mins. A 2g weight is added to the pan arm of the balance choosing the side which causes the transducer arm of the balance to be tipped towards the mounting wire. In order to calibrate the myograph and recorder, the force applied to the transducer must be calculated. This is done using the equation:

$$F_{\text{transducer}} = W \times g \times (\text{arm ratio})$$

When arm ratio = (pan arm) / (transducer arm) and 'g' is the gravitational acceleration (9.81mN/gram)

In the balances used to calibrate the myographs used in these experiments, the pan arm / transducer arm ratio is 0.5.

Thus, for a 2g load, the load on the transducer is $2 \times 9.81 \times 0.5 = 9.81\text{mN}$.

When calibrating the myograph models 500A, 600M and 610M which were attached to Linseis chart recorders, the channel corresponding to the myograph block being calibrated is switched to calibrate before the 2g weight is placed on the balance. When the weight is placed on the balance, the transducer arm touches the wire and the pen is deflected across the chart paper. The recorder has been calibrated so that each small box represents 0.123mN. Therefore, a 2g load producing 9.81mN of force should cause a deflection of 80 small boxes. If the deflection is too short, the variance is adjusted by turning the variance screw anti-clock-wise and if the deflection is too long, the variance screw is turned in a clock-wise direction until the pen is 80 small boxes from its baseline. Once that pen is calibrated, the switch is turned back to the

variance scale. The balance is removed from the first chamber and placed in the next. The balance is left in this position for 30mins before adding the 2g load. This process is repeated for each of the 4 myograph blocks. The myograph model 610M also shows the force generated by the 2g load in mN on its display.

When calibrating myograph model 610M attached to a PC running the Myodaq 2.01 programme, the procedure is identical to that conducted on the myograph models attached to pen recorders until the 2g weight is applied. The calibration menu is selected and the chamber containing the balance is highlighted. The 2g weight is placed on the balance adding 9.81mN of force to the wire. When the display has settled on a figure, press select to calibrate that channel. The force on the transducer is shown as a deflection on the screen of the PC and on the display of the myo-interface in mN. This is repeated for each of the 4 chambers. The Myodaq 2.01 programme automatically adjusts itself so that the addition of the 2g weight always causes a deflection of the correct size to be shown on the screen.

2.7. Setting of transmural pressure:

The myography experiments are conducted at a transmural pressure that is experienced by the vessel *in vivo*. Laplace's Law of pressure within a sphere is the basis of the equation used to determine the pressure of a blood vessel. Laplace's Law states that the pressure (P) within a sphere is indirectly proportional to the internal radius (r):

$$P = \frac{2T}{r}$$

Tension (T) is defined as stress (S) multiplied by the wall thickness (w). Stress is the force per unit cross sectional area of wall. Therefore, Laplace's Law can be written as:

$$P = \frac{2Sw}{r}$$

This law states that as the radius of the sphere increases, the magnitude of the inward component of the wall stress decreases which causes less pressure to be generated inside the sphere. This law has been expanded upon to devise an equation which allows the stretch of a vessel needed to produce a certain effective pressure (P_i) to be determined.

The Laplace relationship can be used to determine the effective pressure in KPa, which is an *estimate* of the pressure necessary to extend the vessel to the measured internal circumference (IC).

$$P_i = \text{wall tension} / \text{IC} / (2 \times \pi)$$

The IC can be measured as follows:

X_0 is the point where the wires are touching each other:

As the wires are $40\mu\text{m}$ in diameter, this point is calculated as:

$$2 + \pi \times 40, \text{ so at } X_0, \text{ the IC}_0 \text{ is } 205.6\mu\text{m}$$

X_1 is the point where the wires are apart and some initial tension has been applied to the vessel:

Therefore, IC = (micrometer reading after tension applied [X_1] – micrometer reading at X_0) x 2 + IC at X_0

The IC is converted to mm before being put into the equation i.e. 205.6 μ m is now 0.2056mm. The wall length is measured then doubled since there is an upper and lower wall.

Wall tension is the measured force divided by the wall length so:

$$\text{Wall tension} = \frac{\text{force (F)}}{(\text{length} \times 2)}$$

$$P_i = \text{wall tension} / \text{IC} / 2 \times \pi$$

$$P_i = \frac{(2 \times \pi) \times \text{wall tension}}{\text{IC}}$$

$$P_i = \frac{(2 \times \pi) \times F}{2 \times \text{length} \times \text{IC}}$$

$$P_i = \frac{2 \times \pi \times \alpha \times \#}{2 \times l \times \text{IC}}$$

where α is calibration factor 0.123mN and # is the number of boxes needed to increase the pressure in the vessel to a given pressure.

The pressure calculated by this equation is in KPa. The pressure exerted by a 1mm tall column of mercury (1mmHg) is 133Pa. Therefore, the effective pressure is divided by 0.1333 to calculate the pressure in mmHg. If the tension is too low, more tension is applied (by moving the wires further apart) before redoing the calculation.

The effective transmural pressure of human and rat pulmonary resistance arteries is 16mmHg as seen *in vivo*. The transmural pressure of chronic hypoxic rat pulmonary resistance arteries is 32mmHg. The transmural pressure of systemic resistance arteries from abdominal adipose tissue is 90mmHg.

2.8. Small animal hypobaric hypoxic chamber design:

The two chambers used by our lab (see **Figure 2.4**) were designed and manufactured by The Royal Hallamshire Hospital, Sheffield. The chambers are made from clear plexiglass with a removable panel which acts as a door to allow the insertion of the animal cages. The chambers can accommodate two animal cages, both housing up to four rats at a time. The cages are placed in the chamber with the food and water dispensers at the back of the chamber to allow a clear view of both the rats and the water and food supplies. The chamber is continuously ventilated by an air flow of 45 L/min and the air is also removed continuously via a tube connected to a pump which creates a vacuum that controls the pressure inside the chamber by operating the inlet valve located on the front door of the chamber. A pressure gauge at the rear of the chamber displays the pressure within and a safety switch which stops the pump if the pressure falls below 460mbar. The temperature (~ 21°C) in the chamber is monitored by the insertion of a mercury thermometer.

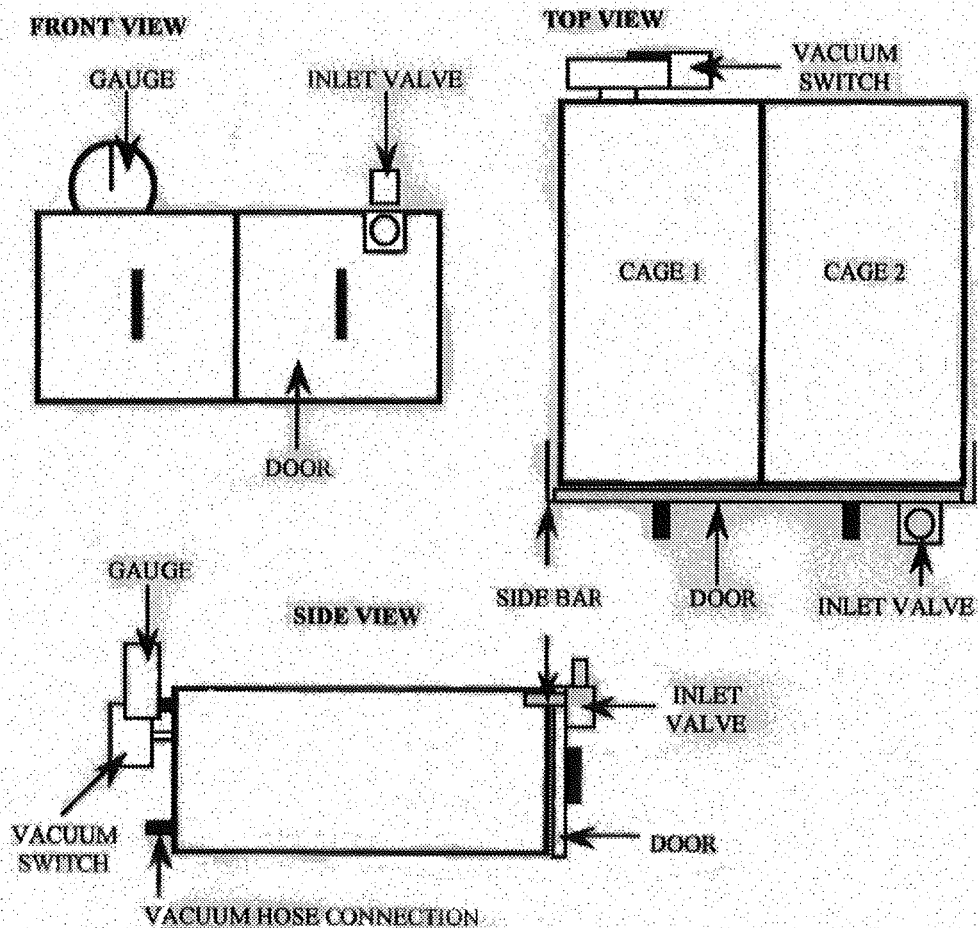


Figure 2.4: Diagrammatic representation of hypobaric chamber (not to scale). At the rear of the chamber, the vacuum hose tube leaves the chamber and is connected with the pump. The inlet valve located on the door of the chamber is rotated to control the pressure inside the chamber (anticlockwise-decrease pressure and clockwise-increase pressure). The safety vacuum switch located on the back of the chamber cuts the pump if the pressure inside the chamber falls dangerously low. The pressure gauge is also located at the rear of the chamber.

2.9. Maintenance of animals:

The chambers are located in a specially designed, sealed room in which the environment is strictly controlled with filtered air so that the temperature is $\sim 21^{\circ}\text{C}$ and there is 55% humidity. Any change in the environmental conditions activated an alarm in the lab and the university gate house so that any problems during out of hours periods would be noticed and dealt with. All rats used in these studies were male Wistar Kyoto rats. Animals destined for the chamber were ordered so that they were 30 days old on the day they entered the chamber. Age-matched controls were ordered and delivered at the same time. The rats arrived 5 days before the start of the 14 day experimental period, using this time to acclimatise. On the first day of the experiment, the rats were divided into chamber and age-matched control groups. The experimental rats were placed in the chamber and the door put in position before switching on the pump. Once the pump is running, the door is held in place while a seal is made. Once the chamber is properly sealed, the inlet valve is gradually closed to reduce the pressure by 50mbar every 30-45mins until the pressure inside the chamber was 750mbar. On the second day of the experimental 14 day period, the pressure in the chamber was reduced in the same manner until it reached the experimental set point of 550mbar. The pressure was checked every 15 mins for an hour after manipulation of the pressure was completed for the day to ensure that the pressure remained stable. The chambers were gradually returned to normal atmospheric pressure every 3-4 days in order to clean out the cages and replenish water and food supplies. The chambers were off for 30mins during this cleaning period before being gradually returned to the experimental pressure. The time course for the pressure manipulations before and after cleaning were ~ 2 hrs, faster than the

initial decreasing of pressure at the start of the experimental period. The chambers were checked by staff from the Glasgow University animal facility at the weekend.

At the end of the experimental period, the chamber was returned to atmospheric pressure and the rats removed. The rats were killed by overdose of sodium pentobarbitone immediately on removal from the chamber. The heart and lungs were removed for studying that day or to be placed in a vial of ice cold Krebs for studying the next day. The age-matched controls were killed and used in the same way.

2.10. Validation of hypobaric hypoxic rat model:

The hypobaric hypoxic rat model has been used for several years by this group and all of the validation of our model of PHT was done by Dr. K.M. McCulloch, the first PhD student in this lab, as part of her doctoral thesis (McCulloch, 1996). The validation of this model was achieved through the *in vivo* and *in vitro* assessment of three characteristic features which demonstrate the development of PHT: pulmonary artery pressure (PAP), ventricular ratio, and percentage of thick walled pulmonary vessels (TWPVs). As well as demonstrating that chronic exposure to the hypobaric hypoxic conditions in the chamber results in the development of PHT, Dr. McCulloch also determined the correct transmural pressure to which the control and chronic hypoxic PRAs should be set. These studies revealed that the PRAs from control rats should be set up under low tension (~ 16mmHg) while chronic hypoxic rat PRAs should be set up under high tension (~ 36mmHg) (McCulloch, PhD thesis, 1996; MacLean & McCulloch, 1998). These are the transmural pressures experienced *in vivo* by PRAs from control and pulmonary hypertensive rats (Herget *et al.*, 1978).

Previous studies have shown the PAP to be significantly increased in rats exposed to 14 days of hypobaric hypoxia than controls, including the validation studies of this lab's model (Chen *et al.*, 1995; Eddahibi *et al.*, 1991; McCulloch, 1996). A recent study by this group revealed an increased right ventricular pressure in this rat model, confirmation that this rat model exhibits pulmonary hypertension (Keegan *et al.*, 2001). An earlier study also showed that hypoxia did not result in an increase in mean arterial pressure of the systemic circulation (Rabinovitch *et al.*, 1979). Therefore, this model results in an increase in pulmonary vascular resistance leading to an increase in PAP and right ventricular pressure.

The previous validation of this lab's hypobaric chronically hypoxic rat model demonstrated a significant increase in the percentage of TWPVs (see **Figure 1.2** and **1.3**) with a thickening of both the *tunica media* and the *tunica adventitia* in the pulmonary resistance arteries (PRAs) of chronic hypoxic rats compared to the controls (McCulloch, 1996). Earlier studies have shown significant hypertrophy of the vascular smooth muscle cells (VSMCs) and an increase in the amount of collagen in the medial layer of large calibre and resistance arteries (100-300µm) of the pulmonary circulation after chronic hypoxic exposure (Hunter *et al.*, 1974; McCulloch, 1996; Meyrick & Reid, 1978; Rabinovitch *et al.*, 1981). Therefore, this model of hypobaric hypoxic rat model exhibits the characteristic vascular remodelling associated with secondary PHT.

A reliable indicator of the development of PHT is the assessment of right ventricular hypertrophy as measured by calculating the ventricular ratio:

$$R.V. / L.V. + S$$

Where: R.V. = right ventricle, L.V. = left ventricle, and S = septum.

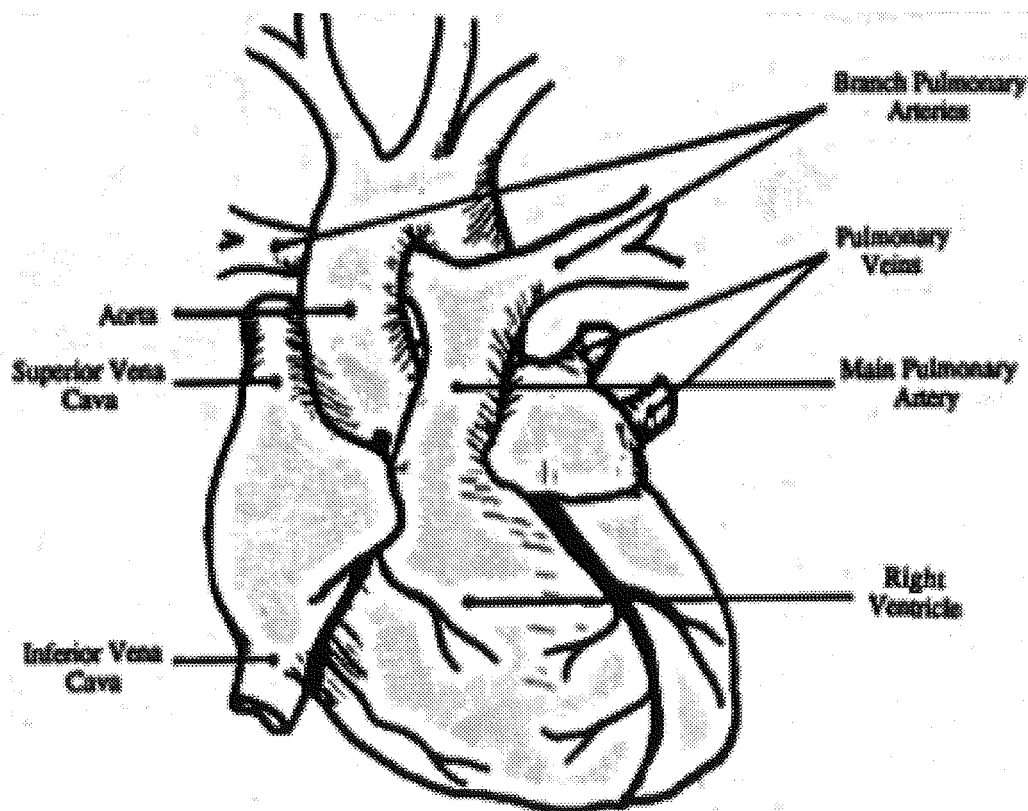


Figure 2.5: Diagram of the heart (not to scale). To prepare the heart for measurement of R.V. / L.V. + S ratio to determine the presence of PHT, the arteries, veins and atria are carefully dissected away from the ventricles.

The ventricular ratio is a reliable index of right ventricular hypertrophy which results from the increased pulmonary vascular resistance which occurs in response to hypoxia (Hunter *et al.*, 1974; Leach *et al.*, 1977; McCulloch, 1996; Rabinovitch *et al.*, 1981). The increase in the ventricular ratio reveals the development and severity of

PHT. A recent study demonstrated the development of right ventricular hypertrophy in this rat model (Keegan, *et al.*, 2001).

In order to minimise the use of animals, the ventricular ratio is the only method used in this current thesis to demonstrate the presence of right ventricular hypertrophy and PHT in the hypobaric chronically hypoxic rat. Once the rats had been sacrificed, the thoracic cavity was opened and the heart and lungs were dissected free. The heart was pinned down before the aorta and pulmonary vessels were removed to leave only the ventricular mass. The ventricular mass was delicately dissected along the free wall of the right ventricle so that the right ventricle was now separate from the left ventricle plus septum (Fulton *et al.*, 1952). After being rinsed in Krebs solution, the ventricles were carefully blotted on a tissue before being weighed. The R.V. / L.V. + S ratio was calculated for each control and chronic hypoxic rat used (expressed as mean \pm SEM). These values can be seen in the appropriate results chapters.

2.11. Data analysis:

All experimental data was analysed using the same analysis methods. The vasoactive response to the various vasoconstrictor and vasodilator substances used in this thesis, in the presence and absence of various antagonists of receptors or downstream mediators, were calculated as changes in wall tension and expressed in mN. The data was plotted in graphical form as a percentage of the maximum vasoconstriction of 50mM KCl in the case of the vasoconstrictor peptide, (endothelin-1) ET-1, and as a percentage of the precontraction elicited by either 10 or 30 μ M of 5-HT or 0.3 μ M of ET-1 in the case of the vasodilator peptide human urotensin-II (hU-II) or acetylcholine, respectively. All the data from the resulting cumulative concentration

response curves (CCRCs) were fitted to an equation describing a one-site sigmoidal dose response curve of variable slope using GraphPad Prism 3.01 (San Diego, California, USA). The equation used for analysis in GraphPad Prism allows the calculation of the maximum response, EC_{50} and the Hill slope of the curve. The EC_{50} is the molar concentration of an agonist that produces 50% of the maximum effect of that agonist (Jenkinson *et al.*, 1995). The equation used is:

$$E = \frac{a \cdot [A]^{nh}}{[A]_{50}^{nh} + [A]^{nh}}$$

where E = response, a = maximum response, [A] = concentration of agonist, $[A]_{50}$ = concentration of agonist which produces 50% of the maximum response (a), and nh = Hill coefficient (Alexander *et al.*, 1999).

This equation was used to determine the EC_{50} of all agonists, in the presence and absence of antagonists, used in this thesis. The EC_{50} was calculated for each individual CCRC then converted into a pEC_{50} value which is the negative logarithm to the base 10 of the EC_{50} of an agonist (pEC_{50} ; Jenkinson *et al.*, 1995). All agonist response data and pEC_{50} values were calculated for individual CCRCs before an average was taken of the data and expressed as the mean \pm SEM.

Studies involving the reversible competitive mixed ET_A/ET_B antagonists were analysed using the method described above. The potency of an antagonist can be quantified by calculating the dissociation equilibrium constant (K_B) for the combination of a reversible competitive antagonist (B) with the receptor, the molar

concentration of ligand required to occupy 50% of the receptor population (Jenkinson *et al.*, 1995). The potency of the antagonist is expressed in this thesis as a pK_B value, the negative logarithm to the base 10 of the molar concentration of the dissociation equilibrium constant. The pK_B values could not be calculated for the mixed ET_A/ET_B antagonists in the human study of left ventricular dysfunction (chapter 5) as the maximum response to ET-1 in the presence of one concentration of each of these antagonists did not reach the vasoconstrictor response observed in vessels without antagonist (Kenakin, 1982). A pA_2 value, the negative logarithm to the base 10 of the molar concentration of antagonist that makes it necessary to double the concentration of agonist needed to elicit the original submaximal response, could not be calculated for the mixed ET_A/ET_B antagonists in the rat study of hypobaric hypoxia (chapter 6) as there was no clear parallel shift of the ET-1 CCRC between the three concentrations tested in the chronic hypoxic rat vessels (Schild, 1947; Arunlakshana & Schild, 1959; Jenkinson *et al.*, 1995). Therefore, an estimated pK_B was calculated for $1\mu\text{M}$ of these antagonists using the following equations:

$$r = \frac{[A']}{[A]}$$

where: r = concentration ratio, $[A']$ = EC_{50} in the presence of antagonist, $[A]$ = EC_{50} in the absence of antagonist. Then:

$$K_B = \frac{[\text{Antagonist}]}{r - 1}$$

$$pK_B = -\log K_B$$

An estimated pK_B value was calculated for each individual CCRC then averaged and expressed as mean \pm SEM.

2.12. Statistical analysis:

Comparisons were made between two groups using Students' t-test for unpaired data. A *P* value of $< 0.05^*$ was considered to be statistically significant. Comparisons were made between four or more groups using a one-way ANOVA with a Dunnetts' post-test. A *P* value of $< 0.05^*$ was considered to be statistically significant. The statistics package used for both of these analyses was GraphPad Prism 3.01.

2.13. Drugs and solutions:

The composition of the Krebs-bicarbonate buffer was (in mM): NaCl 118.4, NaHCO₃ 25, KCl 4.7, CaCl₂ 2.5, KH₂PO₄ 1.2, MgSO₄ 1.2, and glucose 11. This buffer has a pH of 7.4.

The following drugs were used: endothelin-1 and substance P (Calbiochem, Beeston, Nottingham, U.K.). Human Big Endothelin₃₈, acetylcholine chloride, adrenomedullin₅₂, sodium nitroprusside, isoprenaline, 5-hydroxytryptamine, apamin, indomethacin and N^ω-nitro-L-arginine methylester (Sigma, Poole, Dorset, U.K.). Ketanserin tartrate and GR 55562 dihydrochloride (Tocris, Avonmouth, Bristol, U.K.). SB 247083, SB 234551, SB 217242, SB 224289, BRL 15572, human urotensin-II, porcine urotensin-II and rat urotensin-II (gifted by SmithKline Beecham, King of Prussia, Pennsylvania, U.S.A.). Charbydotoxin (gifted by M. Randall, Nottingham University, U.K.).

Endothelin-1, human Big endothelin₃₈, substance P, acetylcholine chloride, adrenomedullin₅₂, sodium nitroprusside, isoprenaline, 5-hydroxytryptamine, apamin, ketanserin tartrate, GR 55562 dihydrochloride, N ω -nitro-L-arginine methylester, SB 234551, SB 217242, human urotensin-II, porcine urotensin-II and rat urotensin were all dissolved in distilled water. SB 24708 was dissolved in DMSO. Indomethacin was dissolved in a 0.5M NaHCO₃ solution.

Chapter 3

**The mediators involved in the
ACh-induced vasodilator
response:
the effect of chronic hypoxia**

3.1.1. Vasodilator response to ACh in control and chronic hypoxic rats:

Previous studies have shown that chronic hypoxia influences the vasodilator response induced by acetylcholine (ACh). The small pulmonary resistance arteries (PRAs) of chronic hypoxic rats were found to have an increase in their endogenous tone, which is uncovered by the addition of the nitric oxide synthase (NOS) inhibitor, L-NAME. The rat PRAs exhibit an increased release of basal NO to antagonise the increase in the inherent tone of the vessels seen in PHT (MacLean & McCulloch *et al.*, 1998). These vessels were also shown to exhibit an increased vasodilator response to ACh than vessels from age-matched control rats. The pIC₅₀ of ACh-induced relaxation was significantly decreased from 5.77 ± 0.15 in control rats to 7.12 ± 0.19 in the hypoxic rats and the maximum vasodilator response to ACh was significantly increased from $28.2 \pm 2\%$ (of 5-HT-induced tone) in control rats to $72.1 \pm 0.2\%$ in chronic hypoxic rats (MacLean & McCulloch, 1998). A recent study has shown that there is a progressive up-regulation of the eNOS isoform in the large and small pulmonary arteries of chronic hypoxic rats during hypoxia of 2, 7 and 14 days (Demiryurek *et al.*, 2000). The level of nitrotyrosine is increased in a similar time-dependent manner to endothelial NOS (eNOS) revealing an increase in the formation of the oxidant peroxynitrite in response to hypoxia (Demiryurek *et al.*, 2000). Therefore, the compensatory mechanism of an increase of eNOS in response to PHT may exacerbate lung damage by leading to an increase in peroxynitrite formation.

3.1.2. Endogenous vasodilator mediators of pulmonary arteries:

These findings required further investigation to determine whether the increase in the maximum response and decreased pIC_{50} of ACh-induced vasodilatation in chronic hypoxic rat PRAs was mainly mediated by an increased release of NO as the results of the up-regulated eNOS would suggest or whether the release of other vasodilator mediators was also increased. An early study showed that ACh- and histamine-induced vasodilatation was mediated by two different endothelium-dependent vasodilator mediators. ACh-induced vasodilatation was inhibited by the NOS inhibitor, L-NMMA. L-NMMA also potentiated the contractile response to hypoxia in perfused rat lungs but did not inhibit histamine-induced vasodilatation, this relaxation was inhibited by the non-selective K^+ channel blocker, tetraethylammonium (TEA) (Hasunuma *et al.*, 1991). These findings suggested NO mediated ACh-induced vasodilatation and modulated the hypoxic pressor response. The histamine-induced vasodilatation may be mediated by an endothelium-derived factor which causes relaxation by hyperpolarising VSMCs beyond their resting potential termed an 'endothelium-derived hyperpolarising factor' (EDHF) (Hasunuma *et al.*, 1991). A study on the effect of pulmonary hypertension on the relaxation induced by the calcium ionophore, ionomycin, showed that the NOS inhibitor L-NOARG attenuated the relaxation response in the main and first order branches of the pulmonary artery of control sheep but did not inhibit this response in chronic hypoxic sheep vessels (Kemp *et al.*, 1995). In chronic hypoxic sheep arteries bathed in Krebs with a high K^+ concentration, L-NOARG was able to completely abolish the ionomycin-induced vasodilatation. These findings revealed the presence of a compensatory K^+ channel-mediated vasodilatation mechanism mediated by EDHF which takes over the vasodilator response in the absence of NO during PHT in sheep large pulmonary

arteries (Kemp *et al.*, 1995). Other studies have also shown that NO modulates the release of EDHF during physiological conditions but, during pathophysiological conditions, the loss of NO-induced vasodilation causes the up-regulation of EDHF and allows the EDHF to maintain vasodilator responses (Bauersachs *et al.*, 1996; McCulloch *et al.*, 1997). However, another study showed that ACh-induced relaxations in rat hepatic arteries were mediated by NO, EDHF and another endothelium-derived hyperpolarising factor generated by the cyclooxygenase pathway, probably PGI₂. This study also found that neither the cyclooxygenase product nor NO regulated EDHF release, therefore, showing that EDHF-mediated relaxation is not just a compensatory mechanism but is involved in the vasodilator response in normal physiological conditions in this vessel (Zygmunt *et al.*, 1998). A recent study showed that in, the guinea pig coronary and mammary arteries, ACh-induced relaxation was dependent on EDHF, NO and PGI₂ (Tare *et al.*, 2000). Hyperpolarisation was required for the mediation of relaxation to EDHF and PGI₂ but not for NO-mediated relaxation as its effect was not dependent on membrane potential (Tare *et al.*, 2000). These findings suggest that these arteries exhibit relaxation which is both dependent and independent of membrane potential and that these different mechanisms are important in preserving the relaxation in pathophysiological conditions (Tare *et al.*, 2000).

The endothelium-derived relaxing factor mediating ACh-induced relaxation of arterial smooth muscle was identified as being nitric oxide (NO) (Furchgott & Zawadzki, 1980). NO is synthesised in endothelial cells from L-arginine by NOS which is activated in response to the rise in [Ca²⁺]_i in response to an agonist stimulating a receptor. NO diffuses to the vascular smooth muscle cell (VSMC) where it activates

soluble guanylate cyclase to convert guanosine triphosphate (GTP) to cyclic guanosine 3'5'-monophosphate (cGMP). The rise in cGMP activates protein kinase G (PKG) which phosphorylates and subsequently inhibits targets in the VSMC. These targets include inhibiting the production of inositol triphosphate (IP₃) and diacyl glycerol (DAG) from phosphatidylinositol diphosphate (PIP₂) which inhibits the release of Ca²⁺ from intracellular stores. PKG also phosphorylates and inhibits voltage-operated Ca²⁺ channels resulting in the inhibition of the influx of Ca²⁺ from the extracellular space. This results in a decrease [Ca²⁺]_i which leads to a decrease in the Ca²⁺-calmodulin complex and a decrease in myosin light chain kinase (MLCK). This results in the inactivation of the contractile proteins and a subsequent relaxation of the vascular smooth muscle. There is also evidence that NO can activate K⁺ channels either directly or indirectly via PKG (Barnes & Belvisi, 1993; Hasunuma *et al.*, 1991; Bolotina *et al.*, 1994; Zygmunt *et al.*, 1998; Jiang *et al.*, 2000; and Tare *et al.*, 2000). Therefore, NO may play a role in mediating the vasodilatation to ACh in the control and chronic hypoxic rat small muscular PRAs.

Prostacyclin (PGI₂) is an arachidonic acid metabolite synthesised by cyclo-oxygenase (COX) in endothelial cells which is activated by a rise in [Ca²⁺]_i in response to an agonist stimulating a surface-bound receptor. There are 2 isozymes of COX, COX-1 and COX-2, which are differentially expressed in different cells. COX-1 is a constitutive enzyme found in most cells. COX-2 is an inducible enzyme found in inflammatory cells which is stimulated by the release of cytokines (Meade *et al.*, 1993; Mitchell *et al.*, 1993). Therefore, the isozyme producing PGI₂ in the endothelial cells is COX-1.

PGI₂ diffuses into the VSMC where it activates the IP receptor which is coupled to a G_s protein which activates soluble adenylate cyclase (AC) to convert adenosine triphosphate (ATP) to cyclic adenosine 3'5'-monophosphate (cAMP). The rise in cAMP activates protein kinase A (PKA) which phosphorylates and subsequently inhibits targets in the VSMC. These targets include inhibiting the production of inositol triphosphate (IP₃) and diacyl glycerol (DAG) from phosphatidylinositol diphosphate (PIP₂) which inhibits the release of Ca²⁺ from intracellular stores. PKA also phosphorylates and inhibits voltage-operated Ca²⁺ channels which inhibits the influx of Ca²⁺ from the extracellular space. This results in a decrease [Ca²⁺]_i which leads to a decrease in the Ca²⁺-calmodulin complex and a decrease in myosin light chain kinase (MLCK). PKA decreases the sensitivity of MLCK to Ca²⁺ as well as decreasing its activation by Ca²⁺-calmodulin complex. This results in the inactivation of the contractile proteins and a subsequent relaxation of the vascular smooth muscle. There is also evidence that PGI₂ can activate K⁺ channels either directly or indirectly via PKA (Voelkel *et al.*, 1991; Zygmunt *et al.*, 1998; Gambone *et al.*, 1997; Jiang *et al.*, 2000; Tare *et al.*, 2000). Therefore, PGI₂ may be involved in mediating the ACh-induced relaxation of control and chronic hypoxic rat small muscular PRAs.

It has been suggested that EDHF may mediate vasodilatation via K⁺ channel-mediated hyperpolarization which reduces Ca²⁺ influx into VSMC's via voltage-dependent Ca²⁺ channels. This could have an important action in small PRAs as the VSMC phenotype found in vessels of this size are more dependent on Ca²⁺ influx to mediate contraction compared to the VSMC phenotype found in the large arteries (Garland *et al.*, 1995). The identity of EDHF has not yet been elucidated but it has been postulated that EDHF could be one of a number of arachidonic acid,

epoxyeicosatrienoic acid or eicosapentaenoic acid metabolites produced by cytochrome P-450 epoxygenase, or even K^+ itself (Bauersachs *et al.*, 1996; McCulloch *et al.*, 1997; Edwards *et al.*, 1998; Quilley & McGiff, 2000; Dora & Garland, 2001; Zhang *et al.*, 2001). Previous studies have shown that EDHF can mediate relaxation and hyperpolarization of vascular smooth muscle by activating the Na^+ - K^+ ATPase pump or different types of K^+ channels depending on the artery being studied and the agonist used to induce vasodilatation (Garland *et al.*, 1995; Chen & Cheung, 1997; Gambone *et al.*, 1997; Zygmunt *et al.*, 1998; Jiang *et al.*, 2000). Previous studies have shown that the presence of EDHF-mediated relaxation and hyperpolarization gains a greater significance as the size of the vessel being studied decreases (Shimokawa *et al.*, 1996). Therefore, it might be expected that EDHF has a role in mediating the ACh-induced vasodilatation of small muscular pulmonary arteries of the control and chronic hypoxic rat.

These studies led to the investigation of the roles of NO, PGI_2 and EDHF in the mediation of ACh-induced vasodilatation and whether the relative importance of these individual mediators changes with respect to chronic hypoxia in the small muscular PRAs of the rat.

3.2. Methods

Wistar rats were placed in a hypobaric chamber at 30 days old. The chamber was depressurized to 550mbars over a period of 48 hours. When the chamber was at 550mbars, the oxygen concentration was at 10%. The temperature of the chamber was maintained at $\sim 21^{\circ}\text{C}$ with a ventilation rate of 45 L/min. The rats remained in these hypoxic conditions for 14 days and sacrificed upon removal from the chamber. Age-matched controls were kept in room air for the same time period (MacLean *et al.*, 1995; and MacLean & McCulloch, 1998). The right ventricle was dissected free from the left ventricle and septum, blotted carefully with a tissue and then weighed. The ratio of right ventricular (R.V.) weight / left ventricular + septum (L.V. + S) weight is calculated to assess the presence of PHT (Hunter *et al.*, 1974; Leach *et al.*, 1977; MacLean & McCulloch, 1998). This has recently been confirmed by direct measurement of right ventricular pressure (Keegan *et al.*, 2001).

The rats were killed by an overdose of sodium pentobarbitone by intra-peritoneal injection. The thorax was opened and the heart and lungs were dissected free then placed in ice cold Krebs. Second order intralobal small muscular resistance arteries ($< 250\mu\text{m}$) were dissected out of the lung tissue and carefully cleaned of surrounding parenchyma with the aide of a microscope. The vessels from both groups of rat were taken from the same region of the left lobe of the lung. The vessels were trimmed to a length of 2mm before passing two wires ($40\mu\text{m}$ in diameter) through the lumen of the vessel and mounting it on a wire myograph (Mulvaney & Halpern, 1977). The myography bath contained Krebs solution at 37°C and bubbled with 16% O_2 / 5% CO_2 / balance N_2 from a gas pipe connected to a Douglas bag. Previous studies have measured the gas tensions in the baths using these parameters and found the O_2

tension to be 120 mmHg and CO₂ tension to be 35 mmHg, which is equivalent to the gas tensions seen in the alveolar and pulmonary arteries *in vivo* (MacLean & McCulloch, 1998).

The vessels were left to equilibrate for an hour after being mounted in the baths. Tension was carefully applied to the vessels so that the control rat vessels were set at ~ 16 mmHg and the hypoxic rat vessels were set at ~ 36 mmHg, tensions which are equivalent to those experienced by the vessels *in vivo* (Herget *et al*, 1978; MacLean & McCulloch, 1998). After the tension was stabilised at appropriate level, the vessels were left to equilibrate for a further 45 minutes. The viability of the vessels was then assessed by the addition of 50mM KCl to the baths. Once the vasoconstriction had levelled off, the baths were washed out several times until the tension had returned to the baseline. The KCl addition was repeated until two reproducible vasoconstrictions were obtained. The viability of the endothelium was then assessed by vasoconstriction of the vessels with 30µM 5-HT and subsequent vasodilatation by 1µM ACh. However, the vessels displayed desensitization to 5-HT when it was used to pre-constrict the vessels for the main experiment. ET-1 could not be used to vasoconstrict the vessels to determine endothelial integrity as ET-1 is resistant to wash out and would interfere with the main experiment (Maguire *et al.*, 2000). Therefore, it was assumed that the vessels all had an intact endothelium. This assumption was proved during the experiment by the ACh-induced vasodilatation.

The submaximal doses of 30µM 5-HT and 10µM 5-HT, in the control and hypoxic Wistar rats respectively, were used to pre-constrict the vessels before a cumulative concentration response curve (CCRC) to ACh was conducted. A lower dose of 5-HT

was used in the chronic hypoxic rats as it has been shown that the presence of hypoxia-induced PHT increases the 5-HT response (MacLean & Morecroft, 2001). Some subsets of vessels were incubated with an inhibitor of various vasodilator mediators to assess the mechanisms behind ACh-induced vasodilatation in the small muscular pulmonary arteries. A subset of the vessels was pre-constricted to 5-HT and left as time controls. Some vessels were pre-constricted to 5-HT before the CCRC to ACh was conducted. Some were incubated for an hour with 0.1mM of the nitric oxide synthase (NOS) inhibitor, L-NAME, before the 5-HT pre-constriction and ACh CCRC to determine the role of NO in the ACh-induced vasodilatation. A subset of vessels was incubated for an hour with 1 μ M of the cyclooxygenase (COX) inhibitor, indomethacin, before the 5-HT pre-constriction and ACh CCRC. As well as having a differential distribution, the two COX isozymes are differentially sensitive to various nonsteroidal anti-inflammatory drugs (NSAIDs) and are pharmacologically distinct. Indomethacin preferentially inhibits COX-1, the isozyme responsible for the production of PGI₂, thromboxane A₂ (TXA₂), PGF₂, PGD₂, and PGE₂ in the endothelial cells. Therefore, indomethacin was used to inhibit PGI₂ synthesis in this study. This was to determine the role of PGI₂ in the ACh-induced vasodilatation.

Another group of vessels was incubated for an hour with 0.1 μ M of two K⁺ channel inhibitors. One of the K⁺ channel inhibitors used is an inhibitor of the large and intermediate conductance Ca²⁺-activated K⁺ channels (BK_{Ca} and IK_{Ca}) inhibitor, charybdotoxin (ChTX), and the other inhibitor used is an inhibitor of the small conductance Ca²⁺-activated K⁺ channels (SK_{Ca}), apamin. These K⁺ channel inhibitors were used to investigate the role of endothelium-derived hyperpolarizing factor

(EDHF) in the vasodilator effects of ACh. Two subsets of vessels were pre-constricted with 50mM KCl instead of 5-HT, with one set being left as a KCl time control and the other set undergoing a CCRC to ACh to investigate further the possible role of EDHF as mediator of ACh-induced vasodilatation, as high concentrations of KCl has been shown to inhibit EDHF release.

3.3. Results

3.3.1. Presence of pulmonary hypertension:

The right ventricular to left ventricular + septum ratio is a reliable index for the presence of PHT (Hunter *et al.*, 1974; Leach *et al.*, 1977). Previous studies have shown that 14 days of hypobaric treatment was sufficient to cause PHT in rats as the ratio was significantly greater in the hypoxic rats when compared with control rats (MacLean *et al.*, 1995; and MacLean & McCulloch, 1998). The results from this present study show that the ratio is significantly greater in the hypoxic rats ($P < 0.001$) when compared with control rats (**Table 3.1**). This demonstrates that the hypoxic rats in this study had developed significant PHT. **Tables 3.4** and **3.5** demonstrate an equivalent contractile response to 50mM KCl and 30 μ M 5-HT in the different protocol groups of control rat PRAs.

Experimental Group	Control Wistar Rat	Hypoxic Wistar Rat
R.V. / L.V. + S Ratio	0.22 ± 0.01	0.31 + 0.01***
n = number	n = 12	n = 11

Table 3.1: Measurement of the right ventricle (R.V.) /left ventricle + septum

(L.V. + S) ratio in the control and hypoxic Wistar rat groups. Data expressed as mean ± SEM. n = number of individual heart preparations. Statistical comparison was made using Students' unpaired t-test. $P < 0.001^{***}$ vs. control rat ratio.

3.3.2. Differences between the ACh-induced vasodilatation in control and hypoxic rats:

Previous studies have shown that the 5-HT-induced vasoconstrictor response is enhanced in PRAs from chronic hypoxic rats (MacLean *et al.*, 1996; MacLean & Morecroft, 2001). Therefore, these studies were used to determine the concentration of 5-HT that should be used to pre-constrict PRAs from the control (30µM) and chronic hypoxic (10µM) rats. However, despite the use of different concentrations of 5-HT to induce pre-constriction in the control and chronic hypoxic rat PRAs, the final tone achieved was higher in the hypoxic rat PRAs (see **Table 3.5** and **Table 3.9**). There was a significant augmentation in the 5-HT pre-constriction achieved in the 5-HT time control ($P < 0.05$) and apamin & charybdotoxin ($P < 0.01$) protocol groups from hypoxic rats when compared to the pre-constriction achieved by 5-HT in the control protocol groups.

There was no significant difference between the potency of ACh in the control and hypoxic Wistar rats. These results are shown in **Table 3.2**. However, there was a significant difference between the maximum vasodilator response to ACh in the control and hypoxic Wistar rat PRAs as the maximum relaxation response is greatly augmented in the hypoxic rat ($P < 0.01$). These results are displayed in **Table 3.3**. The ACh-induced relaxation response in control and chronic hypoxic rat PRAs is shown in **Figure 3.1**.

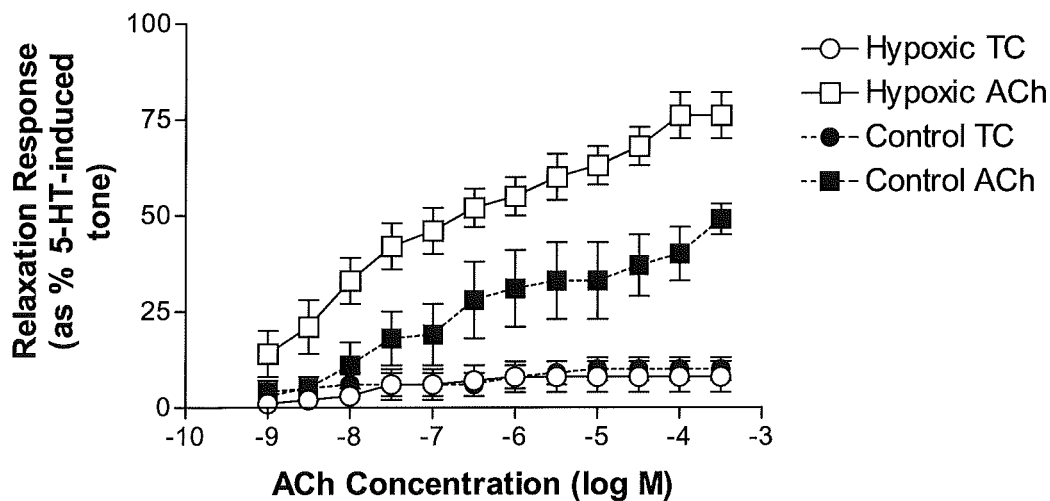


Figure 3.1: Vasodilator response to ACh in the control and chronic hypoxic Wistar rat PRAs. Control 5-HT time control (TC) (n=6); control ACh (n=6); hypoxic 5-HT time control (TC) (n=8); hypoxic ACh (n=8). Data expressed as percentage of 30 μ M and 10 μ M 5-HT-induced tone respectively. Each point represents the mean \pm SEM. n = number of individual PRAs from the same number of individual lung preparations.

Protocol Group	pEC₅₀ value	n number
Control ACh	6.38 ± 0.63	n= 6
Hypoxic ACh	7.71 ± 0.30 ^{ns}	n = 8

Table 3.2: pEC₅₀ values for ACh in control and hypoxic Wistar rat PRAs. Data are expressed as mean ± SEM. n = number of individual PRAs from the same number of lung preparations. Statistical comparison was made using Students' t-test. ns = not significant vs. control rat ACh pEC₅₀.

Protocol Group	Max. relaxation	n number
Control ACh	40 ± 7	n= 6
Hypoxic ACh	76 ± 6**	n = 8

Table 3.3: Maximum ACh-induced relaxation response values in control and hypoxic Wistar rat PRAs as % of 30 and 10µM 5-HT-induced tone respectively. Data expressed as mean ± SEM. n = number of individual PRAs from the same number of individual lung preparations. Statistical comparison was made using Students' t-test. $P < 0.01^{**}$ vs. control rat ACh-induced maximum vasodilator response.

3.3.3. Control Wistar rat PRAs:

ACh induced vasodilatation in control Wistar rat PRAs with a pEC_{50} of 6.38 ± 0.63 ($n = 6$) and a maximum relaxation response of $40 \pm 7\%$ (as % of 5-HT-induced tone). A summary of pEC_{50} values are shown in **Table 3.6**. The ACh-induced vasodilatation was significantly different from the time control fall off of tone ($P < 0.01$). The vasodilator responses to ACh are displayed in **Figure 3.2**.

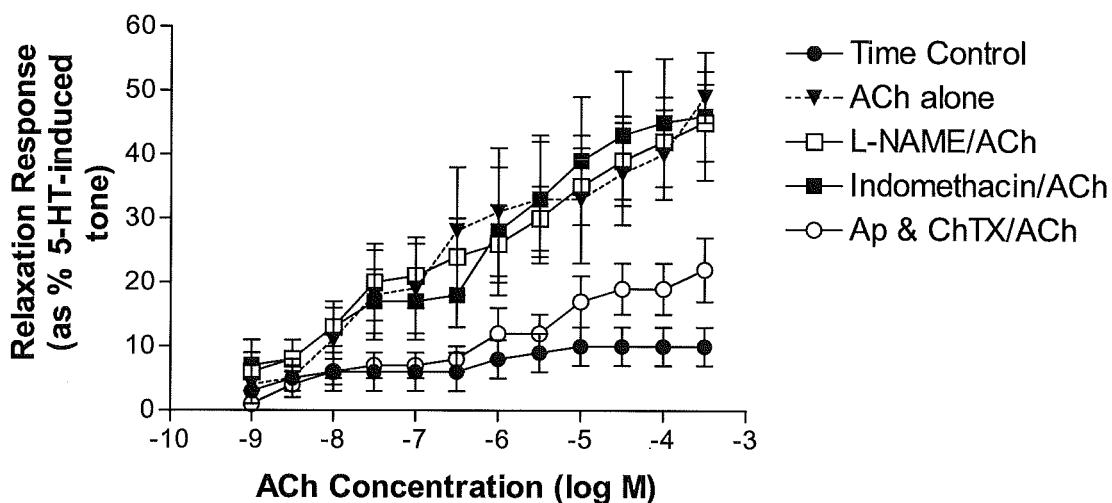


Figure 3.2: Vasodilator response to ACh in the control Wistar rat PRAs in the presence and absence of various vasodilator inhibitors. 5-HT Time control ($n=6$); ACh alone ($n=6$); L-NAME ($n=6$); indomethacin ($n=6$); and apamin (Ap) & charybdotoxin (ChTX) ($n=6$). Data expressed as percentage of $30\mu\text{M}$ 5-HT-induced tone. Each point represents the mean \pm SEM. $n =$ number of individual PRAs from the same number of individual lung preparations.

ACh induced vasodilatation in control Wistar rat PRAs with a pEC_{50} of 6.38 ± 0.63 ($n = 6$) and a maximum relaxation response of $40 \pm 7\%$ (as % of 5-HT-induced tone). A summary of pEC_{50} values are shown in **Table 3.6**. The ACh-induced

vasodilatation was significantly different from the time control fall off of tone ($P < 0.01$). The vasodilator responses to ACh are displayed in **Figure 3.2**.

ACh-induced vasodilatation in the presence of $100\mu\text{M}$ of the NOS inhibitor L-NAME ($n=6$), was significantly different from the fall off in tone ($P < 0.01$). There was no significant decrease in the potency of ACh in the presence of L-NAME. A summary of the pEC_{50} values can be seen in **Table 3.6**. There was no attenuation of the relaxation response to ACh in the presence of L-NAME, nor was there any significant difference between the vasodilatation effected at any given concentration of ACh. A summary of these results is shown in **Table 3.7**. The presence of L-NAME did not affect the basal tone of the control rat PRAs.

ACh-induced vasodilatation was significantly different from the fall off of tone in the presence of $1\mu\text{M}$ of the COX inhibitor, indomethacin ($n=6$) ($P < 0.01$). There was no significant decrease in the potency of ACh in the presence of indomethacin. A summary of the pEC_{50} values can be seen in **Table 3.6**. There was no attenuation of the relaxation response to ACh in the presence of indomethacin, nor was there any significant difference between the vasodilatation effected at any given concentration of ACh. A summary of these results is shown in **Table 3.7**. The presence of indomethacin had no effect on the basal tone of the control rat PRAs.

ACh-induced vasodilatation in the presence of $0.1\mu\text{M}$ of K_{Ca} channel blockers, apamin & charybdotoxin (ChTX) ($n=6$), was not significantly different from the fall off in 5-HT-induced tone. As there was no real relaxation response in the vessels incubated with these K_{Ca} channel blockers, the pEC_{50} could not be calculated. A

summary of pEC₅₀ values can be seen in **Table 3.6**. However, there was a significant attenuation of the maximum vasodilator response to ACh in the presence of apamin and ChTX ($P < 0.05$). A summary of these results is shown in **Table 3.7**. The presence of apamin and ChTX did not affect the basal tone of the control rat PRAs.

Protocol Group	5-HT Time Control	ACh alone	L-NAME	Indomethacin	Apamin & ChTX	KCl Time Control	KCl / ACh
KCl-induced Constriction (mN)	2.81 ± 0.70	4.03 ± 1.23	3.17 ± 0.38	3.54 ± 0.60	3.93 ± 0.67	1.50 ± 0.30	1.63 ± 0.24
Vessel Size (µm)	198 ± 15	192 ± 11	210 ± 16	212 ± 12	173 ± 17	221 ± 16	199 ± 25
n = number	n = 6	n = 6	n = 6	n = 6	n = 6	n = 4	n = 4

Table 3.4: Dimensions and measurements of 50mM KCl-induced tone achieved in the various protocol groups before antagonists added. Data expressed as mean ± SEM. n = number of individual PRAs from the same number of individual lung preparations.

Protocol Group	5-HT Time Control	ACh alone	L-NAME / hU-II	Indomethacin	Apamin & ChTX
5-HT-Induced Pre-tone (mN)	0.87 ± 0.09	1.17 ± 0.36	1.30 ± 0.31	1.24 ± 0.21	1.06 ± 0.11
n = number	n = 6	n = 6	n = 6	n = 6	n = 6

Table 3.5: Measurements of 30 μ M 5-HT-induced pre-constriction achieved in the PRAs of various protocol groups from control Wistar rats. Data expressed as mean \pm SEM. n = number of individual PRAs from the same number of individual lung preparations.

Protocol Group	pEC ₅₀ value	n number
ACh alone	6.38 ± 0.63	n= 6
L-NAME / ACh	6.65 ± 0.59 ^{ns}	n = 6
Indomethacin / ACh	6.64 ± 0.58 ^{ns}	n = 6
Apamin & ChTX / ACh	Not Calculated	n = 6

Table 3.6: pEC₅₀ values for ACh ± various vasodilator inhibitors in control Wistar rat PRAs. Data are expressed as mean ± SEM. n = number of individual PRAs from the same number of lung preparations. Statistical comparisons were made using one-way ANOVA with a Dunnetts' post-test. ns = not significant vs. ACh control.

The raising of tone in small resistance arteries with 50mM KCl has been shown to inhibit the release of endothelium-derived hyperpolarising factor (EDHF). Therefore, experiments were conducted in which the tone of the arteries was raised by the addition of 50mM KCl instead of 30µM 5-HT before conducting the ACh CCRC. There was no significant difference in the relaxation response induced by ACh in the KCl/ACh protocol group compared to the fall off of tone in the KCl time control group at any given concentration of ACh (both n=4). However, the ACh-induced vasodilatation after pre-constriction with KCl is significantly less than the relaxation effected by ACh after 5-HT pre-constriction ($P < 0.01$) at the highest concentration

of ACh. A summary of these results is shown in **Table 3.7**. There is no graph of these results as the decrease in KCl-induced pre-constriction was so small as to be difficult to distinguish from the x axis of the graph.

ACh Bath Conc ⁿ	5-HT / L-NAME	5-HT / Indomethacin	5-HT / Ap & ChTX	KCl / ACh
-9	6 ± 3 ^{ns}	7 ± 4 ^{ns}	1 ± 1 ^{ns}	0 ± 0
-8.5	8 ± 3 ^{ns}	8 ± 3 ^{ns}	4 ± 2 ^{ns}	0 ± 0
-8	13 ± 3 ^{ns}	13 ± 4 ^{ns}	6 ± 2 ^{ns}	0 ± 0
-7.5	20 ± 6 ^{ns}	17 ± 5 ^{ns}	7 ± 2 ^{ns}	0 ± 0
-7	21 ± 5 ^{ns}	17 ± 5 ^{ns}	7 ± 2 ^{ns}	1 ± 1 ^{ns}
-6.5	24 ± 6 ^{ns}	18 ± 5 ^{ns}	8 ± 2*	1 ± 1*
-6	26 ± 6 ^{ns}	28 ± 10 ^{ns}	12 ± 4*	1 ± 1*
-5.5	30 ± 5 ^{ns}	33 ± 9 ^{ns}	12 ± 3*	1 ± 1*
-5	35 ± 6 ^{ns}	39 ± 10 ^{ns}	17 ± 4*	1 ± 1*
-4.5	39 ± 7 ^{ns}	43 ± 10 ^{ns}	19 ± 4*	1 ± 1*
-4	42 ± 7 ^{ns}	45 ± 10 ^{ns}	19 ± 4*	1 ± 1*
-3.5	42 ± 7 ^{ns}	47 ± 10 ^{ns}	19 ± 4*	1 ± 1**

Table 3.7: Control rats: The measurement of vasodilatation as % of 30µM 5-HT- or 50mM KCl-induced tone effected at each point in the ACh CCRC. L-NAME (n=6); indomethacin (n=6); apamin (Ap) & charybdotoxin (ChTX) (n=6); and KCl/ACh (n=6). Data expressed as mean ± SEM. Statistical comparisons were made using a one-way ANOVA with a Dunnetts' post-test. $P < 0.5^*$, $P < 0.01^{**}$ vs. ACh control. ns = not significant.

3.3.4. Hypoxic Wistar rat PRAs:

ACh induced vasodilatation in hypoxic Wistar rat PRAs with a pEC_{50} of 7.71 ± 0.30 ($n = 8$) and a maximum relaxation response of $76 \pm 6\%$ (as % of 5-HT-induced tone). The ACh-induced vasodilatation in chronic hypoxic rats is compared with that observed in the control rats later in the results section. A summary of pEC_{50} values are shown in **Table 3.10**. The ACh-induced vasodilatation was significantly different from the time control fall off of tone ($P < 0.01$). The vasodilator responses to ACh are displayed in **Figure 3.3**.

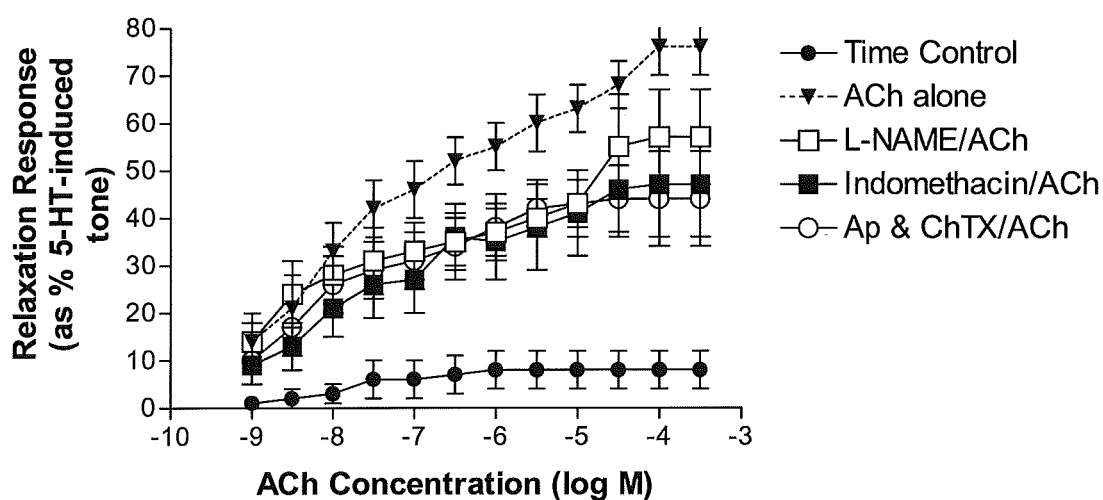


Figure 3.3: Vasodilator response to ACh in the hypoxic Wistar rat PRAs in the presence and absence of various vasodilator inhibitors. 5-HT Time control ($n=8$); ACh alone ($n=8$); L-NAME ($n=6$); indomethacin ($n=8$); and apamin & charybdotoxin ($n=7$). Data expressed as percentage of $10\mu\text{M}$ 5-HT-induced tone. Each point represents the mean \pm SEM. n = number of individual PRAs from the same number of individual lung preparations.

Tables 3.8 and 3.9 demonstrate an equivalent contractile response to 50mM KCl and 10 μ M 5-HT in the different protocol groups of chronic hypoxic rat PRAs. However, the contraction to 50mM KCl in the indomethacin and KCl/ACh protocol groups is significantly smaller than that observed in the protocol group treated with ACh alone ($P < 0.05$).

Protocol Group	5-HT Time Control	ACh alone	L-NAME	Indomethacin	Apamin & ChTX	KCl Time Control	KCl / ACh
KCl-induced Constriction (mN)	4.25	4.80	5.08	1.63	4.72	1.70	2.04
	\pm 1.31	\pm 1.09	\pm 0.91	\pm 0.31*	\pm 0.94	\pm 0.43*	\pm 0.33
Vessel Size (μm)	135	147	160	168	156	176	158
	\pm 11	\pm 13	\pm 14	\pm 14	\pm 18	\pm 30	\pm 26
n = number	n = 8	n = 8	n = 6	n = 8	n = 7	n = 4	n = 4

Table 3.8: Dimensions and measurements of 50mM KCl-induced tone achieved in the various protocol groups. Data expressed as mean \pm SEM. n = number of individual PRAs from the same number of individual lung preparations.

Protocol Group	5-HT Time Control	ACh alone	L-NAME	Indomethacin	Apamin & ChTX
5-HT-induced Pre-tone (mN)	2.55 ± 0.58	2.40 ± 0.69	3.25 ± 1.31	1.16 ± 0.25	3.68 ± 0.58
n = number	n = 8	n = 8	n = 6	n = 8	n = 7

Table 3.9: Measurements of 10 μ M 5-HT-induced pre-constriction achieved in the PRAs of various protocol groups from hypoxic Wistar rats. Data expressed as mean \pm SEM. n = number of individual PRAs from the same number of individual lung preparations.

ACh-induced vasodilatation in the presence of 0.1mM of the NOS inhibitor, L-NAME (n=6), was significantly different from the fall off of tone at 0.3mM ACh ($P < 0.01$). The vasodilator response to ACh in the presence of L-NAME is displayed in **Figure 3.3**. There was no significant decrease in the potency of ACh in the presence of L-NAME. A summary of the pEC₅₀ values can be seen in **Table 3.10**. There was no attenuation of the maximum relaxation response to ACh in the presence of L-NAME, however, there was a significant difference between the vasodilatation effected between 0.3 μ M-3 μ M ACh ($P < 0.05$). A summary of these results is shown in **Table 3.11**. The presence of L-NAME caused a 5 \pm 1% increase in the basal tone of the chronic hypoxic rat PRAs.

ACh-induced vasodilatation in the presence of 1 μ M of the COX inhibitor, indomethacin (n=8), was significantly different from the fall off of tone at 0.3mM

ACh ($P < 0.01$). The vasodilator response to ACh in the presence of indomethacin is displayed in **Figure 3.3**. There was no significant decrease in the potency of ACh in the presence of indomethacin. A summary of the pEC_{50} values can be seen in **Table 3.10**. There was a significant attenuation of the maximum relaxation response to ACh in the presence of indomethacin, and there were significant differences between the vasodilatation effected by 30 M and 0.3mM of ACh ($P < 0.05$). A summary of these results is shown in **Table 3.11**. The presence of indomethacin did not affect the basal tone of the chronic hypoxic rat PRAs.

ACh-induced vasodilatation in the presence of 0.1 μ M of K_{Ca} channel blockers, apamin & charybdotoxin (ChTX) (n=7), was significantly different from the fall off of 5-HT-induced tone ($P < 0.01$). The vasodilator response to ACh in the presence of apamin & charybdotoxin is displayed in **Figure 3.3**. There was no significant decrease in the potency of ACh in the presence of apamin & ChTX. A summary of pEC_{50} values can be seen in **Table 3.10**. However, there was a significant attenuation of the maximum vasodilator response to ACh in the presence of apamin and ChTX and in the relaxation effected between 0.3 μ M – 0.3mM ($P < 0.05$). The K_{Ca} channel blockers significantly inhibited the relaxation response at concentrations of 0.3 μ M-0.3mM of ACh. A summary of these results is shown in **Table 3.11**. The presence of apamin and ChTX did not affect the basal tone of the chronic hypoxic rat PRAs.

Protocol Group	pEC ₅₀ value	n number
ACh alone	7.71 ± 0.30	n= 8
L-NAME/ ACh	7.82 ± 0.39 ^{ns}	n = 6
Indomethacin / ACh	7.23 ± 0.44 ^{ns}	n = 8
Apamin & ChTX / ACh	7.38 ± 0.41 ^{ns}	n = 7

Table 3.10: pEC₅₀ values for ACh ± various vasodilator inhibitors in hypoxic Wistar rat PRAs. Data are expressed as mean ± SEM. n = number of individual PRAs from the same number of lung preparations. Statistical comparisons were made using a one-way ANOVA with a Dunnetts' post-test. ns = not significant vs. ACh control.

The raising of tone in small resistance arteries with KCl has been shown to inhibit the release of endothelium-derived hyperpolarising factor (EDHF). Therefore, experiments were conducted in which the tone of the arteries was raised by the addition of 50mM KCl instead of 10µM 5-HT before conducting the ACh CCRC. There was no significant difference in the relaxation response induced by ACh in the KCl/ACh protocol group compared to the fall off of tone in the KCl time control group at any given concentration of ACh (both n=4). However, the ACh-induced vasodilatation after pre-constriction with KCl is significantly less than the relaxation effected by ACh after 5-HT pre-constriction ($P < 0.01$) at the highest concentration of ACh. Therefore, the pre-constriction of hypoxic PRAs with 50mM KCl inhibits any

subsequent relaxation response to ACh, an effect not seen when the PRA is pre-constricted with 10 M 5-HT. A summary of these results is shown in **Table 3.11**.

Ach Bath Conc ⁿ	5-HT / L-NAME	5-HT / Indomethacin	5-HT / Ap & ChTX	KCl / ACh
-9	14 ± 4 ^{ns}	9 ± 4 ^{ns}	10 ± 5 ^{ns}	0 ± 0
-8.5	24 ± 7 ^{ns}	13 ± 5 ^{ns}	17 ± 6 ^{ns}	0 ± 0
-8	28 ± 6 ^{ns}	21 ± 6 ^{ns}	26 ± 6 ^{ns}	0 ± 0*
-7.5	31 ± 7 ^{ns}	26 ± 7 ^{ns}	29 ± 6 ^{ns}	0 ± 0*
-7	33 ± 6 ^{ns}	27 ± 7 ^{ns}	31 ± 6 ^{ns}	1 ± 1**
-6.5	35 ± 5*	36 ± 7 ^{ns}	34 ± 7*	1 ± 1**
-6	37 ± 5*	35 ± 8 ^{ns}	38 ± 7*	1 ± 1**
-5.5	40 ± 4*	38 ± 9 ^{ns}	42 ± 6*	1 ± 1**
-5	43 ± 5 ^{ns}	41 ± 9 ^{ns}	43 ± 7*	1 ± 1**
-4.5	55 ± 11 ^{ns}	46 ± 10*	44 ± 7*	1 ± 1**
-4	57 ± 10 ^{ns}	47 ± 11*	44 ± 10*	1 ± 1**
-3.5	58 ± 10 ^{ns}	47 ± 9*	44 ± 10*	2 ± 1**

Table 3.11: Chronic hypoxic rat: The measurement of vasodilatation as % of 10 M 5-HT- or 50mM KCl-induced tone effected at each point in the ACh CCRC in chronic hypoxic rat PRAs.. L-NAME (n=6); indomethacin (n=8); apamin (Ap) & charybdotoxin (ChTX) (n=7); and KCl/ACh (n=4). Data expressed as mean ± SEM. Statistical comparisons were made using a one-way ANOVA with a Dunnetts' post-test. $P < 0.5^*$, $P < 0.01^{**}$ vs. ACh control. ns = not significant.

3.4. Discussion

3.4.1. Chronic hypoxic rat model of PHT:

The right ventricular to left ventricular + septum ratios of the rats used in this study display the presence of significant right ventricular hypertrophy in the hypoxic Wistar rats. Therefore, the treatment of rats for 14 days in a hypobaric chamber produces a reliable and useful animal model of primary PHT (MacLean *et al.*, 1995; MacLean & McCulloch, 1998).

3.4.2. ACh-induced vasodilatation in control and chronic hypoxic rats:

The 5-HT pre-constriction achieved was higher in the chronic hypoxic rat PRAs than in the control rat PRAs, despite using a smaller concentration of 5-HT in the chronic hypoxic rat PRAs. However, this augmentation of the 5-HT pre-constriction was only significant in the 5-HT time control and apamin & charybdotoxin protocol groups. It is not clear if this disparity would have had any influence over the results in the chronic hypoxic group. A previous study involving the chronic hypobaric hypoxia rat model revealed that the tension at which vessels were set at during wire myography experiments changed the potency of and maximum response to ET-1 and sarafotoxin (STX_{s6c}) (MacLean & McCulloch, 1998). This study showed that PRAs from control rats were more sensitive to ET-1 when set at ~16mmHg, while STX_{s6c} showed an increased maximum vasoconstrictor response when set at ~35mmHg. STX_{s6c} was more potent than ET-1 in the chronic hypoxic PRAs, but the potency of STX_{s6c} was increased further in vessels set at ~35mmHg. These results showed that the basal tone of the PRAs influenced the effect produced by STX_{s6c} and ET-1. It is unclear if the degree of 5-HT-induced tone has effected the ACh-induced relaxation, but, this limitation of the study should be remembered while reviewing these results.

A previous study regarding the ACh-induced relaxation in control and chronic hypoxic rat PRAs found that the potency of, and maximum vasodilator response to, ACh was significantly greater in the chronic hypoxic rat vessels (MacLean & McCulloch, 1998). This present study also found that the maximum relaxation response was significantly augmented in the chronic hypoxic rats, but did not find an increase in the potency of ACh in these vessels. Therefore, the vasodilator response to ACh is augmented in the presence of PHT.

3.4.3. Mediators of ACh-induced vasodilatation in control rat PRAs:

This study has revealed that the NOS inhibitor, L-NAME, did not inhibit the relaxation produced at any given concentration of ACh. L-NAME did not decrease the potency of ACh in these vessels. Therefore, NO does not play a role in mediating the vasodilator response to ACh in control rat PRAs. However, a previous study showed that there is a NO component in the ACh-induced vasodilatation in all the branches of the mesenteric arterial bed. These findings reveal a differential mediator profile of the ACh-induced relaxation depending on the vascular bed being studied (Parsons *et al.*, 1994). The inhibition of NO with 100 μ M of the NOS inhibitor, L-NAME, did not affect the basal tone of the control rat arteries. These results are in agreement with earlier studies, in both perfused whole lung preparations and isolated small muscular arteries, that showed that NO is not involved in the maintenance of the low vascular tone seen in the pulmonary circulation in control rats (Hasunuma *et al.*, 1991; MacLean & McCulloch, 1998). The findings of the present study, taken with the results from the afore mentioned studies showing no NO component in the

regulation of vascular tone in control animals, suggests that NO has no role in the regulation of the low pulmonary vascular tone or ACh-induced vasodilatation in the control rat PRAs.

The presence of indomethacin, a COX inhibitor, did not inhibit the vasodilatation effected by any given concentration of ACh. Indomethacin also failed to decrease the potency of ACh in these vessels. Therefore, COX products such as PGI₂ do not play a role in mediating the vasodilator response to ACh in control rat PRAs. There was no increase in the basal tension of the control rat PRAs after the addition of indomethacin, suggesting that basal release of prostaglandins such as PGI₂ are not the regulator of the low vascular tone of these vessels under normal physiological conditions.

The addition of the K_{Ca} channel blockers charybdotoxin and apamin, inhibitors of the large & intermediate (BK_{Ca} & IK_{Ca}) and small (SK_{Ca}) conductance channels respectively, significantly attenuated the maximum relaxation response produced by ACh in the control rat PRAs. These K⁺ channel blockers did not decrease the potency of ACh. The addition of apamin and ChTX did not affect the basal tone of the control rat PRAs, so EDHF acting via K_{Ca} channels is not involved in the regulation of the low vascular tone observed in these vessels. Raising the tone of the vessels with KCl resulted in an extremely significant inhibition of the ACh-induced vasodilatation in the control rat PRAs. Previous studies have shown that pre-constriction with KCl inhibits the activity of EDHF in the arteries of various vascular beds (Plane & Garland, 1993; Garland *et al.*, 1995; Shimokawa *et al.*, 1996; Urakami-Harasawa *et al.*, 1997; Ohlmann *et al.*, 1997). Therefore, EDHF, acting via

intermediate and small K_{Ca} channels, is a mediator of the ACh-induced vasodilatation in the control rat PRAs. These findings are in accordance with those of previous studies which showed that the presence of EDHF-mediated vasodilatation was inversely proportional to vessels size. It was shown in the mesenteric arteries of the rat that the importance of EDHF-mediated relaxation increased as the size of the vessel decreased and that EDHF-induced hyperpolarization is an essential mechanism of vasodilatation in the small resistance arteries (Garland *et al.*, 1995; Shimokawa *et al.*, 1996; Urakami-Harasawa *et al.*, 1997). These results suggest that EDHF is involved in the maintenance of the low pulmonary vascular tone in physiologically normal lungs. However, a previous study had suggested that EDHF-mediated regulation of vascular tone in the pulmonary artery is produced through the activation of K_{ATP} channels (Quayle & Standen, 1994). Therefore, it is unsurprising that EDHF, acting via IK_{Ca} and SK_{Ca} channels, mediates part of the ACh-induced vasodilatation response in the small muscular pulmonary resistance arteries. However, to really prove that EDHF is involved would require electrophysiological studies to be conducted.

EDHF has been shown to mediate vasodilatation and hyperpolarization in rat mesenteric arteries; guinea pig coronary arteries and submucosal arterioles; and human subcutaneous resistance arteries (Chen & Cheung, 1997; Coleman *et al.*, 2001; McIntyre *et al.*, 2001). However, non-NO-, non-prostanoid-dependent relaxation mediated by EDHF has been shown to act via mechanisms other than IK_{Ca} and SK_{Ca} channels in several vascular preparations in various species. Previous studies have shown that EDHF-mediate relaxation and hyperpolarization via the Na^+-K^+ ATPase

extrusion pump as ouabain inhibits the EDHF-mediated effects in the small mesenteric and renal arteries of the rat (Jiang *et al.*, 2000; Dora & Garland, 2001).

There has been considerable speculation over the identity of EDHF. It has been postulated that EDHF could be one of a number of arachidonic acid, epoxyeicosatrienoic acid or eicosapentanoic acid metabolites produced by cytochrome P-450 epoxygenase, or even K^+ itself (Bauersachs *et al.*, 1996; McCulloch *et al.*, 1997; Edwards *et al.*, 1998; Quilley & McGiff, 2000; Dora & Garland, 2001; Zhang *et al.*, 2001). Recent studies have revealed the mechanism by which EDHF released from the endothelial cells mediates hyperpolarization of the vascular smooth muscle. These studies have showed that EDHF-mediated K^+ channel activation is almost instantaneous in the endothelial and vascular smooth muscle cells suggesting that the two layers of cells act as a single syncytium due to the presence of myoendothelial gap junctions which allow the electrotonic spread of the hyperpolarization to affect the VSMC (Dora *et al.*, 1999; Harris *et al.*, 2000; Coleman *et al.*, 2001).

The results from these studies support the theory that EDHF may not be a single substance but a family of substances. It has been suggested that there may be variations in the type of EDHF released and the K^+ channels and other effector targets stimulated by its release depending on the vascular bed and species being studied (Jiang *et al.*, 2000). Therefore, the results from this study could be explained by the fact that one type of EDHF, which acts via the IK_{Ca} and SK_{Ca} channels is released from the endothelium in response to concentrations of ACh 0.3 μ M and above, and that another type of EDHF may be released to maintain the low vascular tone seen in normoxic PRAs which acts through other K^+ channels and / or Na^+-K^+ ATPase.

However, this study did not determine the other mechanisms of EDHF-induced relaxation and hyperpolarization involved in the ACh-induced vasodilatation in the control rat PRAs.

3.4.4. Mediators of ACh-induced vasodilatation in chronic hypoxic rat PRAs:

This study revealed that L-NAME significantly inhibited the ACh-induced vasodilatation between the concentrations of 0.3 μ M - 3 μ M. However, L-NAME did not decrease the potency of ACh in these vessels. These results are in contrast to the finding of a recent study which documented a decrease in the NO release and NO-mediated vasodilatation in the intrapulmonary arteries of chronic hypoxic rats (Murata *et al.*, 2001). Therefore, NO plays a significant role in mediating the ACh-induced vasodilatation in the chronic hypoxic rat PRAs. This is consistent with earlier studies showing an increased level of eNOS in the large and small pulmonary vessels from chronic hypoxic rats (Le Cras *et al.*, 1996; Demiryurek *et al.*, 2000). This increased expression of eNOS is not accompanied by a subsequent increase in ACh-induced vasodilatation in all arteries as ACh-induced relaxation is attenuated in the large pulmonary arteries while being augmented in the small PRA in the presence of hypoxia (MacLean *et al.*, 1995; MacLean & McCulloch, 1998). These observations are confirmed by the levels of cGMP found in these vessels as the levels are decreased in the large pulmonary arteries while remaining unchanged in the PRAs (MacLean *et al.*, 1996). A recent study has revealed an increase in the activity of cGMP-specific phosphodiesterase V, (PDE5), in large pulmonary arteries from chronic hypoxic rats through the *de novo* synthesis of the PDE5A2 protein, resulting in decreased levels of cGMP and subsequent attenuation of ACh-induced vasodilatation in these vessels (Murray *et al.*, in press). However, PDE5 levels

remain unchanged in the presence of hypoxia in the PRAs which accounts for the ability of ACh to induce vasodilatation in PRAs, indeed, this vasodilator effect of ACh may be augmented due to increased levels of guanylate cyclase in these vessels (Li *et al.* 1999). These findings are consistent with the previous observations that sildenafil, a selective PDE5 inhibitor, selectively induces vasodilatation of the large pulmonary arteries but does not affect the PRAs (Oka *et al.*, 2001). A recent study has also shown that mice treated with sildenafil were protected from the development of hypoxia-induced PHT (Zhao *et al.*, 2001). The presence of L-NAME revealed the higher endogenous tone of these vessels suggesting that NO is also involved in the inhibitory mechanism which attempts to compensate for the increased pulmonary vascular tone in chronic hypoxic PRAs as seen in previous studies (Hasunuma *et al.*, 1991; MacLean & McCulloch, 1998). These results agree with a previous study which found that there was a significant up-regulation of eNOS in the pulmonary arteries of chronic hypoxic rats as no involvement of NO in the ACh-induced vasodilatation was seen in the control rat PRAs. Therefore, it can be hypothesised that although the increase in NO production and release facilitates the ACh-induced relaxation of chronic hypoxic rats, there is also an increase in peroxynitrite production which may exacerbate damage to these vessels (Demiryurek *et al.*, 1998). NO mediates relaxation by activating guanylate cyclase which increases the concentration of cGMP in the vascular smooth muscle cells which activates protein kinase G which inhibits IP₃-stimulated release of intracellular Ca²⁺ resulting in relaxation. NO can mediate relaxation by activating K⁺ channels via PKG activation and that NO can also directly activate K_{Ca} channels (Hasunuma *et al.*, 1991; Bolotina *et al.*, 1994; Tare *et al.*, 2000). A previous study showed that NO caused hyperpolarization of VSMC's of the rabbit aorta independently of guanylate cyclase activation (Bolotina *et al.*,

1994). Another study investigating the mediators involved in the ACh-induced vasodilatation in the coronary and mammary arteries of the guinea-pig using an integrated approach to study the effects of NO on the tension and membrane potential of these vessels found that while NO caused hyperpolarisation of the membrane potential via K_{ATP} channels, the hyperpolarization was not important to the vasodilator effect of NO in these vessels (Rand & Garland., 1992; Tare *et al.*, 1998). As this present study did not take an integrated approach, the presence of NO-mediated hyperpolarization in response to ACh, and its relationship with the vasodilator effect of NO in the PRAs of the chronic hypoxic rat can only be speculated upon.

The presence of indomethacin, a preferential inhibitor of COX-1, significantly attenuated the vasodilatation effected by ACh at concentrations of 30 μ M and above. However, indomethacin failed to decrease the potency of ACh in these vessels. Therefore, PGI₂ does play a role in mediating the vasodilator response to ACh in chronic hypoxic rat PRAs. The incubation of chronic hypoxic rat PRAs did not result in an increase of the basal tone of these vessels. Therefore, PGI₂ is not involved in the inhibitory mechanism which attempts to compensate for the increased basal pulmonary vascular tone observed in these vessels. This result is surprising considering that prostacyclin synthase (PGI₂-S) expression has been shown to be significantly reduced in pulmonary vessels of all sizes in patients with severe primary PHT (Tuder *et al.*, 1999). Previous studies have shown that the expression of PGI₂-S can inhibit the development of PHT in various animal models. A study involving transgenic mice designed to over-express PGI₂-S showed that the transgenic mice had a lower right ventricular pressure and decreased pulmonary vascular remodelling than

non transgenic mice after chronic hypobaric hypoxia (Geraci *et al.*, 1999). Another study found that rats with monocrotaline-induced PHT showed a reduction in the mean pulmonary arterial pressure and total pulmonary vascular resistance when transfected with PGI₂-S compared to control rats (Nagaya *et al.*, 2000). There was no increase in the basal tension of the chronic hypoxic rat PRAs after the addition of indomethacin, suggesting that basal release of PGI₂ is not a regulator of the low vascular tone of the pulmonary vasculature of control or chronic hypoxic rats. PGI₂ mediates vasodilatation in the VSMCs by activating adenylate cyclase which increases cAMP which stimulates protein kinase A resulting in a reduction of intracellular calcium release and decreasing the sensitivity of the contractile apparatus to Ca²⁺ leading to VSMC relaxation (Gambone *et al.*, 1997; Zygmunt *et al.*, 1998; Tare *et al.*, 2000). Previous studies have also shown that PGI₂ can mediate hyperpolarisation in the coronary and mammary arteries of the guinea-pig, the renal artery of the rat and superior mesenteric arteries of the hamster. In rat the PGI₂-mediated hyperpolarization was resistant to inhibition by glibenclamide and / or ChTX plus apamin suggesting that the effect on membrane potential in the rat arteries were not produced via ATP-sensitive K⁺ or IK_{Ca} and SK_{Ca} channels. (Zygmunt *et al.*, 1998). In the guinea-pig arteries, the PGI₂-mediated hyperpolarisation was inhibited by glibenclamide revealing the role of K_{ATP} channels in this effect (Tare *et al.*, 2000). The PGI₂-mediated hyperpolarisation of the hamster superior mesenteric artery has also been shown to be caused by the opening of K_{ATP} channels (Thapaliya *et al.*, 2000). The integrated investigation of the guinea-pig arteries showed that, in contrast to NO, the PGI₂-mediated hyperpolarisation was important to its vasodilator effect (Tare *et al.*, 2000). As this present study was not an integrated study, the role of

PGI₂-induced hyperpolarisation and its relationship with the PGI₂-mediated vasodilatation in response to ACh was not investigated.

The addition of the K_{Ca} channel blockers charybdotoxin and apamin, inhibitors of the large & intermediate (BK_{Ca} & IK_{Ca}) and small (SK_{Ca}) conductance channels respectively, significantly attenuated the maximum relaxation response produced by 0.3µM and above of ACh in the chronic hypoxic rat PRAs. These K⁺ channel blockers did not decrease the potency of ACh. Raising the tone of the vessels with KCl resulted in an extremely significant inhibition of the ACh-induced vasodilatation in the chronic hypoxic rat PRAs. However, the concentration of KCl used in this thesis (50mM) could have resulted in such a strong depolarization that no vasodilator mediator would have elicited a relaxation. This possibility must be considered due to the fact that there was no relaxation in CH PRAs pre-constricted with KCl even though NO and PGI₂ are involved in the relaxation in these vessels. Previous studies have shown that pre-constriction with KCl inhibits the release of EDHF in the arteries of various vascular beds (Plane & Garland, 1993; Garland *et al.*, 1995; Shimokawa *et al.*, 1996; Urakami-Harasawa *et al.*, 1997; Ohlmann *et al.*, 1997). Therefore, EDHF, acting via intermediate and small K_{Ca} channels, is a mediator of the ACh-induced vasodilatation in the chronic hypoxic rat PRAs. There was no increase in the basal tension of the chronic hypoxic rat PRAs after the addition of ChTX and apamin, suggesting that basal release of EDHF acting via IK_{Ca} and SK_{Ca} channels is not a regulator of the low vascular tone of the pulmonary vasculature of control rats and is not involved in the inhibitory mechanism which attempts to compensate for the increased pulmonary vascular tone observed in chronic hypoxic rats. However, EDHF acting via other K⁺ channels or Na⁺-K⁺ ATPase may play a role in the

maintenance of the low vascular tone in the pulmonary vasculature of control and chronic hypoxic rats as previous studies have shown that other types of EDHF mediate relaxation and hyperpolarization via these mechanisms (Jiang *et al.*, 2000; Dora & Garland, 2001). It is unlikely that another type of EDHF, whose mechanism of action is not inhibited by the K_{Ca} channel blockers, was released in these vessels at concentrations of ACh below $10\mu\text{M}$ as L-NAME inhibits the ACh-induced vasodilatation between $0.3\text{-}3\mu\text{M}$.

3.4.5. Interaction of mediators involved in the ACh-induced vasodilatation:

Previous studies have displayed interactions between the endogenous vasodilator mediators in some vessels and that the role of certain mediators is only revealed when the other mediators are inhibited or lost through disease processes. Several earlier studies displayed an inhibition of EDHF-mediated effects in the presence of functional NO. NO was the mediator of ionomycin (calcium ionophore)-induced vasodilatation in large pulmonary arteries of control sheep. However, NO and EDHF mediated the relaxation to ionomycin in the large pulmonary arteries of chronic hypoxic sheep, and that the effects of EDHF are only revealed by the inhibition of NO production (Kemp *et al.*, 1995). The NOS inhibitor, L-NNA, was found to reveal an EDHF component to the ACh-mediated vasodilatation of the rabbit carotid and porcine coronary arteries (Bauersachs *et al.*, 1996). In the superior mesenteric artery of the rat, NO and EDHF mediate the vasodilatation induced by the muscarinic agonist, carbachol. The EDHF component of the relaxation was increased in the presence of L-NAME and decreased in the presence of increased levels of cGMP (McCulloch *et al.*, 1997). The results of these studies suggest that EDHF-mediated vasodilatation is merely a compensatory backup system which could maintain blood

flow and tissue perfusion should the effects of NO be lost. There has been evidence that NO release is impaired in patients with pulmonary hypertension, systemic hypertension, congenital heart disease, asthma, or in those who smoke (Barnes & Belvisi, 1993; Kharitonov *et al.*, 1994; Persson *et al.*, 1994; Schilling *et al.*, 1994; Berger *et al.*, 2001). EDHF release has also been shown to be down-regulated in the large human arteries in patients who were effected by old age, hypertension, or diabetes (Urakami-Harasawa *et al.*, 1997; Coleman *et al.*, 2001). However, another study found that EDHF was not modulated by the release of NO and was, therefore, not merely a compensatory vasodilator mechanism in the rat hepatic artery (Zygmunt *et al.*, 1998). A previous study in canine large pulmonary arteries found that NO and PGI₂ synergistically mediated the bradykinin-induced vasodilatation of these arteries. This synergy was abolished by the K_{ATP} channel inhibitor glibenclamide (Gambone *et al.*, 1997). However, this vasodilator mediator profile was not observed in these vessels when the agonist inducing vasodilatation was ACh or the calcium ionophore, A23187. These results suggest that the vascular bed and species of animal the vessels are being studied from shows variation in whether there is antagonism or synergy between the vasodilator mediators as well as influencing which mediators are released in response to agonist-induced stimulation. This present study did not investigate the possibility of vasodilator mediator interaction by combining the inhibitors of two or more mediators at the same time. However, the fact that NO, PGI₂, and EDHF all play a part in the ACh-mediated relaxation of chronic hypoxic rat PRAs suggests that there is no inhibition of EDHF-mediated effects in these vessels. Therefore, EDHF does not appear to be a compensatory back up system for NO and PGI₂-mediated relaxation.

The involvement of all three endogenous mediators in one vessel would ensure the maintenance of blood flow in the event of a loss of one of these vasodilator pathways due to disease (Zygmunt *et al.*, 1998; Tare *et al.*, 2000). The fact that the small muscular pulmonary arteries of the chronic hypoxic rat exhibit the involvement of all three mediators when compared with the same vessels from the control rat may reflect the need for a greater vasodilator capacity to counterbalance the raised endogenous tone found in the hypoxic lungs and the importance of keeping these arteries open ensuring adequate perfusion of the alveoli.

3.5. Conclusion

EDHF is the mediator of ACh-induced relaxation in the control rat PRAs. This effect is mediated partly by activation of IK_{Ca} and SK_{Ca} channels. However, other types of EDHF acting through other K^+ channels and the Na^+-K^+ ATPase pump may mediate the low vascular tone observed in control rat PRAs.

NO, PGI_2 , and EDHF all play a role in the ACh-induced vasodilatation of chronic hypoxic rat PRAs. EDHF appears to be mainly mediated through the K_{Ca} channels in these vessels. The involvement of all three mediators in the relaxation response in chronic hypoxic but not control rat PRAs may be a protective mechanism to ensure the adequate perfusion of the alveoli despite a greater level of endogenous tone in these vessels.

Chapter 4

**Effect of human urotensin-II on
human small muscular resistance
arteries of the pulmonary and
systemic circulations**

4.1.1. History of urotensin-II:

Urotensin-II (U-II) is a cyclic peptide first isolated from the caudal neurosecretory system of the goby fish (*Gillichthys mirabilis*) (Bern & Lederis, 1969). Goby U-II is a 12 amino acid residue peptide (see **Figure 4.1**) (Davenport & Maguire, 2000). As well as inducing widespread contraction of smooth muscle in fish, goby U-II has been shown to elicit a vasoactive response in the vascular smooth muscle of isolated mammalian arteries from species such as the rat (Gibson, 1987; Itoh *et al.*, 1987). Previous studies using rat major arteries, particularly the thoracic aorta showed that goby U-II induced a vasoconstrictor and endothelium-dependent vasodilator effect in this tissue (Gibson, 1987; Itoh *et al.*, 1987). These results revealed a possible physiological role for U-II in the cardiovascular systems of mammalian species.

4.2.2. U-II synthesis:

The 124 amino acid residue precursor of human U-II (hU-II), prepro-urotensin-II was cloned from human colon tumour samples (Coulouarn *et al.*, 1998). hU-II is an 11 amino acid peptide with a hexapeptide sequence at the c-terminal which has been conserved from the goby U-II isoform (see **Figure 4.1**) and a variable sequence at the N-terminal. The discovery of the conserved region of the U-II between the human and goby isoforms increased the evidence for a physiological role for U-II in mammals. The distribution of human prepro-U-II mRNA was found to be at its highest level in the spinal cord, particularly in the ventral horn motor neurones, and the medulla oblongata (Coulouarn *et al.*, 1998; Ames *et al.*, 1999; Coulouarn *et al.*, 1999). Both prepro-U-II and hU-II mRNA and immunoreactivity have been found in low levels in peripheral tissues in mammals, such as in skeletal muscle, liver and

kidney, while UT receptor mRNA has been found in the lung and the pancreas (Elshourbagy *et al.*, 2002).

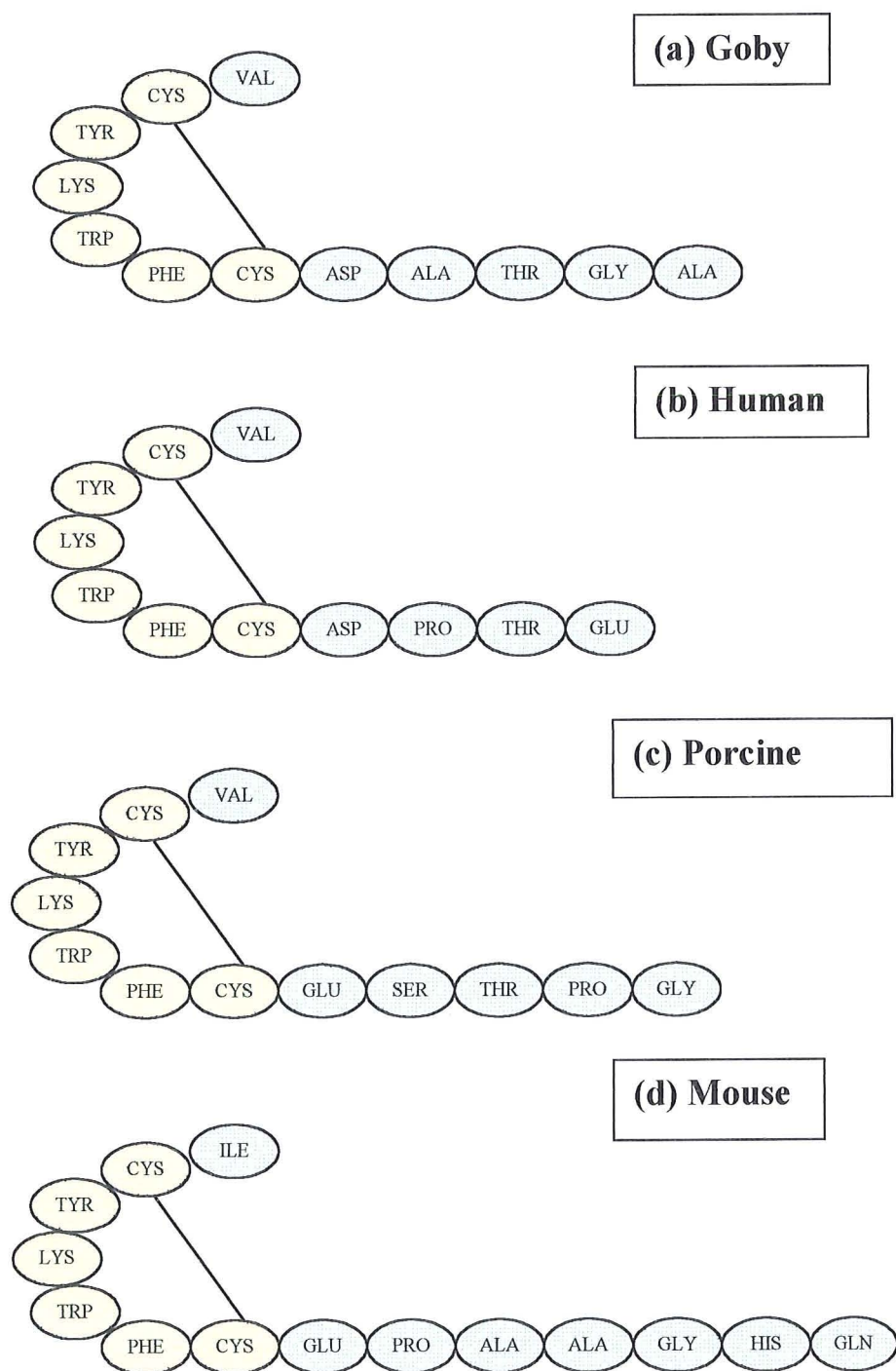


Figure 4.1: Amino acid sequences for (a) goby; (b) human; (c) porcine U-II. The predicted sequence of (d) mouse (Coulouarn *et al.*, 1999; Davenport & Maguire, 2000). Illustration adapted from Davenport & Maguire, 2000.

These peptides were found to be expressed in tissues of humans and primates such as cardiac smooth muscle cells and coronary atherosclerotic plaques; the kidneys and adrenal glands (Coulouarn *et al.*, 1998; Ames *et al.*, 1999; Davenport & Maguire, 2000).

4.2.3. U-II isoforms:

The mouse; porcine; and goby U-II isoforms were also isolated and were found to be comprised of 14; 12; and 12 amino acid peptides respectively (see **Figure 4.1**). These isoforms also exhibited the conserved hexapeptide sequence at the C-terminal, suggesting that the biological activity of U-II is conferred by the C-terminal (Coulouarn *et al.*, 1998; Mori *et al.*; 1999; Davenport & Maguire, 2000). This conserved hexapeptide sequence has an acidic D/E N-terminus and a carboxyl residues which are also conserved between species. This conserved octapeptide sequence is the minimum required sequence which allows full biological activity of the U-II peptide as truncation of the N-terminus of the peptide only affects biological activity when the truncation interrupts this conserved octapeptide sequence (Itoh *et al.*, 1988; Elshourbagy *et al.*, 2002). The amino acid sequences of preproU-II reveals differentiation between higher and lower vertebrates with 93% homology between human and monkey, 48% between human and mouse and 25% between human and carp C-terminus of these sequences (Elshourbagy *et al.*, 2002). There is also a differentiation in the amino acid sequence homology of UT receptors between higher and lower vertebrates. The importance of U-II was further secured when an endogenous receptor was discovered. The rat orphan G-protein coupled receptor 14 (GPR14) was found to be selectively activated by the isoforms of U-II which induced Ca^{2+} mobilisation in cells expressing the receptor (Ames *et al.*, 1999; Mori *et al.*,

1999; Davenport & Maguire, 2000; Elshourbagy *et al.*, 2002). GPR14 is now referred to as the U-II receptor and is designated as UT-II. The sequence of the monkey UT receptor shows 97 and 77% homology with human and rat UT receptors, while mouse UT receptors show 76 and 93% homology with human and rat UT receptors respectively (Elshourbagy *et al.*, 2002). Expression of UT-II mRNA and radioligand binding assays revealed the presence of UT-II receptors in human cardiovascular tissues including the cardiomyocytes of the left atrium and ventricles; the endothelial and smooth muscle cells of the coronary artery and the aorta (Ames *et al.*, 1999; Davenport & Maguire, 2000; Maguire *et al.*, 2000; Affolter & Webb, 2001). No significant difference can be found in the affinities of each of the U-II isoforms from higher and lower vertebrate species for the recombinant UT-II receptor (Ames *et al.*, 1999; Elshourbagy *et al.*, 2002). The highest density of UT-II receptors was found in skeletal muscle. However, peripheral distribution of UT-II receptors included densities in the kidney; spleen; adrenal; and pituitary glands (Maguire *et al.*, 2000; Affolter & Webb, 2001; Totsune *et al.*, 2001). hU-II-like immunoreactivity has been observed in human plasma and a role as a circulating cardiovascular regulating hormone after release from peripheral tissues has been proposed (Affolter & Webb, 2001; Totsune *et al.*, 2001). The expression of UT-II mRNA in cardiovascular tissues has created an interest of the possible pathophysiological role of U-II in the development of coronary atherosclerosis; systemic hypertension; and chronic heart failure (Ames *et al.*, 1999; Davenport & Maguire, 2000; Affolter & Webb, 2001). However, the distribution of U-II and UT receptor mRNAs in the peripheral tissues outwith the CNS and the cardiovascular system suggest that U-II may modulate many physiological systems throughout the body, including influencing endocrine function and release (Elshourbagy *et al.*, 2002).

4.1.4. U-II action:

The systemic administration of hU-II in the anaesthetised rat causes a minor increase in the cardiac output and a small, decrease overall in the total peripheral resistance of the rat vasculature while causing cardiovascular collapse as a result of a decreased myocardial contractility and an overall increase in total peripheral resistance in anaesthetised cynomolgus monkeys (Ames *et al.*, 1999; Davenport & Maguire, 2000). The different species-dependent consequences of systemic hU-II administration may be explained by the vasoconstrictor profile of hU-II on the isolated blood vessels from various vascular beds. hU-II was found to elicit a potent vasoconstrictor effect (-log [EC₅₀] of 9.09 ± 0.19 , n = 13) in the rat thoracic aorta, proximal to the aortic arch, yet has no vasoconstrictor activity in the more distal, abdominal aorta (Gibson, 1987; Ames *et al.*, 1999; Douglas *et al.*, 2000; Maguire *et al.*, 2000). This is an example of the anatomical variation of the vasoconstrictor profile of hU-II. hU-II was more potent, but produced a lower maximum response, than ET-1 in this and every other isolated blood vessel preparation so far studied in various species (Ames *et al.*, 1999; Douglas *et al.*, 2000; Maguire *et al.*, 2000; MacLean *et al.*, 2000). In the human coronary artery, hU-II was 50 times more potent than, but only elicited a maximum response of 25% of that produced by ET-1 (Maguire *et al.*, 2000). The diversity in hU-II-induced vasoconstriction between species is also observed in the pulmonary circulation. hU-II causes a potent vasoconstriction in the main pulmonary artery of the rat, however, no contraction was observed in the pulmonary artery of the dog (MacLean *et al.*, 2000; Douglas *et al.*, 2000). This is another example of the species variation in the vasoconstrictor profile of hU-II. hU-II is a vasoconstrictor peptide of both the venous and arterial sides of the cardiovascular system (Douglas *et al.*, 2000; Maguire *et al.*, 2000). hU-II does not induce vasoconstriction of any arteries so far

studied in the mouse (Douglas *et al.*, 2000). hU-II-induced vasoconstriction is observed in the thoracic aorta; common carotid; and main pulmonary artery of the rat (Douglas *et al.*, 2000; MacLean *et al.*, 2000). The vasoconstrictor effect was limited to the left circumflex and anterior descending coronary arteries in dogs (Douglas *et al.*, 2000). The marmoset and pig displayed a variable vasoconstrictor profile of hU-II-induced constriction. In the pig, the thoracic aorta; pulmonary; internal mammary; and common carotid arteries showed variable hU-II-induced constriction (Douglas *et al.*, 2000). hU-II induced variable vasoconstriction was seen in the thoracic aorta; abdominal aorta; common carotid; and mesenteric arteries of the marmoset (Douglas *et al.*, 2000). The most widespread vasoconstrictor profile was observed in the cynomolgus monkey. hU-II-induced vasoconstriction was seen in the thoracic and abdominal aortae; the left circumflex and anterior descending coronary arteries; the pulmonary; renal; internal mammary; femoral; basilar; common carotid; and mesenteric arteries. Vasoconstriction was also shown in the pulmonary; saphenous; and jugular veins (Douglas *et al.*, 2000). So far, hU-II has been shown to vasoconstrict the human coronary; mammary; and radial arteries but not the endothelium-intact small muscular pulmonary resistance arteries (MacLean *et al.*, 2000; Maguire *et al.*, 2000; Russell *et al.*, 2001). However, 30% of small muscular pulmonary resistance arteries (PRAs) incubated with L-NAME did display a hU-II-induced vasoconstriction of variable efficacy (MacLean *et al.*, 2000). hU-II was shown to have no vasoconstrictor activity in human internal mammary artery or saphenous veins with a functional endothelium in patients with chronic heart failure and healthy volunteers (Hillier *et al.*, 2001). However, a recent *in vitro* study in humans showed that removal of the endothelium, inhibition of NOS, and presence of chronic hypoxia either increased the potency and/or efficacy of hU-II in the rat main

pulmonary artery (MacLean *et al.*, 2000). This reveals that the vasoconstrictor effect of hU-II can be seen when one or several endothelium-derived vasoactive substances are removed or inhibited. This suggests a pathophysiological role for U-II in the cardiovascular system. hU-II also vasoconstricts endothelium denuded human saphenous and umbilical veins (Maguire *et al.*, 2000). A recent *in vivo* study revealed a vasoconstrictor effect of hU-II in humans. This study revealed that infusion of hU-II through the brachial artery resulted in a very significant reduction in forearm blood flow, demonstrating that hU-II has a potent *in vivo* vasoconstrictor effect in humans (Bohm & Pernow, 2002). hU-II has also been shown to increase the contractility of the myocardium of the right human atrium and ventricle (Russell *et al.*, 2001). Activation of the UT-II receptor was found to elicit an increase in Ca^{2+} mobilisation (Ames *et al.*, 1999). hU-II-induced vasoconstriction and increase in IP_3 generation in the rabbit thoracic aorta was inhibited by the phospholipase C inhibitor, NCDC (Opgaard *et al.*, 2000). These findings suggest that the UT-II receptor is a G_q protein-coupled receptor that mediates contraction via the release of Ca^{2+} from internal stores due to phospholipase C activation causing IP_3 generation. hU-II was shown to be a more potent positive inotropic peptide than ET-1 in human myocardial cells. hU-II did not cause arrhythmias in this tissue as readily as ET-1, and hU-II did not interfere with the time taken for the myocardium to relax to 50% of the tone of the original contraction (Russell *et al.*, 2001).

Intravenous administration of goby U-II in the rat caused a minor increase in cardiac output with a small reduction in regional vascular resistance resulting in a small vasodepressor effect (Ames *et al.*, 1999). Endothelium-dependent relaxation of rat aortic strips has previously been observed (Gibson, 1987). These results suggest that

the hU-II may induce vasodilatation in some vessels in the same way that the vasoconstrictor peptide ET-1 can induce vasodilatation via its subpopulation of ET_B receptors. A previous study on rat arteries showed that hU-II-induced both a vasoconstrictor and vasodilator effect in the left anterior descending coronary artery, a vasodilator effect in the mesenteric artery, and neither a vasodilator or vasoconstrictor effect in the rat basilar artery (Bottrill *et al.*, 2000). hU-II-induced vasodilatation was observed in the coronary artery of the perfused rat heart after an initial transient vasoconstriction (Katano *et al.*, 2000).

The recently revealed evidence of a vasodilator effect of hU-II, coupled with the failure of hU-II to constrict human small muscular PRAs without the presence of L-NAME, led to the question of whether or not hU-II would vasodilate these human PRAs. The vasodilator effect was also investigated in the small muscular resistance arteries of a systemic vascular bed, for which the abdominal adipose systemic resistance arteries (SRAs) were chosen.

4.2. Methods

Small muscular pulmonary resistance arteries (PRAs) were dissected free from human lung tissue resected from patients undergoing thoracotomies for bronchial carcinoma. Written consent was obtained from patients to allow the collection of a biopsy of their resected lung for our study. As the anatomical position of the tumour varied between patients, the area of the lung that the biopsy of 'safety margin' tissue is from also varies and cannot be specified. Human small muscular PRAs were dissected free from the surrounding parenchyma and set up on an isometric wire myograph as described in chapter 2 (Mulvaney & Halpern, 1977). The transmural pressure of the vessels was set at $\sim 16\text{mmHg}$.

Small muscular systemic resistance arteries were dissected from a biopsy of abdominal skin and adipose tissue taken from patients undergoing surgery for abdominal hernias. Written consent was obtained from patients to allow the collection of a biopsy of their abdominal tissue for our study. The area of abdomen that the biopsy came from varied as the position of the hernia varied from patient to patient. The small muscular systemic resistance arteries (SRAs) were dissected free from the surrounding adipose tissue and set up on an isometric wire myograph. The transmural pressure of the vessels was set at $\sim 90\text{mmHg}$.

After the tension was stabilised, the vessels were left to equilibrate for 45 minutes. The viability of the vessels was assessed by adding 50mM KCl to the baths. This was repeated until two reproducible vasoconstrictions were obtained. There were several washes in between and a return to baseline before the next addition. The viability of the endothelium was assessed by adding $3\mu\text{M}$ 5-HT to raise tone followed by $1\mu\text{M}$ of

acetylcholine (ACh) to vasodilate the PRAs. The results of the endothelium function tests are shown for each protocol group in **Table 4.6**. Any vessels which did not show a functional endothelium were discarded from the study. Previous studies have shown that the endothelium could not be safely removed manually in these vessels without damaging the thin smooth muscle layer. Therefore, all vessels in this study have an intact and functioning endothelium.

A submaximal dose of 10nM ET-1 was added to the baths to pre-constrict the PRAs in those protocols assessing hU-II-induced vasodilatation after ET-1-induced pre-constriction. A subset of vessels were pre-constricted with ET-1 and left for the duration of the cumulative concentration response curve (CCRC) to hU-II as time controls to show that the smooth muscle cell relaxation induced by hU-II is not merely a consequence of a fall in ET-1-induced tone. A subset of vessels were pre-constricted with ET-1 before being relaxed by porcine U-II to investigate the difference between isoforms of different species in their ability to relax PRAs and SRAs. The vessels of some protocol groups were incubated with one of three inhibitors of endogenous endothelium-derived vasodilators to investigate the mediator(s) involved in the hU-II-induced vasodilatation. The nitric oxide synthase inhibitor, 0.1mM N^G-nitro-L-arginine methyl ester (L-NAME), was added to a subset of vessels to investigate a possible role of NO in the hU-II-induced vasodilatation (Gambone *et al.*, 1997; Parsons *et al.*, 1997; Bottrill *et al.*, 2000; Tare *et al.*, 2000). The cyclooxygenase inhibitor, 1µM indomethacin, was added to a subset of vessels to investigate a possible role for PGI₂ in the hU-II-induced relaxation (Gambone *et al.*, 1997; Bottrill *et al.*, 2000; Tare *et al.*, 2000; MacIntyre *et al.*, 2001). The BK_{Ca} and SK_{Ca} (large and small conductance, respectively) calcium-activated potassium

channel blockers, 0.1 μ M each of apamin (Ap) and charybdotoxin (ChTX), were added to a set of vessels to investigate a possible role for endothelium-derived hyperpolarising factor (EDHF) in the vasodilator effect of hU-II (Garland *et al.*, 1995; Zygmunt *et al.*, 1998; MacIntyre *et al.*, 2001). The K_{Ca} channel blockers and EDHF itself are described more fully in chapter 3. Two subsets of vessels were pre-constricted with 50mM KCl instead of ET-1, with one set acting as the KCl time controls and the other being treated with hU-II to further investigate a possible role of EDHF in the hU-II-induced vasodilatation, as KCl-induced tone has been shown to inhibit EDHF release (Garland *et al.*, 1995; Shimokawa *et al.*, 1996).

Due to the availability of tissue, there were only three protocol groups of abdominal adipose SRAs, those acting as ET-1 time controls; those treated with hU-II; and those treated with porcine U-II. The results of the endothelial viability tests for these vessels can be seen in **Table 4.9**. Any SRAs without a functional endothelial layer were discarded from the study.

The vessels in these studies were used for one CCRC only as both hU-II and ET-1 are resistant to washout with ET-1 being more resistant to removal than hU-II (Maguire *et al.*, 2000).

4.3. Results

4.3.1. Human PRAs:

hU-II-induced a vasodilatation in control human small PRAs. The resulting CCRC is shallow in nature. The pEC_{50} value was 10.78 ± 0.27 ($n=10$) and the maximum relaxation response was $83 \pm 4\%$ (of ET-1-induced tone). A summary of the pre-constriction achieved by 10nM of ET-1 are shown in **Table 4.1**. A summary of pEC_{50} values are shown in **Table 4.3**. The hU-II-induced vasodilatation was significantly different from the time control fall off of tone at $0.1\mu\text{M}$ of hU-II ($P < 0.001$). Therefore, hU-II is a potent vasodilator peptide in human small PRAs. The vasodilator responses to hU-II are displayed in **Figure 4.2**.

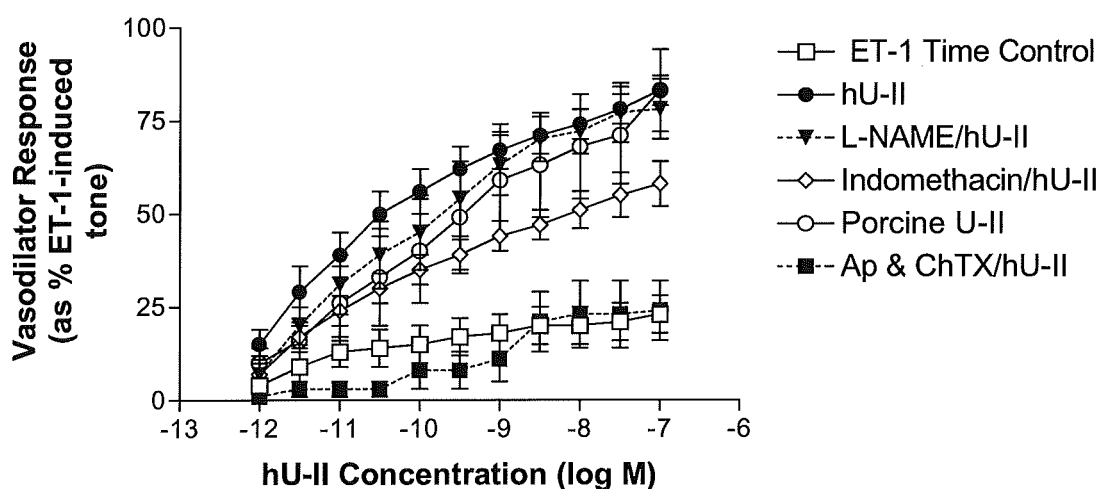


Figure 4.2: Vasodilator response to hU-II in the control human small PRAs in the presence and absence of various vasodilator inhibitors. ET-1 time control ($n=13$); hU-II ($n=10$); porcine U-II ($n=4$); 0.1mM L-NAME ($n=6$); $1\mu\text{M}$ indomethacin ($n=5$); and $0.1\mu\text{M}$ apamin (Ap) & charybdotoxin (ChTX) ($n=5$). Data expressed as percentage of ET-1-induced tone (10nM). Each point represents the mean \pm SEM. n = number of individual PRAs from the same number of individual lung biopsies.

Porcine U-II induced a dose-dependent vasodilatation with a shallow CCRC in control human small PRAs. The pEC_{50} value was 9.85 ± 0.55 ($n=4$) and the maximum relaxation response was $80 \pm 11\%$ (of ET-1-induced tone). A summary of the pre-constriction achieved by 10nM of ET-1 is shown in **Table 4.1**. The porcine U-II-induced vasodilatation was significantly different from the time control fall off of tone at 0.1 μ M of hU-II ($P < 0.001$). Therefore, porcine U-II is a vasodilator peptide in human small PRAs. There was no significant difference in the potency of hU-II- and porcine U-II-induced vasodilator response. The vasodilator responses to hU-II and porcine U-II are displayed in **Figure 4.3**.

Protocol Group	ET-1 Time Control	hU-II Alone	Porcine U-II	L-NAME / hU-II	Indomethacin / hU-II	Ap & ChTX / hU-II
Vessel Size (μm)	160 \pm 11	153 \pm 10	156 \pm 12	157 \pm 11	133 \pm 10	189 \pm 14
ET-1-Induced tone (mN)	1.89 \pm 0.31	2.76 \pm 0.63	1.88 \pm 0.30	1.79 \pm 0.41	2.59 \pm 1.43	1.35 \pm 0.52
n number	n = 13	n = 10	n = 4	n = 6	n = 5	n = 5

Table 4.1: Dimensions and measurement of 10nM ET-1-induced tone achieved in the various protocol groups. Data expressed as mean \pm SEM. n =number of individual PRAs.

Protocol Group	KCl Time Control	KCl / hU-II
Vessel Size (µm)	124 ± 20	123 ± 12
KCl-induced Tone (mN)	1.12 ± 0.21	1.56 ± 0.27
n number	n = 4	n = 4

Table 4.2: Dimensions and measurements of 50mM KCl-induced tone achieved in the various protocol groups. Data expressed as mean ± SEM. n = number of individual PRAs from the same number of individual lung preparations.

hU-II-induced vasodilatation in the presence of 0.1mM of the NOS inhibitor L-NAME (n=6), was significantly different from the time control fall off of tone at 0.1µM of hU-II ($P < 0.001$). A summary of the pre-constriction achieved by 10nM of ET-1 is shown in **Table 4.1**. There was no significant decrease in the potency of hU-II in the presence of L-NAME. A summary of the pEC₅₀ values of hU-II are shown in **Table 4.3**. There was no attenuation of the maximum relaxation response to hU-II nor any significant difference between the vasodilatation effected at any given concentration of hU-II. A summary of these results is shown in **Table 4.4** and **Figure 4.2**.

Protocol Group	pEC₅₀ value	n number
hU-II	10.78 ± 0.27	n = 10
Porcine U-II	9.85 ± 0.55 ns	n = 4
L-NAME / hU-II	10.45 ± 0.37 ns	n = 6
Indomethacin / hU-II	10.71 ± 0.48 ns	n = 5
Ap & ChTX / hU-II	8.73 ± 0.59 **	n = 5

Table 4.3: pEC₅₀ values for porcine U-II and hU-II ± various vasodilator inhibitors in small ACh-sensitive PRAs. Apamin (Ap) & charybdotoxin (ChTX). Data are expressed as mean ± SEM. n = number of individual PRAs from the same number of lung preparations. Statistical comparisons were made using a one-way ANOVA with a Dunnetts' post-test. *P* < 0.01** vs. hU-II control. ns = not significant.

hU-II-induced vasodilatation in the presence of 1µM of the cyclooxygenase (COX) inhibitor, indomethacin (n=5), was significantly different from the fall off of tone in the time control vessels at 0.1µM hU-II (*P* < 0.001). The vasodilator response to hU-II in the presence and absence of 1µM indomethacin is displayed in **Figures 4.2** and **4.4**. A summary of the pEC₅₀ values are shown in **Table 4.3**. There was no

significant decrease in the potency of hU-II in the presence of indomethacin, however, there was a statistically significant attenuation of the maximum relaxation response to hU-II from 30pM and above ($P < 0.05$ then $P < 0.01$ from 30nM). A summary of these results is shown in **Table 4.4**

hU-II-induced vasodilatation in the presence of 0.1 μ M of the K_{ca} channel blockers, apamin (Ap) & charybdotoxin (ChTX) (n=5), was not significantly different from the fall off of tone in the ET-1 time control vessels at any given concentration of hU-II. The effect hU-II in the presence and absence of 0.1 μ M apamin and charybdotoxin is displayed in **Figures 4.2** and **4.5**. There was a significant decrease in the potency of hU-II in the presence of apamin & charbydotoxin ($P < 0.01$). A summary of the hU-II pEC₅₀ values is shown in **Table 4.3**. The maximum vasodilator response to hU-II was also significantly attenuated ($P < 0.01$) as was the response to hU-II at any given concentration ($P < 0.05$ at 1pM then $P < 0.01$ at 3pM and above). A summary of these results is shown in **Table 4.4**.

The raising of tone in small resistance arteries with 50mM KCl instead has been shown to inhibit the release of endothelium-derived hyperpolarising factor (EDHF). Therefore, experiments were conducted in which the tone of PRAs was raised with 50mM KCl instead of 10nM ET-1 before a CCRC to hU-II was carried out. A summary of the pre-constriction caused by 50mM KCl is shown in **Table 4.2**. There was no significant difference in the hU-II response from the KCl time control (n=4). Both KCl protocol groups showed no relaxation which was significantly less than the fall of ET-1-induced tone at 0.1 μ M hU-II ($P < 0.01$). No graph is shown as the tone

had only decreased by a maximum of 5% by the end of the experiment and could not be differentiated from the x-axis of the graph. These results are shown in **Table 4.5**.

hU-II Bath Concⁿ	hU-II alone (n = 10)	L-NAME / hU-II (n = 6)	Indomethacin / hU-II (n = 5)	Ap & ChTX/ hU-II (n = 5)
-12	15 ± 4 %	7 ± 3 % ns	7 ± 5 % ns	1 ± 1 % *
-11.5	29 ± 7 %	20 ± 5 % ns	17 ± 3 % ns	3 ± 2 % **
-11	39 ± 6 %	31 ± 8 % ns	24 ± 4 % ns	3 ± 2 % **
-10.5	50 ± 6 %	39 ± 9 % ns	30 ± 4 % *	3 ± 2 % **
-10	56 ± 6 %	45 ± 10 % ns	35 ± 4 % *	8 ± 5 % **
-9.5	62 ± 6 %	54 ± 10 % ns	39 ± 4 % *	8 ± 5 % **
-9	67 ± 5 %	63 ± 8 % ns	44 ± 4 % *	11 ± 6 % **
-8.5	70 ± 5 %	70 ± 6 % ns	47 ± 4 % *	21 ± 8 % **
-8	74 ± 4 %	72 ± 6 % ns	51 ± 5 % *	23 ± 9 % **
-7.5	78 ± 4 %	77 ± 8 % ns	55 ± 6 % **	23 ± 9 % **
-7	83 ± 4 %	78 ± 8 % ns	58 ± 6 % **	24 ± 8 % **

Table 4.4: The measurement of vasodilatation as % of 10nM ET-1-induced tone effected at each point in the hU-II CCRC. Apamin (Ap) & charybdotoxin (ChTX). Data is expressed as mean ± SEM. Statistical comparisons were made using Student's t-test. $P < 0.05^*$, $P < 0.01^{**}$ vs. hU-II control. ns = not significant.

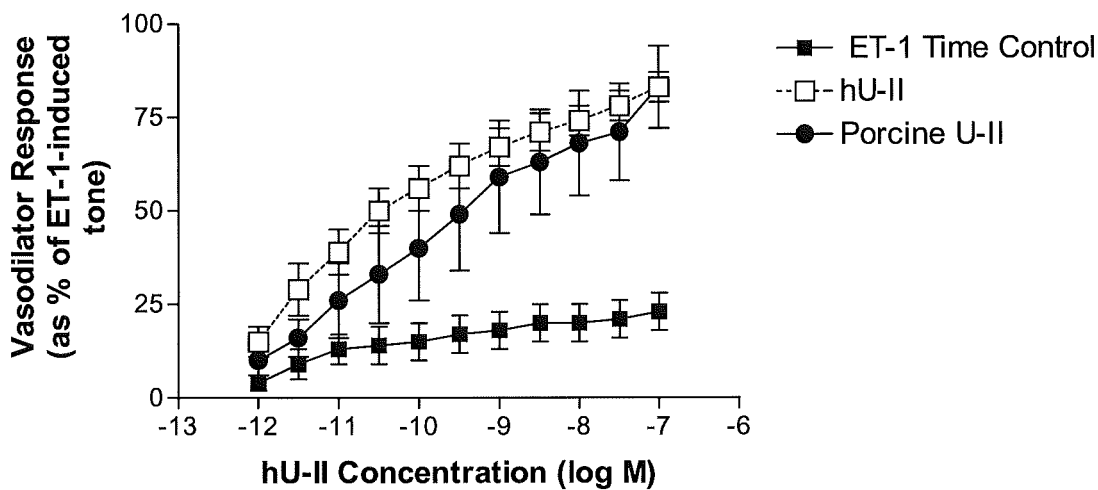


Figure 4.3: Vasodilator response to hU-II and porcine U-II in the control human small PRAs. ET-1 time control (n=13); hU-II (n=10); and porcine U-II (n=4). Data expressed as percentage of ET-1-induced tone (10nM). Each point represents the mean \pm SEM. n = number of individual PRAs.

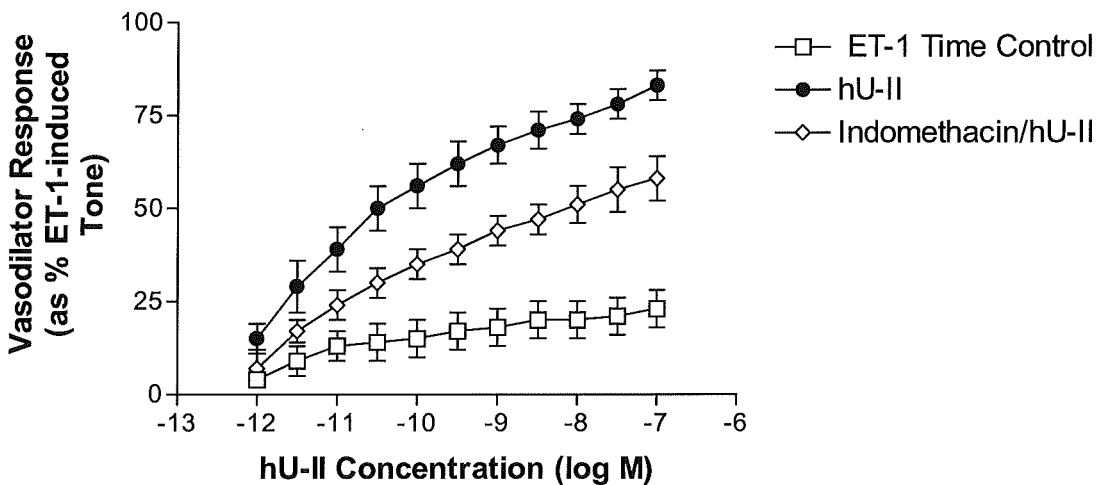


Figure 4.4: Vasodilator response to hU-II in the control human small PRAs in the presence and absence of 1 μ M indomethacin. ET-1 time control (n=13); hU-II (n=10); and indomethacin (n=5). Data expressed as percentage of ET-1-induced tone (10nM). Each point represents the mean \pm SEM. n = number of individual PRAs.

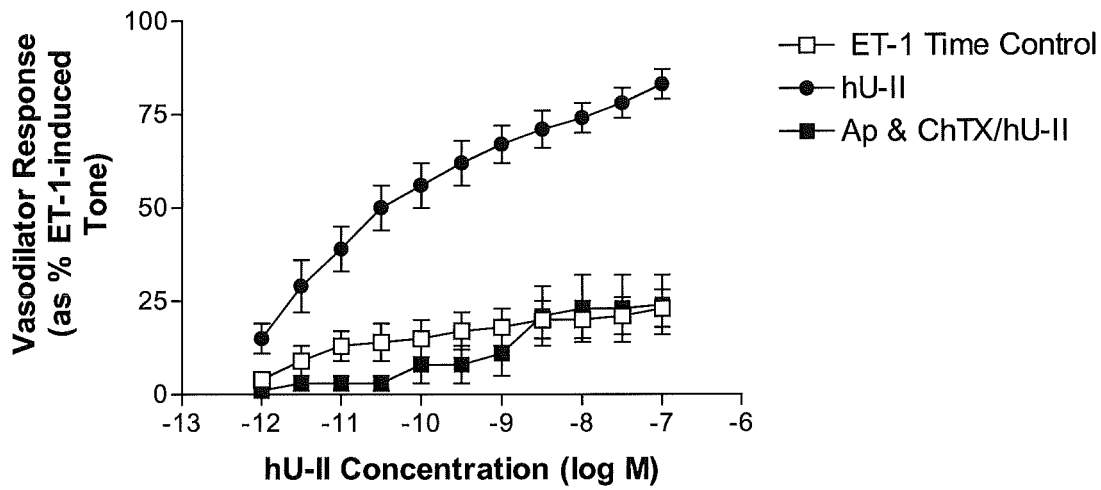


Figure 4.5: Vasodilator response to hU-II in control human small PRAs in the presence and absence of 0.1 μ M apamin & charybdotoxin. ET-1 time control (n=13); hU-II (n=10); and apamin (Ap) & charybdotoxin (ChTX) (n=5). Data expressed as percentage of ET-1-induced tone (10nM). Each point represents the mean \pm SEM.

hU-II Concⁿ	Bath	ET-1 / hU-II	KCl / hU-II
-12		15 ± 4 %	0 ± 0%*
-11.5		29 ± 7 %	0 ± 0%**
-11		39 ± 6 %	0 ± 0%**
-10.5		50 ± 6 %	0 ± 0%**
-10		56 ± 6 %	0 ± 0%**
-9.5		62 ± 6 %	0 ± 0%**
-9		67 ± 5 %	0 ± 0%**
-8.5		70 ± 5 %	0 ± 0%**
-8		74 ± 4 %	0 ± 0%**
-7.5		78 ± 4 %	1 ± 1%**
-7		83 ± 4 %	5 ± 5%**

Table 4.5: The measurement of vasodilatation as percentage of 10nM ET-1- or 50mM KCl-induced tone effected at each point in the hU-II CCRC in PRAs (n = 10 and n = 4, respectively). Data is expressed as mean ± SEM. Statistical comparisons were made using Students' unpaired t-test. $P < 0.05^*$, $P < 0.01^{**}$ vs. ET-1/hU-II control. n = number of individual PRAs from the same number of individual lung biopsies.

Protocol Group	ET-1 Time Control (n = 13)	hU-II (n = 10)	Porcine U-II (n = 4)	L-NAME / hU-II (n = 6)
5-HT-induced tone (mN) & (% of KCl-induced tone)	0.58 ± 0.09 43 ± 5%	0.87 ± 0.26 57 ± 6%	0.89 ± 0.24 48 ± 11%	0.73 ± 0.11 39 ± 9%
ACh-induced relaxation (mN) & (% of 5-HT-induced tone)	0.36 ± 0.07 63 ± 6%	0.39 ± 0.08 55 ± 8%	0.60 ± 0.20 58 ± 8%	0.45 ± 0.10 59 ± 7%

Protocol Group	indomethacin/hU-II (n = 5)	Apamin & ChTX / hU-II (n = 5)	KCl Time Control (n = 4)	KCl / hU-II (n = 4)
5-HT-induced tone (mN) & (% of KCl-induced tone)	0.75 ± 0.21 39 ± 9%	0.46 ± 0.11 60 ± 9%	0.40 ± 0.05 37 ± 6%	0.61 ± 0.06 40 ± 10%
ACh-induced relaxation (mN) & (% of 5-HT-induced tone)	0.50 ± 0.22 60 ± 9%	0.30 ± 0.08 64 ± 8%	0.27 ± 0.04 68 ± 7%	0.40 ± 0.06 67 ± 8%

Table 4.6: The measurements of the endothelial viability tests in human PRAs. The extent of 5-HT-induced tone is shown in mN and as a % of 50mM KCl-induced tone. The extent of the ACh-induced relaxation is shown in mN and as a % of 5-HT-induced tone. Apamin (Ap) & charybdotoxin (ChTX). Data is expressed as the mean ± SEM.

4.3.2. Human abdominal SRAs:

hU-II induced a vasodilatation in human abdominal adipose SRAs with a shallow CCRC. The pEC_{50} was 10.72 ± 0.12 ($n=6$) and the maximum relaxation response was $88 \pm 6\%$ (of 10nM ET-1-induced tone). The hU-II-induced vasodilatation was significantly different from the fall off in tone seen in the time control vessels at $0.1\mu\text{M}$ hU-II ($n=6$) ($P < 0.001$). The effect of hU-II on abdominal adipose SRAs is displayed in **Figure 4.6**.

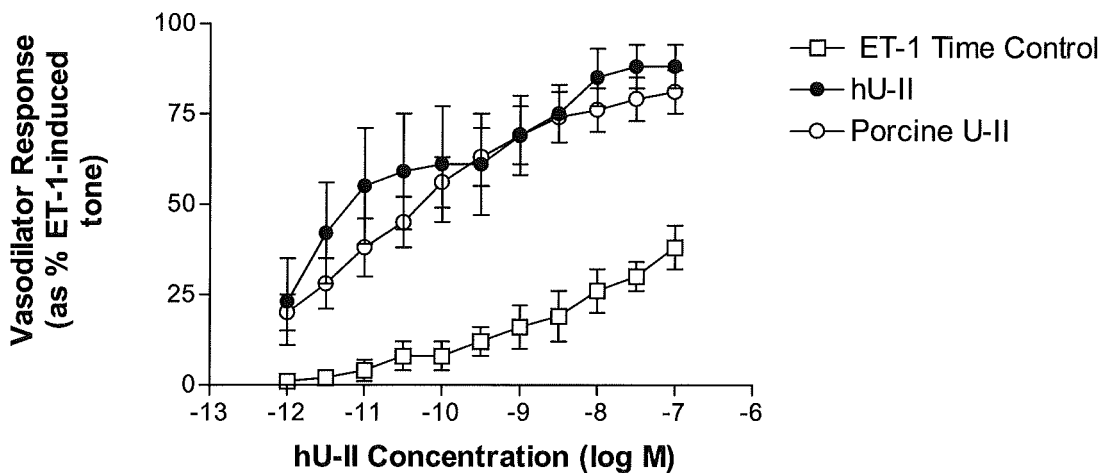


Figure 4.6: The vasodilator response to hU-II and porcine U-II on human abdominal adipose tissue small SRAs. ET-1 time control ($n=6$); hU-II ($n=6$); and porcine U-II ($n=6$). Data expressed as percentage of ET-1-induced tone. Each point represents the mean \pm SEM. n = number of individual SRAs.

Therefore, hU-II is a potent vasodilator peptide in human small abdominal adipose SRAs. There is no significant difference between the potency of hU-II in pulmonary resistance arteries and abdominal adipose systemic resistance arteries. These results

are shown in **Table 4.8**. There is no significant difference between the maximum vasodilatation achieved by hU-II in the pulmonary and systemic resistance arteries.

Protocol Group	ET-1 Time Control	hU-II	Porcine U-II
Vessel Size (μm)	201 \pm 10	192 \pm 16	206 \pm 16
ET-1-induced Tone (mN)	1.81 \pm 0.52	3.08 \pm 1.00	8.30 \pm 2.96
n	n = 6	n = 6	n = 6

Table 4.7: Dimensions and measurements of 10nM ET-1-induced tone achieved in the various protocol groups of SRAs. Data expressed as mean \pm SEM. n = number of individual SRAs from the same number of individual abdominal adipose tissue biopsies.

Porcine U-II caused a vasodilator response in human abdominal adipose systemic resistance arteries. The effect of porcine U-II on abdominal adipose SRAs is displayed in **Figure 4.6**. The pEC₅₀ value was 10.64 \pm 0.35 (n=6) and the maximum relaxation response of 81 \pm 6% (of 10nM ET-1-induced tone). A summary of these results is shown in **Table 4.8**. The vasodilatation produced by porcine U-II was

significantly different from the fall off of tone observed in the ET-1 time control at 0.1 μ M hU-II ($P < 0.001$). Therefore, porcine U-II is a potent vasodilator peptide in abdominal systemic resistance arteries. There is no significant difference between the potency of, and maximum vasodilatation achieved by, porcine U-II between the pulmonary and systemic resistance arteries. There is also no significant difference between the potencies of hU-II and porcine U-II in the abdominal systemic arteries.

Protocol Group	pEC₅₀ value	n number
hU-II	10.72 \pm 0.12	n = 6
Porcine U-II	10.64 \pm 0.35 ns	n = 6

Table 4.8: pEC₅₀ values for porcine U-II and hU-II in small abdominal adipose SRAs. Data are expressed as mean \pm SEM. n = number of individual SRAs from the same number of abdominal adipose tissue biopsies. Statistical comparisons were made using Students' unpaired t-test. ns = not significant.

Protocol Group	ET-1 Time Control	hU-II	Porcine U-II
5-HT-induced tone (mN) & (% of KCl-induced tone)	0.74 ± 0.23 64 ± 12%	2.56 ± 1.17 68 ± 15%	2.99 ± 1.59 41 ± 5%
ACh-induced relaxation (mN) & (% of 5-HT-induced tone)	0.42 ± 0.14 60 ± 7%	1.86 ± 0.95 62 ± 9%	1.50 ± 0.57 67 ± 8%

Table 4.9: The measurements of the endothelial viability tests in human SRAs. The extent of 5-HT-induced tone is shown in mN and as a % of KCl-induced tone. The extent of the ACh-induced relaxation is shown in mN and as a % of 5-HT-induced tone. Data is expressed as the mean ± SEM.

4.3.3. U-II isoforms in normotensive rat PRAs:

I investigated the effect of three isoforms of U-II, human; porcine; and rat on control rat PRAs. None of the isoforms induced vasoconstriction or vasodilatation responses in these vessels under any circumstances (results not shown). Therefore, the vasoactive effects of hU-II in the pulmonary circulation are species specific.

4.4. Discussion

4.4.1. Vasodilator effect of U-II in human PRAs and SRAs:

The human and porcine isoforms of U-II are potent vasodilators of human small PRAs with an intact endothelium. This study is the first to show an hU-II-induced relaxation effect in human vessels. The human and porcine isoforms of U-II are equipotent in these arteries. We compared the potency of hU-II with other vasodilators in human PRAs. This work was published as a rapid communication in the American Journal of Physiology (Stirrat *et al.*, 2001). The order of potency for the vasodilators studied was: hU-II (10.78 ± 0.27) = ADM (10.1 ± 0.4) \gg SNP (7.4 ± 0.2) = ACh (6.8 ± 0.3) in human small PRAs (Stirrat *et al.*, 2001). hU-II was also found to be a potent vasodilator of human abdominal adipose SRAs. These findings were different from those revealed in early studies into the effect of hU-II which showed a potent vasoconstrictor action of hU-II in the vasculature of various species (Itoh *et al.*, 1987; Ames *et al.*, 1999; Douglas *et al.*, 2000, MacLean *et al.*, 2000). However, these findings are consistent with those from previous studies that showed hU-II-induced vasodilatation in the rat small mesenteric and coronary arteries (Bottrill *et al.*, 2000; Katano *et al.*, 2000). These results show that hU-II is able to induce vasoconstriction and vasodilatation in the same vascular bed and in a single arterial preparation. The rat main pulmonary artery is constricted upon application of hU-II while the human small muscular PRAs were dilated and a variable constriction was only seen in 30% of vessels incubated with the NOS inhibitor L-NAME (MacLean *et al.*, 2000; Stirrat *et al.*, 2001). hU-II-induced vasoconstriction and vasodilatation are observed in the coronary artery of the rat (Bottrill *et al.*, 2000; Katano *et al.*, 2000). This evidence suggests the existence of UT-II receptors on both endothelial and vascular smooth muscle cells similar to the distribution of ET_B receptors in pulmonary

arteries. When stimulated, the ET_B receptors located on the endothelial cells mediate ET-1-induced vasodilatation while the ET_B receptors located on the vascular smooth muscle cells mediate vasoconstriction (MacLean *et al.*, 1994; McCulloch *et al.*, 1996; MacLean *et al.*, 1998). These results contrast with radioligand binding assays conducted in skeletal muscle which suggested a single, homogeneous population of receptors (Ames *et al.*, 1999). hU-II has a similar heterogeneous vasoactive profile to ET-1 as both of these peptides can elicit vasodilatation and vasoconstriction. hU-II is a more potent and efficacious vasodilator of human small muscular PRAs than ACh while being a more potent but less efficacious vasoconstrictor of these vessels than ET-1 (Ames *et al.*, 1999; Maguire *et al.*, 2000; MacLean *et al.*, 2000; Stirrat *et al.*, 2001).

4.4.2. Mediators involved in the hU-II-induced vasodilatation in human PRAs:

These results show that hU-II-induced vasodilatation is mediated by EDHF and a role for a cyclooxygenase (COX) product, possibly PGI_2 . The involvement of EDHF was uncovered by the inhibition of the large and small conductance K^+ Ca^{2+} -activated channels with charybdotoxin (ChTX) and apamin respectively. These K^+ channel blockers totally inhibited hU-II-induced vasodilatation. A role for PGI_2 was revealed by the COX inhibitor, indomethacin, which resulted in an attenuation of the maximum dilation induced by hU-II but not a decrease in its potency. The absence of an effect by L-NAME suggests that NO was not involved in the hU-II-induced vasodilatation in human small muscular pulmonary resistance arteries.

Studies into the relaxation effect of well known vasodilators acetylcholine (ACh) and bradykinin have shown variations in the second messenger systems mediating their

relaxation response. Variation was also observed when their relaxation was studied in vessels from different vascular beds (Gambone *et al.*, 1997). Therefore, different agonists produce their relaxation effects by different signal transduction pathways. In the isolated canine main and first order pulmonary arteries, ACh and bradykinin elicit vasodilatation via different endothelium-derived mediators. ACh-induced relaxation is mediated by NO alone at low concentrations and by NO and EDHF at high concentrations. However, bradykinin mediates its vasodilator effect via NO and PGI₂ at low concentrations and by NO; PGI₂; and EDHF at high concentrations (Gambone *et al.*, 1997). A previous study showed that hU-II-induced vasodilatation was mediated by NO alone in the rat left anterior descending coronary artery. However, EDHF probably mediates the relaxation induced by hU-II in rat small mesenteric arteries with NO playing only a minor role (Bottrill *et al.*, 2000). This earlier study revealed an anatomical difference in the signal transduction pathways mediating the relaxation effect of hU-II in rat arteries (Bottrill *et al.*, 2000). My results suggest the relaxation of human small muscular PRAs by hU-II is mediated predominantly by EDHF with a minor role for PGI₂. However, electrophysiological studies are required to confirm this. The differences in the vasodilator mediators behind hU-II-induced vasodilatation in the vessels studied so far could be attributed to anatomical variation and more studies are needed in other species to investigate the possibility that species variation will affect the signal transduction pathways activated by hU-II to produce relaxation. The study investigating ACh-induced vasodilatation in chronic hypoxic rats, described in chapter 3, showed that the maximum dilator response to ACh was increased in PRAs from chronic hypoxic rats. This study also revealed that the vasodilator mediator profile involved in the ACh-induced vasodilatation changed in the presence of PHT. It is proposed that EDHF mediates

the relaxation in response to ACh in the control rats while NO, PGI₂ and EDHF are involved in mediating the relaxation in the chronic hypoxic rats. It would be interesting to see whether the potency of hU-II or the maximum vasodilator response to hU-II is increased in the PRAs of patients with PHT. The study described in chapter 5 involved patients with PHT secondary to different degrees of left ventricular dysfunction, but the availability of this tissue would not allow for extra investigation into the vasodilator effects of hU-II in these vessels. We can only speculate that, as with ACh, the vasodilator mediator profile of hU-II-induced vasodilatation would be different from that observed in patients with out PHT. Would this mediator profile include a role for NO as observed in the vasodilator response to ACh in chronic hypoxic rat PRAs? The study described here, and other studies (Bottrill *et al.*, 2000) are consistent with the hypothesis that small calibre arteries are more likely to be dependent on relaxations mediated by EDHF than large calibre arteries. This hypothesis proposes that as the internal diameter of the artery decreases, the importance of EDHF mediated relaxation increases, as witnessed in mesenteric arteries (Garland *et al.*, 1995; Shimokawa *et al.*, 1996).

4.4.3. Possible pathophysiological role of hU-II:

A possible pathophysiological role for hU-II has been proposed in a variety of conditions, especially those in which endothelial dysfunction is thought to play a part in the disease process. hU-II may be involved in coronary atherosclerosis; systemic hypertension; chronic heart failure; and chronic renal failure (Ames *et al.*, 1999; Davenport & Maguire, 2000; Affolter & Webb, 2001; Totsune *et al.*, 2001). However, any pathophysiological role for hU-II in these conditions would be as a consequence of its vasoconstrictor effects. However, a decrease in the vasodilator

response to hU-II may uncover a vasoconstrictor response. This is supported by studies showing that L-NAME uncovers vasoconstrictor responses in human PRAs and constrictor responses are more prominent in endothelium-denuded human arteries (Davenport & Maguire, 2000; MacLean *et al.*, 2000). This new evidence of hU-II-induced vasodilatation in human vessels may suggest a protector role of hU-II in the cardiovascular system. Further in depth investigations of the vasoconstrictor and vasodilator profiles of hU-II are needed to clarify the potential cardiovascular pathophysiological / protection role of the peptide. These studies should be carried out in human vessels as previous studies have shown considerable species variations in the hU-II-induced effects which make it difficult to extrapolate results seen in another species, such as the rat, to humans.

4.5. Conclusion

hU-II is a very potent and efficacious vasodilator peptide in human small muscular pulmonary and abdominal adipose systemic resistance arteries. In the PRAs, the hU-II-induced vasodilatation is mediated predominantly by EDHF with a minor role for a prostanoid, PGI₂. Further investigation with UT-II subtype specific antagonists is needed to explore the possibility of whether antagonism of the hU-II-induced vasoconstrictor, or stimulation of the vasodilator effect could provide a future therapeutic target for the treatment of various cardiovascular diseases.

Chapter 5

**The effect of mixed ET_A/ ET_B
antagonists in the treatment of
human PHT secondary to left
ventricular dysfunction**

5.1.1. Endothelin structure:

An endothelium-derived contracting factor (EDCF) was identified and isolated from vascular endothelial cells. This vasoactive substance was found to be a 21-amino acid peptide and was named endothelin (ET). It was soon discovered that, not only was ET one of three isoforms (ET-1; ET-2; and ET-3), these isoforms were structurally related to other vasoactive peptides, the sarafotoxins (STXs), and vasoactive intestinal peptide (VIP). Each of these peptide isoforms contain a pair of disulphide bonds in their structure (see **Figure 5.1**) (Yanagisawa *et al.*, 1988; Fleminger *et al.*, 1989; Cody *et al.*, 1991; Rubyani & Botelho, 1991; Rubyani & Polokoff, 1994).

5.1.2. Endothelin biosynthesis and expression:

All the members of this family show complete homology of peptide positions 1; 3; 8; 10; 11; 15; 16; 18; 20; and 21. The amino acids at position 1; 3; 11; and 15 are the cysteine residues which are involved in the disulphide bonds, cysteine 1 and 15 form one disulphide bridge and cysteine 3 and 11 form the other (Rubyani & Polokoff, 1994). The chromosomal location of the genes of the three ET isoforms have been mapped to chromosome 6 (ET-1), chromosome 1 (ET-2), and chromosome 20 (ET-3) in many mammalian species, including humans (Rubyani & Polokoff, 1994). The 21-amino acid peptide ET is the end product of a three step process from gene product to biologically active product. The stimulation of ET-1 mRNA expression in vascular endothelial cells can be elicited by interleukin-1 β (IL-1 β); transforming growth factor- β (TGF- β); thrombin; phorbol ester; angiotensin-II; vasopressin; tumour necrosis factor- α (TGF- α); and shear stress (Yanagisawa *et al.*, 1988; Ohta *et al.*, 1990; Resink *et al.*, 1990; Yoshizumi *et al.*, 1990; Rubyani & Botelho, 1991; Harrison *et al.*, 1998).

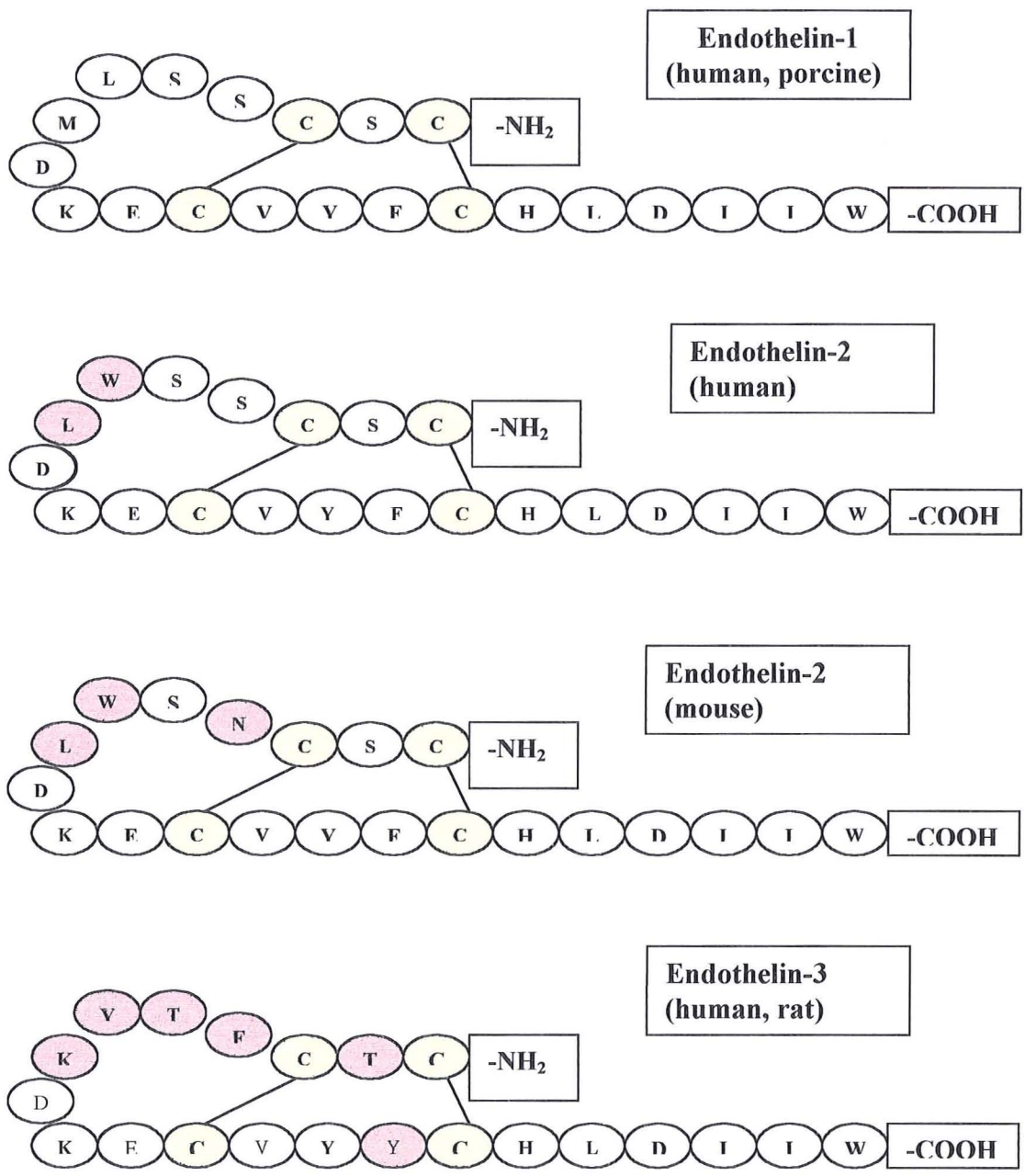


Figure 5.1. Amino acid heterogeneity of the endothelin isoforms, in their 21 amino acid sequence, from various species. Cysteine residues forming disulphide bonds are represented by the yellow circles. The pink circles denote changes in the amino acid sequence compared with the sequence of ET-1. Illustration adapted from Rubyani & Polokoff, 1994.

When discussing the biosynthesis of ET-1, human ET-1 will be used as an example. The form of ET-1 produced by the ET-1 gene is known as PreproET-1 and is 203 amino acids long. This peptide undergoes proteolytic cleavage at the 18th amino acid by signal peptidase to form proET-1 peptide. The proET-1 peptide (large ET-1) is then cleaved at the 53rd and 92nd amino acids by a diabasic amino acid-specific endopeptidase cleavage carboxypeptidase to form big ET-1. The third and final step is the cleavage of big ET-1 at the 73rd amino acid by endothelin-converting enzyme (ECE), a furin-like specific endopeptidase to form ET-1 (Cys⁵³ to TRP²³) (Rubyani & Botelho, 1991; Rubyani & Polokoff, 1994; Kido *et al.*, 1998). It is likely that the metalloproteinase ECE, will be different for each of the three ET isoforms. Expression of ECE has been found intracellularly and on the cell surface of human coronary artery preparations. This study also showed that ECE expression is both continuous by a constitutive pathway and by a regulated pathway that can be activated if needed, analogous to the constitutive and inducible forms of nitric oxide synthase (NOS) enzyme (Russel *et al.*, 1998). There is evidence that patients with PHT; cardiac disease and damage such as that resulting from myocardial infarction have an increased plasma level of ET-1 and that an increase in ECE-1 expression and activity is responsible for this observation (Bohnemeier *et al.*, 1998).

5.1.3. Endothelin receptors:

All of the known ET receptors are found in the cardiovascular system. The ET_A receptors are found on the vascular smooth muscle cells of both arteries and veins of the pulmonary and systemic circulations. The ET_A receptors are also found on cardiac myocytes of the atria and ventricles (Mulder *et al.*, 1998; Modesti *et al.*, 1999; Pieske *et al.*, 1999; Kelso *et al.*, 2000; Love *et al.*, 2000; Moraes *et al.*, 2000;

Miyuuchi *et al.*, 2000; Telemaque-Potts *et al.*, 2000; Berger *et al.*, 2001). The ET_{B1} receptors are found on the vascular endothelial cells of the pulmonary and systemic circulations of both arteries and veins. The ET_{B1} receptors are also present on the cardiac myocytes (Modesti *et al.*, 1999; Moraes *et al.*, 2000; Sawaki *et al.*, 2000). The ET_{B2} receptors are found on the arterial and venous sides of the pulmonary and systemic circulations (McCulloch *et al.*, 1996; MacLean *et al.*, 1998; Cowburn *et al.*, 1999; Modesti *et al.*, 1999; Love *et al.*, 2000; Moraes *et al.*, 2000). ET-1 activation of ET_A receptors mediates vasoconstriction, vascular smooth muscle cell and cardiac myocyte proliferation and hypertrophy, a positive inotropic effect in cardiac myocytes, and a direct cytotoxic effect on cardiac myocytes (Iwasaka *et al.*, 1998; Pieske *et al.*, 1999; Kelso *et al.*, 2000; Love *et al.*, 2000; Miyauchi *et al.*, 2000; Moraes *et al.*, 2000). It has been shown that although ET_A receptors are upregulated in CHF patients, there is evidence of attenuation of various ET_A-mediated effects in the cardiovascular system such as vasoconstriction and the inotropic effects. This suggests that the 'blunting' of ET_A-mediated effects in patients with CHF caused by desensitization of the ET_A receptor by G-protein-coupled receptor kinase mediating phosphorylation of the receptors (Pieske *et al.*, 1999; Love *et al.*, 2000; Moraes *et al.*, 2000). ET-1 activation of ET_{B1} receptors mediates vasodilatation by the release of NO and PGI₂ and may act as a clearance site of ET-1 (Modesti *et al.*, 1999; Moraes *et al.*, 2000; Sawaki *et al.*, 2000). ET-1 activation of ET_{B2} receptors mediates vasoconstriction and modulates the renin -angiotensin-II – aldosterone system (RAAS) (McCulloch *et al.*, 1996; MacLean *et al.*, 1998; Ohnishi *et al.*, 1998; Cowburn *et al.*, 1999; Love *et al.*, 2000; Moraes *et al.*, 2000; Sawaki *et al.*, 2000; Channick *et al.*, 2001).

5.1.4. Endothelin action:

Endothelin has a variety of actions depending on which isoform is released and which tissue they are acting on. As my study is concerned with the role of ET in secondary PHT as a consequence of heart failure, we will concentrate on the actions of endothelin in the cardiovascular system.

The i.v. infusion of ET-1 results in a biphasic effect, a transient vasodilatation precedes a sustained and potent vasoconstriction in a variety of mammalian species, including man (LeMonnier de Gouville *et al.*, 1990; Rubyani & Polokoff, 1994).

ET-1 contributes to the basal tone of the blood vessels of the cardiovascular system (Haynes & Webb, 1994; Rubyani & Polokoff, 1994; Barnes & Liu, 1995). Small amounts of ET-1 in the cardiovascular system would potentiate the effect of other vasoconstrictors such as noradrenaline and 5-HT (MacLean *et al.*, 1993; Rubyani & Polokoff; Kita *et al.*, 1998). A recent study revealed that the presence of ET-1 pre-contraction augmented the vasoconstrictor response induced by 5-CT in small pulmonary arteries from control and chronically hypoxic rats. The 5-CT-induced contractile response was further enhanced by the incubation of the PRAs with the nitric oxide synthase (NOS) inhibitor, L-NAME, as well as ET-1 pre-tone (MacLean & Morecroft, 2001).

ET-1 is produced by cultured endocardial cells which suggest that ET-1 could be involved in an autocrine mechanism in the heart, with ET binding sites found throughout the heart (Rubyani & Botelho, 1991; Rubyani & Polokoff, 1994).

ET-1 has a positive chronotropic effect on isolated heart muscle preparations, but results in bradycardia *in vivo*, possibly due to baroreflex stimulation. The duration of

the cardiac action potential is also increased due to the increase in Ca^{2+} influx accompanying the positive inotropic effect (Rubyani & Polokoff, 1994).

The cardiac output is decreased when ET-1 is administered by i.v. infusion *in vivo*. This decrease is probably a response to the increase in total peripheral resistance (TPR) that is caused by ET-1 so that mean arterial blood pressure is kept within the normal range (Rubyani & Polokoff, 1994). In systemic large arteries and veins, ET-1 was found to be the most potent endogenous vasoconstrictor causing a slow but sustained contraction which is more potent in the veins than in the arteries, resulting in an increased preload. However, in the pulmonary circulation, the large arteries are more sensitive than the large veins. This difference could be attributed to their relative blood gas concentrations as systemic veins and pulmonary arteries are low PO_2 vessels ($\text{PO}_2 \sim 40\text{mmHg}$) when compared with systemic arteries and pulmonary veins ($\text{PO}_2 \sim 100\text{mmHg}$). The pulmonary arterial sensitivity to ET-1 is increased during hypoxia, along with the sensitivity of the heart (MacLean *et al.*, 1989; Rubyani & Polokoff, 1994; MacLean & McCulloch, 1996; McCulloch *et al.*, 1998).

ET-1 is a potent vasoconstrictor of isolated microvessel beds. The microcirculations of hypertensive rats are more sensitive to the vasoconstriction caused by ET-1 than those of normotensive rats (MacLean & M^cGrath, 1990; Rubyani & Polokoff, 1994). ET-1 stimulates the release of nitric oxide (NO) from vascular endothelial cells, which would vasodilate the vessels (Warner *et al.*, 1989; Rubyani & Polokoff, 1994). ET-1 can also stimulate the release of prostacyclin (PGI_2) from vascular endothelial cells, which accounts for the anti-aggregatory effects of ET-1 (Rakugi *et al.*, 1989; Rubyani & Polokoff, 1994).

ET-1 is a potent bronchoconstrictor of the trachea and bronchi of many mammalian species, including humans. The ET-1 is secreted by bronchial epithelial cells. However, removal of the epithelium only increased the vasoconstriction caused by ET-1 (Hay *et al.*, 1993; Rubyani & Polokoff, 1994). As in the blood vessels of the cardiovascular system, ET-1 administration causes an initial transient relaxation followed by a sustained and potent vasoconstriction of airway smooth muscle cells *in vivo* (Rubyani & Polokoff, 1994).

Members of the sarafotoxin (STX) family of peptides can also cause these effects on the heart and lungs as they can activate the ET_B receptors which mediate these responses (Rubyani & Polokoff, 1994; M^cCulloch *et al.*, 1996; MacLean & M^cCulloch, 1998; M^cCulloch *et al.*, 1998).

5.1.5. Role of endothelin in chronic heart failure:

ET-1 has been implicated as having a role in some disease states. Many studies have shown increased levels of circulating immunoreactive ET-1 (irET-1) in diseases such as heart failure and PHT (Love & McMurray, 1996; MacLean, 1998). An increase in the levels of irET-1 has been observed in patients with chronic heart failure (CHF). This increase in ET-1 could promote the progression of the patient towards CHF in a number of ways. ET-1 synthesis has a reciprocal synergistic relationship with the renin-angiotensin-aldosterone system which would enhance sodium retention and vasoconstriction resulting in the weakened heart being placed under even greater stress. ET-1 augments the vasoconstriction elicited by other vasoconstrictors such as noradrenaline. Thus, ET-1 can augment the effect of sympathetic innervation on the heart. As ET-1 also has the ability to promote mitogenesis in smooth and cardiac

muscle cells, ET-1 enhances the process of myocardial and peripheral vascular remodelling that occurs with CHF (Rubyani & Polokoff, 1994; Love & McMurray, 1996; Kita *et al.*, 1998). Therefore, ET-1 over-production can augment all the processes that eventually lead to CHF. As mentioned earlier, the family of sarafotoxins (STXs) are structurally similar to the three ET isoforms. The venom of the burrowing asp, *Atractaspis Engaddensis* is an STX. The venom of the burrowing asp has been demonstrated to cause death by heart failure. The resulting heart failure is a consequence of the stimulation of coronary vasospasm and atrio-ventricular node block. These two effects of STX appear to be mediated via an ET_B receptor (Lee *et al.*, 1986).

5.1.6. Role of endothelin in pulmonary hypertension:

Studies have shown an increase in the irET-1 level in patients with PHT of both primary and secondary natures. This increased irET-1 level appears to occur due to a decrease in clearance of ET-1 from the circulation and an increase in ET-1 production. The increase in ET-1 production could be due to the fact that increases in ET-1 mRNA and ECE-1 expression and decreases in ET-1 clearance have been observed in PHT patients, especially in the small PRAs and right atrium (Yoshiyoshi *et al.*, 1991; Moraes *et al.*, 2000). There is a statistically significant directly proportional relationship between the concentration of ET-1 in the pulmonary circulation and the degree of pulmonary vascular resistance in PHT patients. In PHT, the elevated plasma ET-1 levels appear to be a consequence of ET-1 spillover from the pulmonary circulation (Yoshiyoshi *et al.*, 1991; Love & McMurray, 1996; MacLean, 1998; Moraes *et al.*, 2000). The evidence suggests that an increased ET-1 production is a major cause of the development of PHT. Hypoxia of the pulmonary

circulation induces an increase in ET-1 production which may sustain the increase in mean pulmonary arterial pressure occurring as a result of hypoxia, such as that seen in people living at high altitude. An increase in plasma ET-1 levels are seen in patients with emphysema, adult respiratory distress syndrome, heart disease, and cystic fibrosis (Yoshiyoshi *et al.*, 1991; Rubyani & Polokoff, 1994; MacLean, 1998; Moraes *et al.*, 2000).

5.1.7. Endothelin receptor second messenger systems:

Many studies have been carried out on cultured vascular smooth muscle cells and isolated artery or vein preparations in order to determine the 2nd messenger systems coupling the different ET receptor subtypes to their physiological effect. Most studies have been concerned with how ET-1 causes vasoconstriction via the ET_A receptor. There is evidence that ET-1 induces a biphasic increase in $[Ca^{2+}]_i$. The initial, rapid, transient increase is mediated by release of Ca^{2+} from intracellular stores. This intracellular store overlaps with the caffeine-sensitive intracellular store (Miasiro *et al.*, 1988; Kai *et al.*, 1989; Rubyani & Polokoff, 1994). The slow, sustained increase in $[Ca^{2+}]_i$ is likely to be due to Ca^{2+} influx from the extracellular fluid (Simpson & Ashley, 1989). Other studies have found that ET-1 caused an increase in $[Ca^{2+}]_i$ via a nifedipine-insensitive Ca^{2+} channel and not by an L-type Ca^{2+} VOC (Rubyani & Polokoff, 1994). The intracellular Ca^{2+} is mobilised from the stores by PIP₂ hydrolysis product, IP₃. It is proposed that ET-1 activates the ET_A receptor which is coupled to a Gq protein which phosphorylates phospholipase C (PLC) causing the breakdown of PIP₂ to IP₃ and diacylglycerol (DAG). IP₃ stimulates the release of Ca^{2+} from an intracellular store (probably the sarcoplasmic reticulum) and DAG activates protein kinase C (PKC). PKC activates many target proteins within the cell

such as Ca^{2+} VOC's and contractile proteins. Both of these steps increase $[\text{Ca}^{2+}]_i$ and sensitises the myosin light chain kinase (MLCK) to Ca^{2+} , resulting in contraction (Resink *et al.*, 1988; Marsden *et al.*, 1989; Suguira *et al.*, 1989; Sunako *et al.*, 1989; Rubyani & Polokoff, 1994). The PKC inhibitor, staurosporine, can greatly decrease the contraction elicited by ET-1 (Rubyani & Polokoff, 1994).

There is evidence that ET-1 causes vasodilatation via the ET_B receptor which is coupled to a different Gq protein than the ET_A receptor and stimulates PLA_2 . PLA_2 activation causes the breakdown of arachidonic acid to PGI_2 in the endothelial cell by cyclo-oxygenase then peroxidase, and finally, by prostacyclin synthetase. PGI_2 then acts on the IP receptor which stimulates adenylate cyclase (AC) then cAMP via a G_s protein. The increased cAMP activates protein kinase A (PKA) which phosphorylates various target proteins to decrease $[\text{Ca}^{2+}]_i$ and renders the MLCK Ca^{2+} -insensitive so that any increase in $[\text{Ca}^{2+}]_i$ would not cause contraction. ET-1 acting via the ET_B receptor also stimulates the release of NO which causes vasodilatation via cGMP and protein kinase G (PKG) activation (Rubyani & Polokoff, 1994).

It has also been suggested that ET-1 directly modulates intracellular cyclic nucleotides. ET-1 activates ET_A receptors in the vascular smooth muscle cells to stimulate a G_i protein to decrease AC and cAMP (Rubyani & Polokoff, 1994). Hypoxia can modulate the levels of cAMP found in the various arteries of the pulmonary system (Mullaney *et al.*, 1998; Mullaney *et al.*, 2000). Hypoxia causes a decrease in the basal level of cAMP in all the different pulmonary arteries except the small PRAs. ET-1 decreases the cAMP level of the main and first branch of control rat extralobar arteries, an effect partially blocked by inhibiting the ET_A receptor in

control rats. However, all hypoxic pulmonary arteries displayed an increase in cAMP with ET-1. This study demonstrates that hypoxia can modulate basal and ligand-activated levels of cAMP either directly or via cross-talk by G proteins, and that this modulation varies depending on what artery is being studied (Mullaney *et al.*, 1998). An earlier study substantiates these findings by looking at the phosphodiesterase (PDE) activities in the pulmonary circulation. The cAMP PDE activity and the cGMP PDE activity was found to have increased in all hypoxic arteries, except the small PRAs. This would account for the decrease in cAMP basal level seen in the later study. The increased cAMP PDE activity was due to an increase in PDE 3 (cilostimide-inhibited PDE). The increased cGMP PDE activity was due to an increase in PDE 1 (Ca²⁺/calmoduli-stimulated PDE) and PDE 5 (zaprinast-inhibited PDE). These results reveal that changes in the cyclic nucleotides in response to HPV is due to increased PDE activities and that these alterations are differentially modulated with respect to artery location and PDE type (MacLean *et al.*, 1997).

5.1.8. Another endothelin receptor subtype:

As discussed above, although the 2nd messenger systems coupling the ET receptor subtypes to their physiological actions is complicated and can undergo cross-talk and differentiated modulation, the receptor subtypes themselves seemed quite straight forward. It appeared that ET_A receptors caused stimulation and contraction of tissues while ET_B mediated inhibition and relaxation of tissues. However, recent studies in the different pulmonary arteries of various mammalian species, including man, have appeared to expose this classification as over-simplistic using novel ET antagonists. A study looking at the receptor mediating vasoconstriction in isolated rabbit and human pulmonary arteries found vasoconstriction of the rabbit artery that was not

completely inhibited by ET_A antagonists. This suggested that ET_B receptors were capable of mediating vasoconstriction as well as vasodilatation (Fukuroda *et al.*, 1994). In that study, the receptors mediating contraction of the pulmonary arteries were not the same subtypes. However, studies on the small muscular PRAs of 150-250µm in diameter, where most of the increase in pulmonary arterial pressure originates, have displayed similar receptor subtypes mediating ET-1-induced vasoconstriction in these vessels of rats, rabbits, and humans (MacLean *et al.*, 1994; McCulloch & MacLean, 1995; McCulloch *et al.*, 1996; Docherty & MacLean, 1998; MacLean & McCulloch, 1998; MacLean *et al.*, 1998a; MacLean *et al.*, 1998b; McCulloch *et al.*, 1998, Cowburn *et al.*, 1999). In rabbits, ET-1-induced vasoconstriction of PRAs is partly mediated by a heterogeneous population of ET_B receptors, including an atypical ET_B-like receptor (ET_{B2}). The agonist potency rank order for this receptor is: STX_{6c} > ET-1 = ET-3 which is not typical for either the ET_A or the ET_B receptor (Docherty & MacLean, 1998). In addition, responses to ET-1 were not blocked by either ET_A- or ET_B-receptor antagonists. Further studies on rabbit PRAs looked for differences between receptor subtypes in normal rabbits and rabbits with PHT that was secondary to LVD, induced as a result of coronary artery ligation. The ET receptor subtype mediating vasoconstriction in the PRAs from rabbits with LVD was the atypical ET_{B2} receptor as only the mixed ET_A/ET_B antagonist, SB 209670, inhibited the vasoconstriction. However, NO appeared to modify the response to ET-1 mediated by these receptors in the PHT rabbits (Docherty & MacLean, 1998).

It has been possible to study a secondary form of PHT by keeping rats in a hypobaric chamber for 2 weeks (MacLean & McCulloch, 1998). Therefore, studies could look

at the differences between receptor subtype populations in control and chronic hypoxic rat small PRAs. Studies have revealed that rat PRA vasoconstriction is mediated via an atypical ET_{B2} receptor with an agonist rank order of potency of: $STX_{6c} = ET-3 > ET-1$ (McCulloch & MacLean, 1995; McCulloch *et al.*, 1998). The maximum contraction induced by ET-1 is increased in chronic hypoxic (CH) rats. This appears to be due to an increase in the typical vasoconstrictor ET_A receptor activation in CH rat PRAs which could contribute to the increase in ET-1 maximal contraction (McCulloch & MacLean, 1995; McCulloch *et al.*, 1998). There could also be an up-regulation of ET_{B2} receptors in CH rat, however, there is no specific antagonist which would allow us to confirm this hypothesis as yet. A similar atypical ET_{B2} receptor response appears to mediate ET-1 induced vasoconstriction in human PRAs. This ET_{B2} receptor, as in the rat, needs the mixed ET_A/ET_B antagonist SB 209670 to inhibit ET-1 action in human PRAs (McCulloch & MacLean, 1995; McCulloch *et al.*, 1998; MacLean, 1998). However, despite the pharmacological evidence for 'atypical' ET_B -mediated responses, it has to be acknowledged that only two genes for ET_A and ET_B receptors have been identified in the human genome (Li *et al.*, 1994a; Li *et al.*, 1994b).

The 2nd messenger system that couples the atypical ET_{B2} receptor to its physiological effect of vasoconstriction has yet to be fully elucidated. However, recent evidence has been gathering to suggest that ET-1 modulates K^+ currents in the vascular smooth muscle cell to cause depolarisation and, eventually, contraction. It has been demonstrated that inhibition of K^+ channels in rat main pulmonary artery smooth muscle cells cause a depolarisation of the cell membrane which leads to the opening of Ca^{2+} VOC's, resulting in contraction via an increase in $[Ca^{2+}]_i$. The K^+ channel

involved in this depolarisation is the delayed rectifier K^+ channel (K_V) (Salter *et al.*, 1998; and Yuan *et al.*, 1998).

As well as the vasoconstriction mediated by these receptors, ET-1 has been previously shown to inhibit various K^+ channels resulting in a depolarization of the vascular smooth muscle cells (VSMCs) and subsequent vasoconstriction. Earlier studies have shown that ET-1 inhibited the voltage-dependent K^+ channels (K_V) of the intrapulmonary arterial SMCs of the rat; the delayed rectifier K^+ current (I_{KV}) $K_V1.5$ in the pulmonary arteries of the rat; and the Ca^{2+} -activated K^+ (K_{Ca}) channels in human pulmonary artery smooth muscle cells isolated from patients with and without chronic obstructive pulmonary disease (Larissa *et al.*, 1998; Peng *et al.*, 1998; Salter *et al.*, 1998; Larissa *et al.*, 1999). Therefore, ET-1 elicits vasoconstriction by inhibiting various K^+ currents resulting in membrane depolarization as well as an increase in intracellular Ca^{2+} concentration.

5.1.9. Characterisation of endothelin receptors:

The initial characterisation of ET receptors in to ET_A receptors mediating contraction and ET_B receptors mediating relaxation was done only on the basis of physiological effects of ET-1. The detailed studies into receptor subtypes only became possible when ET antagonists became available. Only by the development of novel selective ET antagonists has it become possible to distinguish between vasoconstriction mediated by ET_A receptors from that mediated by the atypical ET_{B2} receptors. Most of the antagonists developed so far have been ET_A antagonists. BQ-123 and BQ-153 are synthetic analogues of the natural ET_A antagonist BE-I8257a isolated from *Streptomyces misakiensis*. Both are selective ET_A antagonists (Ihara *et al.*, 1991; Eguchi *et al.*, 1992; Fukuroda *et al.*, 1992; Bonvallet *et al.*, 1994). BQ-123 causes a

dose-dependent inhibition of IP₃ generation (Eguchi *et al.*, 1992). BQ-123 can inhibit the DNA synthesis involved in vascular smooth muscle cell proliferation seen in PHT as well as inhibiting vasoconstriction by its antagonistic effect on ET_A receptors. Due to the inhibition of DNA synthesis and vasoconstriction, BQ-123 can attenuate the development of PHT caused by hypoxic conditions (Bonvallet *et al.*, 1994). The ET_A antagonists A-127722; PD 156707; and FR 139317 will also inhibit vasoconstriction and vascular smooth muscle cell proliferation (Sogabe *et al.*, 1992; Reynolds *et al.*, 1995; Opgenorth *et al.*, 1996). The ET_A antagonists can reduce ET-1-induced PHT to some extent, but ET_A is not the only receptor to mediate vasoconstriction. The ET_B antagonist BQ-788 abolished the initial rapid transient vasodilator response of ET-1, resulting in augmentation of a sustained vasoconstriction (Ishikawa *et al.*, 1994). BQ-788 did not inhibit the ET-1-induced vasoconstriction mediated by the atypical ET_{B2} (Docherty & MacLean, 1998; MacLean *et al.*, 1998). No antagonists of ET were able to inhibit the ET_{B2}-mediated vasoconstriction until the emergence of novel mixed ET_A/ET_B antagonists. SB 209670 was developed as an orally active, mixed ET_A/ET_B antagonist (Ohlstein *et al.*, 1994). However, it was discovered that this novel antagonist inhibited vasoconstriction in the PRAs of various mammalian species which are the site of the biggest alterations in response to PHT (Docherty & MacLean, 1998; McCulloch *et al.*, 1998; MacLean, 1998; MacLean *et al.*, 1998). Three new mixed ET_A/ET_B antagonists have emerged and also appear to inhibit the atypical ET_{B2} receptor response, SB 247083; SB 234551; and SB 217242 (Ohlstein *et al.*, 1996; Douglas *et al.*, 1998; MacLean *et al.*, 1998). The inhibition of the ET-1 response by mixed ET_A/ET_B antagonists was assessed to reveal which of these is the most likely candidate for therapeutic use.

5.1.10. Chronic heart failure and secondary PHT:

The cardiac myocytes in the failing myocardium display a reduced force of contractility which leads to a reduction in ejection fraction. The decrease in ejection fraction increases the blood volume remaining in the left ventricle, causing stretch of the cardiac myocytes leading to a further decrease in contractility. This results in an increase in the left ventricular end diastolic pressure and a dilatation of the left ventricle. This results in an increase in mean pulmonary artery pressure (MPAP), If this situation is sustained for any length of time, PHT secondary to CHF develops. Secondary PHT is characterised by an increase in MPAP from $< 15\text{mmHg}$ to $> 19\text{mmHg}$. An increase in pulmonary vascular resistance (PVR) from $67 \pm 30 \text{ dynes.s.cm}^{-5}$ to $149 \pm 14 \text{ dynes.s.cm}^{-5}$ and vascular remodelling where there is a progressive muscularisation of the pulmonary vascular tree (Cowburn *et al.*, 1998; Maclean, 1998; Moreas *et al.*, 2000; Huang *et al.*, 2001). There is an increase in vascular tone of both the systemic and pulmonary circulations secondary to CHF. Pulmonary vascular remodelling further enhances PVR and decreases alveolar-capillary membrane diffusion capacity leading to a decrease in gaseous transfer in the alveoli (Puri *et al.*, 1995; Huang *et al.*, 2001). The combination of the increase in PVR and the decreased gas transfer correlated with the exercise intolerance seen in patients with CHF as PHT increases ventilation – perfusion mismatching. The receptor densities of ET receptors in the pulmonary arterial circulation have the ET_A to ET_B ratio of 9:1, and in the left ventricular cardiac myocytes, the ratio is 84:16 in favour of the ET_A receptor. (Modesti *et al.*, 1999; Moreas *et al.*, 2000; Reindl *et al.*, 1998). There is an increase in vascular tone of both the systemic and pulmonary circulations

in PHT secondary to CHF also. The severity of secondary PHT is directly correlated to the prognosis and mortality of patients with CHF (Moreas *et al.*, 2000). CHF is treated with a standard triple drug regimen comprising of a diuretic; digoxin; and an ACE inhibitor such as enalapril. However, despite this treatment, many patients remained symptomatic with little improvement in secondary PHT (Sutch *et al.*, 1998). Therefore, new therapeutic approaches are needed to alleviate the symptoms of CHF and secondary PHT.

ET-1 is implicated in the pathophysiology of CHF and in the PHT which occurs as a consequence of CHF or congenital heart disease, and in idiopathic or primary PHT that has no obvious cause or PHT that occurs as a consequence of sustained hypoxia. Plasma concentrations of ET-1 and ET-1-like immunoreactivity in the myocardium and pulmonary circulation are raised in patients with PHT secondary to CHF and congenital heart defects (Yoshiyayashi *et al.*, 1991; Kiowski *et al.*, 1998; Fukachi & Giaid, 1998; Cowburn *et al.*, 1998a; Cowburn *et al.*, 1998b; Maclean, 1998; Meada *et al.*, 1998; Sutch *et al.*, 1998; Moraes *et al.*, 2000; Huang *et al.*, 2001; Love & McMurray, 1996) and is significantly correlated with the haemodynamic changes associated with, and the severity of, CHF. ET-1 spillover in the lungs is significantly correlated with the raised pulmonary and systemic vascular resistances (PVR and SVR, respectively) and the increased ratios of PVR : SVR seen in such patients. (Yoshiyayashi *et al.*, 1991; Love & McMurray, 1996; Kiowski *et al.*, 1998; Fukachi & Giaid, 1998; Cowburn *et al.*, 1998a; Cowburn *et al.*, 1998b; Maclean, 1998; Meada *et al.*, 1998; Sutch *et al.*, 1998; Moraes *et al.*, 2000; Huang *et al.*, 2001). ET-1 levels are increased during exercise and this is inversely correlated with peak exercise capacity in CHF patients. This evidence suggests that raised ET-1 levels in secondary

PHT may contribute to the exercise intolerance seen in CHF patients (Moraes *et al.*, 2000). ET-1 is a potent and efficacious vasoconstrictor of the arterial and venous sides of both the pulmonary and systemic vascular circulations (MacLean, 1998; Love *et al.*, 2000). Both ET-1 and endothelin-converting enzyme-1 (ECE-1) have been shown to be synthesised in the vascular endothelial cells and macrophages of the failing myocardium (Fukuchi & Giaid, 1998). Cowburn *et al.* (1998a) infused exogenous ET-1 (at a concentration observed in CHF patients) into the pulmonary artery of patients with CHF subsequent to left ventricular dysfunction. This resulted in an increase in the systemic, but not mean pulmonary, artery pressure while cardiac index fell (Cowburn *et al.*, 1998 a & b). Therefore, exogenous ET-1 caused systemic vasoconstriction without affecting the pulmonary vasculature. This evidence is fuel for the continuing debate over whether the increase in plasma levels of ET-1 seen in patients with secondary PHT is the cause/mediator of, or is merely a marker of the severity of the condition. A definitive answer is still proving to be elusive (Cowburn *et al.*, 1998 a & b; MacLean, 1998; Moraes *et al.*, 2000).

5.1.11. Endothelin antagonists in heart failure:

Studies have previously shown the effect of ET_A selective antagonists on haemodynamics in CHF patients. The ET_A-selective antagonist, LU 135252, has been shown to significantly improve endothelium-dependent, flow-mediated vasodilatation that is normally impaired in CHF patients resulting in exercise intolerance (Berger *et al.*, 2001). LU 135252 also significantly lowers systemic systolic BP, increases cardiac output, and limits the progressive left ventricular remodelling that causes dilatation of the left ventricle leading to a decrease in ejection fraction (Mulder *et al.*, 1998). BMS-19388 has been shown to reduce the hypertrophy of the cardiac

myocytes of the right ventricle, which starts to fail as a consequence of sustained PHT. This antagonist also reduces the pre-load to the right ventricle which will decrease the right ventricular end diastolic pressure and benefit the right failing ventricle (Miyachi *et al.*, 2000). The ET_A-selective antagonists, FR 139317 and BMS 182874, inhibited the ET-1-induced vasoconstriction at concentrations > 1nM in human small PRAs (McCulloch *et al.*, 1996).

A previous study involving the ET_B-selective antagonist, BQ-788, has shown that it inhibited the first phase of the ET-1-mediated biphasic vasoconstrictor response (<1nM) observed in human small PRAs (McCulloch *et al.*, 1996). The ET_B-selective antagonist K-8794 has been shown to increase both systemic BP and SVR as a result of inhibition of ET_{B1}-mediated vasodilatation. However, this same study showed that K-8794 significantly attenuated the activation of the RAAS, therefore, limiting the increase in blood volume and vasoconstriction caused by this neurohumoral system (Sawaki *et al.*, 2000).

The mixed ET_A/ET_B receptor antagonist, bosentan, has been used in several studies investigating its haemodynamic effects in patients with secondary PHT as a consequence of CHF. Bosentan treatment showed a significant decrease in mean arterial pressure, mean pulmonary arterial pressure (MPAP), pulmonary capillary wedge pressure (PCWP), SVR, PVR, and right ventricular pressure, whilst increasing the CO. These haemodynamic responses were seen within one day of treatment. After two weeks of treatment, bosentan further reduced both SVR and PVR, whilst CO was further increased. The plasma ET-1 level was increased after bosentan administration (Sutch *et al.*, 1998; and Moraes *et al.*, 2000). Bosentan treatment

resulted in an improvement of the haemodynamics of both the pulmonary and systemic circulations in patients who had been symptomatic while on the standard triple therapy regime (Sutch *et al.*, 1998). Bosentan is now in phase III trials for CHF and has recently been approved by the Food and Drug Administration (FDA) for use in primary PHT. The mixed ET_A/ET_B receptor antagonists, SB 209670; SB 217242; and SB 234551, all inhibited the ET-1-mediated vasoconstriction of human small PRAs (MacLean *et al.*, 1998).

These previous studies have not provided a definitive answer as to which type of ET receptor antagonist would be the most therapeutically beneficial in the treatment of CHF and secondary PHT. However, as the blockade of ET_{B2} is beneficial in the attenuation of vasoconstriction and in the suppression of the RAAS, ET_B blockade is a desirable effect, despite the inhibition of ET_{B1} -mediated vasodilatation. Antagonism of both ET_A and ET_B receptors may be required to fully suppress the pathophysiological effects of ET-1 in CHF. Therefore, our group investigated the effects of three novel, mixed ET_A/ET_B antagonists on human small PRAs in patients with different degrees of left ventricular dysfunction. This study compared the ET-1-mediated vasoconstriction in the small PRAs of patients with good, moderate, and poor left ventricular ejection fractions and control patients to see if there is a change in the vasoconstrictor effect of ET-1 as the severity of left ventricular dysfunction increases. This study will also characterise the ability of the three novel, mixed ET_A/ET_B antagonists to inhibit the ET-1-induced vasoconstriction in these tissues and to compare their effect between the different patient subgroups.

5.1.12. Novel mixed ET_A/ET_B antagonists:

The chemical name of SB 247083 is: ((E)-[1-butyl-5-[2-(2-carboxyphenyl)methoxy-4-chlorophenyl]-1H-pyrazol-4-yl]-2-[5-methoxydihydrobenzofuran-6-yl]-2-propionic acid)). SB 247083 has been characterised as a non-peptide, orally active ET_A-selective antagonist which inhibited the ET_A-mediated ET-1-induced vasoconstriction of the isolated rat aorta, but was less potent at inhibiting the ET_B-mediated STX_{s6c}-induced vasoconstriction of isolated rabbit pulmonary arteries (Douglas *et al.*, 1998). This antagonism profile is due to the greater affinity of SB 247083 for ET_A than ET_B receptor subtypes (K_i 0.41 and 467nM, respectively) (Douglas *et al.*, 1998; Willette *et al.*, 1998).

The chemical name of SB 234551 is: ((E)-alpha-[[1-butyl-5-[2-[(2-carboxyphenyl)methoxy-phenyl]-1H-pyrazol-4-yl]methylene]-6-methoxy-1,3-benzodioxole-5-propanoic acid). SB 234551 has been characterised as an orally available, non-peptide ET_A-selective antagonist. Previous studies have shown that SB234551 caused a rightward shift of the ET_A-mediated ET-1 concentration / response curves in the isolated rat aorta and large human pulmonary arteries. However, SB 234551 also caused a rightward shift in the ET_B-mediated STX_{s6c}-induced vasoconstriction of the isolated rabbit pulmonary artery (Ohlstein *et al.*, 1998). SB 234551 inhibited the ET-1-induced vasoconstriction of isolated human PRAs (MacLean *et al.*, 1998). A study investigating the effect of SB234551 on the ET-1-induced decrease in glomerular filtration rate and renal plasma flow revealed that SB234551 not only inhibited these pathophysiological effects of ET-1 in the renal circulation but actually increased the renal plasma flow (Brooks *et al.*, 1998). As SB 234551 has also been shown to have only a weak inhibitory effect on the ET_B-mediated STX_{s6c}-

induced vasodilatation of the isolated rabbit pulmonary artery, SB 234551 has been shown to inhibit vasoconstriction by both ET_A and ET_B receptor subtypes while still allowing ET_B-mediated vasodilatation (Brooks *et al.*, 1998; Ohlstein *et al.*, 1998). This antagonism profile is due to the greater affinity of SB 234551 for ET_A than ET_B receptor subtypes (K_i 0.13 and 500nM, respectively) (Brooks *et al.*, 1998; MacLean *et al.*, 1998; Ohlstein *et al.*, 1998; Willette *et al.*, 1998).

The chemical name of SB 217242 is: (1S, 2R, 3S)-3-[2-(2-hydroxyeth-1-yloxy)-4-methoxyphenyl]-1-(3,4-methylenedoxyphenyl)-5-(prop-1-yloxy)indan-2-carboxylic acid. SB 217242 has been classed as a non-peptide, orally active ET_A-selective antagonist (Underwood *et al.*, 1998; Underwood *et al.*, 1999). In earlier studies SB 217242 was shown to inhibit the increase in pulmonary artery pressure, the increase in right ventricular hypertrophy and medial thickening of PRAs in high altitude-sensitive rats resulting from 14 days chronic hypoxia exposure (Underwood *et al.*, 1998; Underwood *et al.*, 1999). SB 217242 inhibited the ET-1-induced vasoconstriction of isolated human PRAs (MacLean *et al.*, 1998). This antagonism profile is due to the greater affinity of SB 217242 for ET_A than ET_B receptor subtypes (K_i 1.1 and 111nM, respectively) (Underwood *et al.*, 1998; MacLean *et al.*, 1998; Willette *et al.*, 1998; Underwood *et al.*, 1999).

5.2. Methods

5.2.1. *In vivo* study:

Our group teamed up with two cardiothoracic surgeons from the cardiology dept. of Glasgow Western Infirmary, Mr. John Lu and Mr. Michael Flynn, to assess the effect of various vasoactive substances on the cardiovascular system *in vivo* and *in vitro*. This was a BHF funded project with local ethical permission granted. The *in vivo* assessment of the vasoconstrictor effects of ET-1 and 5-HT, and the vasodilator effects of PGI₂ were carried out by the surgeons involved in the study. Therefore, all results of the *in vivo* study discussed in this chapter have been supplied by Mr. John Lu and Mr. Michael Flynn. Patients involved in the study were admitted to the hospital for one day a week prior to the coronary artery bypass graft the *in vivo* component of the study which includes thermodilution catheterisation to assess cardiovascular haemodynamics and echocardiographic assessment of left ventricular function. Under local anaesthesia, a pulmonary artery flotation catheter was inserted into either the femoral, antecubital brachial or internal jugular vein and fed through to its destination in the pulmonary artery under fluoroscopy. After a 30 minute period of bed rest, the haemodynamic baselines were stabilised and measurements of the right heart pressures, pulmonary artery wedge pressure, SVR, PVR and cardiac output were taken. The first infusion involved PGI₂ at 4, 8, and 12ng/kg/min to assess the maximum vasodilator reserve. After a 30 minute washout period, 15pmol/min of ET-1, 0.5 ng/kg/min of 5-HT or saline were infused in a random sequence. All infusions were followed by a 30 minute washout period during which all haemodynamic parameters returned to baseline levels. Heparin (5000 IU) was given to all patients before 5-HT and ET-1 infusion to inhibit platelet aggregation. During these infusions, all patients received continuous ECG monitoring. As the *in vitro*

experiments in this chapter only involve ET-1 and the effect of mixed ET_A/ET_B antagonists on this response, I will only discuss the results of the ET-1 component of the *in vivo* study.

5.2.2. *In vitro* study:

Small muscular PRAs were dissected free from human lung tissue biopsies from patients undergoing coronary bypass grafts to alleviate coronary artery occlusion and left ventricular dysfunction. Written consent was obtained from patients to allow the collection of a biopsy of their lung during surgery. As mentioned above, cardiothoracic surgeons at Glasgow Western Infirmary had previously assessed the function of the left ventricle by echocardiographic measurement of the ejection fraction of patients undergoing this surgery. Patients with an ejection fraction of >40% were classed as being in the good LVF group. Patients with an ejection fraction of between 30-40% were classed as being in the moderate LVF group. Patients with an ejection fraction of <30% were classed as being in the poor LVF group. Once isolated from the surrounding parenchyma, the small muscular PRAs of each of these patient groups were set up on an isometric wire myograph (Mulvaney & Halpern, 1997). The transmural pressure of the vessels was set at ~16mmHg.

Another 'group' of vessels was studied. They were small muscular pulmonary resistance arteries (PRAs) were dissected free from human lung tissue resected from patients undergoing thoracotomies for bronchial carcinoma. Written consent was obtained from these patients to allow the collection of a biopsy of their resected lung for our study. The patients were given the designation of control left ventricular function (control LVF) as these patients did not have coronary artery disease.

After an equilibration period of 45 minutes, tension was applied to the isolated vessels by the method described in chapter 2. Once the tension had stabilised, the vessels were left to equilibrate for a further 45 minutes. 50mM KCl was added to the baths to determine the viability of the vessels. KCl additions were repeated until two reproducible vasoconstrictions were observed. Between each addition of KCl, there were repeated washes of the baths until the tension returned to its baseline level.

The vessels were incubated for one hour with either 1 μ M SB 247083, SB 234551, or SB 217242. During each experiment, one vessel was not incubated with an ET_A/ET_B antagonist and this vessel acted as a control ET-1 response. After the incubation period was over, a cumulative concentration response curve (CCRC) to ET-1 was carried out in all vessels. The vessels were only used for one ET-1 CCRC as ET-1 is resistant to washout (Maguire *et al.*, 2000). The ET-1 response achieved in the antagonist treated vessels did not reach a maximum in many cases. However, due to the very expensive cost of ET-1, the highest concentration that could be used was 0.3 μ M which did not always allow the ET-1 response to reach a maximum in the antagonist treated vessels.

5.3. Results

5.3.1. *In vivo* study (carried out by surgeons Mr. John Lu and Mr. Michael Flynn):

An infusion of ET-1 at a rate of 15pmol/min was infused into good, moderate, and poor LVF group patients. The haemodynamic parameters tested before and after infusion were mean PAP, capillary wedge pressure, mean arterial pressure, CI, heart rate, SVR and PVR. These parameters were compared between the different patient groups before ET-1 infusion. The only parameter to show a significant difference between the groups was the PVR at rest which showed a significant increase in the poor LVF group compared with the good LVF group. These results are shown in

Table 5.1.

LVF Group	Good (at rest)	Poor (at rest)
PVR (dynes.s.cm⁻⁵)	139.14 ± 11.40	189.50 ± 13.25*
n	14	6

Table 5.1: The pulmonary vascular resistance (PVR) values measured in patients from the good and poor LVF groups. Data are expressed as mean ± SEM. n = number of patients. Statistical comparisons were made using an unpaired Students' t-test. $P < 0.05^*$ vs. good LVF group.

After infusion of ET-1 (15pmol/min), the only parameters to show a significant difference between the groups were PVR and mean arterial pressure. Infusion of ET-1 caused a significant increase in the PVR value of the good LVF group when compared to the PVR at rest in this group. These results are shown in **Table 5.2**.

LVF Group	Good (at rest)	Good (with ET-1)
PVR (dynes.s .cm⁻⁵)	139.14 ± 11.40	171.29 ± 10.86*
n	14	14

Table 5.2: The PVR value measured in patients of the good LVF group at rest and after infusion of ET-1 (15 pmol/min). Data are expressed as mean ± SEM. n = number of patients. Statistical comparisons were made using an unpaired Students' t-test. $P < 0.05^*$ vs. PVR at rest.

Infusion of ET-1 caused a significant increase in the mean arterial pressure of the moderate LVF group when compared with the good LVF group. These results are shown in **Table 5.3**.

LVF GROUP	Good (with ET-1)	Moderate (with ET-1)
Mean arterial pressure (mmHg)	85.57 ± 3.11	96.86 ± 3.14*
n	14	14

Table 5.3: The mean arterial pressure measured after infusion of ET-1

(15 pmol/min) in the good and moderate LVF groups. Data are expressed as mean ± SEM. n = number of patients. Statistical comparisons were made using an unpaired Students' t-test. $P < 0.05^*$ vs. good LVF group.

5.3.2. *In vitro* study

5.3.2.1. Comparison of ET-1 response between groups:

ET-1 induced a potent vasoconstriction in the human small PRAs from the control, good, moderate, and poor LVF groups. The ET-1 CCRC appears to be characteristically biphasic in nature with a first slow, shallow component and a second fast, steep component. The PRAs in this study are classed with regards to the patient's ejection fraction. Patients undergoing a thoracotomy to resect a bronchial carcinoma, but have no coronary artery disease, are classed as controls. PRAs from patients undergoing a coronary artery bypass with an ejection fraction of > 40% are classed as having a good LVF. PRAs from patients undergoing a coronary artery bypass with an ejection fraction of 30-40% are classed as having a moderate LVF. PRAs from patients undergoing a coronary artery bypass with an ejection fraction of

<30% are classed as having a poor LVF. The vasoconstrictor response to ET-1 in these groups is displayed in **Figure 5.2**. The vessels sizes and maximum contractile responses to 50mM KCl from each of the different LVF groups are shown in **Table 5.4**. There was no significant difference in the potency of ET-1 between the patient groups. These results are shown in **Table 5.5**. There was no significant difference in the maximum constrictor response to ET-1 between the groups. These results are displayed in **Table 5.6**.

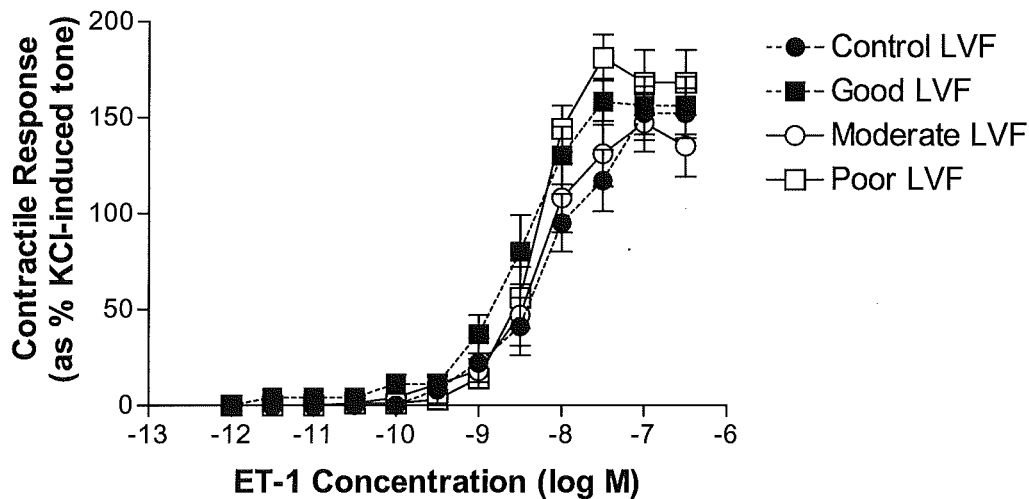


Figure 5.2: The vasoconstrictor response to ET-1 in the human small PRAs of the various LVF groups. Control (n = 12); good LVF (n = 7); moderate LVF (n = 12); and poor LVF (n = 8). Data expressed as percentage of 50mM KCl-induced vasoconstriction. Each point represents the mean \pm SEM.

Protocol Group	Control	Good LVF	Moderate LVF	Poor LVF
Vessel Size (μm)	191 \pm 21	180 \pm 32	213 \pm 14	194 \pm 25
KCl-Induced Tone (mN)	3.17 \pm 0.40	1.42 \pm 0.45	1.94 \pm 0.45	1.52 \pm 0.46
n	12	7	12	8

Table 5.4: Dimensions and measurements of 50mM KCl-induced vasoconstriction in the control ET-1 protocol group of the four different LVF groups. Data are expressed as mean \pm SEM. n = number of patients.

LVF Group	Control	Good LVF	Moderate LVF	Poor LVF
pEC₅₀ values	8.13 \pm 0.12	8.53 \pm 0.17 ^{ns}	8.24 \pm 0.14 ^{ns}	8.32 \pm 0.07 ^{ns}
n	12	7	12	8

Table 5.5: pEC₅₀ values for ET-1 in the human small PRAs of the control, good, moderate and poor LVF groups. Data are expressed as mean \pm SEM. n = number of patients. Statistical comparisons were made using a one-way ANOVA with a Dunnetts' post-test. ns = not significant vs. control group.

Protocol Group	Control	Good	Moderate	Poor
ET-1 Max. Response (as % KCl-Induced Tone)	152 ± 13	141 ± 16 ^{ns}	135 ± 16 ^{ns}	168 ± 17 ^{ns}
n	12	7	12	8

Table 5.6: The maximum contractile response to 0.3µM ET-1 as percentage of 50mM KCl-induced vasoconstriction in the human small PRAs of the control, good, moderate and poor LVF groups. Data are expressed as mean ± SEM. n = number of patients. Statistical comparisons were made using a one way ANOVA with a Dunnetts' post-test. ns = not significant vs. control group.

5.3.2.2. The effect of the mixed ET_A/ET_B antagonists in the control group:

ET-1 induced a vasoconstriction which had a characteristically biphasic CCRC in the small muscular PRAs in the presence and absence of the mixed ET_A/ET_B antagonists except for SB 247083 in the control group (**Figure 5.3**). The vessels sizes and maximum contractile responses to 50mM KCl in the control PRAs are shown in **Table 5.7**.

The vasoconstrictor response to ET-1 in the presence and absence of 1 μ M SB 247083; SB 234551; and SB 217242 in the control group is shown in **Figure 5.3**. A summary of pEC₅₀ values is shown in **Table 5.8**. A summary of the maximum responses to ET-1 is displayed in **Table 5.9**.

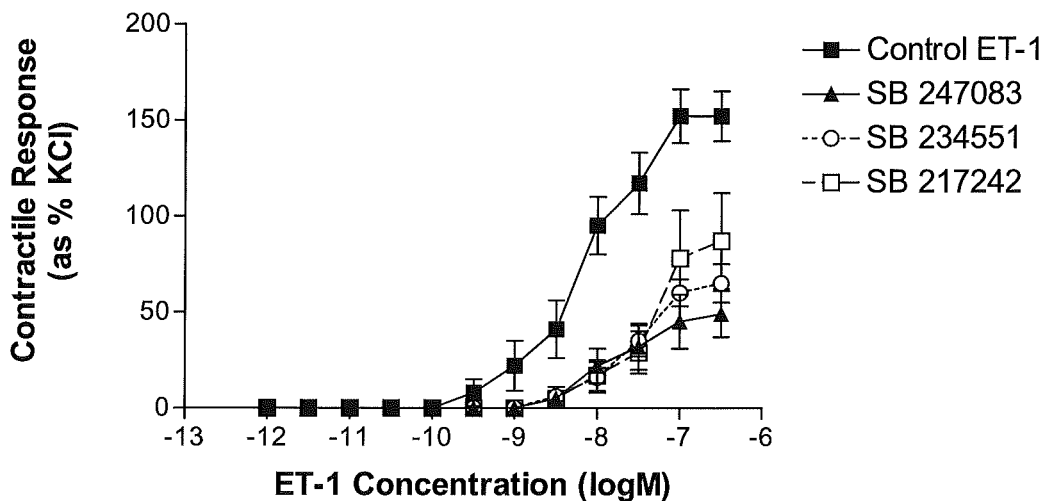


Figure 5.3: The vasoconstrictor response to ET-1 in the human small PRAs in the presence and absence of 1 μ M of a mixed ET_A/ET_B antagonist in the control LVF group. Control ET-1 (n = 12); SB 247083 (n = 10); SB 234551 (n = 8); and SB 217242 (n = 8). Data expressed as percentage of 50mM KCl-induced vasoconstriction. Each point represents the mean \pm SEM.

Protocol Group	Control ET-1	SB 247083	SB 234551	SB 217242
Vessel Size (µm)	191 ± 21	202 ± 15	216 ± 18	194 ± 25
KCl-Induced Tone (mN)	3.17 ± 0.40	3.58 ± 0.89	1.23 ± 0.28	1.52 ± 0.46
n	12	10	8	8

Table 5.7: Dimensions and measurements of 50mM KCl-induced vasoconstriction in the various protocol groups of the control group. Data are expressed as mean ± SEM. n = number of patients.

SB 247083 significantly decreases the potency of ET-1 (n = 10, $P < 0.05$).

SB 247083 significantly attenuates the maximum response to ET-1 ($P < 0.01$).

SB 234551 significantly decreases the potency of ET-1 (n = 8, $P < 0.05$). SB 234551 significantly attenuates the maximum response to ET-1 ($P < 0.01$). SB 217242 significantly decreases the potency of ET-1 (n = 8, $P < 0.05$). SB 217242 significantly attenuates the maximum response to ET-1 ($P < 0.05$) (**Tables 5.8 and 5.9**).

Protocol Group	Control ET-1	SB 247083	SB 234551	SB 217242
pEC₅₀ values	8.13 ± 0.12	7.59 ± 0.15*	7.66 ± 0.12*	7.56 ± 0.18*
n	12	10	8	8

Table 5.8: pEC₅₀ values for ET-1 in the human small PRAs of the control group ± 1µM of a mixed ET_A/ET_B antagonist. Data are expressed as mean ± SEM.

n = number of patients. Statistical comparisons were made using a one-way ANOVA with a Dunnetts' post-test. $P < 0.05^*$ vs. control ET-1.

Protocol Group	Control ET-1	SB 247083	SB 234551	SB 217242
ET-1 Max. Response (as % KCl-Induced Tone)	152 ± 13	49 ± 12**	65 ± 10**	87 ± 25*
n	12	10	8	8

Table 5.9: The maximum contractile response to 0.3µM ET-1 as percentage of 50mM KCl-induced vasoconstriction in the human small PRAs of the control group. Data are expressed as mean ± SEM. n = number of patients. Statistical comparisons were made using a one-way ANOVA with a Dunnetts' post-test. $P < 0.05^*$, $P < 0.01^{**}$ vs. control ET-1 response.

5.3.2.3. The effects of the mixed ET_A/ET_B antagonists in the good LVF group:

ET-1 induced a vasoconstrictor response with a characteristically biphasic CCRC in the small muscular PRAs in the presence and absence of the mixed ET_A/ET_B antagonists in the good LVF group, except for in the presence of SB 217242 which removed the first component of the CCRC. The vessel sizes and maximum contractile responses to 50mM KCl in the good LVF PRAs are shown in **Table 5.10**.

The vasoconstrictor response to ET-1 in the presence and absence of 1 μ M

SB 247083; SB 234551; and SB 217242 in the good LVF group is shown in **Figure**

5.4. A summary of pEC₅₀ values is shown in **Table 5.11**. A summary of the maximum responses to ET-1 is displayed in **Table 5.12**.

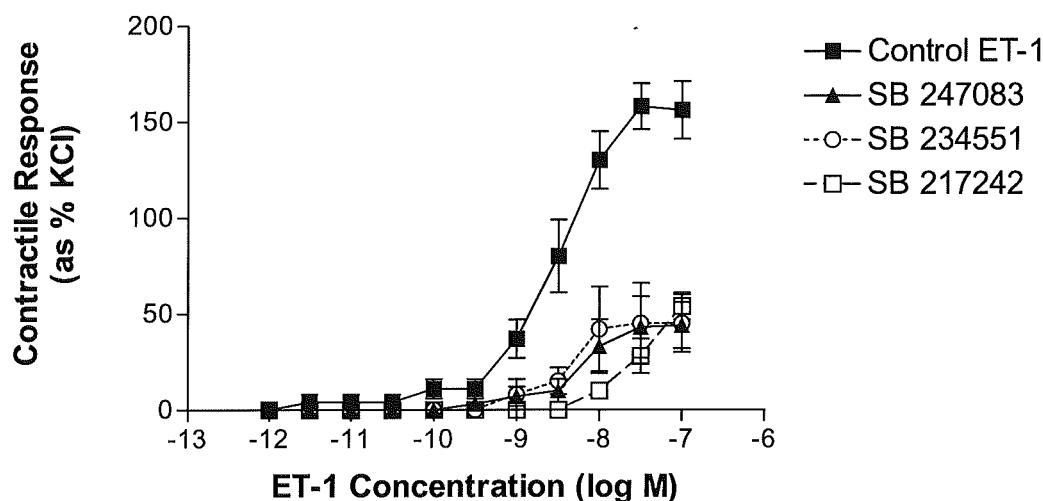


Figure 5.4: The vasoconstrictor response to ET-1 in the human small PRAs in the presence and absence of 1 μ M of a mixed ET_A/ET_B antagonists in the good LVF group. Control ET-1 (n = 7); SB 247083 (n = 6); SB 234551 (n = 4); and SB 217242 (n = 4). Data expressed as percentage of KCl-induced vasoconstriction. Each point represents the mean \pm SEM.

SB 247083 significantly decreases the potency of ET-1 ($n = 6, P < 0.05$). SB 247083 significantly attenuates the maximum response to ET-1 ($P < 0.01$). SB 234551 significantly decreases the potency of ET-1 ($n = 4, P < 0.05$). SB 234551 significantly attenuates the maximum response to ET-1 ($P < 0.01$). SB 217242 significantly decreases the potency of ET-1 ($n = 4, P < 0.01$). SB 217242 significantly attenuates the maximum response to ET-1 ($P < 0.01$). (Tables 5.11 and 5.12).

Protocol Group	Control ET-1	SB 247083	SB 234551	SB 217242
Vessel Size (μm)	180 \pm 32	190 \pm 10	204 \pm 14	183 \pm 19
KCl-Induced Tone (mN)	1.42 \pm 0.45	2.19 \pm 0.83	0.89 \pm 0.23	1.27 \pm 0.09
n	7	6	4	4

Table 5.10: Dimensions and measurements of 50mM KCl-induced vasoconstriction in the various protocol groups of the good LVF group. Data are expressed as mean \pm SEM. n = number of patients.

Protocol Group	Control ET-1	SB 247083	SB 234551	SB 217242
pEC ₅₀ values	8.53 ± 0.17	7.87 ± 0.19*	7.77 ± 0.24*	7.40 ± 0.09**
n	7	6	4	4

Table 5.11: pEC₅₀ values for ET-1 in the human small PRAs of the good LVF group ± 1 μM of a mixed ET_A/ET_B antagonist. Data are expressed as mean ± SEM.

n = number of patients. Statistical comparisons were made using a one-way ANOVA with a Dunnetts' post-test. $P < 0.05^*$, $P < 0.01^{**}$ vs. control ET-1.

Protocol Group	Control ET-1	SB 247083	SB 234551	SB 217242
ET-1 Max. Response (as % KCl-Induced Tone)	141 ± 16	50 ± 9**	49 ± 19**	61 ± 3**
n	7	6	4	4

Table 5.12: The maximum contractile response to 0.3 μM ET-1 as percentage of 50mM KCl-induced vasoconstriction in the human small PRAs of the good LVF group. Data are expressed as mean ± SEM. n = number of patients. Statistical comparisons were made using a one-way ANOVA with a Dunnetts' post-test.

$P < 0.01^{**}$ vs. control ET-1 response.

5.3.2.4. The effects of mixed ET_A/ET_B antagonists in the moderate LVF group:

ET-1 induced a vasoconstriction which had a characteristically biphasic CCRC in the small muscular PRAs in the presence and absence of the mixed ET_A/ET_B antagonists in the moderate LVF group, except for SB 247083. The vessels sizes and maximum contractile responses to 50mM KCl in the moderate LVF PRAs are shown in **Table 5.13**.

The vasoconstrictor response to ET-1 in the presence and absence of 1 μ M SB 247083; SB 234551; and SB 217242 in the moderate LVF group is shown in **Figure 5.5**. A summary of pEC₅₀ values is shown in **Table 5.14**. A summary of the maximum responses to ET-1 is displayed in **Table 5.15**.

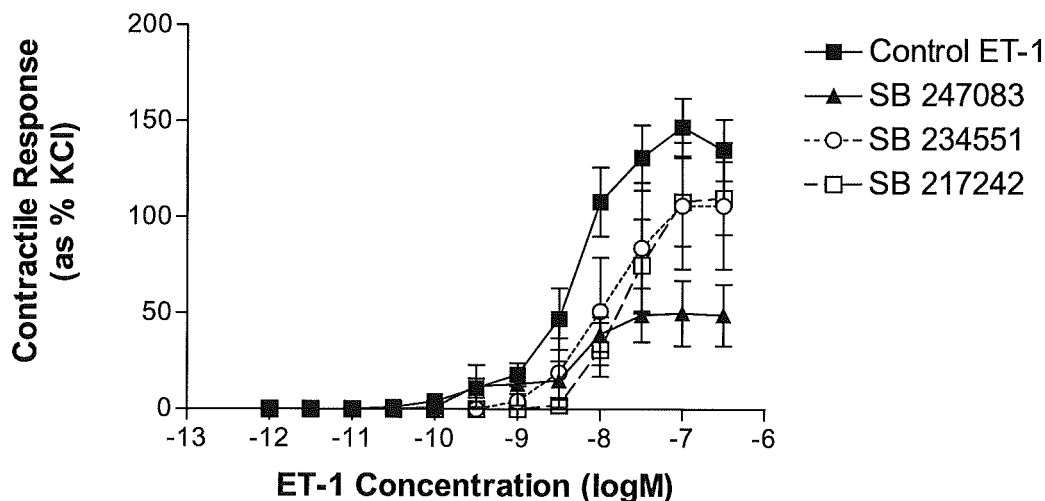


Figure 5.5: The vasoconstrictor response to ET-1 in the human small PRAs in the presence and absence of 1 μ M of a mixed ET_A/ET_B antagonists in the moderate LVF group. Control ET-1 (n = 12); SB 247083 (n = 7); SB 234551 (n = 7); and SB 217242 (n = 6). Data expressed as percentage of 50mM KCl-induced vasoconstriction. Each point represents the mean \pm SEM.

Protocol Group	Control ET-1	SB 247083	SB 234551	SB 217242
Vessel Size (µm)	213 ± 14	168 ± 17	197 ± 22	200 ± 12
KCl-Induced Tone (mN)	1.94 ± 0.45	1.14 ± 0.46	0.84 ± 0.27	1.09 ± 0.25
n	12	7	7	6

Table 5.13: Dimensions and measurements of 50mM KCl-induced vasoconstriction in the various protocol groups of the moderate LVF group. Data are expressed as mean ± SEM. n = number of patients.

SB 247083 did not significantly decrease the potency of ET-1 in the moderate PRAs. SB 247083 significantly attenuates the maximum response to ET-1 (n = 7, $P < 0.05$). SB 234551 did not significantly decrease the potency of ET-1. SB 234551 did not significantly attenuate the maximum response to ET-1. SB 217242 did not significantly decrease the potency of ET-1. SB 217242 did not significantly attenuate the maximum response to ET-1. (Tables 5.14 and 5.15).

Protocol Group	Control ET-1	SB 247083	SB 234551	SB 217242
pEC₅₀ values	8.24 ± 0.14	8.30 ± 0.36 ^{ns}	8.10 ± 0.18 ^{ns}	7.67 ± 0.15 ^{ns}
n	12	7	7	6

Table 5.14: pEC₅₀ values for ET-1 in the human small PRAs of the moderate LVF group ± 1 μM of a mixed ET_A/ET_B antagonist. Data are expressed as mean ± SEM.

Statistical comparisons were made using a one-way ANOVA with a Dunnetts' post-test. ns = not significant.

Protocol Group	Control ET-1	SB 247083	SB 234551	SB 217242
ET-1 Max. Response (as % KCl-Induced Tone)	135 ± 16	49 ± 16*	106 ± 32 ^{ns}	110 ± 19 ^{ns}
n	12	7	7	6

Table 5.15: The maximum contractile response to 0.3 μM ET-1 as percentage of 50mM KCl-induced vasoconstriction in the human small PRAs of the moderate LVF group. Data are expressed as mean ± SEM. n = number of patients. Statistical comparisons were made using a one-way ANOVA with a Dunnetts' post-test.

P < 0.05* vs. control ET-1 response. ns = not significant.

5.3.2.5. The effects of the mixed ET_A/ET_B antagonist the poor LVF group:

ET-1 induced a vasoconstriction which had a characteristically biphasic CCRC in the small muscular PRAs in the presence and absence of the mixed ET_A/ET_B antagonists, except SB 247083 in the poor LVF group. The vessels sizes and maximum contractile responses to 50mM KCl in the poor LVF PRAs are shown in **Table 5.16**. There is no significant difference in the tone induced by 50mM KCl between the control ET-1 group and either of the mixed ET_A/ET_B antagonist groups.

The vasoconstrictor response to ET-1 in the presence and absence of 1 μ M SB 247083; SB 234551; and SB 217242 in the poor LVF group is shown in **Figure 5.6**. A summary of pEC₅₀ values is shown in **Table 5.17**. A summary of the maximum responses to ET-1 is displayed in **Table 5.18**.

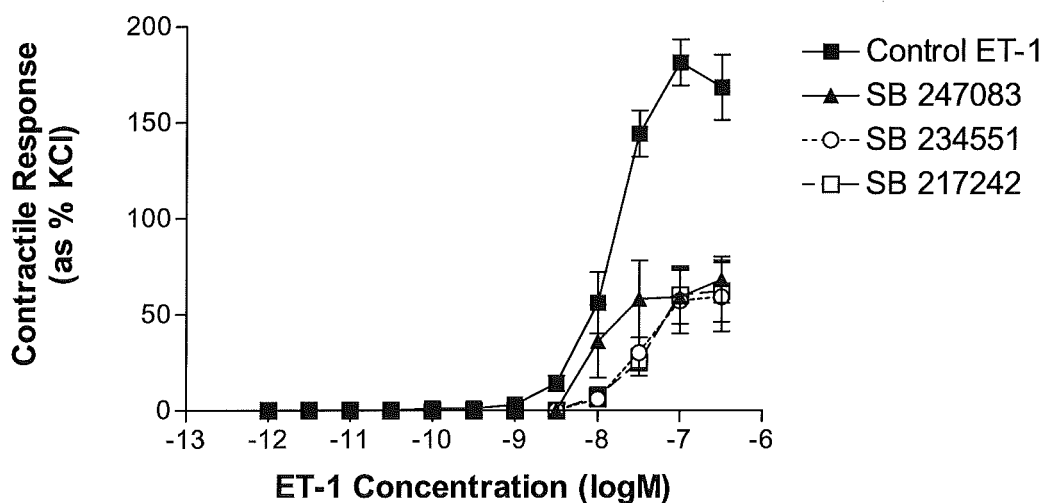


Figure 5.6: The vasoconstrictor response to ET-1 in the human small PRAs in the presence and absence of 1 μ M of a mixed ET_A/ET_B antagonists in the poor LVF group. Control ET-1 (n = 8); SB 247083 (n = 6); SB 234551 (n = 6); and SB 217242 (n = 6). Data expressed as percentage of 50mM KCl-induced vasoconstriction. Each point represents the mean \pm SEM.

Protocol Group	Control ET-1	SB 247083	SB 234551	SB 217242
Vessel Size (µm)	155 ± 26	175 ± 13	180 ± 10	164 ± 17
KCl-Induced Tone (mN)	1.31 ± 0.31	1.23 ± 0.21	0.66 ± 0.13	0.58 ± 0.09
n	8	6	6	6

Table 5.16: Dimensions and measurements of 50mM KCl-induced vasoconstriction in the various protocol groups of the poor LVF group. Data are expressed as mean ± SEM. n = number of patients.

SB 247083 significantly decreases the potency of ET-1 (n = 6, $P < 0.05$). SB 247083 significantly attenuates the maximum response to ET-1 ($P < 0.01$). SB 234551 significantly decreases the potency of ET-1 (n = 6, $P < 0.01$). SB 234551 significantly attenuates the maximum response to ET-1 ($P < 0.01$). SB 217242 significantly decreases the potency of ET-1 (n = 6, $P < 0.01$). SB 217242 significantly attenuates the maximum response to ET-1 ($P < 0.01$). (Table 5.17 and 5.18).

Protocol Group	Control ET-1	SB 247083	SB 234551	SB 217242
pEC₅₀ values	8.32 ± 0.07	7.82 ± 0.17*	7.41 ± 0.12**	7.39 ± 0.07**
n	8	6	6	6

Table 5.16: pEC₅₀ values for ET-1 in the human small PRAs of the poor LVF group ± 1µM of a mixed ET_A/ET_B antagonist. Data are expressed as mean ± SEM.

n = number of patients. Statistical comparisons were made using a one-way ANOVA with a Dunnetts' post-test. $P < 0.05^*$, and $P < 0.01^{**}$ vs. control ET-1.

Protocol Group	Control ET-1	SB 247083	SB 234551	SB 217242
ET-1 Max. Response (as % KCl-Induced Tone)	168 ± 17	68 ± 12**	59 ± 18**	62 ± 16**
n	8	6	6	6

Table 5.18: pEC₅₀ values for ET-1 in the human small PRAs of the poor LVF group ± 1µM of a mixed ET_A/ET_B antagonist. Data are expressed as mean ± SEM.

n = number of patients. Statistical comparisons were made using a one-way ANOVA with a post-test. $P < 0.01^{**}$ vs. control ET-1.

5.4. Discussion

5.4.1. *In vivo* study:

The findings of the *in vivo* study conducted by Mr Lui and Mr Flynn both agreed and disagreed with the results of two previous studies investigating the effect of infused ET-1 on the cardiovascular haemodynamics of CHF patients. The results of the Moraes *et al.* (2000) study showed that the presence of CHF was correlated with the pulmonary haemodynamic parameters of PVR and mean PAP, but not the systemic parameters of CI and SVR. Our group's study found that the only changes in the cardiovascular system that the progression of left ventricular dysfunction caused were in the pulmonary circulation. The PVR of the poor LVF group at rest was significantly increased with respect to the PVR of the good LVF group. This previous study also defined PHT as being present when the mean PAP is ≥ 19 mmHg. The mean PAP of the poor LVF group was 20.33 ± 1.80 mmHg. However, this difference was not significantly different from the good LVF group, but this lack of significance is possibly due to the small number of patients in this group ($n = 6$). Our group's study also agreed with the study conducted by Cowburn *et al.*, 1999, which found that the mean arterial pressure was significantly increased by the infusion of ET-1 in patients with CHF. Our group's study found that the mean arterial pressure was significantly increased after infusion of ET-1 in the moderate, but not the poor, LVF group when compared to the good LVF group. However, this earlier study also found a significant increase in the SVR, but not the PVR, after infusion of ET-1 in CHF patients. This was not seen in our study in any of the patient groups. The infusion of ET-1 only elicited a significant increase in the PVR of patients in the good LVF group compared with their PVR at rest.

5.4.2. *In vitro* study

5.4.2.1. Comparison of ET-1 response between different patient groups:

ET-1 induced a potent and efficacious vasoconstriction in small PRAs from the control and all the heart failure groups. The biphasic nature of the ET-1 CCRC is due to the presence of both ET_A and ET_{B2} receptors mediating the ET-1 response in these vessels (McCulloch *et al.*, 1996; MacLean *et al.*, 1998). Previous studies in human PRAs have shown that the first component of the ET-1 contractile response is slow and shallow (< 1nM), this is mediated by the ET_{B2} receptor. The second fast, steep component of the curve (> 1nM) is mediated by the ET_A receptor (McCulloch *et al.*, 1995; McCulloch *et al.*, 1996, McCulloch *et al.*, 1998; MacLean *et al.*, 1998a).

BQ-788 was able to inhibit both vasodilator and vasoconstrictor ET_B receptors in human PRAs and showed the involvement of a vasoconstrictor ET_B receptor in this preparation (McCulloch *et al.*, 1996). There was no significant difference in the maximum vasoconstriction elicited by ET-1 between the control and heart failure groups. These results show no significant differences in the KCl- or ET-1-induced vasoconstrictor responses of the control patients with bronchial carcinoma and patients with good LVF. Therefore, this study validates the use of lung tissue taken from patients undergoing bronchial carcinoma removal as control tissue for other human pulmonary vascular studies as the presence of carcinoma did not appear to alter the function of the PRAs in this study. The potency of the ET-1-induced constriction was also unaltered by the progression of left ventricular dysfunction. The ET-1-mediated vasoconstriction of the dorsal hand vein, and the positive inotropic effect induced by ET-1 in the ventricular cardiac myocytes, were both attenuated in patients with CHF (Pieske *et al.*, 1999; Love *et al.*, 2000). This 'blunting' of the ET-1-mediated vasoconstriction was not observed in the small PRAs from the CHF

patients compared to controls. Indeed, there was no significant difference in either potency or maximum response of the ET-1-induced vasoconstriction between even the poor left ventricular function and the control groups. Therefore, there is no desensitization of the ET_A receptors in the small PRAs that is seen in other tissue preparations from CHF patients.

5.4.2.2. Effect of the mixed ET_A/ET_B antagonists:

SB 247083 significantly decreased the potency of ET-1 in all the patient subgroups, except for in the moderate LVF group. SB 247083 did markedly reduce the maximum effect of ET-1 in all patient groups. Previous work has shown that this component of the CCRC is mediated by the ET_A-receptor (McCulloch *et al.*, 1996) and, hence, is indicative of the high potency of SB 247083 against the ET_A-receptor (K_i: 0.41nM) (Douglas *et al.*, 1998; Willette *et al.*, 1998). Previous work has been unable to demonstrate inhibition of the first component of the CCRC with a selective ET_A-receptor antagonist, only with a selective ET_B-receptor antagonist (McCulloch *et al.*, 1996). Therefore, the reduction of this component by SB 247083 observed in all groups (except the moderate LVF group) must be due to its moderate affinity at the ET_B receptor (K_i: 467nM) (Douglas *et al.*, 1998; Willette *et al.*, 1998).

SB 234551 significantly decreased the potency of ET-1 in all patient subgroups except for the moderate LVF group. SB 234551 markedly reduced the maximum effect of ET-1 in all the patient subgroups (except for the moderate LVF group), indicative of its high potency against the ET_A receptor (K_i: 0.13nM) (Brooks *et al.*, 1998; MacLean *et al.*, 1998; Ohlstein *et al.*, 1998; Willette *et al.*, 1998). The reduction of the first component of the CCRC by SB 234551 observed in all groups

(except for the moderate LVF group) must be due to its moderate affinity at the ET_B receptor (K_i: 500nM) (Brooks *et al.*, 1998; MacLean *et al.*, 1998; Ohlstein *et al.*, 1998; Willette *et al.*, 1998).

SB 217242 significantly decreased the potency of ET-1 in all the patient subgroups (except for the moderate LVF group). SB 217242 markedly reduced the maximum effect of ET-1 in all the patient groups (except for the moderate LVF group), indicative of its high potency against the ET_A receptor (K_i: 1.1nM) (MacLean *et al.*, 1998; Underwood *et al.*, 1998; Willette *et al.*, 1998; Underwood *et al.*, 1999). The reduction of the first component by SB 217242 observed in all groups (except the moderate LVF group) must be due to its moderate affinity at the ET_B receptor (K_i: 111nM) (MacLean *et al.*, 1998; Underwood *et al.*, 1998; Willette *et al.*, 1998; Underwood *et al.*, 1999).

The reason for the lack of effect of these antagonists in the 'moderate' LVF group is unclear. It may have been due to the 'n' values available, and that an increased sample size would have increased a trend into a significant difference as seen in the other patient groups.

Alternatively, the pulmonary circulations of the moderate LVF group may be undergoing a compensatory physiological mechanism. The PVR is inversely correlated with LVF. The moderate LVF group had an ejection fraction of between 30-40% and an average PVR of 161.14 ± 14.05 dynes·s·cm⁻⁵. One hypothesis is that once the PVR reaches a certain point, a compensatory mechanism is switched on which alters the effects of ET_A and ET_B activation, or alters the characteristics of

these receptors by altering their densities, state of sensitization, or G-protein coupling. This mechanism reduces the effect of the mixed ET_A/ET_B antagonists. Once the PVR increases further in patients with poor LVF, the mechanism is turned off and the effects of the antagonists are restored. As all of the antagonists failed to decrease the potency of ET-1 in this group, this suggests that both antagonists failed to antagonise ET_{B2} receptors which mediate ET-1-induced vasoconstriction up to 1nM (McCulloch *et al.*, 1996). As both SB 234551 and SB 217242 failed to attenuate the maximum contractile response to ET-1 in this group, this suggests that both antagonists failed to antagonise ET_A receptors which mediate ET-1-induced vasoconstriction above 1nM (McCulloch *et al.*, 1996). The compensatory mechanism may result from the differential regulation of both ET_A and ET_B receptors. The cause of the disparity in the results from the moderate LVF group compared with the other groups requires further investigation. However, it should be noted that the moderate LVF group was the only group to experience a significant increase in the mean arterial pressure after the infusion of ET-1. This effect may result from the compensatory mechanism at work in the cardiovascular systems of patients classed as having moderate left ventricular function.

The findings of the study revealed that all three of the novel, mixed ET_A/ET_B antagonists used in this study effectively inhibited the ET-1-induced vasoconstriction of the small muscular PRAs in the control, good, and poor LVF groups. The increase in pulmonary vascular tone observed in patients with CHF and secondary PHT contributes to the exercise intolerance experienced by these patients (Maeda *et al.*, 1998; Moraes *et al.*, 2000). As ET-1 causes pulmonary vasoconstriction *in vivo* and

in vitro, the mixed ET_A/ET_B antagonists may be beneficial in increasing the exercise capacity of patients with CHF

5.5. Conclusion

The results of the *in vivo* study show that the cardiovascular haemodynamic changes subsequent to left ventricular dysfunction vary widely between patients with different levels of disease and that the role that ET-1 plays in causing these changes has yet to be fully elucidated.

The results of the *in vitro* study suggest that the mixed ET_A/ET_B antagonists could be beneficial in the treatment of CHF and secondary PHT as they attenuate the pathophysiological effects of ET-1 in both the pulmonary and systemic circulations. Indeed, the mixed ET_A/ET_B antagonist, bosentan is now in phase III trials in the treatment of heart failure. Therefore, these three, novel mixed ET_A/ET_B antagonists could be of similar therapeutic benefit in CHF, with the added benefit of decreasing PVR.

Chapter 6

**The effect of mixed ET_A/ ET_B
antagonists in the treatment of
hypoxia-induced PHT using the
chronic hypoxic rat model**

6.1.1. Introduction

The infrequent occurrence of PHT makes the study of the pathophysiological processes involved difficult to ascertain, as tissue from patients with this condition is not readily available. However, the chronic hypoxic rat model allows us the opportunity to get as close to pathophysiological secondary PHT conditions as possible as there are no underlying illnesses or genetic predisposition to hypertension or heart failure in the rats used in the study, no surgery such as coronary artery ligation involved, and no drugs were used to induce PHT in this animal model (McCulloch & MacLean, 1995; MacLean *et al.*, 1995; McCulloch *et al.*, 1998; MacLean & McCulloch, 1998).

6.1.2. ET-1 in PHT:

There is an increase in the plasma levels of ET-1 in patients with, and in animal models of, primary and secondary PHT with a directly proportional relationship between the level of ET-1 and the severity of the disease state (Russel & Davenport, 1995; Love & McMurray, 1996; Yang *et al.*, 1997; Cowburn *et al.*, 1998a; MacLean *et al.*, 1998; Underwood *et al.*, 1999; Chen & Oparil, 2000; Miyuachi *et al.*, 2000; Moraes *et al.*, 2000; Telemaque-Potts *et al.*, 2000). It is still unclear whether ET-1 is an important mediator of PHT or simply a marker of the condition.

6.1.3. Effect of chronic hypoxia on ET-1 response:

Chronic hypoxia has shown to increase the maximum response to ET-1 and ET-3 in rat pulmonary resistance arteries (PRAs) (MacLean & McCulloch, 1998; McCulloch *et al.*, 1998). These studies have shown an increase in the endogenous tone of small muscular pulmonary resistance arteries of the chronic hypoxic rat which is equivalent

to an *in vivo* transmural pressure of ~33mmHg (MacLean *et al.*, 1994; McCulloch *et al.*, 1998; MacLean & McCulloch., 1998). Chronic hypoxia increases the level of cAMP in the small muscular pulmonary resistance arteries (Mullaney *et al.*, 1998). A recent study has revealed an increase in the level of immunostaining of α actin in chronic hypoxic rat PRAs compared to controls after hypoxia 2, 7, or 14 days in duration. The presence of α actin is a marker of vascular remodelling and shows that the vessels are undergoing progressive muscularisation associated with the development of PHT in response to hypoxia (Demiryurek *et al.*, 2000).

6.1.4. ET receptors in control and chronic hypoxic rat PRAs:

A previous study has profiled the ET receptors mediating ET-1-induced vasoconstriction in control and hypoxic rat PRAs (McCulloch *et al.*, 1998). In control rats, the contractile response to ET-1 is resistant to blockade by either selective ET_A or selective ET_B receptor antagonists but inhibited by the mixed ET_A/ET_B antagonist SB 209670. In addition, the rank order of agonist potency was STX_{s6c} = ET-3 > ET-1 which indicates an ET_B-like profile. The contractile response to ET-1 was increased in the chronic hypoxic rat PRAs and this increase was inhibited by an ET_A-selective antagonist as well as by SB 209670 (McCulloch *et al.*, 1998). The signalling mechanisms by which the ET_A and ET_B receptors mediate the effects of ET-1 are discussed in chapter 5.

6.1.5. Novel mixed ET_A/ET_B antagonists:

SB 209670 has a K_i at human ET_A receptors of 0.2nM and at ET_B receptors of 18nM (MacLean *et al.*, 1998). Recently, three new mixed ET_A/ET_B antagonists from the same chemical family have been developed, SB 247083, SB 234551 and SB 217242.

The chemical structure and details of these are discussed in chapter 5. In summary, the affinity of SB 247083 for human cloned ET_A and ET_B receptor subtypes is Ki 0.41 and 467nM, respectively, for SB 234551, Ki 0.13 and 500nM, respectively and for SB 217242, Ki 1.1 and 111nM, respectively (Brooks *et al.*, 1998; Douglas *et al.*, 1998; MacLean *et al.*, 1998; Ohlstein *et al.*, 1998; Underwood *et al.*, 1998; Willette *et al.*, 1998; Underwood *et al.*, 1999).

These findings meant that further investigation into the ability of novel mixed ET_A/ET_B antagonists is warranted.

6.2. Methods

Wistar rats were placed in a hypobaric chamber at 30 days old. The chamber was depressurized to 550mbars over a period of 48 hours. When the chamber was at 550mbars, the oxygen concentration was at 10%. The temperature of the chamber was maintained at ~ 21°C with a ventilation rate of 45 L/min. The rats remained in these hypoxic conditions for 14 days and sacrificed upon removal from the chamber. Age-matched controls were kept in room air for the same time period (MacLean *et al.*, 1995; MacLean & McCulloch, 1998). The right ventricle was dissected free from the left ventricle and septum, blotted carefully with a tissue and then weighed. The ratio of right ventricular (R.V.) weight / left ventricular + septum (L.V. + S) weight is calculated to assess the presence of PHT (Hunter *et al.*, 1974; Leach *et al.*, 1977; MacLean & McCulloch, 1998).

The rats were killed by an overdose of sodium pentobarbitone by intra-peritoneal injection. The thorax was opened and the heart and lungs were dissected free then placed in ice cold Krebs. Second order intralobal small muscular resistance arteries (< 250µm) were dissected out of the lung tissue and carefully cleaned of surrounding parenchyma with the aide of a microscope. The vessels from both groups of rat were taken from the same region of the left lobe of the lung. The vessels were trimmed to a length of 2mm before passing two wire (40µm in diameter) through the lumen of the vessel and mounting it on a wire myograph (Mulvaney & Halpern, 1977). The myography bath contained Krebs solution at 37°C and bubbled with 16% O₂ / 5% CO₂ / balance N₂ from a gas pipe connected to a Douglas bag. Previous studies have measured the gas tensions in the baths using these parameters and found the O₂

tension to be 120 mmHg and CO₂ tension to be 35 mmHg, which is equivalent to the gas tensions seen in the alveolar and pulmonary arteries *in vivo* (MacLean & McCulloch, 1998). The vessels were left to equilibrate for an hour after being mounted in the baths. Tension was carefully applied to the vessels so that the control rat vessels were set at ~ 16 mmHg and the hypoxic rat vessels were set at ~ 33 mmHg, tensions which are equivalent to those experienced by the vessels *in vivo* (Herget *et al*, 1978; MacLean & McCulloch, 1998). After the tension was stabilised at appropriate level, the vessels were left to equilibrate for a further 45 minutes. The viability of the vessels was then assessed by the addition of 50mM KCl to the baths. Once the vasoconstriction had levelled off, the baths were washed out several times until the tension had returned to the baseline. The KCl addition was repeated until two reproducible vasoconstrictions were obtained. Vessels in the control ET-1 protocol groups were left to equilibrate until a CCRC to ET-1 was constructed. Some vessels were incubated for an hour with one of the following mixed ET_A/ET_B antagonists, SB 247083, SB 234551, or SB 271242 before a CCRC to ET-1 was constructed. In the control Wistar rats, only a single concentration of each antagonist (1µM) was used as none of the three antagonists at this high concentration were able to inhibit the ET-1-induced vasoconstriction in these vessels. However, three different concentrations of each antagonist (1, 0.3, and 0.1µM) were used in studies using chronic hypoxic rat vessels.

6.3. Results

6.3.1. Development of PHT:

The right ventricular to left ventricular + septum ratio is a reliable index for the presence of PHT (Hunter *et al.*, 1974; Leach *et al.*, 1977). Previous studies have shown that 14 days of hypobaric treatment was sufficient to cause PHT in rats as the ratio was significantly greater in the hypoxic rats when compared with control rats (MacLean *et al.*, 1995; and MacLean & McCulloch, 1998). The results from this present study show that the ratio is significantly greater in the hypoxic rats ($P < 0.001$) when compared with control rats (Table 6.1). This demonstrates that the hypoxic rats in this study had developed right ventricular hypertrophy associated with the development of PHT.

Experimental Group	R.V. /L.V. + Septum Ratio	n = number
Control	0.21 ± 0.01	n = 11
Hypoxic	0.32 ± 0.01***	n = 10

Table 6.1: Measurement of the right ventricle (R.V.) /left ventricle + septum

(L.V. + S) ratio in the control and hypoxic Wistar rat groups. Data expressed as mean ± SEM. n = number of individual heart preparations. Statistical comparison was made using Students' unpaired t-test. $P < 0.001$ *** vs. control rat ratio.

6.3.2. Control rat PRAs in the presence of the mixed ET_A/ET_B antagonists:

ET-1-induced a potent vasoconstriction in the normotensive Wistar rat small PRAs with a pEC₅₀ of 8.00 ± 0.13 (n = 11) and a maximal contractile response of 134 ± 10% (as % KCl-induced contraction). The ET-1 CCRC was characteristically biphasic in nature with a first slow, shallow component and a second fast, steep component. A summary of the maximum contractile response elicited by ET-1 is shown in **Table 6.2**. There was no significant difference in the maximum vasoconstrictor response achieved by 50mM KCl or 0.3µM ET-1 in any of the protocol groups in the control rat. A summary of the pEC₅₀ values of ET-1 are shown in **Table 6.3**. **Figure 6.1** shows the effect of 1µM of the mixed ET_A/ET_B antagonists SB 247083, SB 234551 and SB 217242 on the ET-1 response in control Wistar rat PRAs.

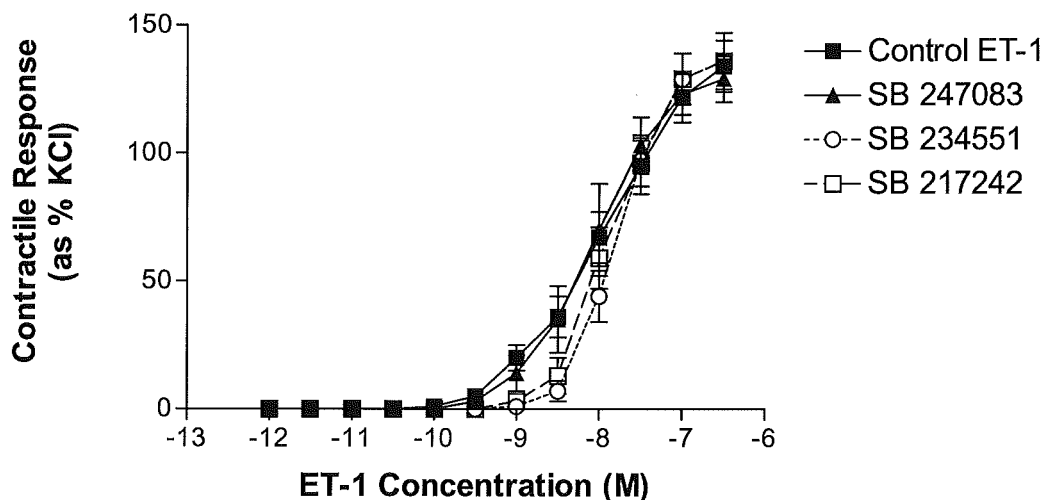


Figure 6.1: Contractile response to ET-1 in the presence and absence of 1µM of the mixed ET_A/ET_B antagonists in normotensive Wistar rat PRAs. Data expressed as percentage of 50mM KCl-induced contraction. Control ET-1 (n = 11); SB 247083 (n = 7); SB 234551 (n = 8); and SB 217242 (n = 9). Each point represents the mean ± SEM. n = number of PRAs from the same number of individual lung preparations.

The maximum vasoconstrictor response to 50mM KCl was significantly smaller in the SB 24551 (n = 9) protocol group than in the ET-1 control (n = 11) ($P < 0.05$).

Protocol Group	ET-1 Control	SB 247083	SB 234551	SB 217242
Vessel Size (μm)	1.42 \pm 11	140 \pm 19	125 \pm 8	171 \pm 12
KCl-Induced Maximum (mN)	2.43 \pm 0.38	2.94 \pm 1.12	1.34 \pm 0.32	2.90 \pm 0.72
ET-1-Induced Max. (mN)	3.15 \pm 0.52	3.83 \pm 1.37	1.89 \pm 0.41	3.97 \pm 0.97
n number	n = 11	n = 7	n = 9	n = 8

Table 6.2: Dimensions and measurement of 50mM KCl- and 0.3 μM ET-1-induced maximum contraction achieved in the various protocol groups in the normotensive Wistar rat PRAs in the presence and absence of 1 μM of mixed ET_A/ET_B antagonist. Data expressed as mean \pm SEM. n = number of individual PRAs from the same number of individual lungs.

The presence of 1 μM SB 247083, SB 234551, or SB 217242 did not result in a decrease of the potency of ET-1 in the normotensive Wistar rat PRAs. However,

SB 234551 and SB 217242 did shift the first component of the CCRC to the right. A summary of the pEC₅₀ values for ET-1 in the presence and absence of 1μM of various mixed ET_A/ET_B antagonists is displayed in **Table 6.3**.

Protocol Group	pEC₅₀ Value	n = number
ET-1 Control	8.00 ± 0.13	n = 11
SB 247083	8.10 ± 0.17 ns	n = 7
SB 234551	7.74 ± 0.11 ns	n = 9
SB 217242	7.99 ± 0.11 ns	n = 8

Table 6.3: pEC₅₀ values for ET-1 in the presence and absence of 1μM of mixed ET_A/ET_B antagonists in normotensive Wistar rat PRAs. Data are expressed as mean ± SEM. n = number of individual PRAs from the same number of lung preparations. Statistical comparisons were made using a one-way ANOVA with a Dunnetts' post-test. ns = not significant.

6.3.3. Chronic hypoxic rat PRAs in the presence of the mixed ET_A/ET_B antagonist, SB 247083:

Figure 6.2 displays the ET-1-induced contractile response in the presence and absence of 1, 0.3, 0.1 μ M of the mixed ET_A/ET_B antagonist, SB 247083, in the PRAs of the chronic hypoxic Wistar rat. The ET-1 CCRC had a characteristically biphasic appearance in the presence and absence of 1, 0.3, and 0.1 μ M of the mixed ET_A/ET_B antagonist, SB 247083. The maximum contractile response to ET-1 in the presence and absence of SB 247083 is shown in Table 6.4.

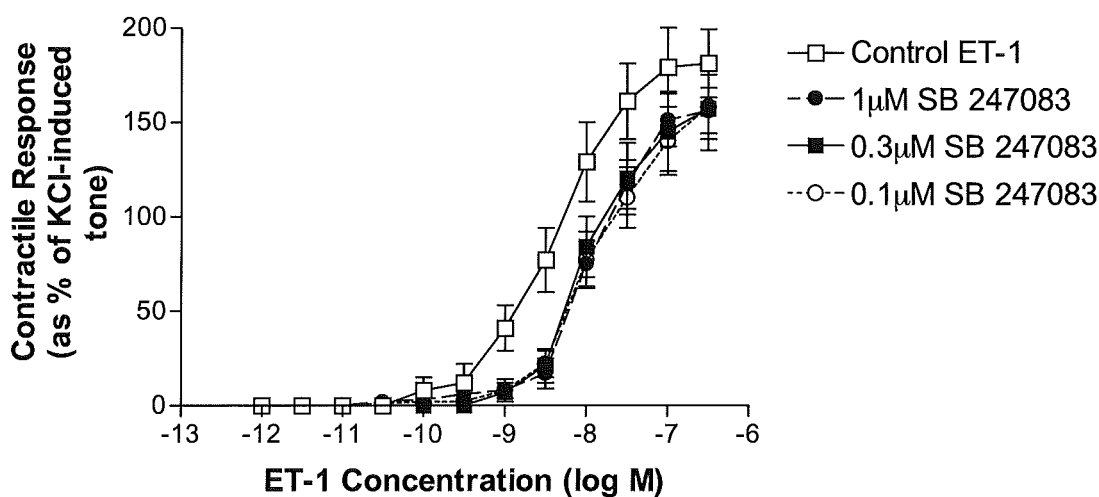


Figure 6.2: Contractile response to ET-1 in the presence and absence of 1, 0.3, and 0.1 μ M of the mixed ET_A/ET_B antagonist, SB 247083, in chronic hypoxic Wistar rat PRAs. Control ET-1 (n = 11); 1 μ M SB 247083 (n = 8); 0.3 μ M SB 247083 (n = 5); and 0.1 μ M SB 247083 (n = 6). Data expressed as percentage of 50mM KCl-induced contraction. Each point represents the mean \pm SEM. n = number of individual PRAs from same number of individual lung preparations.

Protocol Group	ET-1 Control	1 μ M SB 247083	0.3 μ M SB 247083	0.1 μ M SB 247083
Vessel Size (μm)	122 \pm 7	144 \pm 7	159 \pm 16	171 \pm 11
KCl-Induced Maximum (mN)	2.42 \pm 0.43	2.46 \pm 0.34	2.78 \pm 1.11	2.66 \pm 0.71
ET-1-Induced Maximum (mN)	4.06 \pm 0.51	3.60 \pm 0.39	3.96 \pm 1.82	3.75 \pm 1.43
n = number	n = 9	n = 8	n = 5	n = 6

Table 6.4: Dimensions and measurement of 50mM KCl- and 0.3 μ M ET-1-induced maximum contraction achieved in the various protocol groups in the hypoxic Wistar rat PRAs in the presence and absence of 1, 0.3, or 0.1 μ M of the mixed ET_A/ET_B antagonist, SB 247083. Data expressed as mean \pm SEM. n = number of individual PRAs from the same number of individual lungs.

Each concentration of SB 247083 significantly decreased the potency of ET-1 and caused a rightward shift of the CCRC. The potency of ET-1 was significantly decreased by 1 ($P < 0.05$, n = 8), 0.3 ($P < 0.05$, n = 5), and 0.1 μ M ($P < 0.05$, n = 6) SB 247083. A summary of the pEC₅₀ values is shown in **Table 6.5**.

Protocol Group	pEC₅₀ Value	n = number
ET-1 Control	8.46 ± 0.16	n= 9
1µM SB 247083	7.93 ± 0.07*	n = 8
0.3µM SB 247083	7.89 ± 0.10*	n = 5
0.1µM SB 247083	7.81 ± 0.08*	n = 6

Table 6.5: pEC₅₀ values for ET-1 in the presence and absence of 1, 0.3, and 0.1µM of SB 247083 in chronic hypoxic Wistar rat PRAs. Data are expressed as mean ± SEM. n = number of individual PRAs from the same number of lung preparations. Statistical comparisons were made using a one-way ANOVA and a Dunnetts' post-test. *P* < 0.05* vs. ET-1 control.

SB 247083 at concentrations of 1, 0.3, and 0.1µM did not cause parallel shifts of the whole ET-1 concentration / response curve. There was a rightward shift of the first shallow component of the curve by all three concentrations of SB 247083 with 1µM of the drug causing the greatest shift of this component. Therefore, a pA₂ value could not be calculated. However, the estimated pK_B value for 1µM of SB 247083 has been calculated and is shown in **table 6.6**.

Protocol Group	Estimated pK_B values	n = number
SB 247083	6.37 ± 0.24	n = 8

Table 6.6: Estimated pK_B values for $1\mu\text{M}$ of SB 247083 in hypoxic Wistar rat PRAs.

Data are shown as mean \pm SEM. n = number of PRAs from individual lung preparations.

6.3.4. Chronic hypoxic Wistar rat PRAs in the presence of the mixed ET_A/ET_B antagonist, SB 234551:

Figure 6.3 displays the ET-1-induced contractile response in the presence and absence of 1, 0.3, 0.1 μ M of the mixed ET_A/ET_B antagonist, SB 234551, in the PRAs of the chronic hypoxic Wistar rat. The ET-1 CCRC had a characteristically biphasic appearance in the presence and absence of 1, 0.3, and 0.1 μ M of the mixed ET_A/ET_B antagonist, SB 234551. The maximum contractile response to ET-1 in the presence and absence of SB 234551 is shown in Table 6.7.

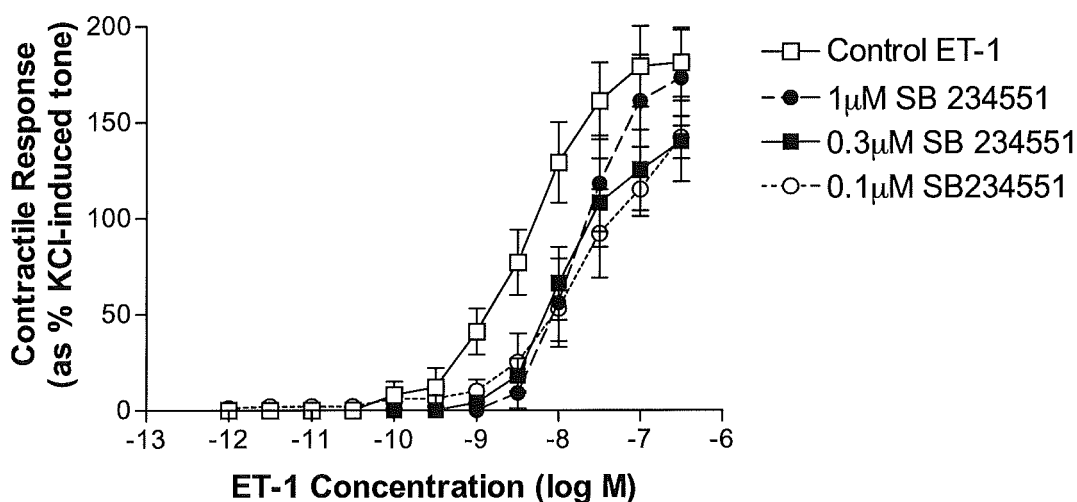


Figure 6.3: Contractile response to ET-1 in the presence and absence of 1, 0.3, and 0.1 μ M of the mixed ET_A/ET_B antagonist, SB 234551, in chronic hypoxic Wistar rat PRAs. Data expressed as percentage of 50mM KCl-induced contraction. Control ET-1 (n = 9); 1 μ M SB 234551 (n = 7); 0.3 μ M SB 234551 (n = 5); and 0.1 μ M SB 234551. Each point represents the mean \pm SEM. n = number of PRAs from the same number of individual lung preparations.

Protocol Group	ET-1 Control	1 μ M SB 234551	0.3 μ M SB 234551	0.1 μ M SB 234551
Vessel Size (μm)	117 \pm 8	133 \pm 5	137 \pm 17	142 \pm 16
KCl-Induced Maximum (mN)	2.42 \pm 0.43	1.46 \pm 0.32	2.30 \pm 0.75	3.16 \pm 1.43
ET-1-Induced Maximum (mN)	4.06 \pm 0.51	2.32 \pm 1.07	5.23 \pm 2.04	4.51 \pm 2.23
n = number	n = 9	n = 7	n = 5	n = 5

Table 6.7: Dimensions and measurement of 50mM KCl- and 0.3 μ M ET-1-induced maximum contraction achieved in the various protocol groups in the chronic hypoxic Wistar rat PRAs in the presence and absence of 1, 0.3, and 0.1 μ M of the mixed ET_A/ET_B antagonist, SB 234551. Data expressed as mean \pm SEM. n = number of individual PRAs from the same number of individual lungs.

Each concentration of SB 234551 significantly decreased the potency of ET-1 and caused a rightward shift of the CCRC. The potency of ET-1 was significantly

decreased by 1 ($P < 0.01$, $n = 7$), 0.3 ($P < 0.05$, $n = 5$), and 0.1 μ M ($P < 0.05$, $n = 5$) SB 234551. A summary of the pEC₅₀ values is shown in **Table 6.8**.

Protocol Group	pEC₅₀ Value	n = number
ET-1 Control	8.46 ± 0.16	n= 9
1 μ M SB 234551	7.73 ± 0.10**	n = 7
0.3 μ M SB 234551	7.83 ± 0.13*	n = 5
0.1 μ M SB 217242	7.66 ± 0.27*	n = 5

Table 6.8: pEC₅₀ values for ET-1 in the presence and absence of 1, 0.3, and 0.1 μ M of SB 234551 in chronic hypoxic Wistar rat PRAs. Data are expressed as mean ± SEM. n = number of individual PRAs from the same number of lung preparations. Statistical comparisons were made using a one-way ANOVA with a Dunnetts' post-test. $P < 0.05^*$, $P < 0.01^{**}$ vs. ET-1 control.

SB 234551 at concentrations of 1, 0.3, and 0.1 μ M did not cause parallel shifts of the whole ET-1 concentration / response curve. There was a parallel shift of the first shallow component of the curve by all three concentrations of SB 234551 with 1 μ M of the drug causing the greatest rightward shift of this component. Therefore, the pA₂

value could not be calculated. However, the estimated pK_B value for $1\mu\text{M}$ of SB 247083 has been calculated and is shown in **Table 6.9**.

Protocol Group	Estimated pK_B values	n = number
SB 234551	6.75 ± 0.26	n = 7

Table 6.9: Estimated pK_B values for $1\mu\text{M}$ of SB 234551 in hypoxic Wistar rat PRAs.

Data are shown as mean \pm SEM. n = number of PRAs from individual lung preparations.

6.3.5. Chronic hypoxic Wistar rat PRAs in the presence of 1, 0.3, and 0.1 μ M of the mixed ET_A/ET_B antagonist, SB 217242:

Figure 6.4 displays the ET-1-induced contractile response in the presence and absence of 1, 0.3, 0.1 μ M of the mixed ET_A/ET_B antagonist, SB 217242, in the PRAs of the chronic hypoxic Wistar rat. The ET-1 CCRC had a characteristically biphasic appearance in the presence and absence of 1, 0.3, and 0.1 μ M of the mixed ET_A/ET_B antagonist, SB 217242. The maximum contractile response to ET-1 in the presence and absence of SB 217242 is shown in Table 6.10. The maximum vasoconstrictor response to 0.3 μ M ET-1 was significantly smaller in the 1 μ M of SB 217242 protocol group (n = 9) than in the control ET-1 group (n = 9) ($P < 0.05$).

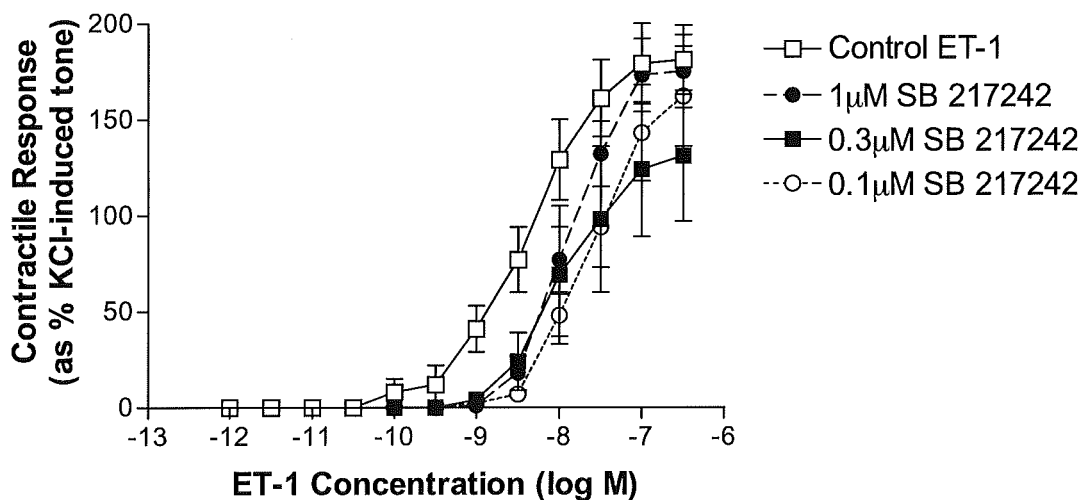


Figure 6.4: Contractile response to ET-1 in the presence and absence of 1, 0.3, and 0.1 μ M of the mixed ET_A/ET_B antagonist, SB 217242, in normotensive Wistar rat PRAs. Data expressed as percentage of 50mM KCl-induced contraction. Each point represents the mean \pm SEM. n = number of PRAs from the same number of individual lung preparations.

Protocol Group	ET-1 Control	1 μ M SB 217242	0.3 μ M SB 217242	0.1 μ M SB 217242
Vessel Size (μm)	140 \pm 12	128 \pm 10	155 \pm 13	160 \pm 9
KCl-Induced Maximum (mN)	2.42 \pm 0.43	1.64 \pm 0.35	1.42 \pm 0.57	2.43 \pm 0.59
ET-1-Induced Maximum (mN)	4.06 \pm 0.51	2.58 \pm 0.39	2.39 \pm 1.34	3.27 \pm 0.39
n = number	n = 9	n = 9	n = 5	n = 6

Table 6.10: Dimensions and measurement of 50mM KCl- and 0.3 μ M ET-1-induced maximum contraction achieved in the various protocol groups in the chronic hypoxic Wistar rat PRAs in the presence and absence of 1, 0.3, and 0.1 μ M of SB 217242. Data expressed as mean \pm SEM. n = number of individual PRAs from the same number of individual lungs.

Each concentration of SB 217242 significantly decreased the potency of ET-1 and caused a rightward shift of the CCRC. The potency of ET-1 was significantly decreased by 1 ($P < 0.05$, $n = 9$), 0.3 ($P < 0.05$, $n = 5$), and 0.1 μ M ($P < 0.01$, $n = 6$) SB 217242. A summary of the pEC₅₀ values is shown in **Table 6.11**.

Protocol Group	pEC₅₀ Value	n = number
ET-1 Control	8.46 ± 0.16	n= 9
1 μ M SB 217242	7.90 ± 0.08*	n = 9
0.3 μ M SB 217242	7.74 ± 0.20*	n = 5
0.1 μ M SB 217242	7.52 ± 0.15**	n = 6

Table 6.11: pEC₅₀ values for ET-1 in the presence and absence of 1, 0.3, and 0.1 μ M of SB 217242 in chronic hypoxic Wistar rat PRAs. Data are expressed as mean ± SEM. n = number of individual PRAs from the same number of lung preparations. Statistical comparison were made using a one-way ANOVA with a Dunnetts' post-test. $P < 0.05^*$, and $P < 0.01^{**}$ vs. ET-1 control.

SB 217242 at concentrations of 1, 0.3, and 0.1 μ M did not cause parallel shifts of the whole ET-1 concentration / response curve. There was a rightward shift of the first shallow component of the curve by all three concentrations of SB 217242. All three

concentrations of SB 217242 appeared to cause the same degree of rightward shift. Therefore, the pA_2 value could not be calculated. However, the estimated pK_B value for $1\mu\text{M}$ of SB 247083 has been calculated and is shown in **table 6.6**.

Protocol Group	Estimated pK_B values	n = number
SB 217242	6.42 ± 0.20	n = 9

Table 6.12: Estimated pK_B values for $1\mu\text{M}$ of SB 217242 in hypoxic Wistar rat PRAs. Data are shown as mean \pm SEM. n = number of PRAs from the same number of individual lung preparations.

6.3.6. Comparison of control and chronic hypoxic rat PRAs:

The potency of ET-1 was significantly increased in response to chronic hypoxia as the pEC₅₀ decreased from 8.00 ± 0.13 (n = 11) to 8.46 ± 0.16 (n = 9) in the normotensive and chronic hypoxia Wistar rat PRAs (*P* < 0.05). A summary of these results is shown in **Table 6.13**. The maximum contractile response was significantly increased in response to chronic hypoxia as the maximum contractile response was increased from 134 ± 10% to 181 ± 18% (as % KCl-induced contraction) in normotensive and chronic hypoxic Wistar rat PRAs (*P* < 0.05). A summary of these results can be seen in **Table 6.14**. There is no significant difference between the pEC₅₀ of ET-1 in the presence of each individual mixed ET_A/ET_B antagonist at the three concentrations studied.

Experimental Group	pEC₅₀ value	n = number
Control	8.00 ± 0.13	n = 11
Hypoxic	8.46 ± 0.16*	n = 9

Table 6.13: pEC₅₀ values for ET-1 in the absence of the mixed ET_A/ET_B antagonists in the control and chronic hypoxic Wistar rat PRAs. Data are expressed as mean ± SEM. n = number of individual PRAs from the same number of lung preparations. Statistical comparisons were made using Students' unpaired t-test. *P* < 0.05* vs. control Wistar rat.

Experimental Group	Maximum contraction (% of KCl)	n = number
Control	134 ± 10	n = 11
Hypoxic	181 ± 18*	n = 9

Table 6.14: Measurement of ET-1-induced maximum vasoconstriction achieved in the control and chronic hypoxic Wistar rat PRAs. Data expressed as mean ± SEM.

n = number of individual PRAs from the same number of individual lungs. Statistical comparisons were made using Students' unpaired t-test. $P < 0.05^*$ vs. control Wistar rat.

6.4. Discussion

6.4.1 Comparison of control and chronically hypoxic rat PRAs:

The results of this study agree with those of earlier studies which saw an increase in the potency of, and maximum contractile response to, ET-1 in the chronic hypoxic rat PRAs (McCulloch & MacLean, 1995; McCulloch *et al.*, 1998; MacLean, 1998; MacLean & McCulloch, 1998). This has been shown to be accompanied by an increase in plasma levels of ET-1 (Chen & Oparil, 2000). As described previously, the response to ET-1 in control rat PRAs is mediated by a heterogeneous ET_B-like receptor population (McCulloch *et al.*, 1998). The potency of ET-1 was significantly increased from 8.00 ± 0.13 (n=11) in control rats to 8.46 ± 0.16 (n=9) in chronic hypoxic rats ($P < 0.05$). The maximum contractile response to ET-1 was also significantly augmented from $134 \pm 10\%$ (n = 11) in control rats to $181 \pm 18\%$ (n = 9) in chronic hypoxic rats ($P < 0.05$). This augmentation of the maximum vasoconstrictor response to, and increased potency of, ET-1 may be due to the up-regulation of ET_A receptors as a consequence of hypoxia as the increased response is inhibited by an ET_A receptor antagonist, causing a decrease in the maximum contraction induced by ET-1 in the chronic hypoxic rat PRAs (McCulloch *et al.*, 1998). Therefore, the potency of, and maximum contractile response to, ET-1 were increased in the chronic hypoxic Wistar rat PRAs as a result of the up-regulation of both ET_A receptors as a consequence of hypoxia. My results are consistent with previous studies in that the antagonist studied had negligible effect on the contractile response to ET-1 in control rat vessels but did inhibit responses to ET-1 in the chronic hypoxic rat vessels, consistent with them behaving as selective ET_A receptor antagonists (see below for further discussion).

6.4.2. Control normotensive rat PRAs:

None of the mixed ET_A/ET_B antagonists were able to decrease the potency of the ET-1-induced vasoconstriction in these vessels. This is consistent with their affinities for the ET_A receptor and the previous studies showing that, the small muscular PRAs of the rat, responses to ET-1 are mediated by an 'atypical ET_B' receptor (McCulloch *et al.*, 1998). However, **Figure 6.1** shows that 1μM SB 234551 and SB 217242 caused rightward shifts of the first component of the ET-1 CCRC. As an ET_B-like receptor is predominantly responsible for the ET-1-induced vasoconstriction in these vessels, the affinity of these two antagonists for the ET_B receptor needs to be considered. The dissociation constant for SB 217242 at ET_B receptors is lower than that of SB 247083 and SB 234551 (K_i 111nM, 467nM and 500nM respectively) (Brooks *et al.*, 1998; Douglas *et al.*, 1998; MacLean *et al.*, 1998; Ohlstein *et al.*, 1998; Underwood *et al.*, 1998; Willette *et al.*, 1998; Underwood *et al.*, 1999). At 1μM of these antagonists, SB 217242 is almost ten fold higher than its dissociation constant and would be able to antagonise the population of ET_{B2} receptors. This would account for the rightward shift of the first component of the ET-1 CCRC by SB 217242. 1μM of SB 234551 is twice as high as its dissociation constant and would antagonise the population of ET_{B2} receptors. However, 1μM of SB 247083 is also twice its dissociation constant at ET_B receptors, yet SB 247083 did not cause a rightward shift of the first component of the ET-1 CCRC. Hence, the effect of these antagonists on this very shallow initial component of the CCRC cannot be fully explained in terms of their affinity at the ET_B receptor. There is no evidence to suggest that these antagonists are inverse agonists. It has to be remembered, however, that the K_i values reported were against the human ET_B receptor and differences may be expected against rat ET receptors.. Therefore, as these antagonists did not inhibit the ET-1-induced vasoconstriction in these vessels,

the results confirm that ET_{B2}-like receptors are the main receptor subtype mediating the ET-1 response in control Wistar rat PRAs. A previous study using the mixed ET_A/ET_B antagonist SB 209670 showed that the potency of ET-1 was decreased in both control and chronically hypoxic rat PRAs (McCulloch *et al.*, 1998). This is different to the results observed using these three novel antagonists and is probably due to SB 209670 having a greater affinity for the ET_B receptor subtype than any of the antagonists used in this study (K_i ET_A: 0.2nM and ET_B: 18nM) (McCulloch *et al.*, 1998). In summary, the three novel antagonists had negligible effect on responses to ET-1 in control rat PRAs. This very different from the observations made in chapter 5 which demonstrated that all three antagonists inhibited the responses to ET-1 in control human PRAs. This is a very good example of species-specific pharmacology and justifies the use of human blood vessels to confirm observations made in animal models.

6.4.3. Chronically hypoxic rat PRAs:

All of the mixed ET_A/ET_B antagonists were able to significantly decrease the potency of ET-1 at all three of the concentrations studied in the chronic hypoxic PRAs. As the antagonists were able to decrease the potency of ET-1, this indicates that there was an increase in the ET_A component of the response, confirming previous studies. The previous study by McCulloch *et al.*, 1998 also showed that the responses to the ET_B receptor agonist STX_{s6c} was not increased in the chronic hypoxic rat vessels and the ET_B-selective antagonist, BQ-788, had no inhibitory effect on this response. Therefore, these results confirm an increase in the ET_A-mediated component of the ET-1 response in the chronic hypoxic rat vessels.

The potency of ET-1 was significantly decreased by 1, 0.3, and 0.1 μ M of SB 247083 from the pEC₅₀ of ET-1 alone, 8.46 ± 0.16 (n = 9), to 7.93 ± 0.07 ($P < 0.05$), 7.89 ± 0.10 ($P < 0.05$), and 7.81 ± 0.08 ($P < 0.05$) respectively (n = 5-8). All three concentrations of SB 247083 caused a rightward shift of the first shallow component of the ET-1 curve. The lack of any further effect of SB 247083 > 0.1 μ M confirms that only a small population of ET_A receptors is present and mediating the constriction to ET-1 and that the antagonist is saturating these ET_A receptors. Only 1 μ M SB 247083 might be expected to exert some effect on the ET_B receptor population (K_i : 0.41nM) but as the results from the control vessel show, this is not observed (Douglas *et al.*, 1998; Willette *et al.*, 1998). Therefore, the effect of this antagonist on contractile response to ET-1 in the hypoxic vessels can be attributed to an effect on a small population of ET_A receptors.

The potency of ET-1 was significantly decreased by 1, 0.3, and 0.1 μ M of SB 234551 to 7.73 ± 0.10 ($P < 0.01$), 7.83 ± 0.13 ($P < 0.05$), and 7.66 ± 0.27 ($P < 0.05$) respectively (n = 5-7). There was a concentration-dependent shift of the CCRC confirming the results observed with SB 247083, that this antagonist is acting as an ET_A receptor antagonist (K_i : 0.13nM) and saturating a small population of ET_A receptors. **Figure 6.3** does suggest that 1 μ M of SB 234551 completely removes the shallow component of the CCRC which may be due to this concentration being sufficient to inhibit 'atypical' ET_B receptors (K_i : 500nM) (Brooks *et al.*, 1998; MacLean *et al.*, 1998; Ohlstein *et al.*, 1998; Willette *et al.*, 1998).

The potency of ET-1 was significantly decreased by 1, 0.3, and 0.1 μ M of SB 217242 to 7.90 ± 0.08 ($P < 0.05$), 7.74 ± 0.20 ($P < 0.05$), and 7.52 ± 0.15 ($P < 0.01$)

respectively (n = 5-9). There was a concentration-dependent shift of the CCRC confirming that this antagonist is acting as an ET_A receptor antagonist (K_i: 1.1nM) and saturating a small population of ET_A receptors. **Figure 6.4** does suggest that all concentrations of SB 217242 completely removes the shallow component of the CCRC which may be due to the higher affinity of this antagonist against 'atypical' ET_B receptors (K_i: 111nM) (MacLean *et al.*, 1998; Underwood *et al.*, 1998; Willette *et al.*, 1998; Underwood *et al.*, 1999).

The results of this study do not help to answer the question of whether ET-1 is a mediator or simply a marker of pulmonary hypertension. However, these results, taken with those from previous studies, reveal an important role for ET-1 in PHT

(MacLean *et al.*, 1995; Yang *et al.*, 1997; MacLean, 1998; MacLean *et al.*, 1998; MacLean & McCulloch, 1998; Underwood *et al.*, 1999; Chen & Oparil, 2000; Miyuachi *et al.*, 2000; Telemaque-Potts *et al.*, 2000).

6.5. Conclusion

The mixed ET_A/ET_B antagonists SB 247083, SB234551, and SB 217242 had no effect on the ET-1 response in the small muscular PRAs of the control rat.

Chronic hypoxia increases both the potency and maximum vasoconstrictor response elicited by ET-1 in the small muscular rat PRAs.

The mixed ET_A/ET_B antagonists SB 247083, SB 234551, and SB 217242 attenuated the increased potency of ET-1 observed in response to chronic hypoxia in the small muscular rat PRAs probably through their activity against the ET_A receptor. The ET-1-induced vasoconstriction in these vessels was mediated by a heterogeneous receptor population, with the ET_{B2} receptor being the predominant receptor involved in this response.

Therefore, new therapeutic advances in the treatment of PHT and right-sided heart failure may come from inhibiting the ET-1 responses.

Chapter 7

General Discussion

7.1. The role of ET-1 in PHT:

The studies described in this thesis have shown that there is an increase in the pulmonary vascular reactivity to ET-1 in pulmonary hypertension (PHT) induced by hypoxia. The rat model of hypobaric hypoxia is a well characterised model of PHT.. This model was used to study the effect of ET-1 and the mixed ET_A/ET_B antagonists in chronically hypoxic rats. The study revealed that there is an increase in the potency of, and maximum vasoconstrictor response to, ET-1 in the small PRAs of these rats. This verifies that ET-1 is a mediator of PHT developed as a consequence of chronic hypoxia. Both the potency of, and maximum contractile response to, ET-1 were increased by the presence of hypoxia-induced PHT. This increase in the vascular reactivity to ET-1 was suggested to be the result of an up-regulation of ET_A receptors. All three of the novel, mixed ET_A/ET_B antagonists, SB 247083; SB 234551; and SB 217242, were able to decrease the potency of ET-1 in the PRAs of the chronically hypoxic rats but did not affect the potency of ET-1 in the control rats. This result suggested that these three antagonists were able to inhibit the up-regulation of ET_A receptors that occurs in the presence of hypoxia-induced PHT.

The studies described in this thesis have shown that, in humans, there is no increase on the pulmonary vascular reactivity to ET-1 in PHT secondary to left ventricular dysfunction (LVD). The study involving patients with varying degrees of (LVD) and control patients undergoing bronchial carcinoma resection revealed that there was no increase in the potency of, or maximum contractile response to, ET-1 within these patient groups. The results of this study were surprising as many previous studies have shown an increase in the plasma levels of ET-1 in the presence of heart failure and PHT. This increase is directly correlated with the severity of disease. However,

this may be associated with a down-regulation of ET receptors in the face of a sustained elevation of ET-1. The results of this human study are in contrast to those observed in the chronic hypoxic rat study which showed that the presence of PHT resulted in an increase in the maximum response to, and potency of ET-1. This difference may be due to the different pathobiologies involved in rat and human PHT and that the chronic hypoxic rats developed more severe PHT. The increased sensitivity to ET-1 in the chronic hypoxic rat may be associated with the advanced development of PHT. As the results of this study display no increase in the vascular reactivity to ET-1 in the presence of PHT, it is suggested that ET-1 is a marker of PHT secondary to LVD. All three novel, mixed ET_A/ET_B antagonists were able to decrease the potency of ET-1 in all four patient groups, except for the moderate LVF group where only SB 217242 was able to decrease the potency. Therefore, these antagonists were able to inhibit the ET_{B2} receptors in these vessels. All three antagonists were also able to attenuate the maximum contractile response of ET-1 in all four patient groups, except for the moderate LVF group where only SB 247083 was able to decrease the maximum response to ET-1. Therefore, these antagonists were also able to inhibit the ET_A receptors in these vessels, if one assumes it is the ET_A receptor mediating the response to higher concentrations of ET-1 as suggested by MacLean *et al.*, 1995 and McCulloch *et al.*, 1998.

The results of these studies suggest that ET-1 may be a mediator of secondary PHT induced by chronic hypoxia, while ET-1 may be a marker of secondary PHT as a consequence of LVD. These studies also display that the three mixed ET_A/ET_B antagonists may be of therapeutic benefit to patients with secondary PHT of either aetiology. This result has been borne out by the fact that the mixed ET_A/ET_B

antagonist bosentan is now in phase III trials for the treatment of chronic heart failure and has just been given approval by the USA Food and Drug Administration for use in primary PHT. Very recent clinical trials involving bosentan in the treatment of chronic heart failure and PHT have revealed mixed results. Bosentan was able to improve the exercise capacity and cardiopulmonary haemodynamics in patients with primary PHT and PHT secondary to connective tissue disease. The patients in this study also saw an improvement in their WHO functional class, Borg dyspnea index and an increase in the time to clinical worsening (Rubin *et al.*, 2002). However, preliminary findings from another study using bosentan as a treatment for chronic heart failure, called the ENABLE trial, reported at a recent American College of Cardiologists meeting found that bosentan did not decrease the mortality rate of patients in the trial. As well as this disappointing result, patients taking bosentan have experienced weight gain along with potentially serious side-effects of a decreased haematocrit and abnormal liver function tests (unpublished communication). Whether these side-effects were dose-related is unclear and that altering the dose administered may eliminate the unwanted effects. However, as bosentan afforded no therapeutic benefit to these patients, it may simply be that bosentan is not the mixed ET_A/ET_B antagonist to use and that other antagonists of this class may be more beneficial. The mixed ET_A/ET_B antagonists SB 247083; SB 234551; and SB 217242 could also be effective drugs in the treatment of primary and secondary PHT of different aetiologies.

7.2. The mediators of ACh-induced vasodilatation: effect of chronic hypoxia:

The rat model of hypobaric hypoxia was used to investigate the effects of PHT on vasodilator response to ACh in the small PRAs. This study revealed that the

maximum ACh-induced vasodilator response was augmented in the presence of PHT induced by chronic hypoxia. This study also investigated the mediators involved in the ACh-induced vasodilatation and the effect that chronic hypoxia would have on the mediator profile. This study revealed that NO and PGI₂ were not mediators of the ACh-induced relaxation in control rat PRAs as the NOS inhibitor, L-NAME, and the cyclooxygenase (COX) inhibitor, indomethacin, were unable to inhibit the ACh-induced response. This lack of involvement by these mediators pointed to the ACh-induced vasodilatation being mediated by EDHF. Previous studies have shown that pre-constriction of vessels with KCl inhibits the release of EDHF. Indeed, this study showed that ACh failed to induce any vasodilatation in vessels pre-constricted with KCl, suggesting the involvement of EDHF. The inhibitors of large & intermediate (BK_{Ca} & IK_{Ca}) and small (SK_{Ca}) Ca²⁺-activated K⁺ channels, charybdotoxin (ChTX) and apamin respectively, attenuated the maximum vasodilator effect elicited by ACh. However, this combination of K⁺ channel blockers was only able to significantly inhibit the highest concentrations of ACh, concentrations well above those needed to produce vasodilatation. The identity of EDHF has not yet been elucidated, but it has been hypothesised that EDHF is a family of substances rather than a single entity which elicit vasodilatation and hyperpolarization via different mechanisms. Other studies have shown a possible EDHF-mediated vasodilatation to ACh via K_{ATP} channels. Therefore, these results suggest that the ACh-induced vasodilator response may be mediated by two different EDHF-like substances in the control rat PRAs.

However, the involvement of EDHF in the ACh-induced vasodilator response requires confirmation through electrophysiological studies. The study revealed that a different mediator profile was involved in the ACh-induced vasodilator response in

PRAs from the chronically hypoxic rats than was observed in the control rats. In the chronic hypoxic rat PRAs, NO; PGI₂; and EDHF are all involved in the ACh-induced vasodilator response. However, the inhibition of these mediators by L-NAME; indomethacin; or a combination of ChTX and apamin, did not alter the potency of ACh but did attenuate the maximum vasodilator response to ACh. Each mediator was involved in different components of the ACh-induced vasodilatation. At low concentrations, the ACh-induced vasodilator response was mediated by NO. PGI₂ mediates the ACh-induced response at higher concentrations than NO and significantly attenuates the maximum relaxation response. An EDHF-like substance acting via IK_{Ca} and SK_{Ca} channels mediates the ACh-induced vasodilatation at the highest concentrations. This suggests that there is a general increase in the synthesis and release of NO, PGI₂, and EDHF in the PRAs in response to PHT induced by chronic hypoxia. There is also an increased basal tone observed in these chronic hypoxic vessels is attenuated by the basal release of NO. These results suggest that there is a basal compensatory vasodilator mechanism which attenuates the increased basal tone of these vessels and an agonist-stimulated mechanism which increases the vasodilator effect of ACh at work in the PRAs of the chronically hypoxic rats attempting to return the pulmonary circulation to its natural low resistance state.

7.3. The vasodilator role of hU-II in the pulmonary circulation:

Early studies involving human urotensin-II (hU-II) showed that hU-II was a potent vasoconstrictor of the vasculature of various species. A previous study conducted by our group showed no vasoconstrictor effect of hU-II in the small muscular PRAs of human control patients. However, the addition of L-NAME revealed a variable

hU-II-induced vasoconstriction in 30% of vessels studied. Therefore, the hU-II-induced vasoconstrictor response appears to be inhibited by the release of NO in these vessels. Recent studies by others have shown that hU-II elicited a vasodilatation in the rat small mesenteric and coronary arteries. Therefore, hU-II can induce either a vasoconstrictor or vasodilator effect depending on the vascular bed and species being studied. The study described in this thesis revealed hU-II to be a potent vasodilator of the human small muscular PRAs, the first study to show hU-II-induced vasodilatation in human vasculature. The potency order of vasodilators in the human PRAs was found to be: hU-II = adrenomedullin (ADM) >> sodium nitroprusside (SNP) = ACh. This study also investigated the mediators involved in the hU-II-induced vasodilatation. The NOS inhibitor, L-NAME, did not inhibit the hU-II-induced vasodilatation at any concentration. Therefore, NO was not involved in mediating the hU-II-induced vasodilator response. The COX inhibitor, indomethacin, significantly inhibited the hU-II-induced vasodilator response at concentrations of 30pM and above to attenuate the maximum vasodilator response. Therefore, a COX product, possibly PGI₂, is involved in mediating the hU-II-induced vasodilator response. The addition of the intermediate and small conductance Ca²⁺-activated K⁺ channel blockers, charybdotoxin (ChTX) and apamin respectively, significantly inhibited the hU-II-induced vasodilator response at every concentration to attenuate the maximum vasodilator response and significantly decrease the potency of hU-II. Therefore, EDHF appears to be involved in mediating the hU-II-induced vasodilator response. However, to confirm the involvement of EDHF, electrophysiological studies are required. EDHF is also involved in the ACh-induced vasodilatation in rat PRAs. EDHF alone mediates the ACh-induced relaxation in control rats and, along with NO and PGI₂, mediates the ACh-induced vasodilatation in chronic hypoxic rats. These

studies agree with earlier studies showing that vasodilatation mediated by EDHF becomes more important with decreasing vessel size.

7.4. Regulation of pulmonary vascular tone:

ET-1 is a potent vasoconstrictor of small muscular PRAs. This potency is increased in the presence of PHT induced by chronic hypoxia but not in the PHT secondary to LVD. A role for ET-1 in 'priming' pulmonary resistance arteries for hypoxic pulmonary vasoconstriction (HPV) by sensitising vascular smooth muscle cells to Ca^{2+} has also been observed. Therefore, ET-1 has a pathophysiological role in PHT. Future treatments for PHT of different aetiologies could include the mixed ET_A/ET_B antagonists, SB 247083; SB 234551; and SB 217242 which are able to inhibit the vasoconstrictor effect of ET-1 in these vessels.

The vasodilator effect of ACh is enhanced in the small muscular PRAs of chronic hypoxic rats. This suggests an increase in the agonist-stimulated vasodilator response which attempts to compensate for the increased vascular reactivity observed as a consequence of PHT. There is an increase in the basal release of NO in the chronically hypoxic vessels which suggests that there is also a mechanism attempting to compensate for the increased basal tone observed in these vessels. These results suggest that compensatory vasodilator mechanisms are activated by the presence of PHT in order to return the pulmonary circulation to its natural low resistance state.

hU-II was previously thought to have a pathophysiological role in a number of disease states such as coronary atherosclerosis; chronic heart failure; chronic renal failure; and systemic hypertension. This was due to the fact that only vasoconstrictor effects

had been observed. However, since recent studies have shown hU-II-induced vasodilatation in various vascular beds of the rat, and the study described in this thesis showed the first vasodilator effect of hU-II in the human vasculature, does hU-II have a protective role in some vascular beds? It would be have been interesting to be have been able to obtain more PRAs from the different patient groups involved in the human LVD study on which to assess the vasodilator effect of hU-II, to see whether the potency or maximum vasodilator response to hU-II changed with advancing LVD. Unfortunately, the number of vessels obtained from this study did not allow for another study to be conducted. If the vasodilator effects could be separated from the vasoconstrictor effects, hU-II could become a potent vasodilator for the treatment of PHT in the way that inhaled NO and analogues of PGI₂ are used at present.

This thesis has two studies showing the likely involvement of EDHF in mediating both ACh- and hU-II-induced vasodilatation. These observations agree with previous studies which have shown that EDHF becomes more important in mediating vasodilatation as the calibre of the vessel decreases. The inhibition of the Ca²⁺-activated K⁺ channels inhibited the maximum vasodilator response to, and potency of, both ACh and hU-II. Many treatments for PHT at present include inhaled NO and the inhalation of analogues of PGI₂. These results suggest that more effective pulmonary vasodilators could come as a result of stimulating the release of EDHF or from drugs which open Ca²⁺-activated K⁺ channels selectively. However, with the identity of EDHF under debate, any possible treatments acting through this mechanism would be a long way off.

7.5. Conclusion

The maintenance of low pulmonary vascular tone is a balance between vasoconstrictors such as ET-1 and vasodilators such as ACh and hU-II (although species differences should be considered when looking at hU-II-induced vasodilatation), as observed in these studies. The presence of PHT of different aetiologies interferes with this balance. Successful treatments for PHT could result from restoring this balance by inhibiting the vasoconstrictor effect of ET-1 with a mixed ET_A/ET_B antagonist or stimulating the vasodilator effects of ACh, and hU-II.

Chapter 8

References

- Affolter, J. & Webb, D.J. (2001) Urotensin-II: a new mediator in cardiopulmonary regulation? *Lancet*, **358**, 774-775.
- Alexander, B., Browse, M.S, Reading, S.J. & Benjamin, I.S. (1999) A simple and accurate mathematical method for calculation of the EC₅₀. *J. Pharmacol. Toxicol.*, **41**, 55-58.
- Ames, R.S., Sarau, H.M., Chambers, J.K., Willette, R.N., Aiyar, N.V., Romanic, A.M., Louden, C.S., Foley, J.J., Sauermelch, C.F., Coatney, R.W., Ao, Z., Disa, J., Holmes, S.D., Stadel, J.M., Martin, J.D., Liu, W-S., Glover, G.I., Wilson, S., McNulty, D.E., Ellis, C.E., Elshourbagy, N.A., Shabon, U., Trill, J.J., Hay, D.W.P., Ohlstein, E.H., Bergsma, D.J. & Douglas, SA. (1999) Human urotensin-II is a potent vasoconstrictor and agonist for the orphan receptor GPR14. *Nature*, **401**, 282-286.
- Arunlakshana, O. & Schild, H.O. (1959) Some quantitative uses of drug antagonists. *Br. J. Pharmacol. And Chemotherapy*, **14**, 48-56.
- Barman, S. (1998) Potassium channels modulate hypoxic pulmonary vasoconstriction. *Am. J. Physiol.*, **275**, L64-L70.
- Barnes, P.J. & Belvisi, .M.G. (1993) Nitric oxide and lung disease. *Thorax*, **48**, 1034-1043.
- Barnes, P.J. & Liu, S.F. (1995) Regulation of pulmonary vascular tone. *Pharmacol. Rev.*, **47**, 87-131.
- Bauersachs, J., Popp, R., Hecker, M., Sauer, E., Fleming, I. & Busse, R. (1996) Nitric oxide attenuates the release of endothelium-derived hyperpolarizing factor. *Circulation*, **94**, 3341-3347.
- Berger, R.M.F., Geiger, R., Hess, J., Bogers, A.J.J. & Mooi, W.J. (2001) Altered arterial expression pattern of inducible and endothelial nitric oxide synthase in pulmonary plexogenic arteriopathy caused by congenital heart disease. *Am. J. Respir. Crit. Care Med.*, **163**, 1493-1499.
- Berger, R., Stanek, B., Hulsmann, M., Frey, B., Heher, S., Pacher, R., Neunteufl, T. (2001) Effects of endothelin A receptor blockade on endothelial function in patients with chronic heart failure. *Circulation*, **103**, 981-986.
- Bern, H.A. & Lederis, K. (1969) A reference preparation for the study of active substances in the caudal neurosecretory system of teleosts. *J. Endocrinol.*, **45**, 11-12.
- Brenner, O. (1935) Pathology of the vessels of the pulmonary circulation (part 1). *Arch. Int. Med.*, **56**, 211-237.
- Bohlen, H.G. (1986) Localization of vascular resistance changes during hypertension. *Hypertension*, **8**, 181-183.
- Bohm, F. & Pernow, J. (2002) Urotensin-II evokes potent vasoconstriction in humans *in vivo*. *Br. J. Pharmacol.*, **135**, 25-27.

Bohnemeier, H., Pinto, Y.M., Horkay, F., Toth, M., Juhasz-Nagy, A., Orzechowski, H.D., Paul, M. (1998) Endothelin-converting enzyme-1 mRNA expression in human cardiovascular disease. *J. Cardiovasc. Pharmacol.*, **31 (suppl. 1)**, S52-S54.

Bolotina, V.M., Najibi, S., Palacino, J.J., Pagano, P.J. & Cohen, R.A. (1994) Nitric oxide directly activates calcium-dependent potassium channels in vascular smooth muscle. *Nature*, **368**, 850-853.

Bonvallet, S.T., Oka, M., Yano, M., Zamora, M.R., McMurtry, I.F. & Stelzner, T.J. (1993) BQ-123, an ET_A-receptor antagonist attenuates endothelin-1-induced vasoconstriction in rat pulmonary circulation. *J. Cardiovasc. Pharmacol.*, **22**, 39-43.

Bonvallet, S.T., Zamora, M.R., Hasunuma, K., Sato, K., Hanasato, N., Anderson, D., McMurtry, I.F. & Stelzner, T.J. (1994) BQ-123, an ET_A-receptor antagonist, attenuates hypoxic pulmonary hypertension in rats. *Am. J. Physiol.*, **266**, H1327-H1331.

Bottrill, F.E., Douglas, S.A., Hiley, C.R. & White, R. (2000) Human urotensin-II is an endothelium-dependent vasodilator in rat small arteries. *B.r. J. Pharmacol.*, **130**, 1865-1870.

Brooks, D.P., DePalma, P.D., Pullen, M., Elliott, J.D., Ohlstein, E.H. & Nambi, P. (1998) SB 234551, a novel endothelin-A receptor antagonist, unmaskes endothelin-induced renal vasodilatation in the dog. *J. Cardiovasc. Pharmacol.*, **31 (suppl. 1)**, S339-S341.

Channick, R.N., Simonneau, G., Sitbon, O., Robbins, I.M., Frost, A., Tapson, V.F., Badesch, Roux, S., Rainisio, M., Bodin, F. & Rubin, L.J. (2001) Effects of the dual endothelin-receptor antagonist bosentan in patients with pulmonary hypertension: a randomised placebo-controlled study. *Lancet*, **358**, 1119-1123.

Chen, G. & Cheung, D.W. (1997) Effect of K⁺-channel blockers on ACh-induced hyperpolarization and relaxation in mesenteric arteries. *Am. J. Physiol.*, **41**, H2306-H2312.

Chen, S., Chen, Y., Meng, Q.C., Durand, J., DiCarlo, V.S. & Oparil, S. (1995) Endothelin receptor antagonist bosentan prevents and reverses hypoxic pulmonary hypertension in rats. *J. Appl. Physiol.*, **79**, 2122-2131.

Chen, Y-F. & Oparil, S. (2000) Endothelin and pulmonary hypertension. *J. Cardiovasc. Pharmacol.*, **35 (suppl. 2)**, S49-S53.

Cody, W.L., Doherty, A.M., He, X., Rapundalo, S.T., Hingorani, G.P., Panek, R.L. & Major, T.C. (1991) Monocyclic endothelins: examination of the importance of the individual disulphide rings. *J. Cardiovasc. Pharmacol.*, **17 (suppl. 2)**, S62-S64.

Coleman, H.A., Tare, M. & Parkington, H.C. (2001) K⁺ currents underlying the action of endothelium-derived hyperpolarizing factor in guinea-pig, rat and human blood vessels. *J. Physiol.*, **531**, 359-373.

- Copock, E.A., Martens, J.R. & Tamkun, M.M. (2001) Molecular basis of hypoxia-induced pulmonary vasoconstriction: role of voltage-gated K⁺ channels. *Am. J. Physiol.*, **281**, L1-L12.
- Coulouarn, Y., Jegou, S., Tostivint, H., Vaudry, H. & Lihmann, I. (1999) Cloning, sequence analysis and tissue distribution of the mouse and rat urotensin-II precursors. *FEBS Lett.*, **457**, 28-32.
- Coulouarn, Y., Lihmann, I., Jegou, S., Anouar, Y., Tostivint, H., Beauvillain, J.C., Conlon, J.M., Bern, H.A. & Vaudry, H. (1998) Cloning of the cDNA encoding the urotensin-II precursor in frog and human reveals intense expression of the U-II gene in motoneurons of the spinal cord. *Proc. Natl. Acad. Sci. U.S.A.*, **95**, 15803-15808.
- Cowburn, P.J., Cleland, J.G.F., McArthur, J.D., MacLean, M.R., Dargie, H.J., McMurray, J.J.V. & Morton, J.J. (1998a) Endothelin-1 has haemodynamic effects at pathophysiological concentrations in patients with left ventricular dysfunction. *Cardiovasc. Res.*, **39**, 563-570.
- Cowburn, P.J., Cleland, J.G.F., McArthur, J.D., MacLean, M.R., McMurray, J.J.V. & Dargie, H.J. (1998b) Pulmonary and systemic responses to exogenous endothelin-1 in patients with left ventricular dysfunction. *J. Cardiovasc. Pharmacol.*, **31** (suppl. 1), S290-S293.
- Cowburn, P.J., Cleland, J.G., McArthur, J.D., MacLean, M.R., McMurray, J.J.V., Dargie, H.J. & Morton, J.J. (1999) Endothelin B receptors are functionally important in mediating vasoconstriction in the systemic circulation in patients with left ventricular systolic dysfunction. *J. Am. Coll. Cardiol.*, **33**, 932-938.
- Davenport, A.P. & Maguire, J.J. (2000) Urotensin-II: fish neuropeptide catches orphan receptor. *Trends Pharmacol. Sci.*, **21**, 80-82.
- Demiryurek, A.T., Cakici, I., Wainwright, C.L., Wadsworth, R.M. & Kane, K.A. (1998) Effects of free radical production and scavengers on occlusion-reperfusion induced arrhythmias. *Pharmacol. Res.*, **38**, 433-439.
- Demiryurek, A.T., Karamsetty, M.R., McPhaden, A.R., Wadsworth, R.M., Kane, K.A. & MacLean, M.R. (2000) Accumulation of nitrotyrosine correlates with endothelial NO synthase in pulmonary resistance arteries during chronic hypoxia in the rat. *Pulm. Pharmacol. Therap.*, **13**, 157-165.
- Docherty, C.C. & MacLean, M.R. (1998). Endothelin-B receptors in rabbit pulmonary resistance arteries: effect of left ventricular dysfunction. *JPET*, **284**, 895-903.
- Dominiczak, A.F. & Bohr, D.F. (1995) Nitric oxide and its putative role in hypertension. *Hypertension*, **25**, 1202-1211.
- Dora, K.A. & Garland, C.J. (2001) Properties of smooth muscle hyperpolarization and relaxation to K⁺ in the rat isolated mesenteric artery. *Am. J. Physiol.*, **280**, H2424-H2429.

Dora, K.A., Martin, P.E.M., Chaytor, A.T., Evans, W.H., Garland, C.J. & Griffith, T.M. (1999) Role of heterocellular gap junctional communication in endothelium-dependent smooth muscle hyperpolarization: inhibition by a connexin-mimetic peptide. *Biochem. Biophys. Res. Commun.*, **254**, 27-31.

Douglas, S.A., Nambi, P., Gellai, M., Luengo, J.I., Xiang, J-N., Brooks, D.P., Roffolo, R.R., Elliott, J.D. & Ohlstein, E.H. (1998) Pharmacologic characterization of the novel, orally available endothelin-A-selective antagonist SB 247083. *J. Cardiovasc. Pharmacol.*, **31** (suppl. 1), S273-S276.

Douglas, S.A., Sulpizio, A.C., Piercy, V., Sarau, H.M., Ames, R.S., Aiyar, N.V., Ohlstein, E.H. & Willette, R.N. (2000) Differential vasoconstrictor activity of human urotensin-II in vascular tissue isolated from the rat, mouse, dog, pig, marmoset and cynomolgus monkey. *Br. J. Pharmacol.*, **131**, 1262-1274.

Duling, B.R., Gore, R.W., Dacey, R.G. & Damon, D.N. (1981) Methods for isolation, cannulation, and *in vitro* study of single microvessels. *Am. J. Physiol.*, **241**, H108-H116.

Eddahibi, S., Humbert, M., Fadel, E., Raffestin, B., Darmon, M., Capron, F., Simonneau, G., Darteville, P., Harmon, M. & Adnot, S. (2001) Serotonin transporter overexpression is responsible for pulmonary artery smooth muscle hyperplasia in primary pulmonary hypertension. *J. Clin. Invest.*, **108**, 1141-1150.

Eddahibi, S., Raffestin, B., Braquet, P., Chabrier, P.E. & Adnot, S. (1991) Pulmonary vascular reactivity to endothelin-1 in normal and chronically pulmonary hypertensive rats. *J. Cardiovasc. Pharmacol.*, **17** (suppl. 7), S358-S361.

Edwards, G., Dora, K.A., Gardener, M.J., Garland, C.J. & Weston, A.H. (1998) K^+ is an endothelium-derived hyperpolarizing factor in rat arteries. *Nature*, **396**, 269-272.

Eguchi, S., Hirata, Y., Ihara, M., Yano, M. & Marumo, F. (1992) A novel ET_A antagonist (BQ-123) inhibits endothelin-1-induced phosphoinositide breakdown and DNA synthesis in rat vascular smooth muscle cells. *FEBS Lett.*, **302**, 243-246.

Elshourbagy, N.A., Douglas, S.A., Shabon, U., Harrison, s., Duddy, G., Sechler, J.L., Ao, Z., Maleeff, B.E., Naselsky, D., Disa, J. & Aiyar, N.V. (2002) Molecular and pharmacological characterization of genes encoding urotensin-II peptides and their cognate G-protein-coupled receptors from the mouse and monkey. *Br. J. Pharmacol.*, **136**, 9-22.

Evans, A.M., Osipenko, O.N. & Gurney, A.M. (1996) Properties of a novel K^+ current that is active at resting potential in rabbit pulmonary artery smooth muscle cells. *J. Physiol.*, **496**, 407-420.

Fishman, A.P. (1973) Hypoxia on the pulmonary circulation – How and where it acts. *Circ. Res.*, **38**, 221-231.

Fishman, A.P. (1988a) Chapter 63: The normal pulmonary circulation. Pulmonary diseases and disorders, 2nd edition. McGraw-Hill Company.

Fishman, A.P. (1988b) Chapter 64: Pulmonary hypertension and cor pulmonale. Pulmonary diseases and disorders, 2nd edition. M^oGraw-Hill Company.

Fleminger, G., Bousso-mittler, D., Bdolah, A., Loog, Y.K. & Sokolovsky, M. (1989) Immunological and structural characterization of sarafotoxin / endothelin family of peptides. *Biochem. Biophys. Res. Commun.*, **162**, 1317-1323.

Frid, M.G., Aldashev, A.A., Dempsey, E.C. & Stenmark, K.R. (1997) Smooth muscle cells isolated from discrete compartments of the mature vascular media exhibit unique phenotypes and distinct growth capabilities. *Circ. Res.*, **81**, 940-952.

Frid, M.G., Moiseeva, E.P. & Stenmark, K.R. (1994) Multiple phenotypically distinct smooth muscle cell populations exist the adult and developing bovine pulmonary arterial media *in vivo*. *Circ. Res.*, **75**, 669-681.

Fukuchi, M. & Giaid, A. (1998) Expression of endothelin-1 and endothelin-converting-enzyme-1 mRNAs and proteins in failing human hearts. *J. Cardiovas. Pharmacol.*, **31 (suppl. 1)**, S421-S423.

Fukuroda, T., Nishikibe, M., Ohta, Y., Ihara, M., Yano, M., Ishikawa, K., Fukami, T. & Ikemoto, F. (1992) Analysis of responses to endothelins in isolated porcine blood vessels by using a novel endothelin antagonist, BQ-153. *Life Sci.*, **50**, 107-112.

Fulton, R.M., Hutchinson, E.C. & Morgan Jones, A. (1952) Ventricular weight in cardiac hypertrophy. *Br. Heart J.*, **14**, 413-420.

Furchgott, R.F. & Zawadzki, J.V. (1980) The obligatory role of endothelial cells in the relaxation of arterial smooth muscle by acetylcholine. *Nature*, **299**, 373-376.

Gambone, L.M., Murray, P.A. & Flavahan, N.A. (1997) Synergistic interaction between endothelium-derived NO and prostacyclin in pulmonary artery: potential role for K⁺_{ATP} channels. *Br. J. Pharmacol.*, **121**, 271-279.

Garland, C.J., Plane, F., Kemp, B.K. & Cocks, T.M. (1995) Endothelium-dependent hyperpolarization: a role in the control of vascular tone. *TiPS*, **16**, 23-30.

Geraci, M.W., Gao, B., Shephard, D.C., Moore, M.D., Westcott, J.Y., Fagan, K.A., Alger, L.A., Tuder, R.M. & Voelkel, N.F. (1999) Pulmonary prostacyclin synthase overexpression in transgenic mice protects against development of hypoxic pulmonary hypertension. *J. Clin. Invest.*, **103**, 1509-1515.

Gibson, A. (1987) Complex effects of *Gillichthys* urotensin-II on rat aortic strips. *Br. J. Pharmacol.*, **91**, 205-212.

Goerke, J. & Mines, A.H. (1988) Chapter 1: Overview of the circulation. Cardiovascular Physiology. Raven Press.

Harris, D., Martin, P.E.M., Evans, W.H., Kendall, D.A., Griffith, T.M. & Randall, M.D. (2000) Role of gap junctions in endothelium-derived hyperpolarizing factor responses and mechanisms of K⁺-relaxation. *Eur. J. Pharmacol.*, **402**, 119-128.

- Harrison, V.J., Ziegler, T., Bouzourene, K., Suci, A., Silacci, P. & Hayoz, D. (1998) Endothelin-1 and endothelin-converting enzyme-1 gene regulation by shear stress and flow-induced pressure. *J. Cardiovasc. Pharmacol.*, **31**, S38-S41.
- Hasunuma, K., Yamaguchi, T., Rodman, D.M., O'Brien, R.F. & McMurtry, I.F. (1991) Effects of inhibitors of EDRF and EDHF on vasoreactivity of perfused rat lungs. *Am. J. Physiol.*, **260**, L97-L104.
- Hay, D.W.P., Luttmann, M.A., Hubbard, W.C. & Udem, B.J. (1993) Endothelin receptors in human and guinea-pig pulmonary tissues. *Br. J. Pharmacol.*, **110**, 1175-1183.
- Haynes, W.G. & Webb, D.J. (1994) Contribution of endogenous generation of endothelin-1 to basal vascular tone. *Lancet*, **344**, 852-854.
- Heath, D. & Edwards, J.E. (1958) The pathology of hypertensive pulmonary vascular disease – A description of six grades of structural changes in the pulmonary arteries with special reference to congenital cardiac septal defects. *Circulation*, **18**, 533-547.
- Heath, D., Edwards, C., Winson, M. & Smith, P. (1973) Effects on the right ventricle, pulmonary vasculature, and carotid bodies of the rat exposed to, and recovery from, simulated high altitude. *Thorax*, **28**, 24-28.
- Heath, D., Smith, P., Gosney, J., Mulcahy, D., Fox, K., Yacoub, M. & Harris, P. (1987) The pathology of the early and late stages of primary pulmonary hypertension. *Br. Heart J.*, **58**, 204-213.
- Herget, J., Sugget, A.J., Leach, E. & Barer, G. (1978) Resolution of pulmonary hypertension and other features induced by chronic hypoxia in rats during complete and intermittent normoxia. *Thorax*, **33**, 468-473.
- Hillier, C., Berry, C., Petrie, M.C., O'Dwyer, P.J., Hamilton, C., Brown, A. & McMurray, J. (2001) Effects of urotensin-II in human arteries and veins of varying calibre. *Circulation*, **103**, 1378-1381.
- Huang, W., Kingsbury, M.P., Turner, M.A., Donnelly, J.L., Flores, N.A. & Sheridan, D.J. (2001) Capillary filtration is reduced in lungs adapted to chronic heart failure: morphological and haemodynamic correlates. *Cardiovasc. Res.*, **49**, 207-217.
- Hunter, C., Barer, G.R., Shaw, J.W. & Clegg, E.J. (1974) Growth of heart and lungs in hypoxic rodents: A model of human hypoxic disease. *Clin. Sci. Mol. Med.*, **46**, 375-391.
- Ihara, M., Noguchi, K., Saeki, T., Fukuroda, T., Tsuchida, S., Kimura, S., Fukami, T., Ishikawa, K., Nishikibe, M. & Yano, M. (1991) Biological profiles of highly potent novel endothelin antagonists selective for the ETA receptor. *Life Sci.*, **50**, 247-255.

Ishikawa, K., Ihara, M., Noguchi, K., Mase, T., Mino, N., Saeki, T., Fukuroda, T., Fukami, t., Ozaki, S., Nagase, T., Nishikibe, M. & Yano, M. (1994) Biological and pharmacological profile of a potent and selective endothelin-B receptor antagonist, BQ-788. *Proc. Natl. Acad. Sci.*, **91**, 4892-4896.

Itoh, H., Itoh, Y., Rivier, J. & Lederis, K. (1987) Contractions of major artery segments of rat by fish neuropeptide urotensin-II. *Am. J. Physiol.*, **252**, R361-R366.

Jenkinson, D.H., Barnard, E.A., Hoyer, D., Humphrey, P.P.A., Leff, P. & Shankley, N.P. (1995) International union of pharmacology committee on receptor nomenclature and drug classification. IX. Recommendations on terms and symbols in quantitative pharmacology. *Pharmacol. Rev.*, **47**, 255-266.

Jiang, F., Li, C.G. & Rand, M.J. (2000) Mechanisms of nitric oxide-independent relaxations induced by carbachol and acetylcholine in rat isolated renal arteries. *Br. J. Pharmacol.*, **130**, 1191-1200.

Kai, H., Kanaide, H. & Nakamura, J.D. (1989) Endothelin-sensitive intracellular Ca^{2+} store overlaps with caffeine-sensitive one in rat aortic smooth muscle cells in primary cultures. *Biochem. Biophys. Res. Commun.*, **158**, 235-243.

Katano, Y., Ishihata, A., Aita, T., Ogaki, T. & Horie, T. (2000) Vasodilator effect of urotensin-II, one of the most potent vasoconstricting factors, on rat coronary arteries. *Eur. J. Pharmacol.*, **402**, R5-R7.

Keegan, A., Morecroft, I., Smillie, D., Hicks, M.N. & MacLean, M,R, (2001) Contribution of the 5-HT(1B)-receptor to hypoxia-induced pulmonary hypertension: converging evidence using 5-HT (1B)-receptor knock-out mice and the 5-HT (1B/1D)-receptor antagonist GR 127935. *Circ. Res.*, **89**, 1231-1239.

Kelso, E.J., McDermott, B.J., Silke, B. & Spiers, J.P. (2000) Endothelin A receptor subtype mediates endothelin-induced contractility in left ventricular cardiomyocytes isolated from rabbit myocardium. *JPET*, **294**, 1047-1052.

Kemp, B.K., Smolich, J.J., Ritchie, B.C. & Cocks, T.M. (1995) Endothelium-dependent relaxations in sheep pulmonary arteries and veins: resistance to block by N^G -nitro-L-arginine in pulmonary hypertension. *Br. J. Pharmacol.*, **116**, 2457-2467.

Kenakin, T.P. (1982) The Schild regression in the process of receptor classification. *Can. J. Physiol. Pharmacol.*, **60**, 249-265.

Kharitonov, S.A., Yates, D., Robbins, R.A., Logan-Sinclair, R., Shinebourne, E.A. & Barnes, P.J. (1994) Increased nitric oxide in exhaled air of asthmatic patients. *Lancet.*, **343**, 133-135.

Kido, T., Sawamura, T. & Masaki, T. (1998) The processing pathway of endothelin-1 production. *J. Cardiovasc. Pharmacol.*, **31 (suppl. 1)**, S13-S15.

- Kiowski, W., Sutch, G., Schalcher, C., Brunner, H-P. & Oechslin, E. (1998) Endothelial control of vascular tone in chronic heart failure. *J. Cardiovasc. Pharmacol.*, **31** (suppl. 1), S67-S73.
- Kita, S., Taguchi, Y. & Matsumura, Y. (1998) Endothelin-1 enhances pressor responses to norepinephrine: involvement of endothelin-B receptor. *J. Cardiovasc. Pharmacol.*, **31** (suppl. 1), S119-S121.
- Leach, E., Howard, P. & Barer, G.R. (1977) Resolution of hypoxic changes in the heart and pulmonary arterioles of rats during intermittent correction of hypoxia. *Clin. Sci. Mol. Med.*, **52**, 153-162.
- Leach, R.M., Hill, H.M., Snetkov, V.A., Robertson, T.P. & Ward, J.P.T. (2001) Divergent roles of glycoysis and the mitochondrial electron transport chain in hypoxic pulmonary vasoconstriction of the rat: identity of the hypoxic sensor. *J. Physiol.*, **536**, 211-224.
- Leach, R.M., Twort, C.H.C., Cameron, I.R. & Ward, J.P.T. (1992) A comparison of the pharmacological and mechanical properties *in vitro* of large and small pulmonary arteries. *Clin. Sci.*, **82**, 55-62.
- Le Cras, T.D., Xue, C., Rengasamy, A. & Johns, R.A. (1996) Chronic hypoxia upregulates endothelial and inducible NO synthase gene and protein expression in rat lung. *Am. J. Physiol.*, **270**, 164-170.
- Lee, S.Y., Lee, C.Y., Chen, Y.M. & Kochva, E. (1986) Coronary vasospasm as the primary cause of death due to the venom of the burrowing asp, *Attractaspis Eggadensis*, **24**, 285-291.
- LeMonnier De Gouville, A.C., Mondot, S., Lipton, H., Hyman, A. & Cavero, I. (1990) Haemodynamic and pharmacological evaluation of the vasodilator and vasoconstrictor effects of endothelin-1 in rats. *JPET*, **252**, 300-311.
- Li, D., Zhou, N. & Johns, R.A. (1999) Soluble guanylate cyclase gene expression and localisation in rat lung after exposure to hypoxia. *Am. J. Physiol.*, **277**, L841-L847.
- Li, H.L., Chen, S., Chen, Y., Meng, Q.C., Durand, J., Oparil, S. & Elton, T.A. (1994a) Enhanced endothelin-1 and endothelin receptor gene expression in chronic hypoxia. *J. Appl. Physiol.*, **77**, 1451-1459.
- Li, H.L., Elton, T.S., Chen, Y.F. & Oparil, S. (1994b) Increased endothelin receptor gene expression in hypoxic rat lung. *Am. J. Physiol.*, **266**, L552-L560.
- Love, M.P., Haynes, W.G., Webb, D.J. & McMurray, J.J.V. (2000) Venous endothelin receptor function in patients with chronic heart failure. *Clin. Sci.*, **98**, 65-70.
- Love, M.P. & McMurray, J.J.V. (1996) Endothelin in chronic heart failure: current position and future prospects. *Cardiovasc. Res.*, **31**, 665-674.

MacLean, M.R. (1998) Endothelin-1: a mediator of pulmonary hypertension? *Pulm. Pharmacol. Ther.*, **11**, 147-149.

MacLean, M.R. (1999) Pulmonary hypertension, anorexigens and 5-HT: pharmacological synergism in action? *Trends Pharmacol. Sci.*, **20**, 490-495.

MacLean, M.R., Alexander, D., Stirrat, A., Gallagher, M., Douglas, S.A., Ohlstein, E.H., Morecroft, I. & Pollard, K. (2000) Contractile responses to human urotensin-II in rat and human pulmonary arteries: effect of endothelial factors and chronic hypoxia in the rat. *Br. J. Pharmacol.*, **130**, 201-204.

MacLean, M.R., Docherty, C.C., McCulloch, K.M. & Morecroft, I. (1998a) Effect of novel mixed ET_A/ET_B antagonists on responses to ET-1 in human small muscular pulmonary arteries. *Pulm. Pharmacol. Therap.*, **11**, 147-149.

MacLean, M.R., Herve, P., Eddahibi, S. & Adnot, S. (2000) 5-hydroxytryptamine and the pulmonary circulation: receptors, transporters and relevance to pulmonary arterial hypertension. *Br. J. Pharmacol.*, **131**, 161-168.

MacLean, M.R., Johnston, E.D., McCulloch, M.R., Pooley, L., Houslay, M.D. & Sweeney, G. (1997) Phosphodiesterase isoforms in the pulmonary arterial circulation of the rat: changes in pulmonary hypertension. *JPET*, **283**, 619-624.

MacLean, M.R., MacKenzie, J.F. & Docherty, C.C. (1998b) Heterogeneity of endothelin-B receptors in rabbit pulmonary resistance arteries. *J. Cardiovasc. Pharmacol.*, **31** (suppl. 1), S290-S293.

MacLean, M.R., McCulloch, M.R. & Baird, M. (1994) Endothelin ET_A- and ET_B-receptor-mediated vasoconstriction in rat pulmonary arteries and arterioles. *J. Cardiovasc. Pharmacol.*, **23**, 838-845.

MacLean, M.R., McCulloch, K.M. & McGrath, J.C. (1993) Influences of the endothelium and hypoxia on α_1 - and α_2 -adrenoceptor-mediated responses in the isolated pulmonary artery. *Br. J. Pharmacol.*, **119**, 917-930.

MacLean, M.R., McCulloch, K.M. & Baird, M. (1994) Endothelin ET_A- and ET_B-receptor-mediated vasoconstriction in rat pulmonary arteries and arterioles. *J. Cardiovasc. Pharmacol.*, **23**, 838-845.

MacLean, M.R., McCulloch, K.M. & Baird, M. (1995) Effects of pulmonary hypertension on vasoconstrictor responses to endothelin-1 and sarafotoxin S6C and on inherent tone in rat pulmonary arteries. *J. Cardiovasc. Pharmacol.*, **26**, 822-830.

MacLean, M.R. & McCulloch, K.M. (1998) Influence of applied tension and nitric oxide on responses to endothelins in rat pulmonary resistance arteries: effects of chronic hypoxia. *Br. J. Pharmacol.*, **123**, 1-8.

MacLean, M.R. & McGrath, J.C. (1990) Effects of endothelin-1 on isolated vascular beds from normotensive and spontaneously hypertensive rats. *Eur. J. Pharmacol.*, **194**, 263-267.

- MacLean, M.R. & Morecroft, I. (2001) Increased contractile response to 5-hydroxytryptamine 1-receptor stimulation in pulmonary arteries from chronic hypoxic rats: role of pharmacological synergy. *Br. J. Pharmacol.*, **134**, 614-620.
- MacLean, M.R., Sweeney, G., Baird, M., McCulloch, K.M., Houslay, M.D. & Morecroft, I. (1996) 5-Hydroxytryptamine receptors mediating vasoconstriction in pulmonary arteries from control and pulmonary hypertensive rats. *Br. J. Pharmacol.*, **119**, 917-930.
- Machado, R.D., Pauciulo, M.W., Thomson, J.R., Lane, K.B., Morgan, N.V., Wheeler, L., Phillips, J.A., Newman, J., Williams, D., Galie, N., Manes, A., McNeil, K., Yacoub, M., Mikhail, G., Rogers, P., Corris, P., Hombert, M., Donnai, D., Martensson, G., Tranebjaerg, L., Loyd, J.E., Trembath, R.C. & Nichols, W.C. (2001) *BMPR2* Haploinsufficiency as the inherited molecular mechanism for primary pulmonary hypertension. *Am. J. Hum. Genet.*, **68**, 92-102.
- Maeda, S., Miauchi, T., Sakai, S., Kobayashi, T., Goto, K., Sugishita, Y. & Matsuda, M. (1998) Endothelin-1 in the heart during exercise. *J. Cardiovasc. Pharmacol.*, **31** (suppl. 1), S392-S394.
- Maguire, J.J., Kuc, R.E. & Davenport, A.P. (2000) Orphan-receptor ligand human urotensin-II: receptor localization in human tissues and comparison of vasoconstrictor responses with endothelin-1. *Br. J. Pharmacol.*, **131**, 441-446.
- Marsden, P.A., Danthuluri, N.R., Brenner, B.M., Ballermann, B.J. & Brock, T.A. (1989) Endothelin action on vascular smooth muscle, inositol triphosphate and calcium mobilization. *Biochem. Biophys. Res. Commun.*, **158**, 86-93.
- Masaki, T., Vane, J.R., & Vanhoutte, P.M. (1989) International union of pharmacology nomenclature of endothelin receptors. *Pharmacol. Rev.*, **46**, 137-142.
- McCulloch, A.I., Bottrill, F.E., Randall, M.D. & Hiley, C.R. (1997) Characterization and modulation of EDHF-mediated relaxations in the rat isolated superior mesenteric arterial bed. *Br. J. Pharmacol.*, **120**, 1431-1438.
- McCulloch, K.M., Docherty, C.C. & MacLean, M.R. (1998) Endothelin receptors mediating contraction of rat and human pulmonary resistance arteries: effect of chronic hypoxia in the rat. *Br. J. Pharmacol.*, **123**, 1621-1630.
- McCulloch, K.M., Docherty, C.C., Morecroft, I. & MacLean, M.R. (1996) EndothelinB receptor-mediated contraction in human pulmonary resistance arteries. *Br. J. Pharmacol.*, **119**, 1125-1130.
- McCulloch, K.M. & MacLean, M.R. (1995) EndothelinB receptor-mediated contraction of human and rat pulmonary resistance arteries and the effect of pulmonary hypertension on endothelin responses in the rat. *J. Cardiovasc. Pharmacol.*, **26** (suppl. 3), S169-76.

McIntyre, C.A., Buckley, C.H., Jones, G.C., Sandeep, T.C., Andrews, R.C., Elliott, A.I., Gray, G.A., Williams, B.C., McKnight, J.A., Walker, B.R. & Hadoke, P.W.F. (2001) Endothelium-derived hyperpolarizing factor and potassium use different mechanisms to induce relaxation of human subcutaneous resistance arteries. *Br. J. Pharmacol.*, **133**, 902-908.

Meade, E.A., Smith, W.L. and DeWitt, D.L. (1993) Differential inhibition of prostaglandin endoperoxide synthase (cyclo-oxygenase) isoenzymes by aspirin and other non-steroidal anti-inflammatory drugs. *J. Biol. Chem.*, **268**, 6610-6614.

Meyrick, B. & Reid, L. (1978) The effect of continued hypoxia on rat pulmonary arterial circulation, an ultrastructural study. *Lab. Invest.*, **38**, 188-200.

Mitchell, J.A., Akaarasereenont, P., Theirermann, C., Flower, R.J. & Vane, J.R. (1993) Selectivity of nonsteroidal anti-inflammatory drugs as inhibitors of constitutive and inducible cyclooxygenase. *Proc. Natl. Acad. Sci.*, **90**, 11693-11697.

Miasiro, N., Yamamoto, H., Kanaide, H. & Nakamura, M. (1988) Does endothelin mobilise calcium from intracellular store sites in rat aortic vascular smooth muscle cells in primary culture? *Biochem. Biophys. Res. Commun.*, **156**, 312-317.

Miyauchi, T., Sato, R., Sakai, S., Kobayashi, T., Ueno, M., Kondo, H., Kawano, S., Goto, K. & Yamaguchi, I. (2000) Endothelin-1 and right-sided heart failure in rats: effects of an endothelin receptor antagonist on the failing right ventricle. *J. Cardiovasc. Pharmacol.*, **36 (suppl. 1)**, S327-S330.

Modesti, P.A., Vanni, S., Paniccia, R., Bandinelli, B., Bertolozzi, I., Polidori, G., Sani, G. & Sernerri, G.G.N. (1999) Characterization of the endothelin-1 receptor subtypes in isolated human cardiomyocytes. *J. Cardiovasc. Pharmacol.*, **34**, 333-339.

Moraes, D.L., Colucci, W.S. & Givertz, M.M. (2000) Secondary pulmonary hypertension in chronic heart failure: The role of the endothelium in pathophysiology and management. *Circulation*, **102**, 1718-1723.

Mori, M., Sugo, T., Abe, M., Shimomura, Y., Kurihara, M., Kitada, C., Kikucji, K., Shintani, Y., Kurokawa, T., Onda, H., Nishimura, O & Fujino, M. (1999) Urotensin-II is the endogenous ligand of a G-protein coupled orphan receptor, SENR (GPR14). *Bioche. Biophys. Res. Commun.*, **265**, 123-129.

Mulder, P., Richard, V., Bouchart, F., Derumeaux, G., Munter, K. & Thuillez, C. (1998) Selective ETA receptor blockade prevents left ventricular remodelling and deterioration of cardiac function in experimental heart failure. *Cardiovasc. Res.*, **39**, 600-608.

Mullaney, I., Vaughan, D. & MacLean, M.R. (1998) Endothelin-1 modulation of camp in rat pulmonary arteries: effect of chronic hypoxia. *J. Cardiovasc. Pharmacol.*, **31 (suppl. 1)**, S112-S114.

Mullaney, I., Vaughan, D.M & MacLean, M.R. (2000) Regional modulation of cyclic nucleotides by endothelin-1 in rat pulmonary arteries: direct activation of Gi2-protein in the main pulmonary artery. *Br. J. Pharmacol.*, **129**, 1042-1048.

Mulvany, M.J. & Aalkjaer, C. (1990) Structure and function of small arteries. *Physiol. Rev.*, **70**, 921-961.

Mulvany, M.J. & Halpern, W. (1976) Mechanical properties of vascular smooth muscle cells *in situ*. *Nature*, **260**, 617-619.

Mulvany, M.J. & Halpern, W. (1977) Contractile properties of small arterial resistance vessels in spontaneously hypertensive and normotensive rats. *Circ. Res.*, **41**, 19-26.

Murata, T., Yamawaki, H., Hori, M., Sato, K., Ozaki, H. & Karkai, H. (2001) Hypoxia impairs endothelium-dependent relaxation in organ cultured pulmonary artery. *Eur. J. Pharmacol.*, **421**, 45-53.

Murphy, D.M.F. & Fishamn, A.P. (1988) Chapter 68. Pulmonary diseases and disorders, 2nd edition. M^cGraw-Hill Company.

Murray, F., MacLean, M. R. & Pyne, N. J. (2002) Increased expression of the cGMP-inhibited cAMP-specific (PDE 3) and cGMP binding cGMP-specific (PDE 5) phosphodiesterases in models of pulmonary hypertension. *In press*.

Nagaya, N., Yokoyama, C., Kyotani, S., Shimonishi, M., Morishita, R., Uematsu, M., Nishikimi, T., Nakanishi, N., Ogihara, T., Yamagishi, M., Miyatabe, K., Kaneda, Y. & Tanabe, T. (2000) Gene transfer of human prostacyclin synthase ameliorates monocrotaline-induced pulmonary hypertension in rats. *Circulation*, **102**, 2005-2010.

Ohlmann, P., Martinez, M.C., Schneider, F., Stoclet, J.C. & Andriantsitohaina, R. (1997) Characterization of endothelium-derived relaxing factors released by bradykinin in human resistance arteries. *Br. J. Pharmacol.*, **121**, 657-664.

Ohlstein, E.H., Nambi, P., Douglas, S.A., Edwards, R., Gellai, M., Lago, A., Leber, J.D., Cousins, R.D., Gao, A., Frazee, J.S., Peishoff, C.E., Bean, J.W., Eggleston, D.S., Elshourbagy, N.A., Kumar, C., Lee, J.A., Yue, T., Loudon, C., Brooks, D.P., Weinstock, J., Feuerstein, G., Poste, G., Roffolo, R.R., Gleason, J.G. & Elliott, J.D. (1994) SB 209670, a rationally designed potent nonpeptide endothelin receptor antagonist. *Proc. Natl. Acad. Sci.*, **91**, 8052-8056.

Ohlstein, E.H., Nambi, P., Hay, D.W., Gellai, M., Brooks, D.P., Luengo, J., Xiang, J.N. & Elliott, J.D. (1998) Nonpeptide endothelin receptor antagonists XI. Pharmacological characterization of SB 234551, a high affinity and selective nonpeptide ETA receptor antagonist. *J. Pharmacol. Exp. Ther.*, **286**, 650-656.

Ohlstein, E.H., Nambi, P., Lago, A., Hay, D.W.P., Beck, G., Fong, K., Eddy, E.P., Smith, P., Ellens, H. & Williot, J.D. (1996) Nonpeptide endothelin receptor antagonists. VI: Pharmacological characterization of SB 217424, a potent and highly bioavailable endothelin receptor antagonist. *JPET*, **276**, 609-615.

- Ohnishi, M., Wada, A., Tsutamoto, T., Fukai, D. & Kinoshita, M. (1998) Comparison of the acute effects of the selective endothelin ET_A and a mixed ET_A/ET_B receptor. *Cardiovasc. Res.*, **39**, 617-624.
- Ohta, K., Hirata, Y., Imai, T., Kanno, K., Emori, T., Shichiri, M. & Marumo, F. (1998) Cytokine-induced release of ET-1 from porcine renal epithelial cell line. *Biochem. Biophys. Res. Commun.*, **169**, 578-584.
- Oka, M. (2001) Phosphodiesterase 5 inhibition restores impaired ACh relaxation in hypertensive conduit pulmonary arteries. *Lung Cell. Mol. Pharmacol.*, **280**, L432-L451.
- Opgaard, O.S., Nothacker, H-P., Ehlert, F.J. & Krause, D.N. (2000) Human urotensin-II mediates vasoconstriction via an increase in inositol phosphates. *Eur. J. Pharmacol.*, **406**, 265-271.
- Opgenorth, T.J., Adler, A.L., Calzadilla, S.V., Chiou, W.J., Dayton, B.D., Dixon, D.B., Goerke, L.J., Henandez, L., Magnusson, S.R., Marsh, K.C., Novasad, E.I., Von Geldern, T.W., Wessale, J.L., Wimm, M. & Wu-Wong, J.R. (1996) Pharmacological characterisation of A-127722: An orally active and highly potent ET_A-selective receptor antagonist. *JPET*, **276**, 473-481.
- Osipenko, O.N., Alexander, D., MacLean, M.R. & Gurney, A.M. (1998) Influence of chronic hypoxia on the contributions of non-inactivating and delayed rectifier K⁺ currents to the resting potential and tone of rat pulmonary artery smooth muscle. *Br. J. Pharmacol.*, **124**, 1335-1337.
- Parsons, S.J.W., Hill, A., Waldron, G.J., Plane, F. & Garland, C.J. (1994) The relative importance of nitric oxide and nitric oxide-independent mechanisms in acetylcholine-evoked dilatation of the rat mesenteric bed. *Br. J. Pharmacol.*, **113**, 1275-1280.
- Peng, W., Michael, J.R., Hoidal, J.R., Karwande, S.V. & Farrukh, I.S. (1998) ET-1 modulates KCa-channel activity and arterial tension in normoxic and hypoxic human pulmonary vasculature. *Am. J. Physiol.*, **275**, L729-L739.
- Perssons, M.G., Zetterstrom, O., Agrenius, V., Ihre, E. & Gustafsson, L.E. (1994) Single-breath nitric oxide measurements in asthmatic patients and smokers. *Lancet*, **343**, 146-147.
- Pieske, B., Beyrman, B., Brue, V., Loffler, B.M., Schlotthauer, K., Maier, L.S., Schmidt-Schweda, S., Just, H. & Hasenfuss, G. (1999) Functional effects of endothelin and regulation of endothelin receptors in isolated human nonfailing and failing myocardium. *Circulation*, **99**, 1802-1809.
- Plane, F. & Garland, C.J. (1993) Differential effects of acetylcholine, nitric oxide and levcromakalim on smooth muscle membrane potential and tone in the rabbit basilar artery. *Br. J. Pharmacol.*, **110**, 651-656.

- Puri, S.P., Baker, L., Dutka, D.P., Oakley, C.M., Hughes, J.M. & Cleland, J.G.F. (1995) Reduced alveolar-capillary membrane diffusing capacity in chronic heart failure. *Circulation*, **91**, 2769-2774.
- Quayle, J.M. & Standen, N.B. (1994) K_{ATP} channels in vascular smooth muscle. *Cardiovasc. Res.*, **28**, 797-804.
- Quilley, J. & McGiff, J.C. (2000) Is EDHF an epoxyeicosatrienoic acid? *Trends Pharmacol. Sci.*, **21**, 121-124.
- Rabinovitch, M., Gamble, W.J., Miettinen, O.S. & Reid, L. (1981) Age and sex influence of pulmonary hypertension of chronic hypoxia and recovery. *Am. J. Physiol.*, **240**, H62-H72.
- Rabinovitch, M., Gamble, W.J., Nadas, A.S., Miettinen, O.S., Reid, L. (1979) Rat pulmonary circulation after chronic hypoxia and recovery. *Am. J. Physiol.*, **236**, H818-H827.
- Rakugi, H., Nakamaru, M., Tabuchi, Y., Nagano, M., Mikami, H. & Ogihara, T. (1989) Endothelin stimulates the release of prostacyclin from rat mesenteric arteries. *Biochem. Biophys. Res. Commun.*, **160**, 924-928.
- Rand, V.E. & Garland, C.J. (1992) Endothelium-dependent relaxation to acetylcholine in the rabbit basilar artery: importance of membrane hyperpolarization. *Br. J. Pharmacol.*, **106**, 143-150.
- Rang, H.P., Dale, M.M. & Ritter, J.M. (1995) Pharmacology, 3rd edition. Churchill-Livingstone.
- Reindl, I., Wernecke, K-D., Opitz, C., Wensel, R., König, D., Dengler, T., Schimke, I. & Kleber, F.X. (1998) Impaired ventilatory efficiency in chronic heart failure: possible role of pulmonary vasoconstriction. *Am. Heart J.*, **136**, 778-785.
- Resink, T.J., Hahn, A.W., Scott-Burden, T., Powell, J., Weber, E. & Buhler, F.R. (1990) Inducible endothelin mRNA expression and peptide secretion in cultured human vascular smooth muscle cells. *Biochem. Biophys. Res. Commun.*, **168**, 1303-1310.
- Resink, T.J., Scott-Burden, T. & Buhler, F.R. (1988) Endothelin stimulates phospholipase C in cultured vascular smooth muscle cells. *Biochem. Biophys. Res. Commun.*, **157**, 1360-1368.
- Resink, T.J., Scott-Burden, T. & Buhler, F. (1989) Activation of phospholipase A_2 by endothelin in cultured vascular smooth muscle cells. *Biochem. Biophys. Res. Commun.*, **158**, 279-286.

- Reynolds, E.E., Keiser, J.A., Haleen, S.J., Walker, D.M., Olszewski, B., Schroeder, R.L., Taylor, D.G., Hwang, O., Welch, K.M., Flynn, M.A., Thompson, D.M., Edmunds, J.J., Berryman, K.A., Plummer, M., Cheng, X., Patt, W.C. & Doherty, A.M. (1995) Pharmacological characterization of PD 156707, an orally active ETA receptor antagonist. *JPET*, **273**, 1410-1417.
- Ross, M.H. & Rommel, L.J. (1989) *Histology: A text and atlas*, 2nd edition. Williams & Wilkins.
- Rubin, L.J., Badesch, D.B., Barst, R.J., Galie, N., Black, C.M., Keogh, A., Pulido, T., Frost, A., Roux, S., Leconte, I., Landzberg, M. & Simonneau, G. (2002) Bosentan therapy for pulmonary arterial hypertension. *N. Engl. J. Med.*, **346**, 896-903.
- Rubyani, G.M. & Botelho, P.L.H. (1991) Endothelins. *FASEB J.*, **5**, 2713-2720.
- Rubyani, G.M. & Polokoff, M.A. (1994) Endothelins. *Pharmacol. Rev.*, **46**, 325-413.
- Russell, F.D. & Davenport, A.P. (1995) Characterization of endothelin receptors in the human pulmonary vasculature using bosentan, SB 209670, and 97-139. *J. Cardiovasc. Pharmacol.*, **26 (suppl. 3)**, S346-S347.
- Russell, F.D., Molenaar, P. & O'Brien, D.M. (2001) Cardiostimulant effects of urotensin-II in human heart *in vitro*. *Br. J. Pharmacol.*, **132**, 5-9.
- Russell, F.D., Skepper, J.N. & Davenport, A.P. (1998) Endothelin peptide and converting enzymes in human endothelium. *J. Cardiovasc. Pharmacol.*, **31 (suppl. 1)**, S19-S21.
- Salter, K., Wilson, C.M., Kato, K. & Kozlowski, R.Z. (1998) Endothelin-1, delayed rectifier K⁺ channels, and pulmonary artery smooth muscle. *J. Cardiovasc. Pharmacol.*, **31 (suppl. 1)**, S81-S83.
- Sasaki, S.I., Kobayashi, N., Dambara, T., Kiro, S. & Sakai, T. (1995). Structural organisation of pulmonary arteries in the rat lung. *Anat. Embryol.*, **191**, 477-489.
- Sawaki, M., Wada, A., Tsutamoto, T., Ohnishi, M., Fujii, M., Matsumoto, T. & Kinoshita, M. (2000) Chronic effects of an orally active selective endothelin-B-receptor antagonist in experimental congestive heart failure. *J. Cardiovasc. Pharmacol.*, **36 (suppl. 1)**, S323-S326.
- Schild, H.O. (1947) pa, a new scale for the measurement of drug antagonism. *Br. J. Pharmacol.*, **2**, 189-206.
- Schilling, J., Holzer, P., Guggenbach, M., Gyurech, D., Marathia, K. & Geroulanos, S. (1994) Reduced endogenous nitric oxide in the exhaled air of smokers and hypertensives. *Eur. Respir. J.*, **7**, 467-471.

Scotland, R.S., Chauhan, S., Vallance, P.J.T. & Ahluwalia, A. (2001) An endothelium-derived hyperpolarizing factor-like factor moderates myogenic constriction of mesenteric resistance arteries in the absence of the endothelial nitric oxide synthase-derived nitric oxide. *Hypertension*, **38**, 833-839.

Shimoda, L.A., Sylvester, J.T. & Sham, J.S.K. (1998) Inhibition of voltage-gated K⁺ current in rat intrapulmonary arterial myocytes by endothelin-1. *Am. J. Physiol.*, **274**, L842-L853.

Shimoda, L.A., Sylvester, J.T. & Sham, J.S.K. (1999) Chronic hypoxia alters effects of endothelin and angiotensin on K⁺ currents in pulmonary arterial myocytes. *Am. J. Physiol.*, **277**, L431-L439.

Shimokawa, H., Yasutake, K., Fujii, M., Owada, K., Nakaike, R., Fukumoto, Y., Takayanagi, T., Nagao, T., Egashira, K., Fujishima, M. & Takeshita, A. (1996) The importance of the hyperpolarizing mechanism increases as the vessel size decreases in endothelium-dependent relaxations in rat mesenteric circulation. *J. Cardiovasc. Pharmacol.*, **28**, 703-711.

Simpson, A.W.M. & Ashley, C.C. (1989) Endothelin evoked Ca²⁺ transients and oscillations in A10 vascular smooth muscle cells. *Biochem. Biophys. Res. Commun.*, **163**, 1223-1229.

Singh, N., Prasad, S., Singer, D.R. & MacAllister, R.J. (2002) Ageing is associated with impairment of nitric oxide and prostanoid dilator pathways in the human forearm. *Clin. Sci.*, **102**, 595-600.

Sogabe, K., Nirei, H., Shoubo, M., Nomoto, A., Ao, S., Notsu, Y. & Ono, T. (1993) Pharmacological profile of FR 139317, a novel, potent, endothelin ETA receptor antagonist. *JPET*, **264**, 1040-1046.

Stirrat, D.S., Levy, R.D., Cernacek, P & Langleben, D. (1991) Increased plasma endothelin-1 in pulmonary hypertension: marker or mediator of disease? *Ann. Intern. Med.*, **114**, 464-469.

Stirrat, A., Gallagher, M., Douglas, S.A., Ohlstein, E.H., Berry, C., Richardson, M. & MacLean, M.R. (2001) Potent vasodilator responses to human urotensin-II in human pulmonary and abdominal resistance arteries. *Am. J. Physiol.*, **280**, H925-H928.

Su, C. & Bevan, J.A. (1976) Pharmacology of pulmonary blood vessels. *Pharmacol. Therap.*, **2**, 275-288.

Sugaira, M., Inagami, T., Hare, G.M.T & Johns, J.A. (1989) Endothelin action: inhibition by protein kinase C inhibitor and involvement of phosphoinositols. *Biochem. Biophys. Res. Commun.*, **158**, 170-176.

Sunako, M., Kawahara, Y., Kariya, K., Araki, S., Fukuzaki, H. & Takai, Y. (1989) Endothelin-induced biphasic formation of 1,2-Diacylglycerol in cultured rabbit vascular smooth muscle cells – mass analysis with a radioenzymatic assay. *Biochem. Biophys. Res. Comm.*, **160**, 744-750.

- Sutch, G., Kiowski, W., Yan, X-W., Hunziker, P., Christen, S., Strobel, W., Kim, J.H., Rickenbacher, P. & Bertel, O. (1998) Short-term oral endothelin-receptor antagonist therapy in conventionally treated patients with symptomatic severe chronic heart failure. *Circulation*, **98**, 2262-2268.
- Sweeney, M. & Yuan, J.X-J. (2000) Hypoxic pulmonary vasoconstriction: role of voltage-gated potassium channels. *Respir. Res.*, **1**, 40-48.
- Sylvester, J.T. (2001) Hypoxic pulmonary vasoconstriction: A radical view. *Circ. Res.*, **88**, 1228-1230.
- Tare, M., Parkington, H.C. & Coleman, H.A. (2000) EDHF, NO and a prostanoid: hyperpolarization-dependent and -independent relaxation in guinea-pig arteries. *Br. J. Pharmacol.*, **130**, 605-618.
- Telemaque-Potts, S., Kuc, R.E., Yanagisawa, M & Davenport A.P. (2000) Tissue-specific modulation of endothelin receptors in a rat model of hypertension. *J. Cardiovasc. Pharmacol.*, **36 (suppl. 1)**, S122-S123.
- Thapaliya, S., Matsuyama, H. & Takewaki, T. (2000) Bradykinin causes endothelium-independent hyperpolarization and neuromodulation by prostanoid synthesis in hamster mesenteric artery. *Eur. J. Pharmacol.*, **408**, 313-321.
- Tortora, G.J. (1992) Principles of human anatomy, 6th edition. HarperCollins.
- Totsune, K., Takahashi, K., Arihara, Z., Sone, M., Satoh, F., Ito, S., Kimura, Y., Sasano, H. & Muakami, O. (2001) Role of urotensin-II in patients on dialysis. *Lancet*, **358**, 810-811.
- Tuder, R., Cool, C.D., Geraci, M.W., Wang, J., Abman, S.H., Wright, L., Badesch, D. & Voelkel, N.F. (1999) Prostacyclin synthase expression is decreased in lungs from patients with severe pulmonary hypertension. *Am. J. Respir. Crit. Care Med.*, **159**, 1925-1932.
- Underwood, D.C., Bochnowicz, S., Osborne, R.R., Loudon, C.S., Hart, T.K., Ohlstein, E.H. & Hay, D.W. (1998) Chronic hypoxia-induced cardiopulmonary changes in three rat strains: inhibition by the endothelin receptor antagonist, SB 217242. *J. Cardiovasc. Pharmacol.*, **31 (suppl. 1)**, S453-S455.
- Underwood, D.C., Bochnowicz, S., Osborn, R.R., Luttmann, M.A., Loudon, C.S., Hart, T.K., Elliott, J.D. & Hay, D.W. (1999) Effect of SB 217242 on hypoxia-induced cardiopulmonary changes in the high altitude-sensitive rat. *Pulm. Pharmacol. Ther.*, **12**, 13-26.
- Urakami-Harasawa, L., Shimokawa, H., Nakashima, M., Egashira, K. & Takeshita, A. (1997) Importance of endothelium-derived hyperpolarizing factor in human arteries. *J. Clin. Invest.*, **100**, 2793-2799.

Voelkel, N.F., Gerber, J.G., McMurtry, I.F., Nies, A.S. & Reeves, J.T. (1981) Release of vasodilator prostaglandin, PGI₂, from isolated rat lung during vasoconstriction. *Circ. Res.*, **48**, 207-213.

Warner, T.D., Mitchell, J.A., De Nucci, G. & Vane, J.R. (1989) Endothelin-1 and endothelin-3 release EDRF from isolated perfused arterial vessels of the rat and rabbit. *J. Cardiovasc. Pharmacol.*, **31 (suppl. 1)**, S85-S88.

Waypa, G.B., Chandel, N.S. & Schumacker, P.T. (2001) Model for hypoxic pulmonary vasoconstriction involving mitochondrial oxygen sensing. *Circ. Res.*, **88**, 1259-1266.

Willette, R.N., Sauermelch, C.F., Storer, B.L., Guiney, S., Luengo, J.I., Xiang, J.N, Elliott, J.D. & Ohlstein, E.H. (1998) Plasma- and cerebrospinal fluid-immunoreactive endothelin-1: effects of nonpeptide endothelin receptor antagonists with diverse affinity profiles for endothelin-A and endothelin-B receptors. *J. Cardiovasc. Pharmacol.*, **31 (suppl. 1)**, S149-S157.

Yanagisawa, M., Kurihara, H., Kimura, S., Tomobe, Y., Kobayashi, M., Mitsui, Y., Yazaki, Y., Goto, K. & Masaki, T. (1988) A novel and potent vasoconstrictor peptide produced by vascular endothelial cells.

Yoshizumi, M., Kurihara, H., Morita, T., Yago, T., On-Hasha, I., Sugayama, T. & Takaku, P. (1990) Interleukin-1 increases the production of endothelin-1 by cultured endothelial cells. *Biochem. Biophys. Res. Commun.*, **166**, 324-329.

Yang, X., Chen, W. & Chen, J. (1997) Change of level and expression of endothelin-1 in the lungs of rats with hypoxic pulmonary hypertension. *Chin. Med. J.*, **110**, 104-108.

Yoshiyoshi, M., Nishioka, K., Nakao, K., Saito, Y., Matsumura, M., Ueda, T., Temma, S., Shirakami, G., Imura, H. & Mikawa, H. (1991) Plasma endothelin concentrations in patients with pulmonary hypertension associated with congenital heart defects. Evidence for increased production of endothelin in pulmonary circulation. *Circulation*, **84**, 2280-2285.

Yuan, X.J., Wang, J., Juhaszova, M., Golovina, V.A. & Rubin, L.J. (1998) Molecular basis and function of voltage-gated K⁺ channels in pulmonary arterial smooth muscle cells. *Am. J. Physiol.*, **274**, L621-L635.

Zhang, Y., Oltman, C.L., Lu, T., Lee, H-C., Dellsperger, K.C. & Vanrollins, M. (2001) EET homologs potently dilate coronary microvessels and activate BKCa channels. *Am. J. Physiol.*, **280**, H2430-2440.

Zhao, L., Mason, N.W., Morrell, N.W., Kojonazarov, B., Sadykov, A., Maripov, A., Mirrakhimov, M.M., Aldashev, A.A. Wilkins, M.R. (2001) Sildenafil inhibits hypoxia-induced pulmonary hypertension. *Circulation*, **104**, 424-428.

Zygmunt, P.M., Plane, F., Paulsson, M., Garland, C.J. & Hogestatt, E.D. (1998) Interactions between endothelium-derived relaxing factors in the rat hepatic artery: focus on regulation of EDHF. *Br. J. Pharmacol.*, **124**, 992-1000.

